Novel findings on the impact of HIV infection: Interplay between T cell development and peripheral T cell homeostasis

Joumana Zeidan

Department of Microbiology and Immunology
Faculty of Medicine
McGill University, Montreal

December 2010

A thesis submitted to McGill University in partial fulfillment of the requirements of the degree of Philosophiae Doctor (Ph.D.)

THESIS ABSTRACT

A hallmark of HIV infection is the gradual decline in CD4 T cells leading to AIDS and failure of the immune system. Depletion of CD4 T cells has been attributed to direct viral cytopathogenicity and hyperimmune activation which all lead to accelerated apoptosis. More recently, impaired thymic function has been shown to contribute to the numerical decline of CD4 T cells. The thymus is the primary source of *de novo* T cells that bear a broadly diverse T cell receptor (TCR) repertoire. In adults, the thymus produces every day approximately 50 million new T cells termed recent thymic emigrants (RTEs). Following their exit from the thymus, RTEs join the naive T cell compartment and upon antigen encounter differentiate into effector and memory T cells.

To further elucidate the perturbations induced by HIV on thymic function and homeostasis of RTEs, we took advantage of a CD4 RTE-specific phenotype ($CD45RA^{+}CD27^{+}CCR7^{+}CD31^{hi}$) recently identified in our laboratory. Herein, we provide evidence that preservation of the RTE pool is key to the maintenance of total CD4 T cells and more specifically central memory T cells (T_{CM}), a subset of memory T cells that are long-lived and have the capacity to persist through homeostatic proliferation, during untreated HIV infection. Our data demonstrates that although proliferation of RTEs during acute/early infection (AEHI) was associated with increased T_{CM} numbers, persistent activation and cell cycle entry of RTEs during chronic HIV infection (CHI) resulted in low RTE, T_{CM} and CD4 T cell numbers. The defects in the regenerative capacity and differentiation of RTEs during CHI were associated with decreased RTE survival, providing evidence that cell cycle entry within the RTE cell pool leads to further depletion, in contrast to replenishment, of RTE and total CD4 T cell counts.

We also investigated the role of thymic output versus peripheral proliferation in CD4 T cell reconstitution following administration of Highly Active Anti-Retroviral Therapy (HAART) during AEHI. HAART is a combination therapy integrating two reverse transcriptase inhibitors along with one or more protease inhibitors. It is generally believed that the increases in CD4 T cell numbers

observed during the first few weeks that follow HAART treatment are due to recirculation of sequestered T cells and not *de novo* T cell production. Our results demonstrate that increases in RTE frequencies together with enhanced intrathymic proliferation four weeks post-HAART correlated with long-term RTE and CD4 T cell recovery. However, failure to decrease cell cycle entry of RTEs following HAART was associated with poor long-term RTE recovery, providing further evidence that thymic output, in contrast to homeostatic expansion, is a key player in the recovery of RTE and total CD4 T cells during immune reconstitution.

We also show a role for IL-7 and IFN-α, two cytokines involved in the regulation of T cell homeostasis, in the observed perturbations of RTE homeostasis and thymic function. IL-7 is an essential cytokine involved in the survival and homeostatic expansion of thymocytes and T cells. However, in untreated HIV infection, high levels of IL-7 were associated with hyperimmune activation and accelerated depletion of RTEs. On the other hand, levels of IL-7 following therapy with HAART were correlated with RTE numbers and survival. We observed that failure to decrease levels of IFN-α, an inflammatory cytokine produced by plasmacytoid dendritic cells (pDCs), following treatment with HAART was negatively associated with levels of intrathymic proliferation and seemed to interfere with the survival-mediated effects of IL-7 on RTEs in the periphery.

Direct assessment of the blockages that IFN-α might exert on thymic function is impeded by the lack of phenotypes that allow isolation of human thymocytes at key developmental stages. Our third set of results demonstrate that $CD3^-$ thymocytes that encompass the $CD31^+CD1a^{low}$ phenotype had not yet undergone β-selection and are the common precursors to both the αβ and γδ lineages. On the other hand, our results show that thymocytes with the $CD31^-CD1a^{hi}$ phenotype were β-selected as demonstrated by their enrichment for the TCRβ molecule. Isolation and co-culture of these subsets within the OP9-DL1 system, consisting of the OP9 bone marrow stromal cell line that ectopically expresses the Notch ligand Delta-like-1, allows for their subsequent maturation, providing a tool for

assessing the impact of inflammatory cytokines produced during HIV infection on intrathymic proliferation.

Overall, the data presented in this thesis illustrate for the first time that HIV infection induces important perturbations in the homeostasis and regenerative capacities of RTEs. This thesis also demonstrates a crucial role for thymic output in T cell reconstitution following HAART therapy and reveals cytokine-mediated defects in RTE homeostasis. Further characterization of the direct impact of inflammatory cytokines on thymopoiesis would help in the development of adjunct therapies aimed at restoring thymic activity and RTE maintenance.

ABRÉGÉ

Une des principales caractéristiques de l'infection par le VIH est la baisse graduelle du nombre de cellules T CD4, laquelle mène à la défaillance du système immunitaire puis SIDA. La déplétion des cellules T CD4 a été attribuée à une cytopathogénicité virale directe et à une hyper-activation immunitaire qui aboutissent à une apoptose accélérée. Il a été démontré récemment, qu'une fonction thymique affaiblie contribue à la diminution du nombre de cellules T CD4. Le thymus est la principale source de cellules T *de novo* qui expriment un répertoire très diversifié de récepteurs des lymphocytes T (TCR). Chez les adultes, le thymus produit chaque jour environ 50 millions de nouveaux lymphocytes T, appelés émigrants thymiques récents (ETRs). À leur sortie du thymus, ces ETRs rejoignent le compartiment des cellules T naïves et, suite au contact avec leur antigène spécifique, elles se différencient en cellules T effectrices et mémoires.

Afin d'évaluer les perturbations causées par le VIH sur la fonction thymique et l'homéostasie des ETRs, nous nous sommes basés sur un phénotype spécifique aux ETRs CD4 ($CD45RA^{+}CD27^{+}CCR7^{+}CD31^{hi}$) mis au point dans notre laboratoire. Dans cette étude, nous avons mis en évidence que l'apport continu en ETRs est la clé du maintien des cellules T CD4 totales et, plus spécifiquement, des cellules T centrales mémoires (T_{CM}). Les T_{CM} sont un sous-groupe de cellules T mémoires qui ont la capacité de persister à long terme grâce à la prolifération homéostatique. Bien que la prolifération des ETRs pendant l'infection aiguë/précoce (AEHI) soit associée à une augmentation du nombre de cellules T_{CM} et à une reprise des cellules T CD4, nos données démontrent qu'une activation persistante ainsi que l'entrée des ETRs dans le cycle cellulaire durant l'infection chronique (CHI) résulte en un faible nombre d'ETRs, de cellules T_{CM} et de cellules T CD4. Le défaut de la capacité de régénération et de différentiation des ERTs lors du CHI est associé à une diminution de la survie des ETRs, prouvant ainsi que la prolifération périphérique au sein du pool de ERTs mène à davantage de déplétion des ERTs et des cellules T CD4 totales.

La thérapie antirétrovirale fortement active (HAART) est une polythérapie qui comprend deux inhibiteurs de transcriptase reverse et un ou plusieurs inhibiteurs de protéases. Il est généralement admis que l'augmentation du nombre de cellules T CD4 observée durant les premières semaines qui suivent un traitement HAART est due à une re-circulation des cellules T séquestrées et non à une production de *novo de* cellules T. Ici, nous montrons que le thymus joue un rôle dans la phase précoce de la reconstitution des cellules CD4. Nos résultats démontrent que l'augmentation du nombre d'ERTs observée quatre semaines post-HAART chez des sujets présentant une fonction thymique accrue, corrèlent avec une restauration à long terme des ERTs et des cellules T CD4. Une augmentation de l'entrée en cycle cellulaire des ERTs à la suite d'un traitement HAART était associée à une restauration des ERTs plus faible. Ceci prouve que la production thymique, contrairement à l'expansion homéostatique, joue un rôle clé dans la restauration des ERTs et des cellules T CD4 lors de la reconstitution immunitaire.

Nous avons également déterminé le rôle de l'IL-7 et l'IFN-α, deux cytokines impliquées dans la régulation de l'homéostasie des cellules T, dans les perturbations de l'homéostasie des ERTs et de la fonction thymique. L'IL-7 est une cytokine essentielle impliquée dans la survie et l'expansion homéostatique des thymocytes et des cellules T. Pourtant, lors des infections au VIH non traitées, des nivaux élevés d'IL-7 sont associés à une hyper activation immunitaire et à une accélération de l'épuisement des ERTs. Cependant, nous avons constaté une corrélation entre les nivaux d'IL-7, le nombre et la survie des ERTs à la suite d'un traitement HAART. Nous avons observé que, suite au traitement HAART, l'absence de réduction des nivaux d'IFN-α, une cytokine inflammatoire produite par les cellules dendritiques plasmacytoïdes, était corrélée négativement avec la prolifération intra-thymique. Ainsi, l'IFN-α semblait interférer avec les effets bénéfiques de l'IL-7 sur la survie des ERTs périphériques.

L'évaluation directe de l'effet exercé par l'IFN-α sur la fonction thymique est entravée par le manque de phénotype permettant l'isolation des thymocytes humains à certains stages clés de leur développement. Nos résultats démontrent

que les thymocytes $CD3^-$ qui comprennent le phénotype $CD31^+CD1a^{low}$ n'avaient pas encore subi la sélection β et ne pouvaient pas se développer vers les stades αβ et γδ. Par contre, les thymocytes qui comprenaient le phénotype $CD31^-CD1a^{hi}$ avaient subi la sélection β, puisqu'ils exprimaient la molécule TCRβ. Nous avons isolé et co-cultivé ces sous-groupes de cellules à l'aide du système OP9-DL1 afin d'étudier leur maturation *in vitro*. Le système OP9-DL1 fournit donc un outil pour l'évaluation de l'impact sur la prolifération intra-thymique des cytokines inflammatoires secrétées lors d'une infection au VIH.

En résumé, les données présentées dans cette thèse démontrent pour la première fois que l'infection par le VIH cause d'importantes perturbations au niveau des capacités d'homéostasie et de régénération des ERTs. Cette thèse illustre aussi le rôle crucial que joue la production thymique dans la reconstitution du compartiment des cellules T suite à un traitement HAART, et révèle un défaut dans l'homéostasie des ERTs médié par certaines cytokines. Une caractérisation plus approfondie de l'impact direct des cytokines inflammatoires sur la thymopoïèse pourrait aider à l'élaboration de thérapies complémentaires visant à restaurer l'activité du thymus et le maintien des ERTs.

ACKNOWLEDGEMENTS

First and foremost, I would like to express my sincerest gratitude to my supervisor, Dr. Rafick-Pierre Sékaly, who has supported me throughout my thesis and provided me with the personal and financial resources for the completion of this work. Through his mentorship, and with his expertise, extensive knowledge, dedication, patience, and attention to details, I have been able to learn and grow professionally.

I would like to express my gratitude to Dr. Elias Haddad for his valuable contribution through the numerous scientific discussions, as well as Dr. Rebeka Bordi her important technical assistance and Dr. Bader Yassine-Diab for his significant help with flow cytometry. I also thank Dr. Simone Fonseca, Dr. Cheryl Cameron, Dr. Denis Gaucher, Dr. Mohamed El-Far and Dr. Clarisse Benne for their editorial assistance.

Outside the scientific world, my family and friends have also played a major role in supporting me during my Ph.D. studies. My parents, Amer and Fadia, were always there for me, encouraging me throughout the years and providing me with financial and emotional support. I thank my sister Lara for her help with graphical editing. I would also like to express my gratitude to Matthieu Briand and Rita Kosseifi for their constant support and encouragement as well as for providing me with valuable advice to manage challenging times.

TABLE OF CONTENT

LIST OF TABLES

CHAPTER 2

CHAPTER 3

LIST OF FIGURES

CHAPTER 1 AND 5

CHAPTER 2

CHAPTER 3

CHAPTER 4

CONTRIBUTION OF AUTHORS

Chapter 2 **Survival of recent thymic emigrants is essential for central memory and total CD4 maintenance in untreated HIV infection**

Joumana Zeidan, Bader Yassine-Diab, Yu Shi, Yoav Peretz, Mohamed-Rachid Boulassel, Marie-Lise Dion, Rebeka Bordi, Lionel Filion, Jean-Pierre Routy, Remi Cheynier, Elias K. Haddad and Rafick-Pierre Sekaly.

J. Zeidan performed the phenotypic staining and flow cytometric analysis of healthy and HIV-infected PBMCs. J. Zeidan, with the help of B. Yassine-Diab, Y. Shi and Y. Peretz, performed the PhosFlow assay. Detection of plasma cytokines by ELISA were performed by M.R. Boulassel. M.-L. Dion, R. Bordi, L. Filion and R. Cheynier, with the help of J. Zeidan, defined the CD31 phenotype. The manuscript and the figures were generated by J. Zeidan, in collaboration with E.K. Haddad, under the supervision of R.-P. Sekaly. J. Zeidan determined the studied HIV cohort's inclusion and exclusion criteria. J.-P. Routy and R.-P. Sekaly provided the HIV-infected samples.

Chapter 3 **Increased intrathymic proliferation and decreased immune activation contribute to the recovery of recent thymic emigrants in HIV-infected individuals under HAART**

Joumana Zeidan, Marie-Lise Dion, Rebeka Bordi, Bader Yassine-Diab, Mohamed-Rachid Boulassel, Lionel Filion, Jean-Pierre Routy, Remi Cheynier, Elias K. Haddad and Rafick-Pierre Sekaly.

J. Zeidan performed the phenotypic staining and flow cytometric analysis of HIV-infected PBMCs (with the help of B. Yassine-Diab). TREC analysis was performed by M.-L. Dion and R. Bordi. Detection of plasma cytokines by ELISA were performed by M.R. Boulassel. M.-L. Dion, R. Bordi, L. Filion and R. Cheynier, with the help of J. Zeidan, defined the CD31 phenotype. The manuscript and the figures were generated by J. Zeidan, in collaboration with E.K. Haddad, under the supervision of R.-P. Sekaly. J. Zeidan determined the studied HIV cohort's inclusion and exclusion criteria. J.-P. Routy and R.-P. Sekaly provided the HIV-infected samples.

Chapter 4 CD31 and CD1a identify human β-selected thymocytes and delineate cells committed to the αβ lineage

Joumana Zeidan, Lionel Filion, Rebeka Bordi, Geneve Awong, Mohamed El-Far, Bader Yassine-Diab, Ali Fellali, Sylvain Gimmig, Elias K. Haddad, Juan Carlos Zúñiga-Pflücker and Rafick-Pierre Sekaly.

J. Zeidan performed thymocyte phenotypic staining, sorting and flow cytometric analysis (with the help of R. Bordi, B. and Yassine-Diab). S. Gimmig performed the FACS sorting on DB Aria. J. Zeidan, with the help of M. El-Far performed the cell lysis for RNA extraction. The genomics platform of the Institute for Research in Immunology and Cancer (Montreal) performed the qRT-PCR. J. Zeidan, with the help of A. Fellali and E.K. Haddad analyzed the qRT-PCR data. J. Zeidan, with the help of G. Awong, performed the co-cultures with OP9-DL1. The manuscript and the figures were generated by J. Zeidan, in collaboration with E.K. Haddad, under the supervision of R.-P. Sekaly. L. Filion provided the thymus samples and J.C. Zúñiga-Pflücker provided the OP9-DL1 cells.

INTRODUCTION

A hallmark of HIV infection is the gradual depletion of naive as well as total CD4 T cells from the periphery and secondary lymphoid tissues [1, 2]. Depletion of naive T cells could be associated with various factors including antigen stimulation and recruitment into the memory T cell pool, cell death and impaired thymic function. The thymus, the primary source of *de novo* T cell production, is susceptible to HIV infection as demonstrated by isolation of the virus from within thymocytes and the expression of the molecules that allow HIV entry (namely CD4 together with CXCR4 or CCR5) by thymocytes as well as stromal cells [3, 4].

Previous work performed in our laboratory has identified a novel method of measuring intrathymic proliferation called the sj/β TREC ratio. This method is based on the quantification of the by-products of TCRB and TCRA rearrangements, namely T cell receptor (TCR) excision circles (TREC). The use of this approach has led to the conclusion that intrathymic proliferation of T cell precursors is severely impaired during primary HIV infection, resulting in progressive CD4 T cell depletion during chronic HIV infection. [5, 6].

Reduced proliferation of thymic precursors has been suggested to a result from indirect effects of HIV infection such as the production of pro-inflammatory cytokines by innate immune cells such as macrophages, mDCs and pDCs [6]. Increased levels of pro-inflammatory cytokines such as IFN-α, TNF-α, and IL-6 have been detected in HIV-infected individuals [7, 8] and IFN-α has been shown to exert a negative impact on T cell homoeostasis [9]. The thymus also contains

pDCs and these cells have been shown to produce IFN-α upon infection with HIV in Thy/Liv SCID-hu mice [10]. Due to its ability to exert anti-proliferative effects on immature thymocytes in mouse models [11], IFN-α is a likely candidate in the observed defects in intrathymic proliferation. However, evaluation of the impact of pro-inflammatory cytokines such as IFN-α on thymopoiesis has been hampered due to the lack of phenotypes associated with key stages of human T cell development, such as β-selection in which the majority of intrathymic proliferation takes place [6].

A caveat of the TREC assay is that it does not permit direct quantification and biological characterization (such as the expression of survival, apoptotic and activation markers) of the cells that have recently exited the thymus, termed recent thymic emigrants (RTEs). This has limited the understanding of the direct impact of impaired thymopoeisis on peripheral homeostasis. To overcome this limitation, our laboratory has recently identified high expression of the adhesion molecule CD31 ($CD31^{hi}$) as a validated phenotype that distinguishes TREC-rich RTEs from TREC-poor 'older' naive T cells, thereby providing a tool to measure frequencies and functional properties of RTEs during HIV infection.

The objectives of the research described in this thesis are:

1) Determine the impact of HIV infection on RTE production and homeostasis, during acute/early (AEHI) and chronic HIV infection (CHI). Are RTEs depleted? If so, at which stage of infection? And what are the mechanisms involved in their depletion?

2) Determine the impact of thymic output on CD4 T cell homeostasis in a longitudinal analysis of HIV-infected individuals in early stage of disease. Does depletion of RTEs lead to impairment in the distribution of memory subsets, specifically T_{CM}, considered to be the stem cells of the memory T cell pool, leading to faster disease progression? Does preservation of the RTE subset result in delayed loss of CD4 T cells in untreated HIV infection?
3) Determine the contribution of the production and survival of RTEs in CD4 T cell reconstitution following treatment with HAART in HIV-infected subjects.
4) Determine the impact of cytokines that play important roles in T cell homeostasis, namely IL-7 and IFN-α, on the magnitude of changes in the sj/β TREC ratio and in RTE numbers post-HAART.
5) Define key stages of early human T cell ontogeny such as β-selection by using the OP9-DL1 culture system, an *in vitro* system that models all stages of thymic development. This will be the basis of future evaluation of the blockages that IFN-α and/or other inflammatory cytokines might exert on human intrathymic proliferation and thymic output.

CHAPTER 1: REVIEW OF THE LITTERATURE

1. Thymopoiesis

The thymus is the primary lymphoid organ in which T cell precursors originating from the bone marrow are educated into functional αβ or γδ T cells. αβ T cells are the predominant subset in the periphery, with γδ T cells comprising only 1-5% of T cells. Mature thymocytes exit the thymus as recent thymic emigrants (RTEs) that colonize peripheral lymphoid organs and contribute to the peripheral naive T cell pool until their encounter with cognate antigens. The unique importance of the thymus in T cell immunity is clearly demonstrated in individuals with DiGeorge Syndrome, a rare congenital disorder characterized by the absence of the thymus which results in severe immunodeficiency and a high susceptibility to infections [12].

1.1. The thymic microenvironment

The thymus is a bilobular organ located in the upper anterior thoracic cavity that is subdivided into numerous lobules, each consisting of a peripheral cortex surrounding a central medulla. T cell development involves continuous interactions between the thymic stroma, a dense network consisting of thymic epithelial cells (TECs), dendritic cells (DCs) and macrophages, and differentiating thymocytes as they migrate through its different compartments in a tightly regulated fashion [13]. Development of T cells in the thymus can be separated into three steps:

1) Thymic colonization and T cell commitment
2) Divergence of the αβ and γδ lineages
3) Functional maturation of αβ and γδ thymocytes. For cells of the αβ lineage, this involves positive and negative selection.

Throughout these processes, thymocytes undergo various transcriptional changes and the different stages of human T cell development can be distinguished by the expression of cell surface markers that include CD34, CD1a, CD4, CD8 and CD3 [14]. These events occur in distinct anatomical regions of the thymus as developing thymocytes are submitted to various decision checkpoints and receive

signals from specialized stromal and dendritic cells located throughout the thymus.

1.2. T cell commitment

Studies in the mouse have shown that hematopoietic progenitor cells enter the thymus parenchyma from the blood by migrating through post-capillary venules located near the cortico-medullary junction [15]. These cells are called early thymus progenitors (ETP). The exact mechanism leading to ETP entry is not fully identified, but seems to be regulated by the availability of intrathymic niches [16]. This process likely involves adhesive interactions between platelet (P)-selectin (CD62P), expressed on the thymic endothelium, and its ligand PSGL-1, found on ETPs. Indeed, it was shown that the thymi of mice lacking PSGL-1 contained fewer progenitors and that the expression of P-selectin by the thymic endothelium was regulated by the number of resident thymic progenitors [17].

Recent studies support the hypothesis that the human thymus is seeded by a stem-cell like progenitor that possesses alternative lineage potential and that T cell commitment occurs in the thymus [18-21]. In the human thymus, the most immature cells do not express CD4 and CD8 and therefore are called double negative (DN). This stage can be further subdivided using the markers CD34 and CD1a [14]. The earliest precursors express CD34, but not yet CD1a, and retain the potential to differentiate into cells of the myeloid and erythroid lineage [21]. On the other hand, $CD34^{+}CD1a^{+}$ are irreversibly committed to the T cell lineage and will not differentiate into non T cells; these cells up-regulate genes specific for T cells such as pTα, RAG-1 and LAT while down-regulating non-T lineage genes such as CD13 and CD33 [21]. Upon T cell commitment, thymocytes undergo rearrangements of their T cell receptor (TCR) γ, δ and β genes. Rearrangement of the TCR germline DNA, also known as somatic recombination, is a stepwise mechanism involving the assembly and fusion of the variable (V), diversity (D) and joining (J) segments to form a vast repertoire of diverse TCR sequences [22].

1.3. Beta-selection vs. gamma delta-selection

In mice, $CD4^-$ $CD8^-$ double negative (DN) thymocytes are further classified into four subgroups, DN1 to DN4, based on their expression of CD25 and CD44 [23]. αβ and γδ-lineage T cells arise from a common DN3 progenitor, in which TCRβ, TCRγ and TCRδ-chain rearrangements are initiated [24]. During TCR rearrangements, TCR diversification is enhanced through the random insertion of deoxyribonucleotides (N nucleotides) and palindromic sequences (P nucleotides) [22]. Consequently, two third of the rearrangements are out-of-frame and do not result in the coding of functional proteins. Thymocytes that have successfully rearranged the TCR β-chain are rescued from apoptosis and selected for further maturation, a process termed β-selection [25]. Survival signals are conferred through the pre-TCR complex, which is generated by the pairing of the productively produced β-chain together with the invariant pre-TCRα chain (pTα) and the CD3 chain [26]. Signal transduction through the pre-TCR complex is not triggered by ligand recognition; instead the pre-TCR can deliver its signals autonomously through its spontaneous oligomerization [27]. Signaling through the pre-TCR involves the SRC-family kinases LCK, ZAP70 and adapter LAT (linker for activation of T cells) which initiate downstream signaling events such as mobilization of calcium and translocation of transcription factors such as NF-κB and NFAT to the nucleus [28]. Pre-TCR signaling activates cell cycle expansion, confers survival signals and induces re-expression of the RAG enzymes, thereby promoting TCRA gene rearrangement [29]. β-selection also leads to complex internalization and lysosomal degradation of the pre-TCR [30], explaining why cell surface expression of the pre-TCR is detectable at very low levels. As a result, detection of the expression of the intracellular TCRβ protein is commonly used as a marker to identify thymocytes that have undergone β-selection [31]. The DN3 cells that have successfully rearranged the TCR β-chain go on to up-regulate CD4 and CD8 and become double-positive (DP) and subsequently CD4 or CD8 single-positive (SP) cells.

Unlike αβ T cells, γδ T cell precursors do not form a pre-TCR and γδ-selection involves a complete TCRγδ complex [32]. With the recent identification of CD27 as a surface marker that is up-regulated on thymocytes undergoing either β- or γδ-selection, it was shown that γδ-selection is analogous to β-selection; it involves similar regulation of T cell development genes such as the RAG enzymes, CD25, pTα, Runx1, Gfi1, SpiB, Notch1 and Notch3 [24]. This study also demonstrated that formation of the TCRγδ induces survival and promotes subsequent maturation of the selected γδ-thymocytes; however, this was shown to involve Bcl-2 while β-selection induces Bcl-xL [24]. DN3 thymocytes that produced a TCRγδ remain DN and progress along the γδ-lineage [33].

In contrast to mice, developing human DN thymocytes up-regulate CD4 before up-regulating CD8 and progress to the DP stage by passing through the immature single positive (ISP) intermediate [34]. In humans, the point of αβ and γδ lineage divergence remains unknown and the stage during which β-selection occurs has not been fully clarified.

1.3. Positive and negative selection of αβ T cells

Following β-selection-mediated expansion, thymocytes re-express the enzymatic machinery that regulates TCR rearrangement and begin to rearrange the TCRA locus [29]. The TCRD gene segments are embedded within the TCRA locus. Therefore, excising the TCRD locus is a pre-requisite for successful TCRA rearrangement within DP thymocytes and irreversibly commits DP cells to the T cell lineage followed by VJα rearrangements [35]. Successful rearrangement of the TCRA gene leads to the expression of a functional TCRα protein, resulting in the formation of a TCRαβ complex at the surface of the cells. Unlike the pre-TCR, the TCRαβ interacts with self-peptide/major histocompatibility complex (MHC) expressed by cortical TECs and dendritic cells, and these interactions are crucial for subsequent maturation and survival. DP thymocytes expressing a TCRαβ that recognizes self-peptide:MHC complexes with low

affinity are rescued from cell death, a process termed positive selection [36]. Signals inferred by positive selection induce DPs to differentiate into CD4 or CD8 SP thymocytes and to migrate from the cortex into the medulla through CCR7-mediated chemotaxis [37] where they will reside for approximately two weeks before exiting into the circulation.

The medulla is the primary site of negative selection, a process by which thymocytes expressing a TCRαβ that engages p:MHC complexes with high affinity are induced to undergo apoptotic cell death, owing to the presence of medullary TECs that express tissue-specific antigens regulated by the transcription factor Aire (autoimmune regulator) [38]. In this manner, negative selection controls the T cell repertoire that is exported to the periphery by ensuring that self-reactive thymocytes are deleted prior to their exit.

About half of positively selected thymocytes undergo negative selection [39], while the remaining SPs up-regulate molecules that promote egress from the thymus such as sphingosine 1-phosphate type 1 receptor (S1P1) [40], CCR7 and CD62L [41] and down-regulate others that lead to their retention within the thymus such as CD69 [42]. Following exit from the thymus, αβ T cells recirculate between the blood and secondary lymphoid organs while γδ T cells reside primarily within epithelial tissues such as the skin, intestinal epithelium and lungs [43].

1.4. IL-7 and Notch Signaling in T cell development

As described above, developing thymocytes undergo several lineage decisions during their journey throughout the thymus. Such cell fate decisions as well as thymocyte survival, proliferation and differentiation are influenced by various signals derived from soluble factors (cytokines and chemokines) as well as molecular interactions requiring cell-cell contact. This section focuses on the roles of Interleukin-7 (IL-7) and Notch signaling in thymopoiesis.

IL-7 is a pleiotropic cytokine produced by stromal cells within the bone marrow and the thymus. IL-7 signals through the IL-7 receptor, a heterodimeric complex composed of CD127 (or IL-7Rα) and CD132, the common γ-chain that is shared

by the receptors for IL2, IL-4, IL-7, IL-9, IL-15 and IL-21 [44]. When IL-7 interacts with its cognate receptor, activation of the Janus kinase-signal transducer and activator of transcription (JAK-STAT) signaling pathway is induced (involving Jak1, Jak3, and Stat-5); this leads to the up-regulation of genes associated with proliferation and survival (such as the anti-apoptotic molecule Bcl-2) [44]. The critical role of IL-7 signaling in human T cell development was highlighted by studies demonstrating that T cells are absent in individuals with IL-7R and JAK3 deficiencies [45, 46]. On the other hand, αβ T cells were detected in mice deficient for IL-7 or IL-7R, albeit at significantly lower numbers [47, 48], suggesting that IL-7 has a more crucial role in human T cell development than in mouse T cell development. IL-7 was shown to be essential for the expansion of human $CD34^+$ progenitor cells committed to the T cell lineage [49] as well as for their survival [50]. This is clearly demonstrated in experiments over-expressing Bcl-2 in IL-$7^{-/-}$ mice, which relieved blockages in early T cell development [51]. In addition, IL-7-mediated up-regulation of Bcl-2 is also necessary for the survival of DP thymocytes following positive selection [51]. IL-7 seems to be involved in inducing TCRβ V(D)J rearrangements as these could not be detected in thymocytes from subjects with X-linked severe combined immunodeficiency (characterized by a deficiency in the common γ-chain of the IL-7 receptor) [45]. This is further supported by the finding that *in vitro* addition of IL-7 enhanced TCRβ rearrangements in fetal thymic organ cultures (detailed in section 2.1.2) [52], and this effect was possibly mediated by STAT-5 [50]. This is not the case in mice, in which IL-7 is not involved in TCRβ rearrangement but rather is crucial for TCRγ rearrangements [53].

Amongst the various interactions between thymocytes and the thymic microenvironment, the activation of Notch receptors on the surface of developing thymocytes by Notch ligands on stromal cells has been shown to regulate thymocyte fate decisions and induce critical developmental changes [33]. Notch receptors are a highly conserved family of transmembrane glycoproteins. When engaged by ligands from the Jagged and Delta families, Notch receptors induce

proteolytic cleavage and translocation of the intracellular domain of Notch into the nucleus [54], where it interacts with various transcriptional factors to induce transcription of its target genes [55]. The importance of Notch signaling in the earliest stages of T cell commitment was demonstrated by complementary experiments showing that the over-expression of the intracellular (active) domain of Notch-1 in human and mouse progenitor cells facilitated the development of DP T cells while abolishing the development of B cells within the bone marrow of reconstituted SCID mice [56, 57]. Conversely, inactivation of Notch-1 signaling in mouse progenitor cells prevented T cell development and resulted in the generation of B cells within the thymus [58, 59]. Furthermore, Notch-1 has been reported to support the expansion of precursors committed to the T cell lineage by sustaining IL-7 receptor expression [49].

Notch signaling was shown to also play a role in commitment to the αβ- versus γδ-lineage in mouse studies. Loss of Notch-1 signaling prior to β-selection resulted in severe perturbation of αβ but not γδ T cell lineage development due to impaired V(D)J β rearrangement [60]. Conversely, over-activation of Notch-1 induced thymocytes bearing functional γδTCR gene rearrangements to adopt the αβ T cell fate [61]. In contrast to what occurs in mice, Notch signaling seems to be required for human γδ T cell development, as cord blood- or thymus-derived $CD34^+$ progenitor cells generate higher frequencies of γδ T cells in culture when transduced with active Notch-1 [56]. More recently, it was shown that higher levels of Notch signaling promoted γδ T cell differentiation at the expense of αβ T cells, whereas lower levels of Notch signaling allowed for the development of αβ T cells [62]. The roles of Notch-1 and IL-7 in human T cell development are illustrated in figure 1.

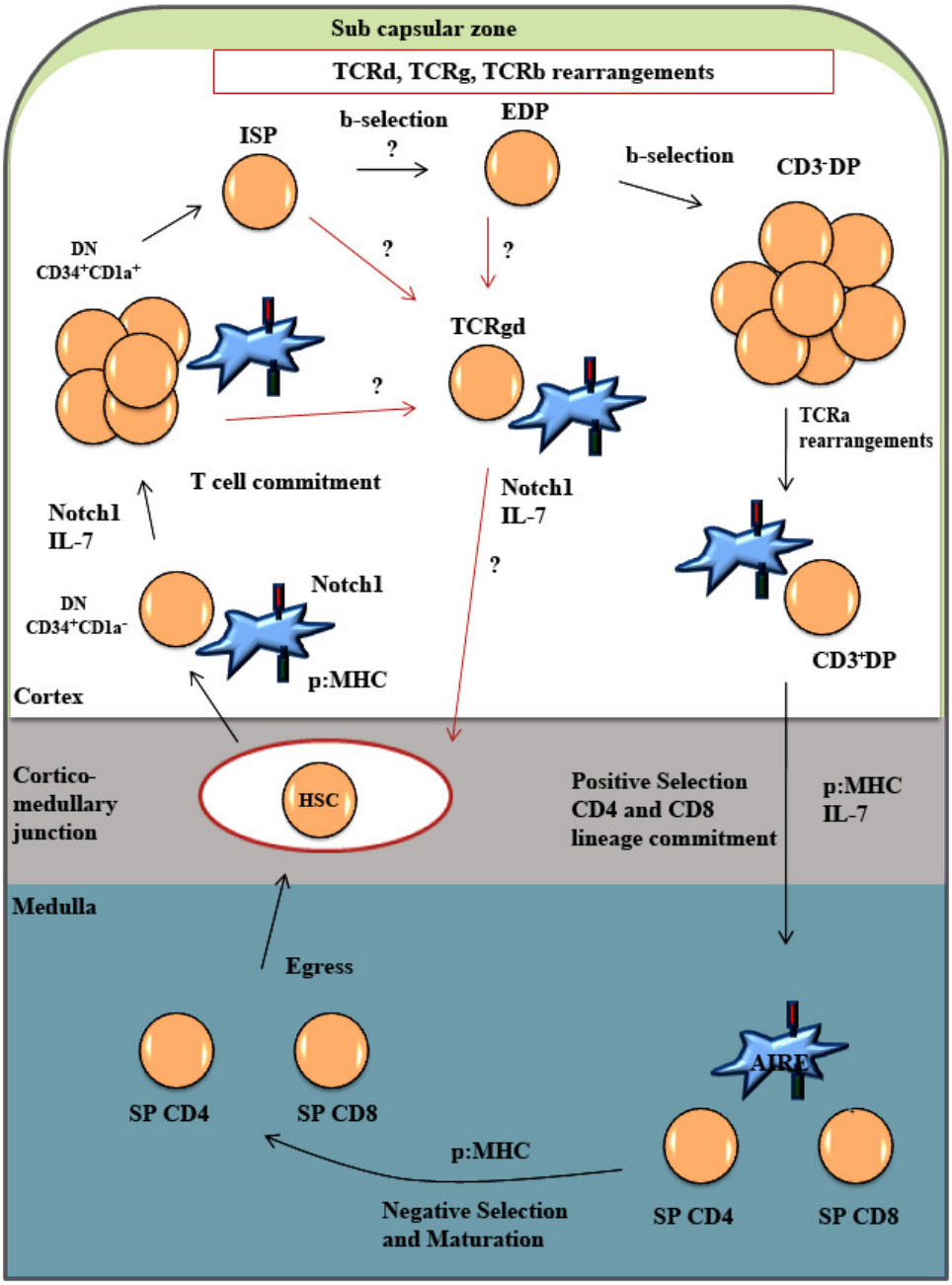

Figure 1: T cell development in the human thymus.
The thymic architecture is organized into discrete cortical and medullary areas, each of which contains specific stromal cells (TECs are represented as the blue cells, Notch-1 and self-p:MHC complex are also illustrated as red and green ligands, respectively) and thymocytes at defined maturation stages (original figure). Question marks highlight the stages of human T cell development that remained unknown prior to the work carried out in this thesis. Explanation within the text body.

2. Evaluation of thymic activity in humans

2.1. Studying T cell development

Both *in vivo* and *in vitro* systems have been developed in order to further our understanding of human T cell development and the various factors and mechanisms that are involved in this process.

2.1.1. Thy/Liv SCID-hu mouse model

The thymus/liver SCID-human mouse is a heterochimeric model designed to study hematopoietic differentiation of human T cells. It involves the grafting of portions of human fetal thymus and human fetal liver hematopoietic stem cells (HSC) into genetically determined severe combined immunodeficiency (SCID) mice [63]. Due to a spontaneous mutation in the gene encoding an enzyme involved in DNA repair, V(D)J recombination does not occur in SCID mice [64]. Consequently, these mice lack T and B cells, enabling them to accept foreign grafts. The implanted HSCs migrate into the implanted human tissues where they mature into T and B cells. This model has proven useful in the study of the development of various lymphoid cells and represents an important animal model in AIDS research [63].

2.1.2. Human fetal thymic organ culture

Fetal thymic organ cultures (FTOC) have been widely used to study aspects of thymocyte development and thymic stromal cell function *in vitro*. This system involves the isolation and culture of fetal thymus lobes from which endogenous thymocytes are depleted. This is followed by the microinjection of progenitor cells that will ultimately undergo differentiation [65]. To overcome limitations in the availability of human thymic tissue, this method can be adapted using thymocyte-depleted fetal mouse thymus lobes in conjunction with human thymocyte progenitors [66].

2.1.3. OP9-DL1

The OP-DL1 culture system consists of OP9 mouse bone marrow stromal cells that are retrovirally transduced to express the Notch ligand Delta-like-1 (DL-1). This cell line lost the ability to support B cell development [67]. Instead, *in vitro* co-culture of mouse embryonic stem cells as well as human cord blood hematopoietic stem cells on OP9-DL1 cells leads to the generation of cells with phenotypes indicative of the T cell lineage, including DPs [67, 68].

Prior to the introduction of the OP9-DL1 system, efforts to monitor thymocyte development *in vitro* in the absence of a thymic microenvironment have been unsuccessful. As reported in section 1.4, Notch signaling is crucial in regulating T cell development. Amongst Notch ligands, DL-1 is a key molecule in governing T cell versus the B cell lineage commitment since its presence instructed $CD34^+$ cord blood progenitor cells to differentiate into DP thymocytes and inhibited B cell development [69]. In fact, DL1 is not expressed by thymic stromal cell monolayer cultures (TSMC) in which T cell lymphopoiesis is not supported, while its expression is maintained in FTOCs [70]. These findings demonstrate that DL1 mimics the thymic stromal environment and are the basis of the OP9-DL1 culture system.

2.2. Studying thymic function

The sampling of human thymic tissue to study thymic activity, due to ethical restrictions, is limited to samples obtained post-mortem or following partial removal of thymic tissue such as in the context of thoracic surgeries. To overcome limitations associated with invasive thymic tissue sampling, a series of indirect methods aimed at evaluating thymic activity and/or thymic output are used instead.

2.2.1. CT scan

Thymic imaging using thoracic computed tomography (CT) scans permits the assessment of the size, shape, and density of the human thymus and provides an estimate of thymic activity [71]. The image obtained is given a grading scale from

0 to 5 based on the amount of functional thymic tissue, with an index of 3 or greater representing abundant thymic tissue [72]. A limitation of the use of CT scans in evaluating thymic size lies in its inability to distinguish between abundant thymic tissue due to enhanced thymic function or infiltration of the perivascular space by mature T cells and other blood cells during inflammation [73]. Therefore, this tool should be used in conjunction with other methods during conditions associated with inflammation such as during HIV infection.

2.2.2. TRECs

Analysis of T cell receptor (TCR) excision circles (TRECs) represents a method that allows detection of recent thymic emigrants (RTEs) and quantification of thymic output. TRECs are excised circular DNA generated following TCR gene rearrangement. Since they are by-products of events occurring during intrathymic development, their measurement is considered an indication of thymic activity. The use of TRECs as a tool to measure thymic function is further supported by their absence in athymic individuals with complete DiGeorge Syndrome [74].

Rearrangement of the VJ TCRA and V(D)J TCRB genes is highly diverse and produces a wide array of TRECs, and no single TREC can be used alone to quantify thymic function. However, deletion of the TCRD locus occurring during TCRA rearrangement in DP thymocytes produces two types of TRECs that are detected in 70% of αβ T cells, a signal joint sjTREC and coding joint cjTREC [75], rendering them widely used for the evaluation of thymic function. Furthermore, as TRECs are stable extra-chromosomal DNA [76], they are not duplicated during mitosis [77] and are therefore 'diluted out' when cells replicate. Therefore, levels of sj and cjTRECs are higher in thymocytes than in naive T cells, and higher in naive T cells than in memory T cells [74]. In addition, their use allows for the distinction of RTEs from resident naive T cells that have divided and reduced their TREC levels [74]. Because TRECs are diluted with each cell division, their levels are not solely determined by thymic output but also by peripheral expansion. Although peripheral TREC levels were shown to correlate strongly with intrathymic TREC values and are therefore a reliable tool

to study thymic function in healthy individuals [78], their measurement does not provide direct evidence of intrathymic impairment in clinical diseases associated with T cell depletion and heightened proliferation.

To overcome these limitations, our laboratory generated a method aimed at measuring intrathymic proliferation by quantifying the various TRECs generated by TCRB and TCRA rearrangements in peripheral blood mononuclear cells and computing the ratio of sj TRECs/β TRECs [6]. Due to the fact that peripheral proliferation would result in an equal dilution of the DJβ and sjTRECs, the sj/β TREC ratio directly reflects the extent of thymocyte proliferation between TCRB and TCRA gene rearrangements. This novel method of quantifying TRECs is therefore not confounded by peripheral T cell division and can be used in HIV infection to assess thymic function [6].

2.2.3. Naive and RTE phenotype

In humans, there are no established cell surface markers to phenotypically distinguish between long-lived naive T cells and cells that have recently emigrated from the thymus. Flow cytometric analysis of cells expressing CD45RA, CD27, CCR7 and CD62L permits the quantification of antigen-naive T cells from the peripheral blood [79] and has been widely used to estimate thymic function. Although RTEs are part of the total naive T cell pool, naive T cells also include long-lived 'older' T cells [80]. In fact, it has been shown that thymectomy in human adults does not lead to a decline in naive T cell numbers [81], and their quantification does not reflect a direct measurement of thymic function. Therefore, the identification of markers that specifically detect RTEs should permit a more direct assessment of thymic output. CD31 (also termed platelet-endothelial cell adhesion molecule 1 (PECAM-1)), an adhesion molecule part of the immunoglobulin (Ig) superfamily [82], has been proposed as an RTE marker for CD4 T cells in humans [83]. CD31 is expressed predominantly at endothelial cell-cell junctions and on the surface of platelets and megakaryocytes, but its expression can also be found on various leukocyte and thymocyte subsets as well as the thymic epithelium [82, 84, 85]. Although it is widely expressed within CD4

naive T cells, it is generally not detected in CD4 memory subsets [86]. The function of CD31 depends on the cell type and binding partner. Homophilic binding between CD31 on endothelial cells and CD31 on neutrophils and monocytes mediates cellular adhesive contacts and promotes extravasation and infiltration of leukocytes at sites of inflammation [87]. In the thymus, CD31-CD38 interactions between the thymic epithelium and developing thymocytes enhance apoptosis [85]. In 2002, Kimmig et al. reported that CD4 naive T cells expressing CD31 contained 8-fold higher TREC levels than $CD31^-$ naive T cells [83]. Although this study demonstrated that $CD31^-$ naive T cells had undergone extensive peripheral proliferation and were 'older' than $CD31^+$ naive T cells, it failed to analyze CD31 levels in the thymus or compare TREC levels between $CD31^+$ T cells and single positive thymocytes. Nonetheless, CD31 seemed a likely candidate for the identification of RTEs since it is progressively down-regulated following TCR engagement and is not re-expressed on memory T cells [88]. In addition, the frequencies of $CD31^+$ cells within the CD4 T pool are elevated (more than 80%) in cord blood samples [89] and are decreased with ageing [83, 89, 90]. Our laboratory has taken this observation further and demonstrated that CD4 naive T cells expressing the highest levels of CD31, termed $CD31^{hi}$ have a similar sjTREC content to that of single positive thymocytes (only a 2-fold reduction) and encompass in average 12-fold more sjTRECs than $CD31^-$ naive T cells (unpublished data). In addition, the frequencies of $CD31^{hi}$ naive T cells correlated with thymic activity, as measured by the sj/β TREC ratio, in healthy controls as well as in HIV-infected individuals (unpublished data). These findings further support the validity of the $CD31^{hi}$ phenotype for RTE assessment.

Having established a phenotype specific for CD4 RTEs, it is now possible to directly isolate and characterize these cells from human samples, as well as analyze the impact of thymic function in clinical settings and immune reconstitution.

3. T cell Homeostasis

The generation and maintenance of T cell numbers as well as TCR repertoire diversity (dependent on the naive T cell pool) and functional efficiency (dependent on the memory T cell pool) is crucial for immune competence. This is achieved by maintaining equilibrium between thymic output, homeostatic peripheral proliferation and rates of apoptosis within the naive and memory T cell pools.

3.1. Naive T cell homeostasis

In human adults, naive T cells are long-lived, with a life span of 3-6 months [91] and seldom divide in steady state conditions. The maintenance of the naive T cell pool is an active process, requiring continuous signals provided by interactions with TCR/self-peptide MHC complexes and members of the common gamma chain (γc) family of cytokines especially IL-7.

3.1.1. Role of the TCR

Positive selection in the thymus generates T cells capable of recognizing self-antigens without inducing autoimmunity. This low self-reactivity is responsible for the survival and maintenance of naive T cells [92]. Initial studies suggested that MHC class I and class II molecules were needed for the maintenance of the CD8 and CD4 T cell populations [93-95]. The requirement for TCR/self-peptide MHC interactions was later confirmed in studies with extensive MHC deficiencies in non-lymphopenic (lymphoreplete) mice. It was found that CD4 naive T cells did not proliferate in MHC class II deficient mice and that their life span was considerably shortened [96]. Similarly, a recent study using bone marrow chimeras demonstrated that the survival rate of CD8 naive T cells was greatly diminished in MHC class I deficient hosts under lymphoreplete conditions [97]. Despite the obvious need for TCR interactions in T cell longevity, the exact intracellular signals leading to survival are not fully elucidated.

Further support for the role of low affinity TCR signaling in naive T cell maintenance stems from studies performed in TCR transgenic mice that

demonstrated that recent thymic emigrants compete with resident naive T cells for survival signals. Naive T cells were shown to survive for long periods of time when transferred into athymic mice due to the presence of empty niches [98]. However; in normal euthymic mice, resident naive T cells were short lived with half of the population being replaced by recent thymic emigrants within four weeks [98]. In a steady state system, the addition of a new cell is counterbalanced by the deletion of another cell. Newly exported cells are therefore constantly competing for the same niche as resident naive T cells; however, the "age" of a cell does not determine its selection advantage. Studies have shown that competition is limited to cells with similar specificity (intraclonal competition) [99] but TCR promiscuity (when a TCR can engage diverse self-peptide MHC ligands) offers certain T cells a selective advantage by allowing them to compete for numerous MHC ligands (interclonal competition) [100]. How intraclonal competition regulates the size and diversity of the naive T cell pool was demonstrated in a recent study with transfer of TCR-transgenic CD4 T cells at different frequencies [101]. When adoptively transferred at low frequencies that resembled the physiological numbers of a specific clone, naive T cells had a considerably longer lifespan than when transferred at higher frequencies [101]. In this manner, competition of newly exported naive T cells is determined by the clonal size of the resident T cells, thereby ensuring the maintenance of a diverse TCR repertoire.

3.1.2. Role of IL-7 signaling

Local production of IL-7 in secondary lymphoid organs (such as lymph nodes) is crucial in providing homeostatic signals to naive and memory T cells [102, 103]. This essential role is clearly demonstrated in studies that block contact with IL-7, whether by injecting normal mice with IL-7 specific blocking monoclonal antibodies [103, 104] or by adoptive transfer of T cells into IL-7 deficient mice [105]. In addition, mice that overexpress IL-7 had increased number of circulating T cells, demonstrating that IL-7 plays a role in controlling the size of the T cell pool.

When IL-7 interacts with its receptor (described in section 1.4), the Janus kinase-signal transducer and activator of transcription (JAK-STAT) signaling pathway becomes activated (involving Jak1, Jak3, and Stat-5). Stat-5 is crucial in mature T cell survival by preventing the mitochondrial pathway of apoptosis, and complete deletion of the Stat-5a and Stat-5b locus in mice leads to severe peripheral T cell depletion [106]. The anti-apoptotic molecules Bcl-2 and Mcl-1 are key downstream targets of IL-7 signaling and they confer survival by blocking the Bcl-2-related pro-apoptotic factors Bim, Bid and Bad (reviewed in [44]). In IL-7Rα chain deficient mice, over-expression of Bcl-2 or knockout of the Bim gene led to a partial recovery of T cell pool in the periphery [51, 107]. The phosphoinositide 3-kinase (PI3K) signaling pathway is also triggered in response to IL-7 and is equally important in maintaining Bcl-2 levels (reviewed in [44]).

IL-7 signaling also results in the down-modulation of the IL-7Rα chain [108], a process believed to ensure optimal T cell numbers in the presence of a limiting source of IL-7 [109]. In fact, constitutive over-expression of transgenic CD127 led to the depletion of the T cell pool [108], highlighting the need for down-regulation of IL-7Rα for optimal IL-7 usage. The PI3k pathway is involved in this negative feedback loop by inactivating forkhead box O1 (foxO1) [110] which in turn induces down-regulation of the IL-7Rα chain [111]. Growth factor independent 1 (GFI-1) has also been reported to have a role in CD127 silencing [108].

3.1.3. Homing to peripheral T cell organs

Naive T cells need to constantly recirculate between the blood and secondary lymphoid tissues in order to access and interact with the limiting self-peptide:MHC and IL-7 molecules required for their survival. CD4 and CD8 naive T cells therefore depend on the expression of factors facilitating migration to the lymph nodes. The transcription factors KLF2 (Kruppel-like transcription factor 2) and FoxO1 are responsible for high expression of the lymph node homing molecules CD62L and CCR7 (ligand of CCL19), respectively [41, 111], which are found on naive T cells. Deficiency in either factor resulted in inefficient

trafficking of naive T cells and shortened lifespan of T cells in secondary lymphoid organs [41, 111]. Blocking CD62L or CCR7 yielded similar results [112]. A subset of fibroblastic reticular cells situated in the T cell zones of lymphoid organs secretes CCL19 in addition to IL-7 [112]. In this manner, CCR7-expressing naive T cells are attracted to the sites of IL-7 production. KLF2 is also essential for expression of sphingosine 1-phosphate receptor 1 ($S1P_1$), which is required for the migration of naive and central memory T cells from lymph nodes to the periphery [41].

3.2. Generation and homeostasis of memory T-cells

Protective immunity against infection relies on antigen-specific memory T cells that persist in peripheral tissues for many years following initial antigen encounter. The establishment of the memory T cell pool is dependent on the ability of the naive T cell pool to respond to multiple antigens. Several models have been proposed for memory T cell differentiation lineages including the progressive differentiation model, the signal strength model, and the asymmetrical division model which state that central memory T cells are generated directly from naive T cells (reviewed in [113]). Memory T cells are identified phenotypically in humans by the high expression of CD45RO and low expression of CD45RA [114]. They comprise a mixture of central memory T cells that are long-lived and home to the lymph nodes via their expression of CD62L and CCR7 and effector memory T cells that are short-lived and migrate to peripheral non-lymphoid tissues [113].

Distinct mechanisms govern the homeostasis of memory T cells. In contrast to naive T cells, cognate antigen [92] and self-pMHC ligands are not required for the long term survival of CD4 and CD8 memory T cells [115, 116]. Instead, survival signals are provided by cytokines: IL-15 and IL-7 are equally essential for the maintenance of CD8 memory T cells [117, 118] while IL-7 plays a predominant role in CD4 memory T cell survival with IL-15 acting as an accessory cytokine [119]. In contrast to naive T cells, memory T cells undergo substantial homeostatic proliferation in lymphoreplete hosts [120] that is antigen-independent

and is mediated solely by cytokine signaling [121]. IL-15 regulates the CD8 memory T cell pool by acting as a limiting factor for cell cycle entry [117] whereas both IL-7 and IL-15 are responsible for CD4 memory T cell homeostatic proliferation [119, 120]. Independent regulation of the different naive and memory T cell compartments permits newly exported naive T cells to seed into peripheral T cell pools without replacing antigen-experienced memory T cells. This, in concert with intraclonal competition (described in section 3.1.1), produces optimal diversity by ensuring that millions of different clones can compete for life-sustaining stimuli within their niche and co-exist in a limited physical space. The differences between naive and memory T cell homeostasis are highlighted in figure 2.

3.3. Lymphopenia: Equilibrium between output and expansion

When the immune system is faced with severe T cell loss such as in the case of chemotherapy, irradiation or certain viral infections such as HIV, reconstitution of the T cell pool occurs via thymic output and/or peripheral expansion.

3.3.1. Role of lymphopenia-induced proliferation (LIP)

Peripheral homeostatic expansion (antigen-independent stimulation) is able to partly restore the size of the T cell pool following adoptive transfer of naive T cells into lymphopenic hosts [122]. However, these dividing naive T cells gradually acquire the phenotype of memory T cells [122, 123]. In addition, restoration of T cell numbers observed shortly following T cell depletion is attributed to extensive expansion of residual memory T cells [124]. Therefore, despite the abundance of open space for naive T cells, peripheral expansion is only capable of regenerating the memory T cell pool. For that reason, the term lymphopenia-induced proliferation (LIP) is preferred to describe this process.

LIP of naive T cells requires both IL-7 [105] and self-peptide:MHC ligands [123], but the mechanisms in place during LIP differ from those occurring in homeostatic survival. The response of T cells to IL-7 and specific self-peptide:MHC ligands (survival versus proliferation) depends on the size of the T

cell pool. Under normal physiological conditions, these interactions elicit survival of resting naive T cells. However; when T cell counts are depleted, IL-7 consumption is consequently reduced. The result is increased availability of IL-7 and self-peptide:MHC ligands in secondary lymphoid organs. Under such altered conditions, increased signaling via the TCR and the IL-7 receptor promotes T cell expansion (illustrated in figure 2). The importance of TCR signaling strength in driving LIP was demonstrated in mouse models using TCR transgenic of different affinity for self-pMHC ligands. Upon adoptive transfer into lymphopenic mice, T cells with high-affinity TCRs had greater rates of LIP and reconstituted the T cell pool faster than low-affinity T cells [125, 126]. In addition, certain negative regulators of TCR signaling such as LAG-3, BTLA-4, and SIT influence the rate of LIP. It has been shown that T cells with low affinity TCRs were better able to undergo LIP in the absence of these molecules [127-129]. Additional studies have further determined that costimulatory molecules such as CD28 and CD40 are not involved in homeostatic responses to self-peptide:MHC ligands (whether survival or LIP), even though they are crucial for responses to foreign antigens [130].

IL-7 is a major player in LIP; excessive amounts of IL-7 drive the proliferation of naive and memory T cells [120]. The proliferative impact of increased availability of IL-7 in lymphopenic hosts can be extrapolated from IL-7 dose response studies which clearly discriminate between low doses of IL-7 (<1 ng/ml) that sustain only survival and high doses of IL-7 (>1 ng/ml) that promote both survival and cell cycling [131]. Even in lymphoreplete hosts, supranormal levels of IL-7 gave rise to extensive T cell proliferation resembling LIP [132]. IL-7-induced proliferation appears to be a consequence of activation of the PI3K pathway [133], which leads to degradation of the cyclin-dependent kinase inhibitor $p27^{kip1}$ [134], thus allowing progression to the S phase of the cell cycle [135].

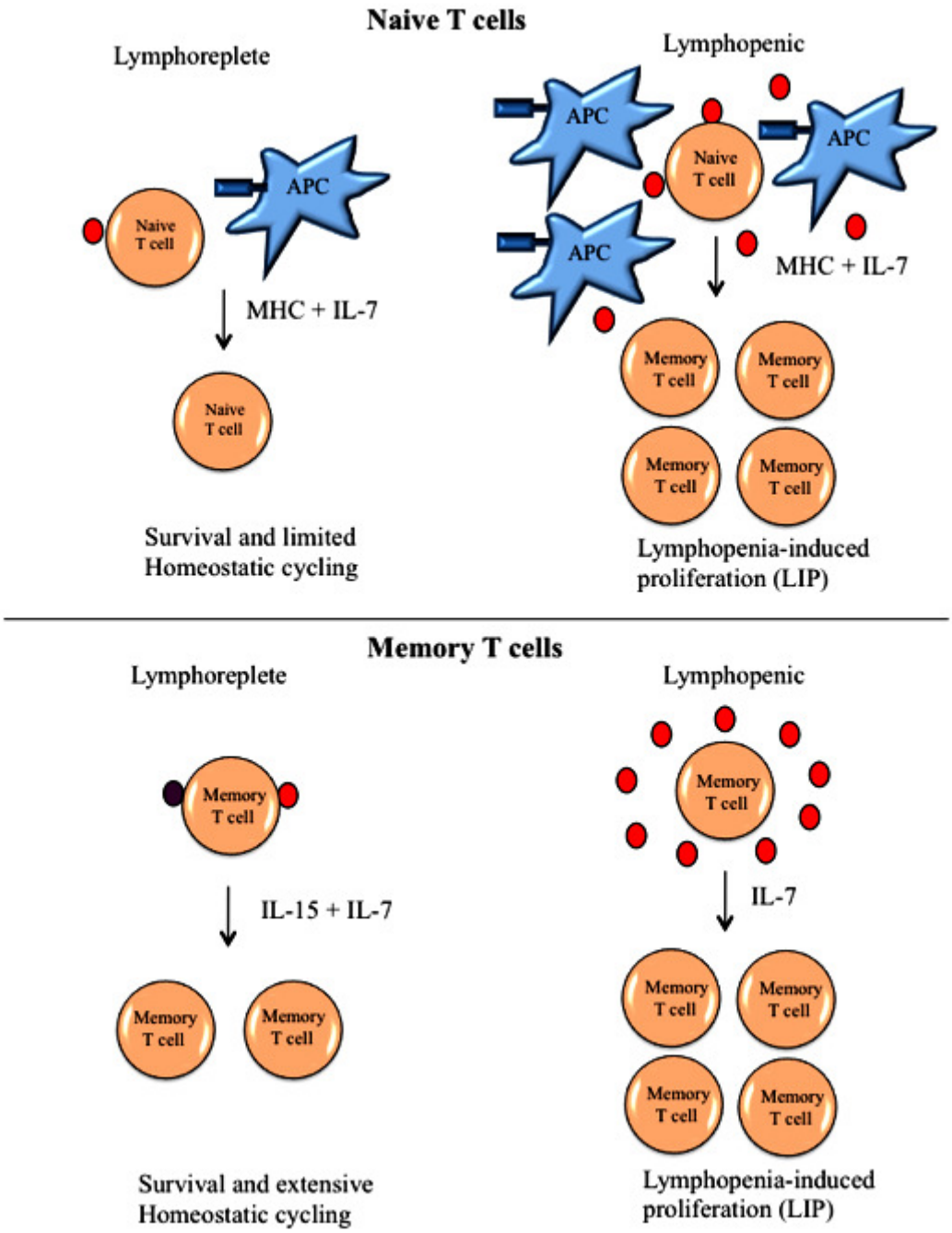

Figure 2: Mechanisms involved in homeostasis of naive and memory T cells in lymphoreplete and lymphopenic environments.
In T cell-sufficient environments, the survival and maintenance of naive T cells depends on both low affinity TCR/self-peptide:MHC ligand interactions and the IL-7 cytokine. Maintenance and homeostatic cycling of memory T cells is not dependent on self-pMHC ligands but on cytokines, mainly IL-15 and IL-7. In a lymphopenic setting, naive T cells undergo extensive proliferation as a result of the increased availability of self-pMHC and IL-7 molecules. This is accompanied with a switch from the naive to the memory phenotype. However, peripheral expansion of memory T cells is mediated solely by IL-7 (original figure).

3.3.2. Role of thymic output

The role of peripheral homeostatic proliferation in the regulation of the size of the naive T cell pool is appreciated in thymectomized mice in which a small portion of naive T cells divide while retaining their naive phenotype [80] and in neonates in which a considerable void needs to be filled by the thymus [123, 136]. However, when faced with the task of T cell reconstitution, LIP is unable to replenish the naive T cell pool since proliferation is linked with an irreversible switch to the memory phenotype and restrained TCR diversity [122]. In fact, efficient generation of naive T cells is accomplished when lymphopenic hosts have an intact thymus [124] or following injection of peripheral T cells together with bone marrow (BM) cells into irradiated hosts [137]. In these irradiated hosts, memory T cells were the first to emerge and were reconstituted by LIP. Thymic export of T cells originating from BM donor cells was initiated one month after grafting and generated the naive T cell pool [137]. This highlights the importance of the thymus in naive T cell reconstitution. Of note, the size of the T cell pool doubled to accommodate exported RTEs. This is comparable to the increase in T cell numbers described following engraftment of thymic lobes [138], and confirms the competence of the thymus in maintaining both TCR repertoire diversity and T cell numbers in mouse models. Similarly, a positive association was found in human studies between thymic function and naive T cell regeneration following hematopoietic stem cell transplantation (HSCT) in both paediatric and adult patients [139, 140]. T cell reconstitution following severe lymphopenia induced by intensive chemotherapy for the treatment of cancer seemed to be dependent on age; T cell reconstitution was faster in patients under 15 years of age (more likely to have a better thymic function) than in patients above 18 years old [141]. However, it remains unclear whether the thymus is capable of responding to lymphopenia by enhancing T cell production. In mice, production of T cells was not increased following mild or severe T cell depletion [142]. Nonetheless, it can be concluded from all these studies that continuous output of naive T cells by the thymus influences the composition of the T cell repertoire, a phenomena not exerted by LIP. In addition, murine RTEs are

efficient at replacing pre-existing naive T cells [122], perhaps because they are exempt from competition for three weeks following their release into the periphery [138]. This indicates that RTEs have a survival advantage over older and less diverse resident naive T cells and suggests that clinical diseases that impact thymic function such as HIV infection would significantly alter the composition of the TCR repertoire of the peripheral T cell pool.

4. HIV Infection

Human immunodeficiency virus (HIV) is a lentivirus, part of the retrovirus family, that if left untreated eventually causes acquired immunodeficiency syndrome (AIDS). HIV is composed of two copies of positive single-stranded RNA that encodes for nine genes: *gag*, *pol*, *env*, *tat*, *rev*, *nef*, *vif*, *vpr*, and *vpu*. A hallmark of HIV infection is the progressive loss and dysfunction of CD4 T lymphocytes in the periphery and mucosal tissues. HIV leads to the specific infection of CD4 helper T cells and although HIV-mediated cell lysis contributes to the observed loss of CD4 T cells, it was shown that the frequency of productively infected cells is very low compared to the massive CD4 T cell death occurring within secondary lymphoid tissues [143], suggesting indirect mechanisms of cell killing. These include abortive HIV infection [143, 144], activation-induced death of uninfected cells and destruction of infected cells by CD8 cytotoxic T cells [1].

4.1. Clinical course of HIV Infection

Acute HIV infection can be divided into different clinical phases based on the variations in HIV viral load. Most of our knowledge on early pathogenesis of mucosal transmission stems from non human primate (NHP) models of HIV infection. Following sexual exposure and viral transmission of simian immunodeficiency virus (SIV), it was shown that it takes around 10 days until viral RNA is detected in the plasma. This period is known as the eclipse phase and is characterized by local infection of mucosal CD4 T cells [145]. At the end of the eclipse phase, the virus spreads into the draining lymph nodes in which

activated $CD4^+$ target cells are further infected. At this point, there is systemic dissemination of the virus that reaches other lymphoid tissues such as the gut-associated lymphoid tissue (GALT) and rapid replication due to the large availability of target cells (namely $CCR5^+$ effector memory T cells), resulting in an exponential increase of viremia [146]. The peak in plasma viremia, usually reaching more than a million RNA copies/ml, occurs 3-4 weeks following virus entry [146]. During this period of high viral replication, HIV-infected individuals may develop non-specific flu-like symptoms such as fever, malaise, lymphadenopathy, pharyngitis, headache, myalgia, night sweats, nausea or vomiting. This period also coincides with significant decreases in circulating CD4 T cells. It was initially suggested that redistribution of CD4 T cells out of the circulation and into the sites of inflammation accounted for CD4 depletion in the periphery [147], and that the extent of this depletion might be overestimated when analyzing the blood compartment in acute infection. However, there is considerable recent evidence that demonstrates that CD4 T cell depletion also occurs within secondary lymphoid tissues during acute HIV [148] and SIV infection [149]. In the GALT, approximately 60% of CD4 T cells can be depleted within the first three weeks of SIV infection by both viral lysis of infected cells and apoptosis of uninfected activated CD4 T cells [149]. Following the peak in viremia, plasma RNA levels slowly decrease to reach a plateau, known as the viral 'set point' [150]. This partial viral control is linked with HIV-specific CD8 T cell responses which peak shortly prior to the decline in viremia. Although it is possible that the drop in viral load is a result of other factors such as depletion of CD4 T cell targets, the presence of CD8 specific T cell responses during acute infection is also important in maintaining viral load at stable levels [151]. In fact, it was shown that individuals that were able to mount immunodominant CD8 T cell responses usually have a lower viral set point than those who do not [152]. Within the same time frame, antibodies against HIV are produced and their detection in the plasma by ELISA is one of the tools used in the diagnosis of HIV infection. However, these antibodies are non-neutralizing and do not contribute to viral load control [153]. Establishment of the viral set point is associated with

increases in circulating CD4 T cells to near normal levels. However, this CD4 T cell rebound does not occur in the GALT [148].

Chronic HIV infection (also called the clinical latency phase), if left untreated, lasts on average 10 years and begins when viral load set point is achieved and CD4 T cells counts are stabilized. Throughout this phase, CD4 T cells are gradually depleted from the circulation [146]. When CD4 T cell counts fall below 200 cells/µl, the immune system is rendered unable to cope with opportunistic infections and tumors, marking the onset of AIDS. The rate of this depletion varies from one individual to another, for reasons that remain to be fully elucidated [154]. The loss of CD4 T cell help is thought to contribute to the inability of CD8 T cells to mount effective responses and control viremia during chronic infection [155, 156]. In addition to quantitative loss of CD4 T cells, the TCR repertoire becomes constrained concomitant with the shift in the proportions of resting naive cells towards increased activated memory and effector cells [157], thereby further compromising one's immune system.

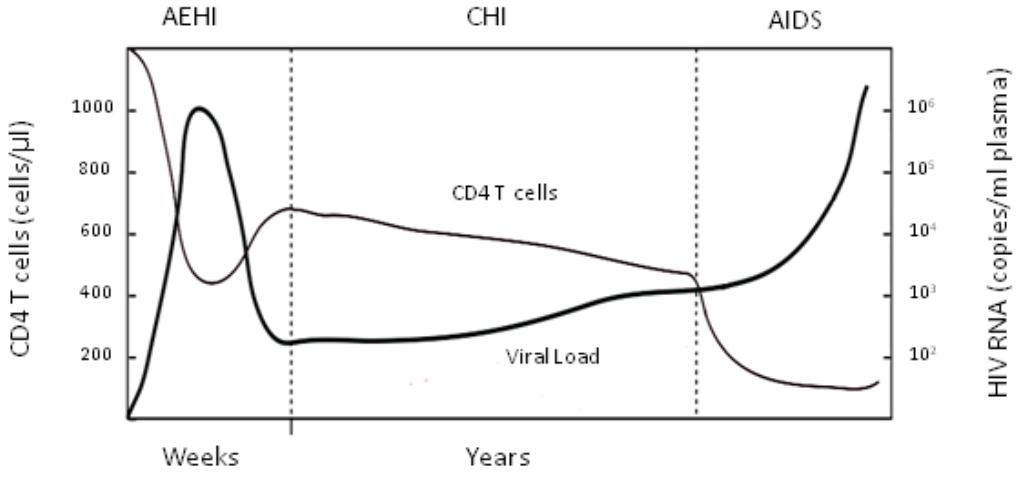

Figure 3: Clinical course of HIV infection.

CD4 T cell numbers and HIV viral load during acute/early HIV infection (AEHI), chronic HIV infection (CHI), and progression to AIDS (original figure).

4.2. Impact of HIV infection on the thymus

A number of studies have clearly shown that not only is HIV capable of entering the thymus, but it also leads to profound morphological changes within the thymus, including but not limited to involution, degeneration of the thymic epithelium and depletion of thymocytes in humans [158-160] and thy/Liv SCID-hu mice [161]. Studies utilizing TREC assays have shown reduced thymic output during HIV infection [6, 74, 162, 163], demonstrating a role for HIV in impaired thymopoiesis. Thymocyte depletion, and hence thymic output, may be mediated by many mechanisms. Over 90% of thymocytes express the HIV receptor CD4 while approximately 50% of thymocytes express the HIV co-receptor CXCR4 making them susceptible to infection and direct killing [4]. In fact, HIV has been visualized within thymocytes using immunohistochemistry [3] and was shown capable of infecting various thymocyte populations *in vitro* [164, 165]. Perturbations in cytokine production (such as IL-2, IL-6 and IFN-γ) within the HIV-infected thymus have been reported in Thy/Liv SCID-hu mouse studies [166]. This could affect development and proliferation of immature thymocytes, as suggested by our previous findings of a low sj/β TREC ratio in a subset of individuals during both acute and chronic HIV infection [6]. In addition to altering thymocyte survival and/or proliferation, HIV infection can result in lower output of new T cells into the periphery by altering export of mature thymocytes. It was recently shown that mature SP thymocytes in the human HIV-infected thymus are activated and express high levels of the activation marker CD69 [167]. As CD69 needs to be down-regulated in order to allow mature SP thymocytes to up-regulate $S1P_1$, a receptor involved in thymocyte egress, activation of thymocytes during HIV infection could further diminish thymic output [168]. All together, these findings demonstrate the susceptibility of the thymus to HIV infection and reinforce the notion that thymic function is altered during HIV infection.

4.3. Highly Active Anti-Retroviral Therapy

Highly Active Anti-Retroviral Therapy (HAART) is a combination therapy that integrates two reverse transcriptase inhibitors along with one or more protease inhibitors and/or integrase inhibitors and leads to efficient suppression of viral replication and augmentation of CD4 T cell numbers in the majority of cases. Following onset of HAART, the plasma viral load undergoes two exponential phases of decay [169]. The initial decline is rapid and results from the loss of productively infected cells which consists mostly of activated CD4 T cells. This is followed by a slower decline which most likely represents the removal of infected macrophages and dendritic cells, which are more resistant to virus-induced cytopathic effects than CD4 T cells. In most individuals treated with HAART, viremia is reduced below 25 copies of viral RNA per ml of plasma (the detection limit of sensitive assays) by week 20 and remains stable except for the occasional transient increases in viral load called viral 'blips' [169], which may be a consequence of activation of latently infected CD4 T cells.

Upon initiation of HAART, CD4 T cell recovery has also been reported to occur in a biphasic fashion. During the first few weeks, a rapid increase in peripheral CD4 T cells was observed which consisted mostly of T cells bearing the memory phenotype [170]. This is believed to be due to redistribution of memory CD4 T cells that were trapped within lymphoid tissues during viral replication [171]. During the next 12 months, CD4 T cell reconstitution proceeded at a slow pace and steady increases of naive CD4 T cells were detected during this second phase [170]. In subjects that responded to HAART treatment, the majority of CD4 T cell recovery occurred during the first year of treatment at an average of 100–200 cells/µl with subsequent increases of around 50 cells/µl per year [172]. An association between younger age and higher CD4 T cell recovery following HAART has been reported by various groups [173], strongly suggesting a role for the thymus in the magnitude of CD4 T cell reconstitution. In support of this, it was shown that CD4 and CD8 naive T cells can be also significantly increased during the first phase of reconstitution in subjects that showed greater thymic size,

as measured by CT scan, following HAART [174]. Individuals with less thymic tissues showed a rise in naive T cells only during the second phase (after four weeks) of HAART [174]. In addition, we have previously shown that intrathymic proliferation is enhanced shortly following HAART in a subgroup of HIV-infected individuals [6]. However, the direct impact of impaired thymopoeisis on peripheral homeostasis is not fully clear due to the lack of tools that permit direct quantification and biological characterization of RTEs.

CHAPTER 2.

Survival of recent thymic emigrants is essential for central memory and total CD4 maintenance in untreated HIV infection

Joumana Zeidan (1,2), Bader Yassine-Diab (2), Yu Shi (2), Yoav Peretz (2), Mohamed-Rachid Boulassel (3), Marie-Lise Dion (2), Rebeka Bordi (2), Lionel Filion (4), Remi Cheynier (5), Jean-Pierre Routy (3),Elias K. Haddad (2,7) and Rafick-Pierre Sekaly (1,2,6,7)*.

1) *Dept. of Microbiology and Immunology, McGill University, Montreal, Quebec, Canada* 2)*, Laboratoire d'Immunologie, CHUM Research Center, Montreal, Quebec, Canada,* 3) *Montreal Chest Institute, MUHC, Montreal, Quebec, Canada, 4) Dept. of Biochemistry Microbiology and Immunology, University of Ottawa, Ottawa, Ontario, Canada,* 5) *Unite des Virus Lents, Institut Pasteur, Paris, France,* 6) *Dept. Microbiologie et Immunologie, Université de Montreal, Montreal, Quebec, Canada, 7) Vaccine and Gene Therapy Institute of Florida Corp, Florida, USA.*

*****Corresponding author:
Dr. Rafick-Pierre Sekaly
Vaccine & Gene Therapy Institute Florida
11350 SW Village Pkwy, 3rd Floor
Port St. Lucie, FL 34987
Telephone Number: 772-345-4785
Fax Number: 772-345-3675
Email: sekaly@vgti-fl.org

Abstract

A hallmark of HIV infection is the progressive depletion of naive and central memory T cells (T_{CM}). The aim of this study was to investigate the depletion of recent thymic emigrants (RTE) in acute/early (AEHI) and chronic HIV infection (CHI) at the single cell level and to define if defects in thymic output specifically impacted the T_{CM} subset. Our data shows that while all untreated subjects displayed lower RTE levels as compared to uninfected controls in AEHI, a subgroup of infected subjects had increased RTEs during CHI to levels similar to what observed in healthy controls. Of note, these subjects showed higher T_{CM} and total CD4 T cell counts 60 weeks post-infection and were defined as slow progressors (SP). Low levels of RTEs at set point were strongly correlated with heightened levels of cell cycle entry and immune activation (as measured by Ki67 and PD-1) within the RTE subset as well as higher IL-7 plasma levels during AEHI. Proliferation of RTEs during AEHI positively correlated with T_{CM} numbers, demonstrating the importance of RTEs in replenishing the T_{CM} pool and stabilizing CD4 T cell numbers. In contrast to AEHI, persistent high levels of Ki67 in RTEs during CHI were associated with decreased T_{CM} and total CD4 numbers. RTEs from SP showed higher Bcl-2 frequencies when compared to progressor (P) subjects; conversely frequencies of $Ki67^+$ cells within RTEs were inversely correlated with frequencies of $Bcl\text{-}2^+$ cells during CHI, suggesting increased susceptibility to apoptosis within RTEs from subjects with chronic immune activation. All together, our data demonstrates that hyperimmune activation is a mechanism that leads to RTE depletion during untreated HIV infection and highlights the importance of RTE survival in the maintenance of the T_{CM} and total CD4 T cell pools during HIV infection.

Introduction

Human immunodeficiency virus type 1 (HIV-1) infection is marked by the progressive loss of CD4 T cells, ultimately leading to immunodeficiency and death. The pathogenesis of T cell depletion in HIV infection is caused by a combination of different mechanisms including increased T cell death, enhanced T cell immune activation and subsequent "dysfunction" (1). This leads to an imbalance in the distribution of several T cell subsets in the circulation as well as in peripheral tissues, a prominent feature of HIV pathogenesis (2). Acute infection is marked by massive depletion of $CCR5^+$ effector memory T cells (T_{EM}) from extra-lymphoid tissues, especially in the gut (3-5). On the other hand, naive and central memory (T_{CM}) CD4 T cells are both progressively depleted throughout infection (6-8), and the rate of CD4 naive T cell depletion has been correlated with disease progression (9). While acute T_{EM} depletion is a common feature to both pathogenic (in rhesus macaques (RM)) and non pathogenic (in sooty mangabeys (SM)) SIV infection, T_{CM} are maintained in the blood and lymph nodes of SM. Preservation of the CD4 T_{CM} cell compartment and of its ability to generate polyfunctional T_{EM} T cells is a key feature of slow disease progression as it was associated with the maintenance of a diminished, but stable, T_{EM} compartment (8-10).

Since the thymus is the source of *de novo* T cell production, examining thymic function during HIV infection is crucial to the understanding of naive T cell dynamics and the impact of their loss on disease progression. Several approaches have been used to measure thymic function in HIV infection including T cell receptor excision circles (TRECs) (11). Their use has demonstrated that HIV results in decreased thymic output (11) as well as intrathymic proliferation (12). Increased T cell turnover is a hallmark of HIV infection (13) and therefore, fluctuations in TREC content not only reflect changes in thymic function but also in peripheral proliferation as TRECs get diluted with each cell division (14).

To assess the impact of peripheral events on the dynamics of recent thymic emigrants (RTEs), flow cytometry was used as it provides us with a quantitative

tool to analyze newly exported T cells and to discriminate them from non-RTE naive T cells. CD31 (or PECAM-1), an adhesion molecule that is part of the Ig superfamily (15), allows us to make that distinction: CD4 naive T cells with high levels of CD31 are more closely associated with thymic output as well age-related thymic involution (unpublished data). We have previously determined that $CD31^{hi}$ naive T cells have the closest developmental proximity to mature thymocytes as they have only a two-fold TREC dilution when compared to exiting single positive thymocytes (unpublished data).

We have previously shown that during primary HIV infection, intra-thymic proliferation and hence thymic output were severely impaired when compared to age-matched controls (12). In the present study, although it is highly probable that defective thymic function plays a role in the observed low RTE values, we focused our aims on evaluating peripheral events that lead to RTE depletion.

Results

Recent thymic emigrants, as defined by CD31hi, are decreased following HIV infection in a subset of individuals.

In this study, we defined CD4 Recent Thymic Emigrants (RTEs) as naive CD4 T cells ($CD45RA^+CCR7^+CD27^+$) expressing high levels of the marker CD31 (the 10% brightest cells by MFI). Using this cut off, we demonstrated that $CD31^{hi}$ naive T cells have a similar sjTREC content to that of single positive thymocytes (only a 2-fold reduction) and encompass in average 12-fold more sjTRECs than $CD31^-$ naive T cells (unpublished data). The gating strategy is illustrated in Figure 1*A*.

Eight HIV-infected individuals recruited at the earliest stage of the disease (mean of 70 days, range 32-140) and whose age ranged from 22 to 35 were studied longitudinally for approximately one year following infection (mean of 415 days, range 202-532). These subjects were subgrouped based on the rate of decline of CD4 T cells during the first year of infection: four out of eight subjects had maintained or increased CD4 T cell numbers, while the remaining four subjects had a negative delta (Δ) CD4 T cell numbers. These two groups were subsequently labeled as slow progressors (SP) and progressors (P); respectively. (Table S1). The RTE frequencies within the CD4 naive T cell population were analyzed in these subjects at various intervals throughout the infection and compared to values in age-matched uninfected controls (N = 6). The $CD31^{hi}$ gate within CD4 naive T cells was set by analyzing CD31 expression within controls at the same time as HIV-infected individuals. Our data shows that mean $CD31^{hi}$ frequencies within CD4 naive T cells were significantly lower in SP and P subjects compared to healthy controls during acute/early HIV infection (AEHI, 10 weeks post-infection) (13.8% ± 0.8 versus 22.9% ± 5.7, $P = .01$; and 4.5% ± 3.4 vs. 22.9% ± 5.7. $P = .01$; respectively); however, only P subjects had significantly lower RTE frequencies compared to healthy controls during chronic HIV infection (CHI, 60 weeks post-infection) (5.3% ± 5.6 vs. 22.9% ± 5.7, $P = .01$) (Figure 1*B*).

In addition, SP showed significantly higher RTE (22.8 vs. 4.1 cells/µl, $P = .01$) as well as higher T_{CM} absolute numbers (136.3 vs. 69.6 cells/µl, $P = .03$) than P subjects during CHI (Figure 1*C*). No differences in the absolute numbers were observed for the other naive T cells, T_{EM} or T_{TM} between these two groups (data not shown). All together, these results show that recent thymic emigrants are rapidly reduced following HIV infection but that normal levels are attained in some subjects during CHI which correlated with slower disease progression, as measured by the rate of CD4 loss.

Baseline RTE frequencies correlate with RTE, T_{CM} and total CD4 counts 1 year post-infection

Longitudinal analysis of all infected subjects (N = 8) revealed that higher frequencies of $CD31^{hi}$ within naive T cells measured during CHI correlated with higher levels detected in AEHI (r = 0.885, N = 9, $P = .002$) (Figure 2*A*), indicating that the magnitude of RTE depletion in acute infection clearly discriminates between SP and P subjects. Accordingly, we observed that higher baseline RTE frequencies were associated with higher absolute numbers of RTEs in CHI (r = 0.83, N = 8, $P = .002$) (Figure 2*B*). To investigate the impact of the RTE subset on disease progression, we sought to determine if baseline RTE frequencies could predict the magnitude of T_{CM} and total CD4 T cell loss later in infection. The frequencies of all three naive subsets ($CD31^{hi}$, $CD31^{low}$ and $CD31^{-}$) at onset of infection were obtained and compared to T_{CM} and CD4 T cell counts measured during CHI (Figure 2*C*). Interestingly, $CD31^{hi}$ (RTE) was the only CD4 naive T cell subset that showed a positive correlation between its initial frequencies and T_{CM} (r = 0.92, N = 8, $P = .002$) as well as CD4 T cell counts (r = 0.796, N = 8, $P = .009$) one year following infection. These results indicate that severe loss of the RTE niche early in infection, but not that of the other naive subsets eventually leads to the accelerated depletion of T_{CM} and total CD4 T cells. These findings suggest that RTE frequencies at the onset of infection could predict disease progression during the chronic phase of infection.

RTEs are the only naive subset that up-regulate PD-1 and Ki67 levels in HIV-infected individuals.

Hyperimmune activation constitutes a major mechanism for the depletion of many T cell subsets during HIV infection (1). To determine whether hyperimmune activation occurs within the RTE subset and contributes to the loss of RTEs and depletion of CD4 T cells, we examined T cell activation and proliferation, as monitored by the activation marker PD-1 and the cell cycle marker Ki67, in the different CD4 naive ($CD31^{hi}$, $CD31^{low}$, and $CD31^{-}$) and memory T cell subsets in untreated SP and P subjects during both AEHI and CHI in comparison to healthy controls (N = 6). Out of the four SP subjects in the study, three had low or undetectable levels of HIV RNA (<500 copies/ml) during CHI while 1 of them had high levels similar to those observed in P subjects (Table S1). This subject was therefore removed from further analysis in order to achieve two distinct and homogenous groups. Our results demonstrate that the frequencies of $Ki67^{+}$ cells within RTEs were 10-fold higher than those observed within other naive subsets in uninfected individuals (mean 1.2% ± 0.9 vs. 0.15% ± 0.13, Student's *t* test *P* = .01 compared to $CD31^{low}$ and vs. 0.1% ± 0.07, *P* = .008 compared to $CD31^{-}$). Of note, the frequencies of $Ki67^{+}$ cells within RTEs in healthy controls, and not that of other naive T cells, were significantly higher than frequencies of $Ki67^{+}$ cells within T_{CM} (2.5-fold higher) and similar to frequencies of $Ki67^{+}$ cells within T_{EM} T cells (mean 1.2% ± 0.9 vs. 0.46% ± 0.22, *P* = .03 and vs. 1.36% ± 1.13, *P* = .84; respectively). These results clearly demonstrate that the proliferation of naive T cells is mostly confined to the RTE subset (Figure 3*A*). During AEHI, Ki67 frequencies within RTEs were significantly increased when compared to those observed in healthy controls (2.5-fold higher, *P* = .04) and remained higher than frequencies of $Ki67^{+}$ cells in other naive T cell subsets (2.7% ± 2.5 vs. 0.36% ± 0.2, *P* = .01 compared to $CD31^{low}$ and vs. 0.87% ± 0.47, *P* = .03 compared to $CD31^{-}$) (Figure 3*A*). Similar differences were also noted during CHI (2.6% ± 2.4 vs. 0.3% ± 0.3, *P* = .03 compared to $CD31^{low}$ and vs. 0.71% ± 0.44, *P* = .05 compared to $CD31^{-}$) (Figure 3*A*). Previous studies have already established peripheral proliferation of memory T cells is increased during HIV infection [16],

and we show here that increased proliferation of naive T cells also occurs during HIV infection but is specifically restricted to the RTE subset.

Longitudinal analysis of Ki67 frequencies within RTEs showed that the frequencies of $Ki67^+$ cells in P subjects peaked early in infection (mean 96 days, range 45-154) and remained high later in infection when compared to the frequencies observed in healthy controls (Figure S1, examples P1-3). On the other hand, SP individuals had low frequencies of $Ki67^+$ cells within RTEs throughout the studied period of infection (Figure S1, example SP1-2).

Similarly to Ki67, PD-1 frequencies increased in the majority of subsets following HIV infection (Figure 4*A*); up-regulation of PD-1 was restricted to the RTE population when compared to other naive T cells (7% ± 4.2 vs. 1.3% ± 0.7, N = 6, $P = .05$ compared to $CD31^{low}$ and vs. 2% ± 1.5, $P = .05$ compared to $CD31^-$) and frequencies within RTEs were similar to those observed for T_{CM} (7% ± 4.2 vs. 6.3% ± 2.6) (Figure 4*A*). As expected (17), T_{EM} and T_{TM} expressed significantly higher frequencies of $PD\text{-}1^+$ cells than did RTE (6% ± 4.2 vs. 19.1% ± 7.7, $P = .001$ and vs. 18.6% ± 5.6, $P < .001$; respectively) (Figure 4*A*). Similar to what we reported for Ki67, frequencies of $PD\text{-}1^+$ cells within RTEs from P subjects were higher than those observed in healthy controls (6-fold higher in AEHI, $P < .001$ and 3.5-fold higher in CHI, $P = .008$) while RTEs from SP subjects showed low frequencies of $PD\text{-}1^+$ cells that overlapped with those observed in healthy controls (mean of 2.5% versus 1.9%, $P = .22$).

We then proceeded to identify the factors driving RTE proliferation. A positive correlation was shown between the frequencies of $Ki67^+$ cells within RTEs and HIV RNA levels during AEHI as well as CHI ($r = 0.89$, N = 7, $P = .006$ and $r = 0.93$, N = 7, $P = .001$; respectively) (Figure 3*B*) suggesting that HIV antigens could trigger RTEs to differentiate into the memory T cell pool. In addition, we also detected a positive correlation between the frequencies of $Ki67^+$ cells within RTEs and levels of IL-7 during both AEHI and CHI ($r = 0.72$, N = 7, $P = .04$ and $r = 0.67$, N = 7, $P = .05$; respectively) (Figure 3*B*); indicating that IL-7 could be responsible for the increased cell cycle entry [18-19]. This is in agreement with a

previous study demonstrating the capability of naive $CD4^+$ $CD31^+$ T cells to proliferate in response to IL-7 triggering (20). In general, the correlations between cell cycle entry and viral load or levels of IL-7 were predominantly observed in the RTE subset (Tables I and II), suggesting that other factors could be responsible for the proliferation of CD4 memory subsets such as IL-2 or IL-15.

Our data show a significant positive association between viral load and the frequencies of PD-1^+ cells within RTEs in AEHI (r = 0.91, N = 7, *P* = .006) and CHI (r = 0.92, N = 7, *P* = .006) (Figure 4*B*). A positive correlation was noted between IL-7 plasma levels and the frequencies of PD-1^+ cells within RTEs in AEHI but not CHI (r = 0.71, N = 7, *P* = .03) (Figure 4*B*). IL-7 has previously been shown to induce PD-1 expression on T cells *in vitro* (21). This up-regulation did not hinder responses to successive IL-7 stimulation, but altered TCR triggered-activation and proliferation (21). The absence of a correlation between levels of IL-7 and PD-1 up-regulation in RTEs during CHI might be due to unresponsiveness to IL-7.

Activation levels in RTEs and plasma IL-7 concentrations early in infection correlate with RTE depletion during chronic infection.

Having established that hyperimmune activation (as defined by PD-1 and Ki67) within RTEs from P subjects was significantly higher than that observed in RTEs from SP subjects, we next sought to determine if frequencies of Ki67 and PD-1 early in infection could predict the magnitude of RTE and CD4 T cell depletion. Our results (Figure 5*A*) showed an inverse correlation between the frequencies of $Ki67^+$ as well as PD-1^+ cells within RTEs during AEHI and RTE numbers one year post-infection (r = -0.8, N = 7, *P* = .02 and r = -0.73, N = 6, *P* = .05; respectively). Furthermore, higher levels of Ki67 and PD-1 within RTEs during AEHI translated into a greater rate of CD4 T cell depletion within the studied time frame, as measured by the Δ CD4 at the one year time frame (r = -0.84, N = 7, *P* = .01 and r = -0.8, N = 6, *P* = .03; respectively) (Figure 5*A*). Of note, the levels of

Ki67 and PD-1 in other naive or memory CD4 subsets during PHI did not correlate with CD4 T cell depletion (r = -0.03, *P* = .47 and r = 0.005 *P* = .49 for $CD31^{low}$, r = 0.14, *P* = .39 and r = -0.55 *P* = .12 for $CD31^{-}$, r = 0.03, *P* = .47 and r = -0.26 *P* = .3 for T_{CM}, r = 0.44, *P* = .19 and r = -0.32 *P* = .26 for T_{EM} and r = -0.45, *P* = .19 and r = -0.32 *P* = .26 for T_{TM}) (data not shown).

In addition, since frequencies of $Ki67^{+}$ and $PD\text{-}1^{+}$ cells in RTEs during AEHI were correlated with levels of IL-7 and HIV RNA (Figures 3*B* and 4*B*), we investigated the possibility that levels of IL-7 in AEHI could predict the counts of RTE and total CD4 T cells later in infection. An inverse correlation was observed between levels of IL-7 measured during AEHI and RTE numbers (r = -0.67, N = 7, *P* = .05) as well as the magnitude of CD4 T cell loss (r = -0.71, N = 7, *P* = .03) during CHI (Figure 5*B*). All together, these results demonstrate that hyperimmune activation within RTEs as well as levels of IL-7 observed during AEHI are associated with lower RTE counts during CHI and faster disease progression, as measured by the magnitude of CD4 T cell loss.

Frequencies of $Ki67^{+}$ cells within RTEs during AEHI are associated with loss of phenotype and recruitment into the central memory T cell pool.

Since frequencies of $Ki67^{+}$ cells within RTEs correlated with plasma IL-7 concentrations during AEHI, we questioned whether increased cell cycle entry during acute infection was a compensatory mechanism to increase total T cell numbers (including RTEs) in the periphery (20). We observed a negative correlation between the frequencies of $Ki67^{+}$ in RTEs and RTE cell counts during AEHI (r = -0.65, N = 7, *P* = .05) (Figure 6*A*). These results suggest that increased RTE cell cycle entry is a response to low RTE numbers and/or increased RTE loss due to increased susceptibility to apoptosis. The latter hypothesis is further supported by the finding that RTE counts were not normalized following the peak of Ki67 expression (data not shown). Interestingly, the frequencies of $Ki67^{+}$ cells in RTEs during AEHI were found to positively correlate with T_{CM} T cell counts (r

= 0.64, N = 7, *P* = .05) (Figure 6*A*) and not with absolute numbers of the other memory subsets (T_{EM} or T_{TM}); these results clearly suggest that proliferating RTEs were recruited into the T_{CM} compartment. T_{CM} cell counts in AEHI also positively correlated with the change in CD4 counts observed following the peak of Ki67 frequencies in RTEs (r = 0.96, N = 7, *P* < .001, data not shown), suggesting that the partial increase in CD4 T cell counts during AEHI could be due to accumulation of T_{CM} T cells.

None of the other naive T cell subsets showed a positive correlation between Ki67 frequencies within their subset and T_{CM} T cell counts in AEHI (data not shown), illustrating a unique role for proliferating RTEs in the initial task of replenishing the central memory T cell pool. This finding is not surprising since we previously observed that the frequencies of $Ki67^+$ cells correlated strongly with viral load during AEHI (Figure 3*B*). All together, our data show that the early decrease of RTEs in AEHI could most likely be attributed to T cell differentiation and loss of the $CD31^{hi}$ phenotype.

Frequencies of Ki67$^+$ cells within RTEs during CHI are associated with low RTE, T_{CM} and total CD4 T cell counts.

We next proceeded to investigate the impact of loss of RTE during CHI. Confirming our findings in AEHI, we observed a negative correlation between the frequencies of $Ki67^+$ cells within RTEs and RTE T cell counts during CHI (r = -0.8, N = 7, *P* = .02) (Figure 6*B*). However, this was now accompanied by a negative correlation between the frequencies of $Ki67^+$ cells within RTEs and T_{CM} as well as total CD4 T cell counts (r = -0.76, N = 7, *P* = .02 and r = -0.79, N = 7, *P* = .02; respectively) (Figure 6*B*), suggesting that cell cycle entry leads to the depletion of RTEs and consequently, over time, T_{CM} and total CD4 T cells instead of their increase (Figure 2*C*). These findings further confirm that preservation of the RTE pool is required for the maintenance of T_{CM} and total CD4 T cell counts.

Even though frequencies of $Ki67^+$ cells in RTEs showed a significant positive correlation with viral load and levels of IL-7 during the chronic phase of HIV infection (Figure 3*B*), our data show that presence of high levels of antigen (viral load) as well as homeostatic proliferation of RTEs are incapable of increasing RTE or T_{CM} numbers, and therefore lead to total CD4 T cell depletion. In fact, during CHI depletion of total numbers of circulating RTEs is associated with depletion of the T_{CM} T cell pool ($r = -0.85$, $N = 7$, $P = .01$) (Figure 3*B*).

All together, our data clearly highlight the distinct impact of RTE cell cycle entry during AEHI and CHI: while constituting a renewal source of T_{CM} T cells in AEHI, hyperimmune activation in CHI does not seem to lead to efficient recruitment of RTEs into the T_{CM} T cell pool.

Chronic immune activation is associated with levels of RTE survival

To verify the hypothesis that the decrease in absolute numbers of RTEs could be due to defective cell cycle entry, we analyzed the expression levels of the IL-7Rα chain, CD127, and its downstream target Bcl-2 by flow cytometry in the various naive and memory CD4 T cell subsets in healthy individuals (N = 6) as well as in AEHI and CHI (N = 6 for both groups). We did not observe any change in the frequencies of $CD127^+$ cells between HIV-infected individuals and healthy controls for all naive and memory subsets (data not shown); in contrast, the frequencies of Bcl-2^+ cells in $CD31^{hi}$ (RTE) and $CD31^{low}$ CD4 naive T cell subsets were reduced during both AEHI and CHI as compared to healthy controls (RTE: 79.5% ± 9.2 vs. 63.4% ± 15.3, $P = .05$ and 57.5% ± 14.8, $P = .01$; respectively. $CD31^{low}$: 77.8% ± 10.8 vs. 60.6% ± 12.4, $P = .04$ and 56.9% ± 15.2, $P = .03$; respectively) (Figure 7*A*). Furthermore, the frequencies of Bcl-2^+ cells in RTEs from P were significantly lower when compared to SP subjects during CHI but not AEHI (mean of 67.1 vs. 47.6%, Student's *t* test $P < .001$, N = 6 time points during CHI for both P and SP subjects) (Figure 7*B*).

To investigate the impact of hyperimmune activation on the survival and maintenance of the RTE population, we monitored the intracellular levels of the anti-apoptotic molecule Bcl-2 in RTEs during CHI. We found a significant inverse relation between the frequencies of $Ki67^+$ cells and that of $Bcl\text{-}2^+$ cells within RTEs (r = -0.63, *P* = .02, N = 11 time points for 7 subjects) (Figure 7*C*); demonstrating for the first time that the previously described association between increased Ki67 frequencies and activation-induced cell death during HIV infection in T_{CM} and total CD4 T cells (16, 22) was also observed in RTEs. It was previously shown that CD8 memory T cells expressing high levels of PD-1 contain lower levels of Bcl-2 (23). Our result show an inverse correlation between frequencies of $PD\text{-}1^+$ and $Bcl\text{-}2^+$ cells within RTEs during CHI (r = -0.8, *P* = .001, N = 11 time points for 7 subjects) (Figure 7*C*); highlighting a potential mechanism by which RTE T cells that are activated and stimulated to enter cell cycle are more prone to activation-induced cell death consequently leading to total CD4 T cell depletion.

High viral load in Progressors is associated with dysfunction in the IL-7/IL-7R system.

The observed negative correlation between Ki67 and Bcl-2 as well as between PD-1 and Bcl-2 frequencies on RTEs during chronic time points suggested that the increased susceptibility to apoptosis could be a consequence of defective IL-7 signaling [24]. To verify this hypothesis, we investigated the possibility that levels of IL-7 in plasma could predict Bcl-2 frequencies throughout HIV infection in SP and P subjects. We observed a significant positive correlation between IL-7 plasma levels and frequencies of $Bcl\text{-}2^+$ cells within RTEs from SP (3 subjects, 12 longitudinal time points over 1 year of infection) (r = 0.54, *P* = 0.03, N = 12 time points) (Figure S2*A*). The positive correlation between IL-7 and Bcl-2 levels in RTEs was no longer significant in P subjects (3 subjects, 12 longitudinal time points over 1 year of infection) (r = 0.24, *P* = 0.22, N = 12 time points) (Figure S2*A*) despite the fact that these subjects showed significantly higher levels of IL-7

as compared to healthy individuals (10.7 vs. 4.7 pg/ml for both SP and healthy controls, Student's *t* test $P < .001$) (Figure S2*B*). As P subjects were also characterized by high HIV viral load (having above 10,000 HIV RNA copies/ml) as compared to SP subjects (less than 500 HIV RNA copies/ml), we investigated the possibility that chronic immune activation rendered the IL-7 receptor unresponsive to IL-7 driven signals. We analyzed levels of basal and *in vitro* IL-7 induced STAT-5 phosphorylation by flow cytometry for evidence of recent IL-7 signaling and the ability of RTEs to respond to IL-7 in a small cohort of untreated HIV-infected subjects characterized with high viral load during PHI and monitored also for one year of infection. Our data show a significant positive association between IL-7 levels in AEHI and IL-7 induced pSTAT-5 levels ($N = 6$, $r = 0.86$, $P = .01$) (Figure 8*A*) and Δ pSTAT-5 ($N= 6$, $r = 0.87$, $P = .01$) (data not shown), suggesting *in vivo* responses to IL-7. However, no correlations were detected between IL-7 and pSTAT-5 levels within RTEs, whether basal or induced, during CHI; instead a negative correlation was found between viral load and IL-7-induced pSTAT-5 during CHI ($N = 6$, $r = -0.76$, $P = .04$) (Figure 8*B*) implying a role for chronic activation in dysfunction of the IL-7/IL-R system. We could not detect changes in Bcl-2 expression following IL-7 stimulation, which is probably due to the short incubation period: 24 hours versus 3 or 6 days (24-15). All together, these results suggest that IL-7 signaling in intact during AEHI but is lost during CHI in subjects without viral control.

Discussion

The loss of $CD31^{hi}$ naive CD4 T cells from the periphery can be associated with many factors including decreased thymic output, entrapment within lymphoid tissues, increased naive T cell destruction caused by the virus as well as antigenic activation leading to loss of the RTE phenotype as these cells are recruited into the memory T cell pool (1). Previously, we have highlighted the importance of the thymus in keeping naive and total CD4 numbers constant despite high plasma HIV RNA levels during untreated chronic HIV infection (7). In this paper, we analyzed recent thymic emigrants directly in the periphery using specific surface markers ($CD45RA^{+}CCR7^{+}CD27^{+}CD31^{hi}$) and investigated the homeostasis of this specific naive subset in AEHI and CHI.

Following the onset of thymic atrophy at puberty, the generation of new T cells slowly decreases with adulthood. It was previously shown that decreased thymic activity following HIV infection is not significant in older individuals when compared to their age-matched controls (12), most probably due to the fact that their thymii are much less active before infection and comprise fewer targets. The increased susceptibility of the younger more active thymus to HIV infection was nicely demonstrated in subjects with higher thymic volume that interrupted HAART treatment and experienced a rapid decline in CD4 T cells thereafter as compared to subjects with lower thymic volume (26). Therefore, we specifically analyzed untreated subjects that were younger than 35 years of age in order to correlate depletion of RTEs over the course of infection with the HIV virus without the influence of natural decreased output of RTE due to aging.

In this paper, we report that RTE frequencies within naive CD4 T cells were significantly reduced during both AEHI and CHI as compared to age-matched uninfected controls. During AEHI, the decrease was observed for all subjects but at varying degrees. However, during CHI only a subset of infected individuals experienced prolonged RTE cell loss. Slow progressors (SP) were characterized by moderate RTE depletion during AEHI and normal absolute numbers as compared to healthy controls during CHI. On the other hand, progressors (P)

showed severe RTE depletion throughout both AEHI and CHI and had a faster rate of T_{CM} and CD4 T cell depletion. Our data demonstrated that maintenance of RTEs is crucial in total CD4 T cell stabilization and their frequencies in AEHI seem to dictate the rate of disease progression, suggesting that T cell regeneration whether by the thymus or peripheral expansion is unable to compensate for severe RTE depletion during AEHI.

Our data show that higher activation and cell cycle entry (as measured by PD-1 and Ki67) within RTEs as well as higher levels of IL-7 during AEHI and CHI discriminated between the SP and P groups and were associated with lower RTE numbers during CHI and faster total CD4 T cell loss. This is in agreement with a number of studies measuring T cell dynamics utilizing deuterated glucose and bromodeoxyuridine (BrdU) incorporation as well as Ki67 expression to show that immune activation and CD4 T cell turnover are increased during CHI (11, 13, 27) and correlate with disease progression (28-29). Plasma IL-7 concentrations correlated with the frequencies of Ki67 within RTEs during AEHI as well as CHI and most likely contributed to the observed heightened activation in P subjects. Our findings of a positive correlation between the levels of IL-7 and Ki67 frequencies within RTEs but not other naive subsets is in agreement with a previous study (20) in which it was demonstrated that that $CD31^+$ but not $CD31^-$ were stimulated to proliferate in response to IL-7 in healthy individuals. In addition, high IL-7 levels in the context of lymphopenia such as that observed in HIV infection were shown to induce naive T cells to bear the memory phenotype independent of foreign antigen (30) and may accelerate RTE differentiation and depletion. In addition, the correlation between high levels of IL-7 during AEHI and disease progression can be further explained by the fact that IL-7 has been proposed to contribute to T cell death in high viral load conditions (31-32).

The finding that RTEs but not other naive subsets showed Ki67 frequencies similar to those observed in memory T cell subsets during HIV infection is novel and helps reconcile conflicting data on the status of naive T cell proliferation during HIV infection. While previous studies have shown that naive T cells have

increased Ki67 frequencies during HIV infection (27), it was later reasoned that inclusion of cells with a transitional phenotype into the naive cell gate ($CD45RA^+$ versus $CD45RA^+CD27^+$) artificially increased the frequencies of $Ki67^+$ cells in the "naive" population and their exclusion lead to the conclusion that naive CD4 T cells did not show increased proliferation during HIV infection (11). In this study, we show that increased cell cycle entry of naive CD4 T cells during AEHI and CHI is limited to the RTE subset. This further explains why increased Ki67 frequencies failed to be detected within the total naive T cell population in certain infected individuals, especially when CD4 numbers are above 500 cells/µl (11).

Although our data demonstrates that higher Ki67 frequencies within RTEs were a strong correlate of RTE depletion throughout infection, proliferation of RTEs during AEHI in progressors was important for the generation of T_{CM} and initial stabilization of CD4 T cell counts. We show that during AEHI high frequencies of $Ki67^+$ cells within RTEs, but not within any other CD4 naive subset, were positively correlated with HIV RNA plasma levels and T_{CM} cell counts, suggesting that proliferation of RTEs during AEHI leads to their recruitment into T cells of the central memory phenotype and concomitant depletion. This, however, led to increased circulating CD4 T cell counts. The rapid RTE differentiation we observed is supported by the findings of a previous study demonstrating that memory CD4 T cells were enriched for sjTRECs during primary HIV infection with only 50% of TRECs contained within naive T cells (33). An analysis of markers of recent TCR engagement such as CD69 and CD25 on $Ki67^+$ RTEs would further validate this hypothesis.

Interestingly, $CD31^{low}$ and $CD31^-$ CD4 naive T cells retained low frequencies of $Ki67^+$ cells in both P and SP individuals which were not dependent on viral load and did not correlate with absolute numbers of any memory subset. This suggests that the generation of immunity to HIV and perhaps other neoantigens is dependent in a large part on the presence of RTEs. This hypothesis is supported by a previous study analyzing $CD31^+$ and $CD31^-$ CD4 naive T cell cycle progression following TCR engagement in which it was observed that $CD31^+$ but

not $CD31^-$ T cells from both uninfected and HIV-infected individuals were induced to express Ki67 in response to TCR stimulation (34). In addition, a separate study also comparing $CD31^+$ and $CD31^-$ CD4 naive T cell found that $CD31^+$ T cells were the only subset that could respond to IL-7 stimulation by proliferating. It remains to be determined whether $CD31^{low}$ represent an intermediate population with a lower capacity to enter cell cycle following TCR and/or IL-7 triggering or if they are impaired similarly to $CD31^-$ T cells. Nonetheless, $CD31^{low}$ and $CD31^-$ CD4 naive T cells have considerably lower TREC content than $CD31^{hi}$ CD4 naive T cells (unpublished data), and it is therefore possible that they represent naive T cells that have undergone extensive proliferation to the point of lacking the capacity to further respond to stimulus and expand. These observations further stress the importance of efficient thymic function during HIV infection: in addition to providing new cells to compensate for the destruction of existing T cells, maintained thymic output would also ensure the presence of naive T cells capable of proliferating in response to viral proteins and homeostatic signals.

In addition, our data revealed different factors involved in RTE depletion during CHI. Although Ki67 frequencies within RTEs were still elevated during CHI, they were associated with lower T_{CM} and total CD4 T cell counts. This illustrates potential defects in the ability of RTEs from P infected individuals to regenerate and/or differentiate into memory T cells. It was previously shown that maintenance of T_{CM} T cells is important in system stabilization since they are needed for the constant replenishment of T_{EM}, a predominantly short-lived subset whose depletion impact disease progression (8). Our data extend these findings by demonstrating that RTE numbers significantly correlated with T_{CM} T cell counts during CHI, an association not detected between any other naive subset and T_{CM} or between RTEs and other memory T cells, and highlights the need for efficient thymopoiesis in disease control.

Although Ki67 is a nuclear antigen identifying cells which have entered proliferation (35), it was reported that most $Ki67^+$ T cells were in G1 phase versus S and G2 + M phases during HIV infection in contrast to normal individuals (36).

In addition, despite Ki67 frequencies correlating strongly with the amount of dividing cells per day, fewer cells were found to be dividing on any given day than were $Ki67^+$ (16). Therefore, unlike BrdU incorporation, Ki67 in the context of HIV infection is not limited to proliferating cells (as it can include activated cells that have not yet entered S-phase and are not actively proliferating (37)) and unlike CFSE, it does not indicate whether labelled cells have completed the cell cycle and successfully divided. Whether $Ki67^+$ RTEs are activated cells attempting to complete the proliferation cycle or cells actively proliferating, our data show that peripheral proliferation is inefficient at restoring T cell numbers.

Although we did not look at specific markers of apoptosis, the finding of lower Bcl-2 frequencies amongst RTEs in P as compared to SP subjects during CHI and of a positive correlation between chronic immune activation and Bcl-2 frequencies within RTEs suggested dysregulated proliferation and preferential loss of activated RTEs from the periphery similarly to that previously shown for CD4 T cells (16), and more specifically, T_{CM} (22) as a mechanism behind severe RTE depletion in CHI. Our findings of a negative correlation between viral load and pSTAT-5 levels also suggested that reduced longevity of RTEs during CHI was mediated in part by their unresponsiveness to IL-7 survival signals as result of excessive TCR triggering. This is in agreement with previous studies which have shown that the IL-7 signaling pathway is deficient in chronic HIV infection (38).

The effect of HIV viremia on RTE hyperimmune activation is likely a combination of both specific TCR engagement and non-specific bystander activation as suggested by the finding of a positive correlation between frequencies of Ki67+ cells within RTEs during CHI and plasma levels of IL-7 as well as IFN-α ($r = 0.87$, $P = .012$, data not shown). Increased levels of inflammatory cytokines and microbial translocation of LPS have been reported during HIV infection (39-40) and S-phase T cells, although expressing markers of activation, did not exhibit signs of recent TCR stimulation (41) confirming non-

specific stimulation. It is also probable that IL-7 acts in concert with viral load in the progressive exhaustion of RTEs.

All together, our data highlights hyperimmune activation as a key determinant in RTE pathogenesis which is mediated by high plasma viral RNA (by both direct and indirect mechanisms) and homeostatic forces (high levels of IL-7). This is in agreement with a previous report that has established a role for homeostasis in addition to virus-specific immune responses in CD4 proliferation, but not for CD8 T cells which were found to proliferate solely in response to viral factors (19). Loss of T_{CM} T cells and their inability to sufficiently replenish the T_{EM} compartment has previously been shown to mediate faster disease progression (8, 10). We propose that RTEs are the only naive subset capable of differentiating into T_{CM} and that their preservation is important in stabilizing total CD4 T cell counts and slowing the rate of disease progression. However, since we did not look at markers of thymic function such as the sj/β TREC ratio, it remains unclear whether RTE depletion in P subjects during CHI results from inadequate replacement of RTEs undergoing cell death, or if accelerated cell death in periphery despite unaltered intact thymic output is the major force driving RTE depletion.

Materials and Methods

Patients and control individuals

Blood or leukapheresis samples were obtained from 10 healthy adult donors and 8 HIV-infected patients. Eight untreated HIV-infected individuals were sampled during the acute/early phase of infection and followed-up for 1 year. The clinical data of each subject are listed in table S1. All samples were obtained with the informed consent of the subjects enrolled and according to the guidelines of the bioethical committee of Centre hospitalier de l'Université de Montreal (CHUM) and McGill University Health Center (MUHC).

Surface and intracellular staining by flow cytometry

Frozen PBMCs were stained simultaneously with the following monoclonal antibodies (mAbs) for the detection of cell proliferation: FITC labeled anti-Ki67 (BD Pharmingen), PE labeled anti-CD31 (BD Pharmingen), APC-Cy7 labeled anti-CD45RA (BD Pharmingen), PECy7 labeled anti-CCR7 (BD Pharmingen), APC labeled anti-PD-1 (BD Pharmingen), Alexa-700 labeled anti-CD27 (eBioscience) Pacific Blue labeled anti-CD4 (BD Pharmingen) and Amcyan labeled anti-CD3 (BD Pharmingen). For the detection of cell survival, the following mAbs were used: FITC labeled anti-Bcl-2 (BD Pharmingen), PECy5 labeled anti-CD127 (eBioscience), PE labeled anti-CD31 (BD Pharmingen), APC-Cy7 labeled anti-CD45RA (BD Pharmingen), PECy7 labeled anti-CCR7 (BD Pharmingen), APC labeled anti-PD-1 (BD Pharmingen), Alexa-700 labeled anti-CD27 (eBioscience) Pacific Blue labeled anti-CD4 (BD Pharmingen) and Amcyan labeled anti-CD3 (BD Pharmingen).

Intracellular staining was carried out following surface staining and cell permeabilization, after which cells were incubated with mAb directed against Ki-67 or Bcl-2 (Becton Dickinson, Pharmingen) or their respective isotype in the dark at room temperature for 30 minutes. The cells were then washed of the excess antibody and fixed in 2% formaldehyde (FA). Data was acquired on a

Becton Dickinson LSR II™ system through 8- or 9-color flow cytometry and analyzed using the DiVa™ software (Becton Dickinson systems).

PhosFlow detection of STAT-5

Antibodies and reagents

Dead cells were eliminated from all analyses with a violet-fluorescent dye from LIVE/DEAD Fixable Dead Cell Stain Kits (Invitrogen). The following antibodies were used for cell surface staining in PhosFlow: CD3-Alexa700, CD4-pacific blue, CD31-FITC, p-STAT5-PE (pY694) (BD Bioscience), CD27-allophycocyanin-Alexa750, and CD45RA-ECD (Beckman Coulter). For stimulation experiments, recombinant human IL-7 (R&D) was used at 0.1 ng/ml, following a dose-titration that allowed quantification of the IC50 (data not shown).

Phospho-specific flow cytometry analysis of pSTAT5

Frozen PBMC were thawed in RPMI 1640 medium containing 10% FBS and rested for 4 hours at 37°C and 5% CO2. PBMCs were initially stained with antibodies CD3, CD27 and CD31 and plus violet-fluorescent dye which was used to detect Live/Dead cells. Following one wash, cells were resuspended at 10 million cells/ml in PBS and stimulated for 15 minutes at 37°C with IL-7. After stimulation, cells were fixed with Cytofix buffer (BD Bioscience) for 10 minutes at 37°C. Cells were pelleted and perrmeabilized in PERM II buffer (BD Bioscience) for 30 minutes on ice. Cells were washed twice with staining buffer (BD Bioscience) and stained with an antibody cocktail containing CD4, CD45RA and p-STAT5. The cells were then washed of the excess antibody and resuspended in PBS 2%FCS. Cells were immediately analyzed on a LSRII flow cytometer (BD Bioscience).

Quantification of IL-7

IL-7 levels were quantified in plasma from 10 healthy controls and 8 untreated HIV-infected individuals using the high sensitivity IL-7 Quantikine HS ELISA kit (R&D Systems) according to manufacturer's instructions. Samples were assayed in duplicate.

Statistics

Statistical analysis (two-tailed Student's *t* test, Pearson correlation test, *r*, and *P* values) was performed using MS Excel and the Vassar college website. An *r* value ≥ 0.4 or ≤ -0.4, and a *P* value ≤ 0.05, were considered significant.

Bibliography

1. McCune, J.M., The dynamics of CD4+ T-cell depletion in HIV disease. Nature, 2001. 410(6831): p. 974-9.

2. Grossman, Z., et al., Pathogenesis of HIV infection: what the virus spares is as important as what it destroys. Nat Med, 2006. 12(3): p. 289-95.

3. Veazey, R.S., et al., Gastrointestinal tract as a major site of CD4+ T cell depletion and viral replication in SIV infection. Science, 1998. 280(5362): p. 427-31.

4. Mazzucchelli, R. and S.K. Durum, Interleukin-7 receptor expression: intelligent design. Nat Rev Immunol, 2007. 7(2): p. 144-54.

5. Mattapallil, J.J., et al., Massive infection and loss of memory CD4+ T cells in multiple tissues during acute SIV infection. Nature, 2005. 434(7037): p. 1093-7.

6. Di Mascio, M., et al., Naive T-cell dynamics in human immunodeficiency virus type 1 infection: effects of highly active antiretroviral therapy provide insights into the mechanisms of naive T-cell depletion. J Virol, 2006. 80(6): p. 2665-74.

7. Dion, M.L., et al., Slow disease progression and robust therapy-mediated CD4+ T-cell recovery are associated with efficient thymopoiesis during HIV-1 infection. Blood, 2007. 109(7): p. 2912-20.

8. Okoye, A., et al., Progressive CD4+ central memory T cell decline results in CD4+ effector memory insufficiency and overt disease in chronic SIV infection. J Exp Med, 2007. 204(9): p. 2171-85.

9. Nishimura, Y., et al., Loss of naive cells accompanies memory CD4+ T-cell depletion during long-term progression to AIDS in Simian immunodeficiency virus-infected macaques. J Virol, 2007. 81(2): p. 893-902.

10. Picker, L.J., et al., Insufficient production and tissue delivery of CD4+ memory T cells in rapidly progressive simian immunodeficiency virus infection. J Exp Med, 2004. 200(10): p. 1299-314.

11. Douek, D.C., et al., Evidence for increased T cell turnover and decreased thymic output in HIV infection. J Immunol, 2001. 167(11): p. 6663-8.

12. Dion, M.L., et al., HIV infection rapidly induces and maintains a substantial suppression of thymocyte proliferation. Immunity, 2004. 21(6): p. 757-68.

13. Mohri, H., et al., Increased turnover of T lymphocytes in HIV-1 infection and its reduction by antiretroviral therapy. J Exp Med, 2001. 194(9): p. 1277-87.

14. Hazenberg, M.D., et al., Thymic output: a bad TREC record. Nat Immunol, 2003. 4(2): p. 97-9.

15. Kohler, S. and A. Thiel, Life after the thymus: CD31+ and CD31- human naive CD4+ T-cell subsets. Blood, 2009. 113(4): p. 769-74.

16. Ribeiro, R.M., et al., In vivo dynamics of T cell activation, proliferation, and death in HIV-1 infection: why are CD4+ but not CD8+ T cells depleted? Proc Natl Acad Sci U S A, 2002. 99(24): p. 15572-7.

17. Trautmann, L., et al., Upregulation of PD-1 expression on HIV-specific CD8+ T cells leads to reversible immune dysfunction. Nat Med, 2006. 12(10): p. 1198-202.

18. Bazdar, D.A. and S.F. Sieg, Interleukin-7 enhances proliferation responses to T-cell receptor stimulation in naive CD4+ T cells from human immunodeficiency virus-infected persons. J Virol, 2007. 81(22): p. 12670-4.

19. Catalfamo, M., et al., HIV infection-associated immune activation occurs by two distinct pathways that differentially affect CD4 and CD8 T cells. Proc Natl Acad Sci U S A, 2008. 105(50): p. 19851-6.

20. Azevedo, R.I., et al., IL-7 sustains CD31 expression in human naive CD4+ T cells and preferentially expands the CD31+ subset in a PI3K-dependent manner. Blood, 2009. 113(13): p. 2999-3007.

21. Kinter, A.L., et al., The common gamma-chain cytokines IL-2, IL-7, IL-15, and IL-21 induce the expression of programmed death-1 and its ligands. J Immunol, 2008. 181(10): p. 6738-46.

22. Sieg, S.F., D.A. Bazdar, and M.M. Lederman, S-phase entry leads to cell death in circulating T cells from HIV-infected persons. J Leukoc Biol, 2008. 83(6): p. 1382-7.

23. Petrovas, C., et al., Differential association of programmed death-1 and CD57 with ex vivo survival of CD8+ T cells in HIV infection. J Immunol, 2009. 183(2): p. 1120-32.

24. Juffroy, O., et al., Dual mechanism of impairment of interleukin-7 (IL-7) responses in human immunodeficiency virus infection: decreased IL-7 binding and abnormal activation of the JAK/STAT5 pathway. J Virol, 2010. 84(1): p. 96-108.

25. Colle, J.H., et al., The correlation between levels of IL-7Ralpha expression and responsiveness to IL-7 is lost in CD4 lymphocytes from HIV-infected patients. AIDS, 2007. 21(1): p. 101-3.

26. Vallejo, A., et al., High thymic volume is associated with viral replication and immunologic impairment only early after HAART interruption in chronic HIV infection. Viral Immunol, 2005. 18(4): p. 740-6.

27. Hazenberg, M.D., et al., T-cell division in human immunodeficiency virus (HIV)-1 infection is mainly due to immune activation: a longitudinal analysis in patients before and during highly active antiretroviral therapy (HAART). Blood, 2000. 95(1): p. 249-55.

28. Giorgi, J.V., et al., Shorter survival in advanced human immunodeficiency virus type 1 infection is more closely associated with T lymphocyte activation than with plasma virus burden or virus chemokine coreceptor usage. J Infect Dis, 1999. 179(4): p. 859-70.

29. Hazenberg, M.D., et al., Persistent immune activation in HIV-1 infection is associated with progression to AIDS. AIDS, 2003. 17(13): p. 1881-8.

30. Murali-Krishna, K. and R. Ahmed, Cutting edge: naive T cells masquerading as memory cells. J Immunol, 2000. 165(4): p. 1733-7.

31. Fluur, C., et al., Potential role for IL-7 in Fas-mediated T cell apoptosis during HIV infection. J Immunol, 2007. 178(8): p. 5340-50.

32. Lelievre, J.D., et al., Interleukin 7 increases human immunodeficiency virus type 1 LAI-mediated Fas-induced T-cell death. J Virol, 2005. 79(5): p. 3195-9.

33. Lewin, S.R., et al., Dynamics of T cells and TCR excision circles differ after treatment of acute and chronic HIV infection. J Immunol, 2002. 169(8): p. 4657-66.

34. Luciano, A.A., et al., Impaired induction of CD27 and CD28 predicts naive CD4 T cell proliferation defects in HIV disease. J Immunol, 2007. 179(6): p. 3543-9.

35. Wersto, R.P., et al., Cell cycle-dependent reactivity with the monoclonal antibody Ki-67 during myeloid cell differentiation. Exp Cell Res, 1988. 179(1): p. 79-88.

36. Combadere, B., et al., CD4+Ki67+ lymphocytes in HIV-infected patients are effector T cells accumulated in the G1 phase of the cell cycle. Eur J Immunol, 2000. 30(12): p. 3598-603.

37. van Oijen, M.G., et al., Positivity of the proliferation marker Ki-67 in noncycling cells. Am J Clin Pathol, 1998. 110(1): p. 24-31.

38. Bazdar, D.A., M. Kalinowska, and S.F. Sieg, Interleukin-7 receptor signaling is deficient in CD4+ T cells from HIV-infected persons and is inversely associated with aging. J Infect Dis, 2009. 199(7): p. 1019-28.

39. Boasso, A. and G.M. Shearer, Chronic innate immune activation as a cause of HIV-1 immunopathogenesis. Clin Immunol, 2008. 126(3): p. 235-42.

40. Brenchley, J.M., et al., Microbial translocation is a cause of systemic immune activation in chronic HIV infection. Nat Med, 2006. 12(12): p. 1365-71.

41. Sieg, S.F., et al., Peripheral S-phase T cells in HIV disease have a central memory phenotype and rarely have evidence of recent T cell receptor engagement. J Infect Dis, 2005. 192(1): p. 62-70.

Figure legends

Figure 1. A subset of HIV-infected individuals maintained normal levels of RTEs during CHI. (A) Gating strategy used to identify $CD31^{hi}$ CD4 (RTEs). $CD3^{+}4^{+}$ PBMCs were first gated on the naive markers CD45RA+, followed by CCR7+ and CD27+ and then divided into 3 subpopulations based on the expression of CD31 with RTEs containing the highest MFI levels. Healthy individuals were always monitored at the same time as HIV-infected subjects as internal controls for $CD31^{hi}$ gating. Memory subsets were gated on CD45RA- and further characterized using CCR7 and CD27: T_{CM} are CCR7+CD27+, T_{EM} are CCR7-CD27-, and T_{TM} are CCR7-CD27+ (B) Untreated HIV-infected individuals were grouped as slow progressors (SP) or progressors (P) based on the rate of decline of CD4 T cell numbers. The frequencies of $CD31^{hi}$ within naive CD4 T cells were measured in AEHI (average of 10 weeks) as well as in CHI (average of 60 weeks) from SP and P subjects and compared to healthy controls. (C) SP subjects showed significantly higher RTE and T_{CM} T cell counts than subjects with lower $CD31^{hi}$ frequencies (P = .02). Horizontal lines represent maximal values, third quartiles, medians, first quartiles, and minimal values, from top to bottom.

Figure 2. Initial RTE frequencies in AEHI predict RTE, T_{CM} and total CD4 T cell counts in CHI. (A) Frequencies of $CD31^{hi}$ were analyzed longitudinally for each of the 8 subjects. Representative FACS histograms compare subjects that maintain high $CD31^{hi}$ frequencies to those that had low $CD31^{hi}$ frequencies. Grey lines represent CD31 expression obtained in AEHI and black lines are for measurements during CHI (B) The frequencies of $CD31^{hi}$ within naive CD4 T cells in AEHI were measured in correlation with RTE T cell counts (cell/µl) 60 weeks later in untreated individuals. RTE counts were calculated by multiplying the percentage of $CD31^{hi}$ within CD4 T cells in each individual by their CD4 T cell counts. (C) The frequencies of $CD31^{hi}$ (◆), $CD31^{low}$ (▲), and $CD31^{-}$ (■) within naive CD4 T cells in AEHI were measured in correlation with T_{CM} and CD4 T cell counts (cell/µl) 60 weeks later in untreated individuals.

Figure 3. Frequencies of Ki67 in RTEs from healthy controls and HIV-infected individuals during AEHI and CHI. (A) Frequencies of $Ki67^+$ cells were detected on the different CD4 subsets ($CD31^{hi}$, $CD31^{low}$, and $CD31^-$ naive T cells as well as T_{CM} and T_{EM} memory T cells) for healthy controls (◆), HIV-infected individuals (4 P and 3 SP) during AEHI (▲) as well as CHI (▲). A representative FACS histogram is shown for Ki67 expression within RTEs in an infected individual (thick black line) versus a healthy control (thin gray line). The isotype control for the Ki67 antibody is shown as shaded gray area. (B) Correlations between frequencies of $Ki67^+$ cells in RTEs and viral load (log copies/ml) and plasma IL-7 (pg/ml) during AEHI and CHI.

Figure 4. Frequencies of PD-1 in RTEs during AEHI and CHI. (A) The frequencies of $PD\text{-}1^+$ cells were determined within the different CD4 subsets ($CD31^{hi}$, $CD31^{low}$, and $CD31^-$ naive T cells as well as T_{CM}, T_{EM}, and T_{TM} memory T cells) for healthy controls (◆), HIV-infected individuals (3 P and 3 SP) during AEHI (▲) as well as CHI (▲). A representative FACS histogram is shown for PD-1 levels within RTEs in an infected individual (thick black line) versus a healthy control (thin grey line). (B) Frequencies of $PD\text{-}1^+$ cells within RTEs were analyzed in correlation with viral load (log copies/ml) and plasma IL-7 (pg/ml) detected during AEHI and CHI.

Figure 5. Hyperimmune activation levels in RTEs and plasma IL-7 concentrations early in infection correlate with disease progression. (A) The frequencies of $Ki67^+$ and $PD\text{-}1^+$ cells in RTEs during AEHI were analyzed in correlation with RTE T cell counts during CHI as well as with the rate of CD4 T cell depletion (measured as the Δ CD4 counts after 1 year of infection).

Figure 6. RTE cell cycle entry in AEHI leads to recruitment to the memory T cell pool while cell cycle entry in CHI leads to RTE, T_{CM} and total CD4 T cell depletion. (A) Frequencies of $Ki67^+$ cells in RTEs during AEHI were analyzed in correlation with RTE and T_{CM} T cell counts obtained during AEHI. (B) The frequencies of $Ki67^+$ cells in RTEs detected during CHI were correlated with

RTE, T_{CM} and CD4 T cell counts during CHI and RTE T cell counts during CHI were also analyzed in correlation with T_{CM} T cell counts.

Figure 7. Chronic immune activation is associated with lower survival of RTEs. (A) The frequencies of Bcl-2^+ cells were determined within the different CD4 subsets ($CD31^{hi}$, $CD31^{low}$, and $CD31^-$ naive T cells as well as T_{CM}, T_{EM}, and T_{TM} memory T cells) for healthy controls (■) and HIV-infected individuals during AEHI (■) as well as CHI (■). A representative FACS histogram is shown for Bcl-2 levels within RTEs in an infected individual (thick black line) versus a healthy control (thin black line). The isotype control for the Bcl-2 antibody is shown as a shaded gray area. (B) The frequencies of Bcl-2^+ cells within RTEs from SP were compared to P subjects for both AEHI and CHI (N = 6 time points for each group). Differences in Bcl-2 frequencies were observed between SP and P during CHI ($P < .001$) and between AEHI and CHI in P ($P = .05$). Horizontal lines represent maximal values, third quartiles, medians, first quartiles, and minimal values, from top to bottom. (C) The frequencies of $Ki67^+$ and PD-1^+ cells within RTEs were analyzed in correlation with the frequencies of Bcl-2^+ cells within RTEs in 6 subjects during CHI (N = 11 time points in CHI).

Figure 8. Response to IL-7 stimulation in HIV-infected individuals with high HIV RNA load. The correlations between levels of IL-7 and basal pSTAT-5 (◆) as well as between levels of IL-7 and IL-7-induced pSTAT-5 (■) were analyzed in subjects with high viral load (having above 10,000 HIV RNA copies/ml) during acute infection (A) and chronic infection (B). A representative FACS histogram is shown for basal pSTAT-5 levels within RTEs in an infected individual (shaded grey area) versus IL-7 triggered pSTAT-5 levels within RTEs (black line).

Figure S1. Longitudinal Ki67 frequencies within RTEs. Ki67 frequencies within RTEs are shown for 3 P and 2 SP subjects. Although highest Ki67 frequencies in P are highest during AEHI, they remains above those observed in healthy controls, while SP have values near healthy controls (mean frequencies of $Ki67^+$ cells in RTEs from healthy controls are marked by a black line).

Figure S2. Levels of IL-7 are positively associated with Bcl-2 expression in RTEs from SP. (A) IL-7 levels were analyzed in correlation with Bcl-2 frequencies within RTEs for both SP and P subjects. (B) IL-7 levels were compared between healthy controls (○), SP (●) and P subjects (●) throughout infection.

Figure 1 A

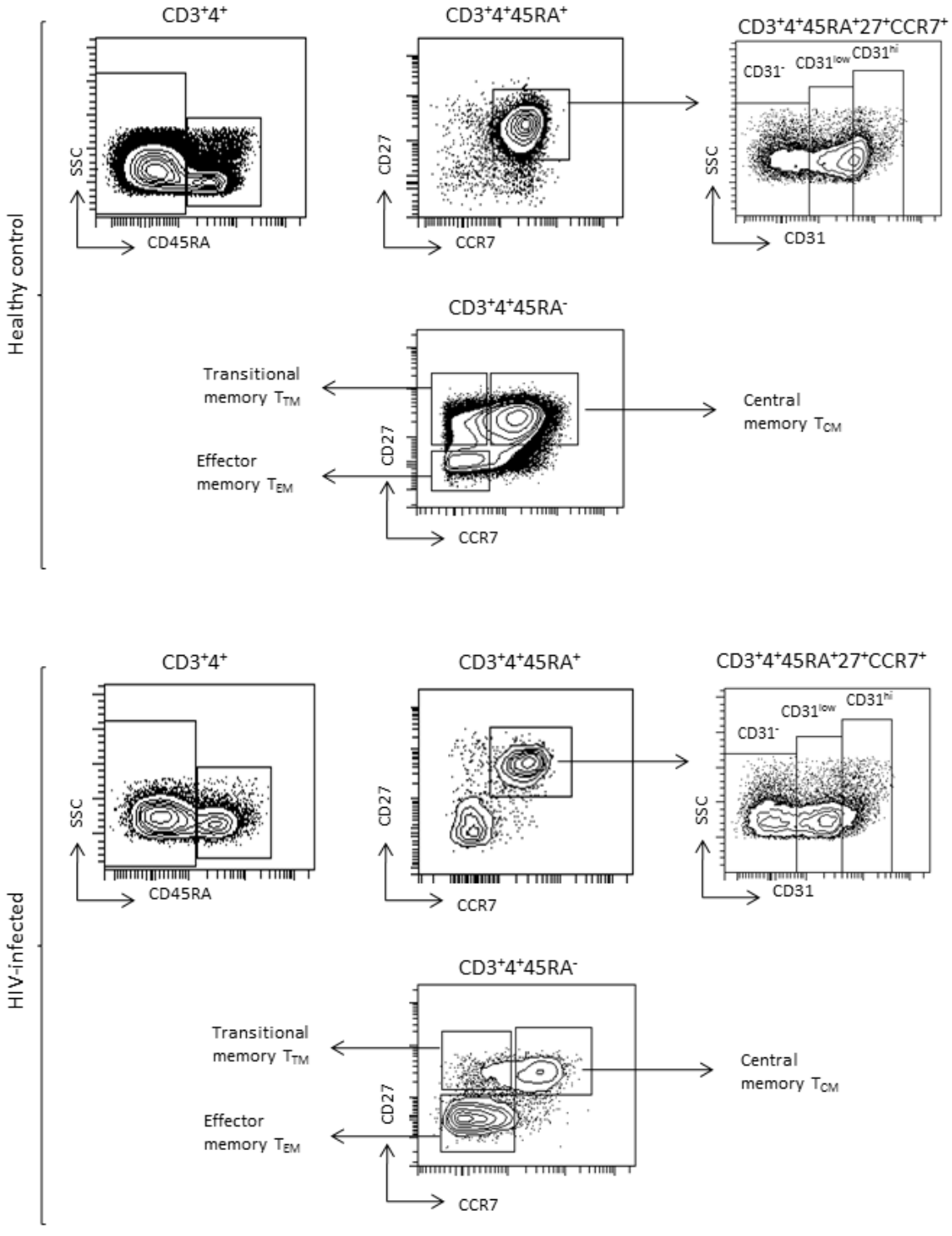
Healthy control
CD3+4+
SSC
CD45RA
CD3+4+45RA+
CD27
CCR7
CD3+4+45RA+27+CCR7+
CD31-
CD31low
CD31hi
SSC
CD31
CD3+4+45RA-
Transitional memory TTM
Effector memory TEM
CD27
CCR7
Central memory TCM
HIV-infected
CD3+4+
SSC
CD45RA
CD3+4+45RA+
CD27
CCR7
CD3+4+45RA+27+CCR7+
CD31-
CD31low
CD31hi
SSC
CD31
CD3+4+45RA-
Transitional memory TTM
Effector memory TEM
CD27
CCR7
Central memory TCM

Figure 1

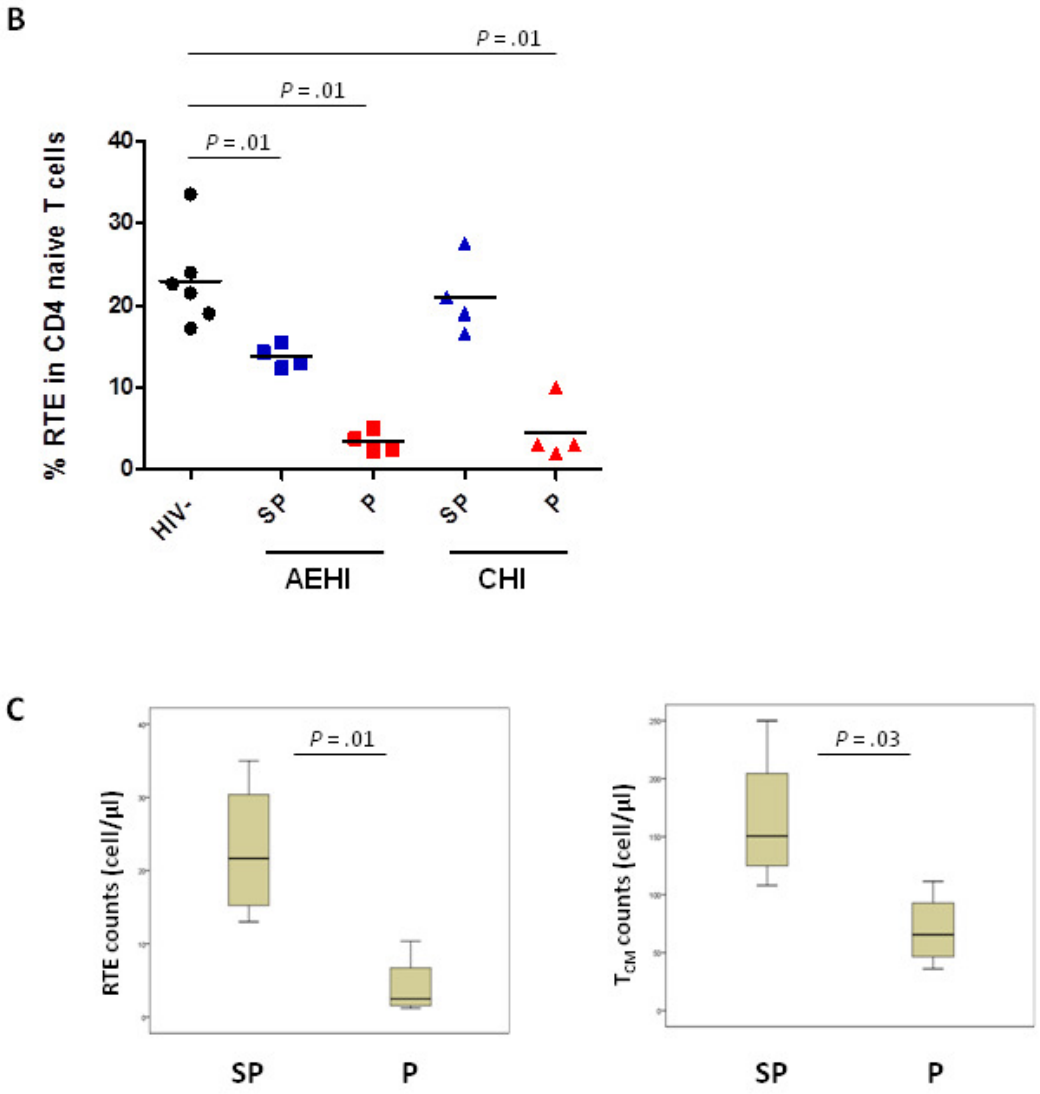
B
P = .01
P = .01
P = .01
% RTE in CD4 naive T cells
40
30
20
10
0
HIV-
SP
P
SP
P
AEHI
CHI
C
P = .01
RTE counts (cell/µl)
SP
P
P = .03
T_{CM} counts (cell/µl)
SP
P

Figure 2

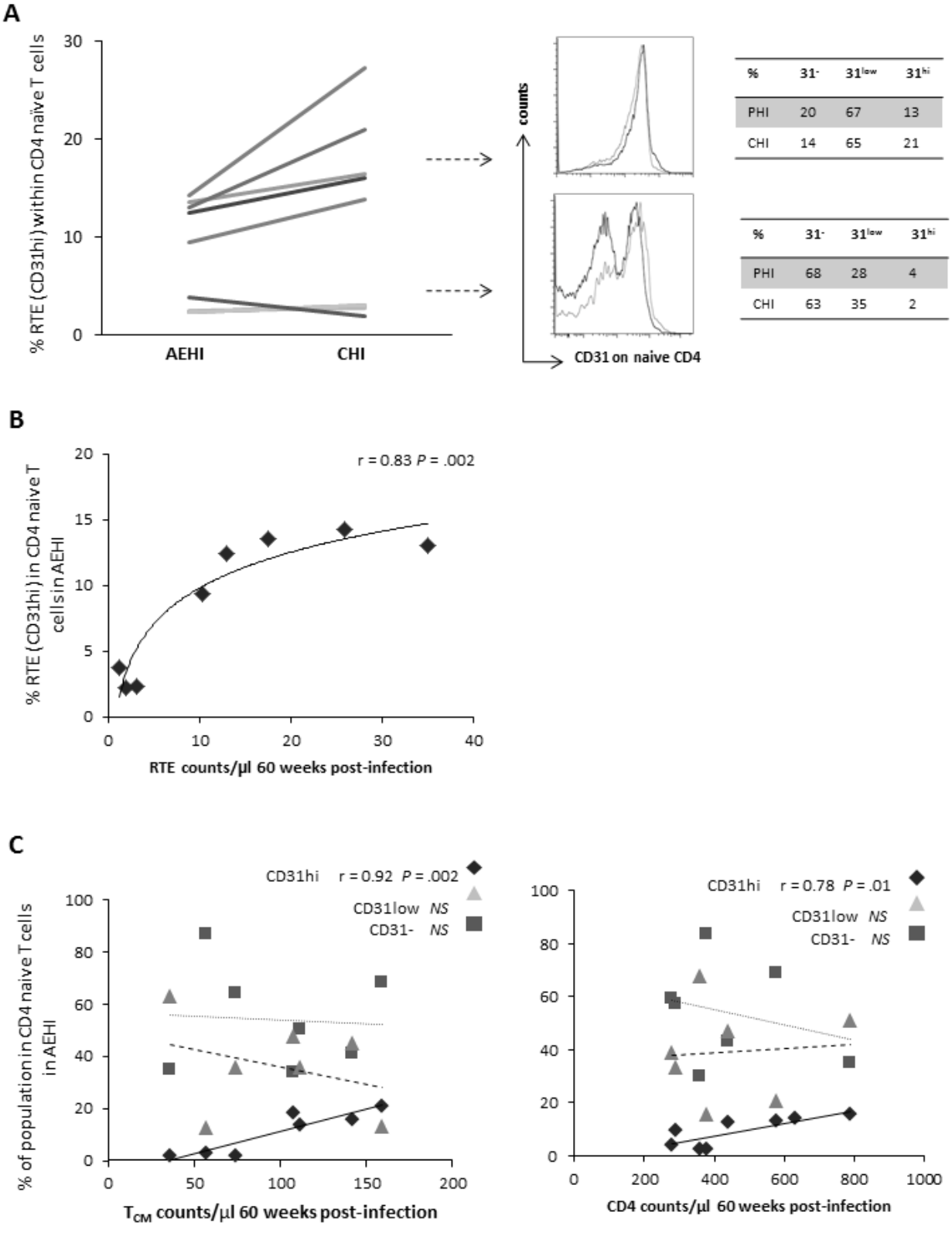

%	31-	31low	31hi
PHI	20	67	13
CHI	14	65	21

%	31-	31low	31hi
PHI	68	28	4
CHI	63	35	2

Figure 3

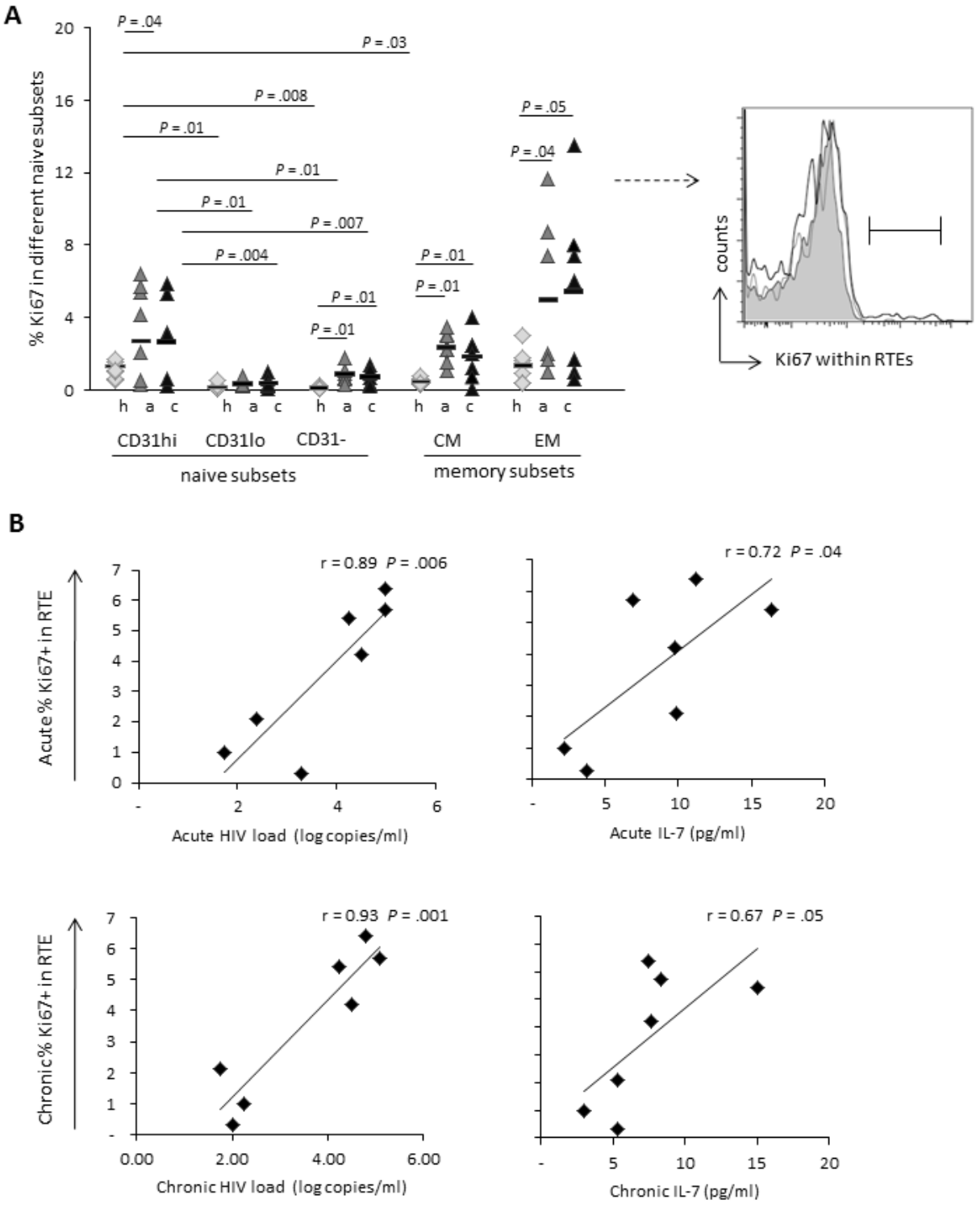
A
% Ki67 in different naive subsets
P = .04
P = .03
P = .008
P = .01
P = .01
P = .01
P = .007
P = .004
P = .01
P = .01
P = .01
P = .01
P = .05
P = .04
h a c
CD31hi
CD31lo
CD31-
CM
EM
naive subsets
memory subsets
counts
Ki67 within RTEs
B
Acute % Ki67+ in RTE
r = 0.89 P = .006
Acute HIV load (log copies/ml)
r = 0.72 P = .04
Acute IL-7 (pg/ml)
Chronic % Ki67+ in RTE
r = 0.93 P = .001
Chronic HIV load (log copies/ml)
r = 0.67 P = .05
Chronic IL-7 (pg/ml)

Table I

Correlations between Ki67 levels expressed within different CD4 subsets with plasma HIV RNA and IL-7 in acute infection

N = 8	RTE	$CD31^{low}$	$CD31^{-}$	T_{CM}	T_{EM}	T_{TM}
HIV RNA	r = 0.89 *P* = .006	r = 0.71 *P* = .02	r = 0.17 *NS*	r = 0.28 *NS*	r = 0.32 *NS*	r = 0.23 *NS*
IL-7	r = 0.72 *P* = .004	r = 0.005 *NS*	r = -0.26 *NS*	r = 0.37 *NS*	r = 0.84 *P* = .004	r = 0.6 *P* = .05

Table II

Correlations between Ki67 levels expressed within different CD4 subsets with plasma HIV RNA and IL-7 in chronic infection

N = 8	RTE	$CD31^{low}$	$CD31^{-}$	T_{CM}	T_{EM}	T_{TM}
HIV RNA	r = 0.93 *P* = .001	r = -0.46 *NS*	r = -0.65 *P* = .04	r = 0.04 *NS*	r = -0.36 *NS*	r = -0.25 *NS*
IL-7	r = 0.67 *P* = .05	r = -0.34 *NS*	r = -0.37 *NS*	r = 0.38 *NS*	r = -0.28 *NS*	r = 0.22 *NS*

Figure 4

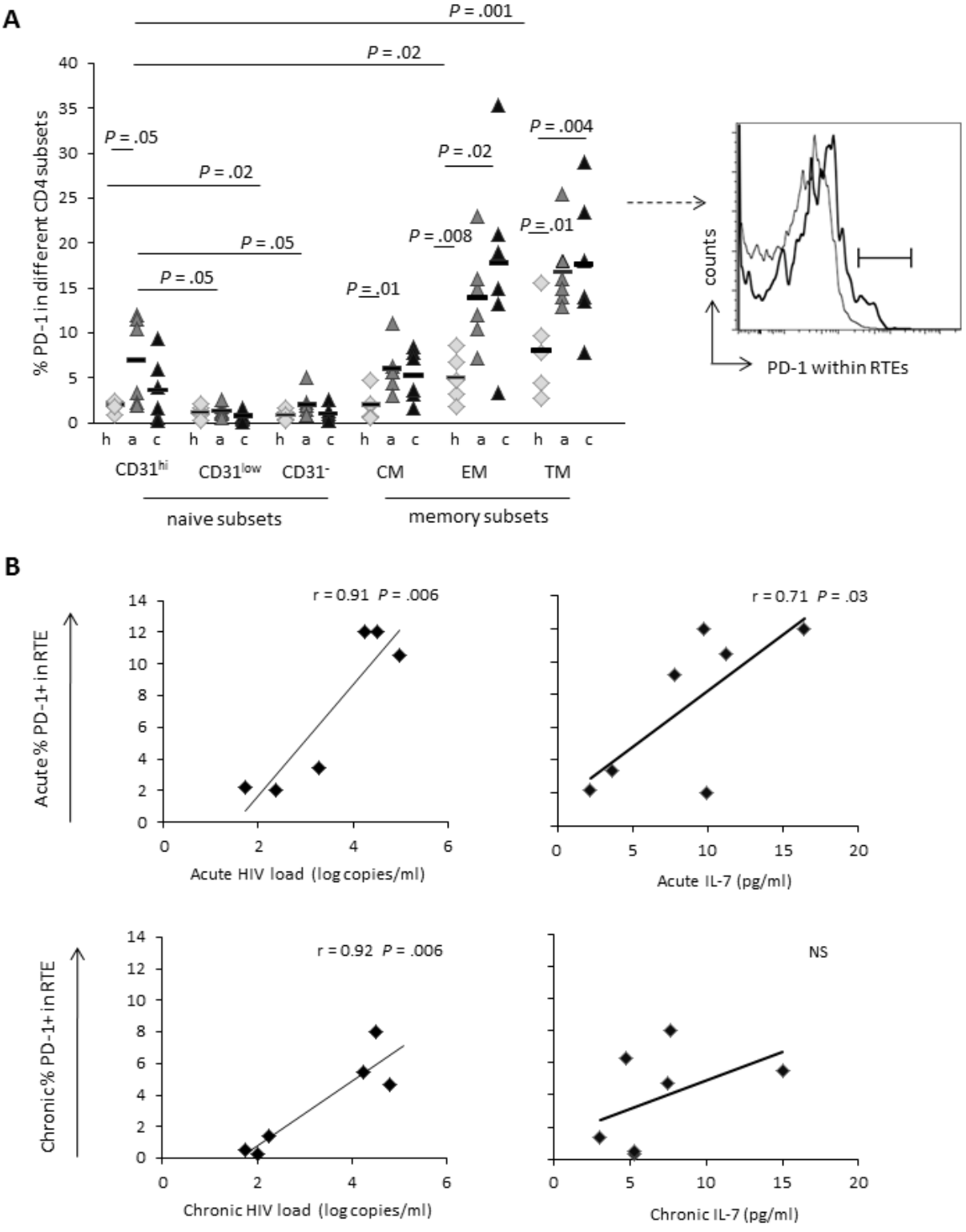
A
P = .001
P = .02
P = .05
P = .02
P = .05
P = .05
P = .01
P = .02
P = .008
P = .004
P = .01
% PD-1 in different CD4 subsets
counts
PD-1 within RTEs
h a c
CD31hi
CD31low
CD31-
CM
EM
TM
naive subsets
memory subsets
B
Acute % PD-1+ in RTE
r = 0.91 P = .006
Acute HIV load (log copies/ml)
r = 0.71 P = .03
Acute IL-7 (pg/ml)
Chronic % PD-1+ in RTE
r = 0.92 P = .006
Chronic HIV load (log copies/ml)
NS
Chronic IL-7 (pg/ml)

Figure 5

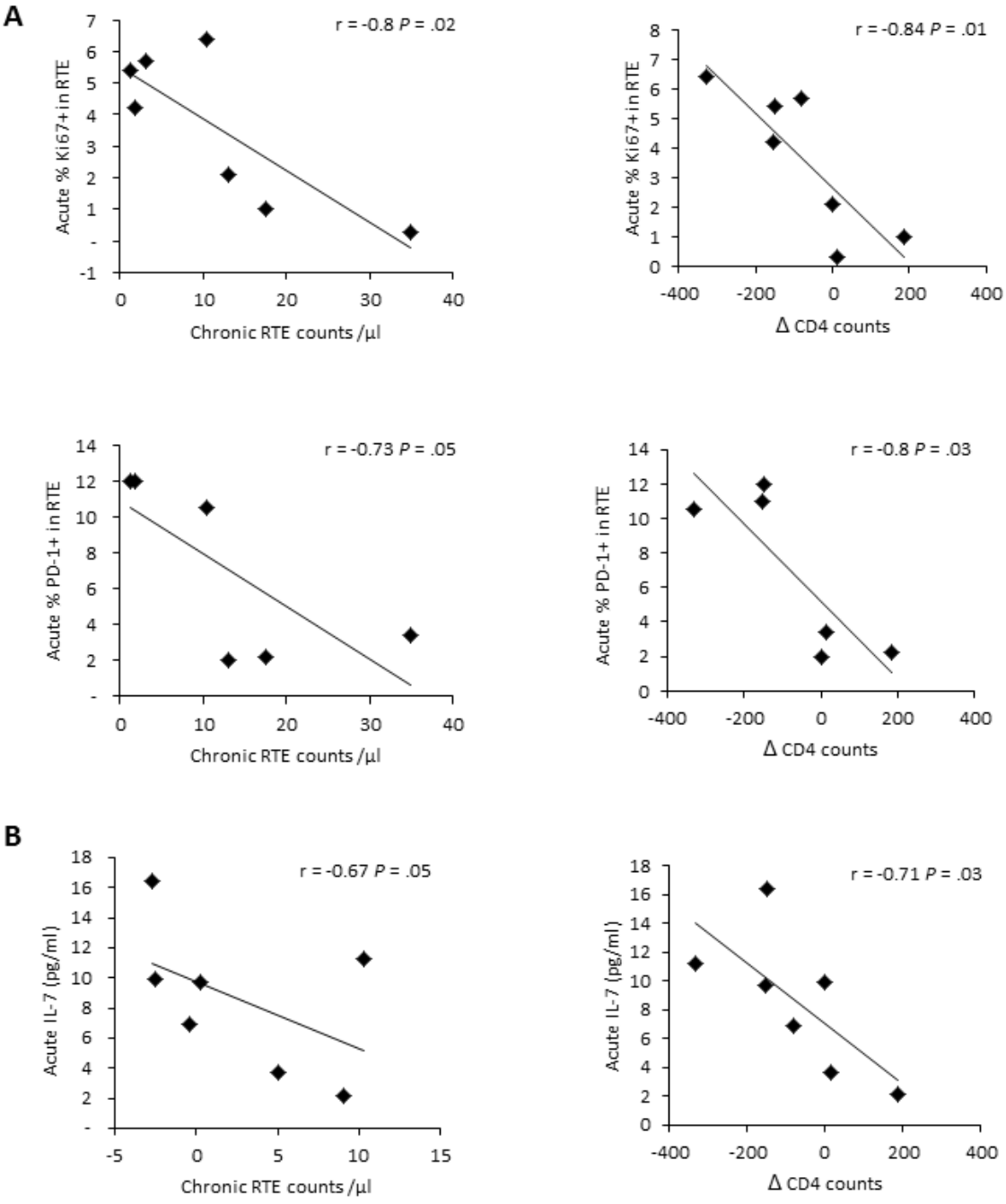
A
r = -0.8 P = .02
Acute % Ki67+ in RTE
Chronic RTE counts /µl
r = -0.84 P = .01
Acute % Ki67+ in RTE
Δ CD4 counts
r = -0.73 P = .05
Acute % PD-1+ in RTE
Chronic RTE counts /µl
r = -0.8 P = .03
Acute % PD-1+ in RTE
Δ CD4 counts
B
r = -0.67 P = .05
Acute IL-7 (pg/ml)
Chronic RTE counts /µl
r = -0.71 P = .03
Acute IL-7 (pg/ml)
Δ CD4 counts

Figure 6

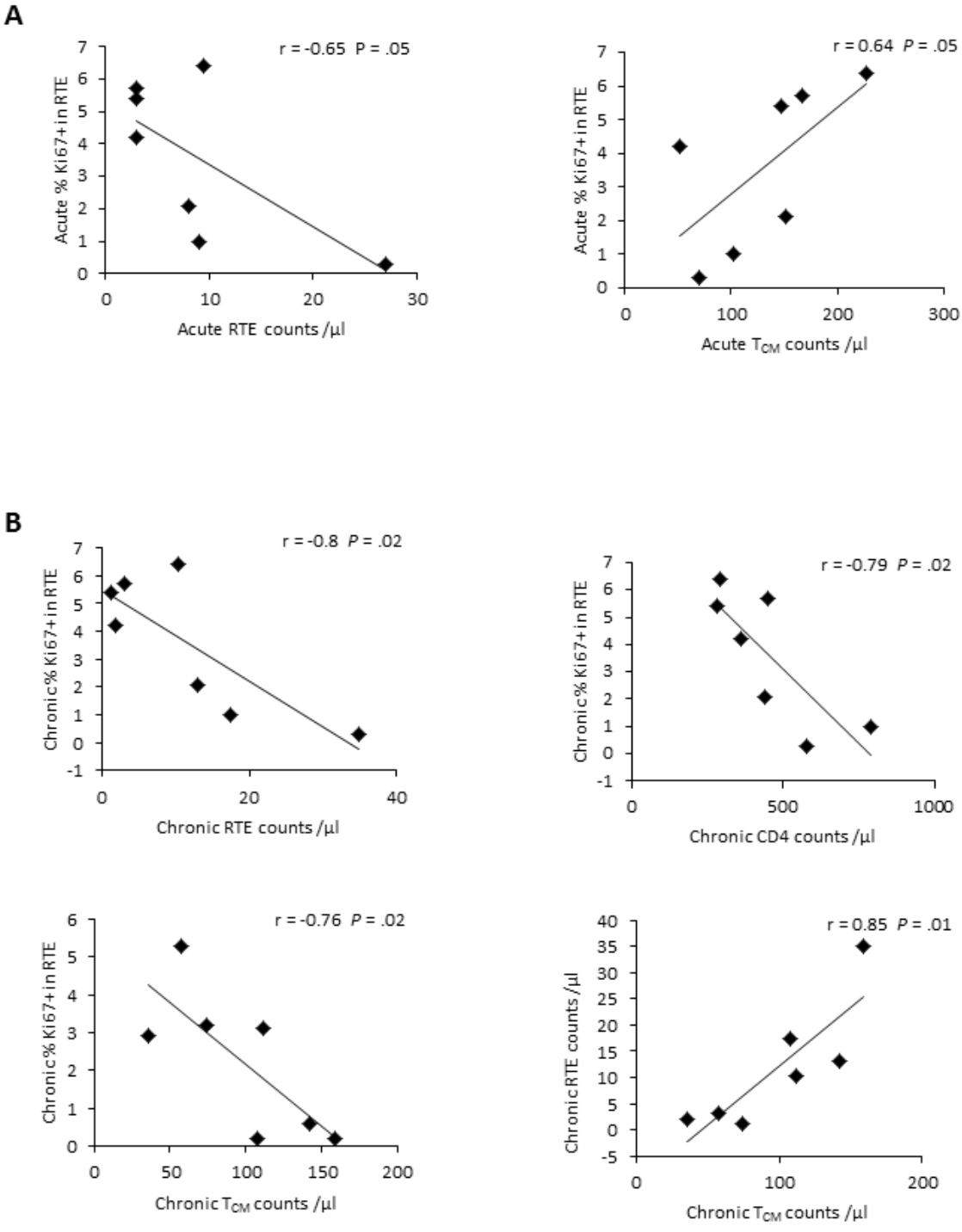
A
r = -0.65 P = .05
Acute % Ki67+ in RTE
Acute RTE counts /µl
r = 0.64 P = .05
Acute % Ki67+ in RTE
Acute T_{CM} counts /µl
B
r = -0.8 P = .02
Chronic % Ki67+ in RTE
Chronic RTE counts /µl
r = -0.79 P = .02
Chronic % Ki67+ in RTE
Chronic CD4 counts /µl
r = -0.76 P = .02
Chronic % Ki67+ in RTE
Chronic T_{CM} counts /µl
r = 0.85 P = .01
Chronic RTE counts /µl
Chronic T_{CM} counts /µl

Figure 7

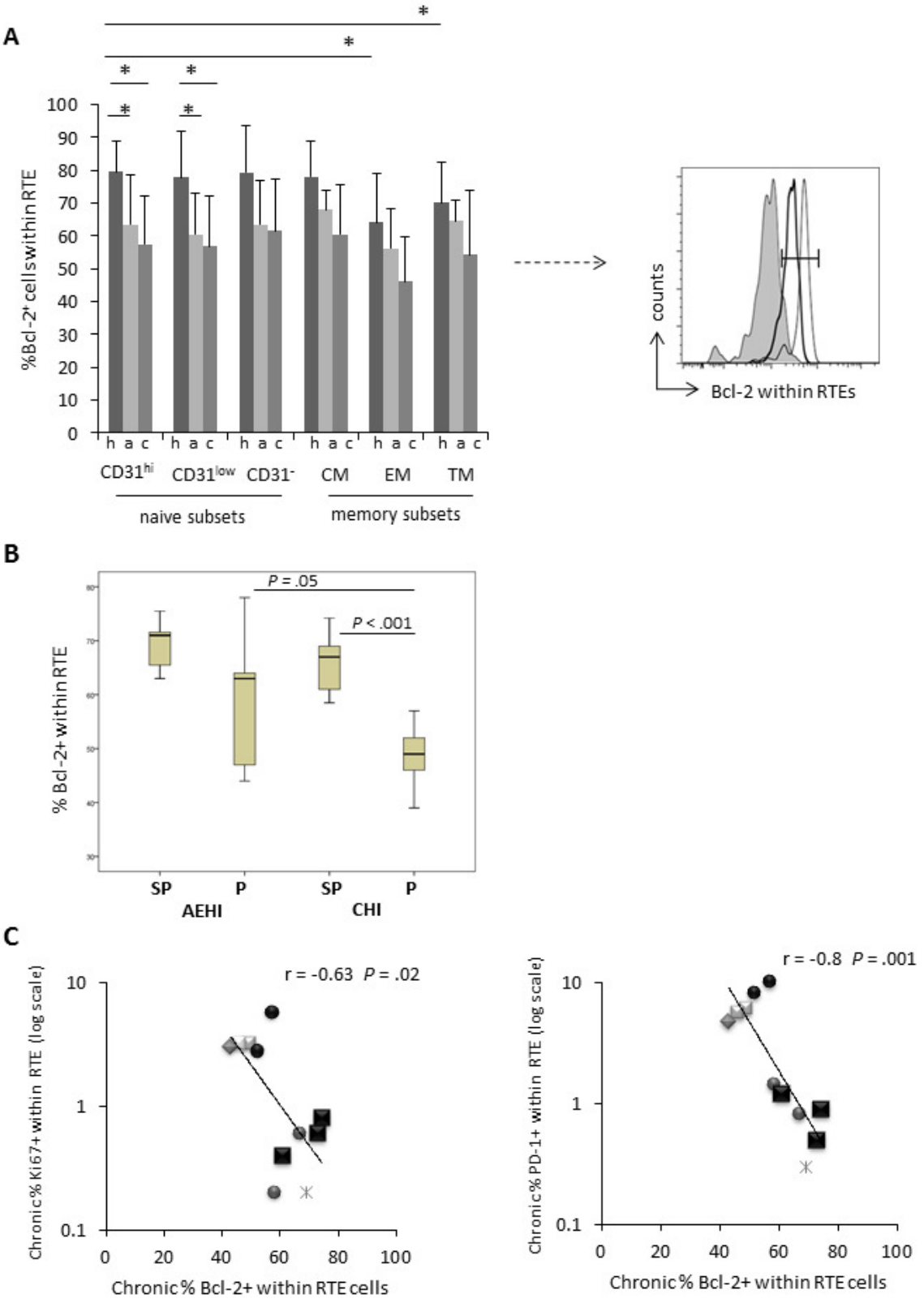
A
%Bcl-2+ cells within RTE
h a c
CD31hi
CD31low
CD31-
CM
EM
TM
naive subsets
memory subsets
counts
Bcl-2 within RTEs
B
% Bcl-2+ within RTE
P = .05
P < .001
SP
P
AEHI
CHI
C
Chronic % Ki67+ within RTE (log scale)
r = -0.63 P = .02
Chronic % Bcl-2+ within RTE cells
Chronic % PD-1+ within RTE (log scale)
r = -0.8 P = .001
Chronic % Bcl-2+ within RTE cells

Figure 8

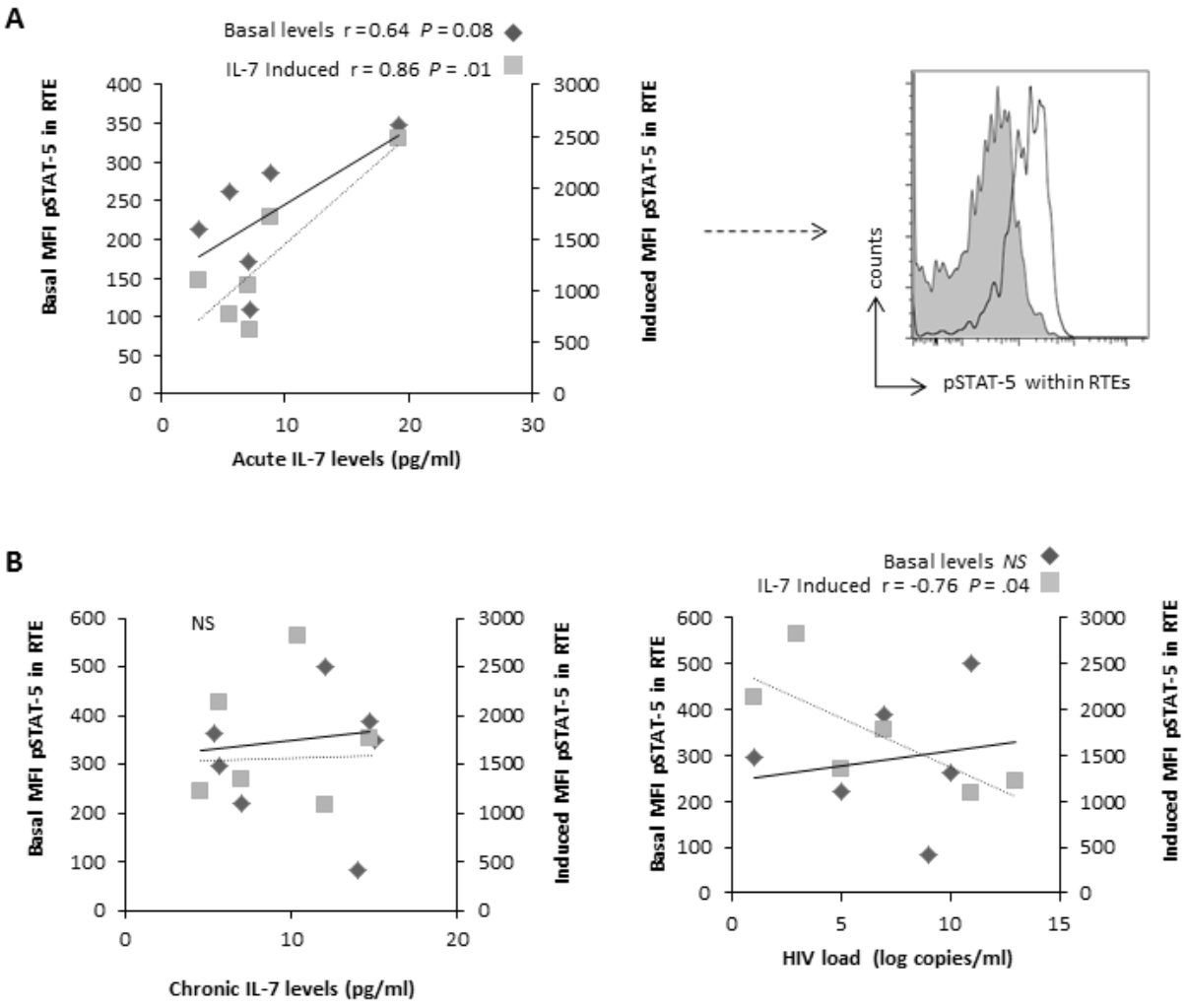
A
Basal levels r = 0.64 P = 0.08
IL-7 Induced r = 0.86 P = .01
Basal MFI pSTAT-5 in RTE
Induced MFI pSTAT-5 in RTE
Acute IL-7 levels (pg/ml)
counts
pSTAT-5 within RTEs
B
NS
Chronic IL-7 levels (pg/ml)
Basal levels NS
IL-7 Induced r = -0.76 P = .04
HIV load (log copies/ml)

Table S1: Untreated and treated primary HIV infected subjects

Patient	Age	Time P.I (days) *	Baseline CD4 count	Δ CD4	Baseline Viral Load (log)	Set point Viral load (log)
SP1 **	30	32	460	130	6.36	4.01
SP2	25	43	603	186	1.72	2.24
SP3	28	78	564	14	3.28	2.00
SP4	35	82	438	1	2.38	1.75
P1	22	45	620	-330	4.97	4.79
P2	27	140	460	-80	4.97	5.08
P3	28	83	513	-153	4.51	4.51
P4	30	57	430	-150	4.25	4.25

•Elapsed time between the sampling date and date of infection. This date was estimated based on the AIEDRP 2002 guidelines

** SP1 is the only SP with high viral load (>10,000 copies/ml) and was therefore omitted from the SP group and all further analysis as of figure 3 to achieve a homogeneous SP sub-group .

Figure S1

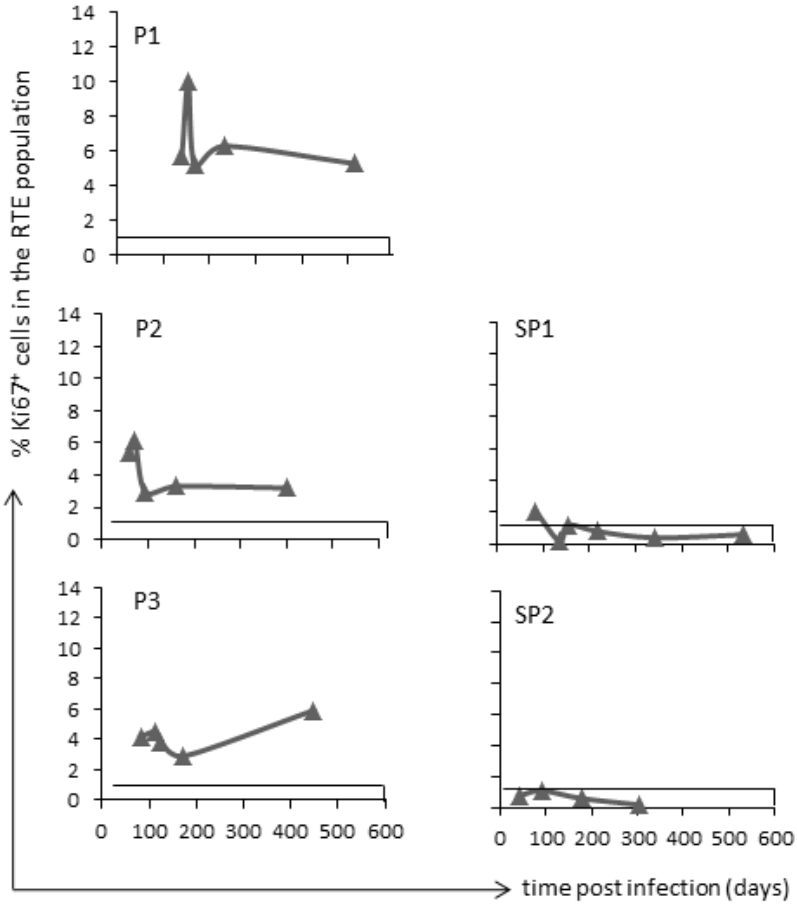
P1
P2
P3
SP1
SP2
% Ki67+ cells in the RTE population
time post infection (days)
0
2
4
6
8
10
12
14
0 100 200 300 400 500 600

Figure S2

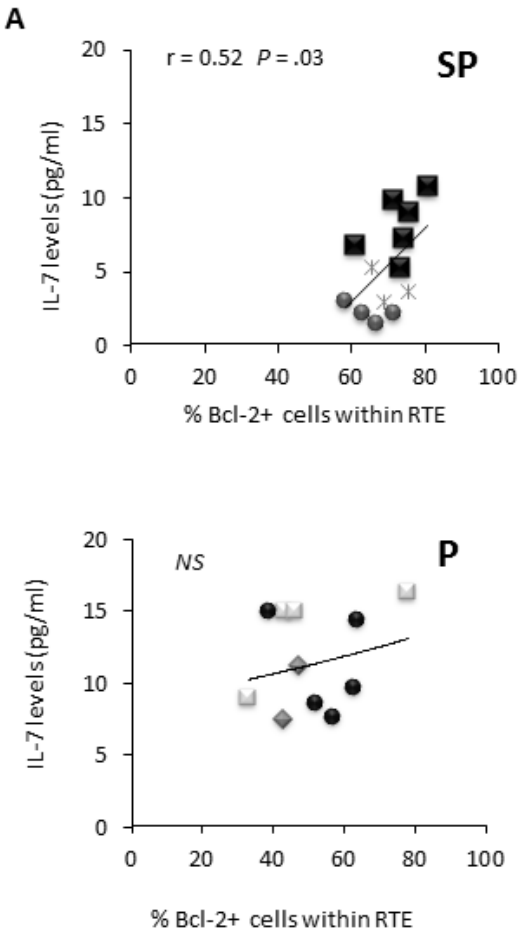
A
r = 0.52 P = .03
SP
IL-7 levels (pg/ml)
% Bcl-2+ cells within RTE
NS
P
IL-7 levels (pg/ml)
% Bcl-2+ cells within RTE
B
P < .001
IL-7 levels (pg/ml)
HC
SP
P

In Chapter 2, the use of the CD4 RTE-specific phenotype ($CD45RA^{+}CD27^{+}CCR7^{+}CD31^{hi}$) in a longitudinal study of HIV-infected individuals enrolled during AEHI demonstrated that alterations within the size of RTE cell pool greatly impacted the magnitude of the central memory T cell (T_{CM}) pool and provide evidence for total CD4 T cell depletion.

In a quest for the mechanisms that lead to such perturbations, we also showed that high levels of plasma IL-7 and IFN-α correlated with increased frequencies of activated RTE cells (as measured by Ki67 and up-regulation of PD-1 expression) during CHI. Hyperimmune activation, in turn, impacted the regenerative capacity and differentiation of RTEs during CHI and was associated with decreased RTE survival, demonstrating that peripheral proliferation within the RTE cell pool is a mechanism that leads to depletion of RTE and total CD4 T cell counts.

In order to determine the role of thymic output and peripheral events on RTE and CD4 T cell reconstitution as well as to show the impact of hyperimmune activation and levels of IL-7 and IFN-α on RTE recovery during HAART, we set up a longitudinal study of HIV-infected individuals treated during AEHI; these subjects were recruited and followed up for up to one year. Within these subjects, we will measure thymic function using the sj/β TREC ratio, assess the CD4 RTE-specific phenotype and evaluate RTE cell survival and proliferation using mAbs against the IL-7R and Ki67.

CHAPTER 3.

Increased intrathymic proliferation and decreased immune activation contribute to the recovery of recent thymic emigrants in HIV-infected individuals under HAART

Joumana Zeidan (1,2), Marie-Lise Dion (2), Rebeka Bordi (2), Bader Yassine-Diab (2), Mohamed-Rachid Boulassel (3), Lionel Filion (4), Jean-Pierre Routy (3), Remi Cheynier (5), Elias K. Haddad (2,7) and Rafick-Pierre Sekaly (1,2,6,7)*.

1) *Dept. of Microbiology and Immunology, McGill University, Montreal, Quebec, Canada* 2)*, Laboratoire d'Immunologie, CHUM Research Center, Montreal, Quebec, Canada,* 3) *Montreal Chest Institute, MUHC, Montreal, Quebec, Canada, 4) Dept. of Biochemistry Microbiology and Immunology, University of Ottawa, Ottawa, Ontario, Canada,* 5) *Unite des Virus Lents, Institut Pasteur, Paris, France,* 6) *Dept. Microbiologie et Immunologie, Université de Montreal, Montreal, Quebec, Canada, 7) Vaccine and Gene Therapy Institute of Florida Corp, Florida, USA*.

*****Corresponding author:
Dr. Rafick-Pierre Sekaly
Vaccine & Gene Therapy Institute Florida
11350 SW Village Pkwy, 3rd Floor
Port St. Lucie, FL 34987
Telephone Number: 772-345-4785
Fax Number: 772-345-3675
Email: sekaly@vgti-fl.org

Abstract

Highly active antiretroviral therapy (HAART) in HIV-infected individuals increases CD4 T cell counts in the majority of patients. The thymus is thought to be involved in immune reconstitution following HAART, but the factors regulating regeneration of T cells are not yet fully elucidated. The aim of this study was to investigate the role of thymic output versus peripheral expansion in the recovery of recent thymic emigrants (RTEs) and the impact of that population on total CD4 T cell reconstitution in 10 HIV-infected subjects that initiated HAART during acute/early HIV infection (AEHI). Our data demonstrates that subjects with baseline CD4 counts above 550 cells/µl had higher baseline RTE numbers than subjects with CD4 counts below 550 cells/µl and exhibited only transient increases in RTE numbers 4 weeks post-HAART which seemed to result from recirculation. Subjects with CD4 counts below 550 cells/µl showed increases at 4 weeks post-HAART that were maintained 52 weeks post-HAART. The magnitude of increases in RTE numbers following HAART was strongly associated with total CD4 T cell reconstitution and was correlated with increases in intrathymic proliferation, as measured by the sj/β TREC ratio, decreases in peripheral proliferation, as measured by Ki67, and increases in RTE survival, as measured by CD127. Baseline levels of IFN-α, a cytokine previously shown to reduce *in vitro* thymocyte proliferation in mouse models, were higher than in uninfected controls and post-HAART decreases were positively associated with greater sj/β TREC ratio and RTE recovery. Levels of IL-7 were significantly increased 4 weeks post-HAART, and the magnitude of this increase was positively associated with short-term and long-term RTE recovery in subjects that showed low levels of IFN-α post-HAART, suggesting that IFN-α might interfere with IL-7 mediated reconstitution. The role of IL-7 in enhancing RTE regeneration seemed to be predominantly mediated via increased survival but not by peripheral expansion of RTEs since levels of IL-7 positively correlated with frequencies of $CD127^+$ cells within RTEs but negatively correlated with frequencies of $Ki67^+$ cells within RTEs.

Introduction

Highly Active Antiretroviral Therapy (HAART) results in viral suppression and total CD4 number increases in the majority of HIV-infected individuals. However, up to 30% of HIV-infected individuals do not increase CD4 T cells more than 100 cells/μl in response to HAART despite full HIV RNA control (1). In addition, the extent of CD4 T cell reconstitution is highly variable, with several factors influencing recovery. Among these is the size of the naive CD4 T cell population in peripheral blood, which was found to strongly predict the magnitude of total CD4 T cell increases following treatment with HAART (2). Thymic function is thought to play an important role in the repopulation of T cells: naive T cell restoration has been linked with greater thymic volume and TREC levels (3), as well as a higher intrathymic proliferation as measured by the sj/βTREC ratio (4). Conversely, it has also been suggested that thymic function is unchanged following HAART, and that other constraints such as naive T cell proliferation as well as cell death rates (5) and/or sequestration within lymph nodes (6-7) are relieved with onset of therapy and result in preservation of the newly exported T cells and accumulation of naive T cells.

IL-7 is a pleiotropic cytokine that plays a critical role in homeostatic proliferation and survival of naive T cells (8). IL-7 mediates its activity through the IL-7 receptor which consists of an IL-7 specific α-chain (also known as CD127) linked with the γc-chain. Levels of IL-7 are increased in HIV-infected individuals (9-10), and it is debatable whether levels decrease following treatment with HAART. Up-regulation of the IL-7/IL-7R system is thought to be an important aspect of immune reconstitution following treatment with HAART and levels of CD127 on CD4 T cells have been associated with enhanced CD4 T cell recovery in HIV-infected individuals following HAART therapy (11). IL-7 is also essential for the development of immature thymocytes (12) and leads to enhanced generation of new T cells by the thymus following its administration in mouse and macaque models (13-14).

IFN-α, a pro-inflammatory cytokine, is predominantly produced by plasmacytoid dendritic cells (pDCs) and is detected at high levels early in HIV infection (15). High levels of IFN-α have been shown to induce an anti-proliferative effect on both immature thymocytes (16) and mature T cells (17-18), and have been associated with T cell dysfunction (19) as well as faster progression into AIDS (18, 20-21).

This study aimed at evaluating the role of thymic function and homeostatic proliferation in the reconstitution of recent thymic emigrants (RTEs) and investigating the impact of IL-7 and IFN-α on thymic function and RTE survival.

Results

RTEs are increased in a subset of patients receiving HAART during AEHI.

To investigate the impact of HAART therapy on RTE reconstitution, 10 HIV-infected individuals that were treated with HAART during acute/early HIV infection (AEHI) (mean of 90 days after onset of infection, range 36-159) were followed for approximately one year after initiation of treatment (mean 375 days, range 303-550). These subjects achieved viral control and reached undetectable HIV RNA levels following HAART treatment. (Subjects are further characterized in Table S1).

Recent Thymic Emigrants (RTEs) were defined as naive CD4 T cells ($CD45RA^+CCR7^+CD27^+$) expressing high levels of the marker CD31 as previously described (Chapter 2). Our data show that subjects with CD4 T cell counts higher than 550 cells/μl prior to HAART initiation (N = 3) exhibited transient increases in RTE cell counts 4 weeks post-treatment (mean of 16 ± 11), after which RTE numbers decreased to levels significantly lower than those observed at baseline (mean of 5 ±) (Figure 1*A*). On the other hand, subjects which contained CD4 T cell counts lower than 550 cells/μl prior to HAART initiation (N = 7) showed significant increases in RTE cell counts at 4 weeks post-HAART (mean of 12 ± 10 vs. 4 ± 2 cells/μl, Student's *t* test $P = .05$) and although we detected heterogeneity in the magnitude of increases in RTE numbers between subjects, RTE recovery was maintained 52 weeks post treatment in this group (mean of 12 ± 10 and 13 ± 10 vs. 4 ± 2 cells/μl, Student's *t* test $P = .05$ and $P = .03$; respectively) (Figure 1*A*). In fact, increases in RTE cell counts 4 weeks post-HAART predicted the magnitude of RTE recovery 52 weeks post-HAART ($r = 0.87$, N = 7, $P < .001$) (data not shown).

To evaluate the impact of RTEs on the recovery of CD4 T cells, we analyzed the magnitude of increases in RTE numbers together with total CD4 T cell increases. Δ RTE, defined as the RTE cell gain over the course of treatment (calculated by subtracting basal values from post-HAART values) was positively correlated with

total Δ CD4 at both 4 weeks and 52 weeks following treatment (r = 0.79, N = 10, *P* = .003 and r = 0.84, N = 10, *P* = .001; respectively) (Figure 1B), highlighting the importance of the RTE population in the reconstitution of CD4 T cells.

Subjects with baseline CD4 T cell counts above 550 cells/μl showed lower viral load (mean of 2.65 ± 0.75 vs. 5.66 ± 0.84 copies/ml (log), Student's *t* test *P* = .004) as well as higher RTE cell counts (mean of 12.2 ± 1.8 vs. 3.8 ± 2.4 cells/μl, Student's *t* test *P* = .001) prior to HAART treatment (Table 1), suggesting that these individuals were not greatly impacted by the virus prior to therapy and therefore did not show recovery in RTE or CD4 T cell counts.

Increased thymic function and CD127 frequencies are associated with RTE reconstitution in HIV-infected subjects receiving HAART.

As mentioned above, our data showed variability in the magnitude of RTE recovery from subject to subject. To gain a better understanding of the factors influencing RTE recovery in HIV-infected individuals under HAART, changes in RTE numbers during follow-up were analyzed in correlation with intrathymic proliferation (as measured by the sj/β TREC ratio), proliferation (as measured by the intracellular expression of the nuclear antigen Ki67) and survival (as measured by cell surface expression of CD127). Our data show a positive association between Δ RTE and the sj/β TREC ratio 52 weeks post-HAART (r = 0.84, N = 7, *P* = .009) (Figure 2*A*), demonstrating that long-term increases in RTE numbers are sustained in individuals with better thymic function. In contrast, we observed a negative correlation between Δ RTE and frequencies of $Ki67^+$ cells within RTEs 52 weeks post-HAART (r = -0.81, N = 10, *P* =.002) (Figure 2*B*). Frequencies of $Ki67^+$ cells within RTEs were also negatively correlated with RTE cell counts 52 weeks post-HAART (r = -0.73, N = 10, *P* =.008) (data not shown), suggesting that peripheral expansion of RTEs could be a mechanism that leads to RTE depletion rather than regeneration in individuals that retained high Ki67 frequencies. We find that RTE gain was also positively associated with the frequencies of $CD127^+$ cells within

RTEs during follow-up (Figure 2*C*), suggesting that an intact IL-7 signaling pathway and increased survival signals impact the magnitude of RTE recovery. Of note, we did not find a significant correlation between age and Δ RTE (r = -0.34, N = 10, *P* = .16) (data not shown).

Role of thymic function versus recirculation and proliferation in short-term and long-term RTE reconstitution in HIV-infected subjects receiving HAART.

We hypothesized that recirculation of RTEs from lymph nodes might be involved in the early and transient increase of RTE cells observed in subjects with baseline CD4 T cell counts above 550 cells/µl. In order to distinguish the mechanisms involved in short-term versus long-term RTE recovery, longitudinal analysis of the frequencies of $CD31^{hi}$ cells amongst naive CD4 T cells simultaneously with RTE cell counts, sj/β TREC ratio and frequencies of $Ki67^{+}$ cells within RTEs was carried out. Lymph nodes were previously shown to contain 2-fold more TRECs than in the peripheral blood (6). Since treatment with HAART significantly reduces virus concentration within lymph nodes (22) and results in TREC increases in the periphery together with decreases in lymph nodes, it is possible that HAART releases sequestered RTEs back into the circulation (23). If the frequencies of RTEs are identical in blood and lymph nodes similarly to what has been reported for TRECs (24), recirculation would increase RTE counts but not their frequencies within naive T cells and would constitute a transient source of new RTE cells. Increased RTE T cell counts as well as RTE frequencies within naive CD4 T cells following HAART could reflect increased RTE output as a result of enhanced thymic function or decreased rate of RTE cell loss.

In figure 3, we show two examples of treated subjects with baseline CD4 T cells < 550 cells/µl (T1-2) in comparison with 2 examples of treated subjects with baseline CD4 T cells > 550 cells/µl (T3-4). T1 and T2 both showed early increases in RTE frequencies and cell counts with concomitant increases in the sj/β TREC ratio. Unlike T1, T2 did not reduce frequencies of $Ki67^{+}$ cells within

RTEs upon HAART and RTE frequencies and cell counts decreased despite continuous increases in the sj/β TREC ratio, suggesting that enhanced thymic function, although crucial, is not the sole determinant in immune reconstitution and that peripheral events such as immune activation also influence RTE recovery. T3 and T4 both showed transient increases in RTE cell counts without increases in the sj/β TREC ratio. Frequencies of $Ki67^+$ cells within RTEs from T3 remained high following treatment with HAART, which may explain the transient increases observed in RTE frequencies and cell counts. T4 had low frequencies of $Ki67^+$ cells within RTEs prior to treatment and did not show increases in RTE frequencies, suggesting recirculation as the most likely source of the observed transient increases in RTE numbers.

Levels of IL-7 but not IFN-α were positively associated with RTE and total CD4 T cell reconstitution.

Pre-HAART IFN-α levels were increased when compared to uninfected controls (mean of 19.99 ± 21.3 vs. 4.29 ± 1.3 pg/ml, P = .045), and levels returned to normal in certain subjects while remaining high in others following treatment with HAART (mean of 15.4 ± 27.3 vs. 4.29 ± 1.3 pg/ml, P = .23) (Figure 4*A*). The Δ IFN-α 52 weeks post-HAART was negatively correlated with the magnitude of increases in RTE numbers (r = - 0.77, N = 10, P = .005) as well as with the magnitude of increases in total CD4 T cell counts (r = - 0.73, N =10, P = .008) (Figure 4B). In addition, Δ IFN-α 52 weeks post-HAART was also negatively correlated with changes in the sj/β TREC ratio (r = - 0.76, N =7, P = .02) (Figure 4C).

Longitudinal analysis revealed increases in the levels of IL-7 4 weeks following onset of HAART (average 1.3–fold increase, P = .01) (Figure 5*A*). Interestingly, these early changes in levels of IL-7 were positively associated with the short-term gain of RTE (r = 0.74, N = 7, P = .028) and CD4 T cell numbers (r = 0.66, N = 7, P = .05) but only in subjects that had reduced their IFN-α levels (Figure 5*B*), suggesting that IFN-α could interfere with IL-7 signaling in RTEs. Higher Δ IL-7

4 weeks post-HAART was also positively correlated with higher RTE counts 52 weeks post-HAART (r = 0.81, N =7, *P* = .012) (data not shown). To determine if the IL-7-mediated increases in RTE numbers occurred through increased proliferation, we investigated the link between levels of IL-7 and frequencies of $Ki67^+$ cells within RTEs in subjects that decreased levels of IFN-α following treatment with HAART (N = 7). We did not detect any correlation between these two parameters at 4 weeks post-HAART (data not shown), but a negative correlation was found between levels of IL-7 52 weeks post-HAART and Ki67 frequencies within RTEs (r = -0.73, N =7, *P* = .031) (Figure 5*C*), indicating that proliferation of RTEs is not the mechanism behind increased RTE numbers. Instead, we detected a positive correlation between levels of IL-7 under HAART and the frequencies of $CD127^+$ cells within RTEs, which was again restricted to subjects that decreased levels of IFN-α after treatment with HAART (r = 0.58, *P* = .018, N = 5 subjects, 13 treated time points) (Figure 5*C*). This suggests that enhanced IL-7/IL-7R signaling following treatment with HAART results in greater rates of immune reconstitution. Of note, we did not detect any association between changes in levels of IL-7 and the sj/β TREC ratio at 4 weeks post-HAART (data not shown), but we did observe a positive correlation between pre-HAART levels of IL-7 and higher sj/β TREC ratio 52 weeks post-HAART (r = 0.71, N = 7, *P* = .036) (Figure S1).

Discussion

The data presented here demonstrate that RTE reconstitution following treatment with HAART is highly variable amongst different subjects and is dependent on both central (thymic activity) and peripheral (homeostasis) events. We show that subjects with baseline CD4 counts above 550 cells/µl exhibited transient increases in RTE numbers 4 weeks post-HAART which seemed to result from recirculation while subjects with CD4 counts below 550 cells/µl showed increases at 4 weeks post-HAART that were maintained 52 weeks post-HAART.

It has been previously proposed that increases in naive T cells occur during the second and slower phase of T cell reconstitution following treatment with HAART in adults with advanced HIV infection (25). However, we detected early increases in RTE cell counts in the majority of subjects, and proceeded to investigate the sources of these increases. Several mechanisms can explain the early and transient increase in RTE numbers observed in subjects with baseline CD4 counts above 550 cells/µl including redistribution from lymphoid tissue to blood or peripheral expansion. It was previously shown that during HIV infection RTEs, as detected by cjTREC quantification, are sequestered within lymphoid tissues, and their levels were positively correlated with the concentration of HIV RNA within the lymph nodes (6). It was therefore postulated that entrapment of RTEs within lymph nodes is a response to the high viral load within these tissue, possibly in order to facilitate differentiation of RTEs into memory T cells. Treatment with HAART reduces viral load and virus replication in lymphoid tissues (26) as well as the frequencies of T cells expressing adhesion molecules (7), and hence promotes the release of T cells back into the circulation. This notion is supported by the findings that 10 weeks post therapy with HAART, a decrease in total lymphocyte numbers was observed in lymph nodes while an increase was found in peripheral blood (7). However, naive T cells are depleted in the lymph nodes during HIV infection (27-28), and although it was reported that that lymph nodes from infected individuals contained 2-fold more TRECs than did PBMCs (6), they still had significantly lower levels of TRECs than those

found in lymph nodes from healthy subjects. Therefore, redistribution would represent a limiting source of new TREC-rich cells into the periphery and could justify the transient increase of RTE numbers observed in certain subjects. Another mechanism for the rapid increases of RTEs post-HAART could be peripheral expansion of RTE subset. Frequencies of $Ki67^+$ cells in RTEs gradually decreased throughout treatment in a significant number of subjects, and in certain treated individuals Ki67 frequencies within RTEs remained high and were even increased. It is possible that suppression of viral load removes the proliferative defects observed in untreated patients and allows for expansion of T cells instead of triggering cell death. However, our data show that proliferation does not constitute a major input of RTEs; on the contrary, we observed an inverse correlation between Ki67 frequencies within RTEs 52 weeks post-HAART and Δ RTE. It is unlikely that this negative association reflects a homoeostatic attempt at replenishing the RTE cell pool through proliferation since our data fail to show a positive link between levels of IL-7 (the major cytokine involved in naive T cell homeostasis) and Ki67 frequencies.

The difference we observed in the proliferative role of IL-7 in untreated subjects (Chapter 2) versus treated patients can be explained by the findings that IL-7 enhances proliferation in response to TCR-triggering (29) and that IL-7, in concert with TCR signals, activates naive T cells during lymphopenia (30). Therefore, the specific effect of IL-7 on RTEs could vary dependent on the presence or absence of viral antigens and the severity of the CD4 T cell depletion. Elevated frequencies of $Ki67^+$ cells within RTEs observed in a subset of HAART-treated individuals could instead reflect chronic immune activation, which would account for the fact these subjects experienced decreases in RTE cell counts despite increases in the sj/β TREC ratio. This notion is supported by the findings of a negative correlation between Ki67 and CD127 frequencies within RTEs post-HAART ($r = -.066$, $P = .05$, data now shown). It was previously reported that high frequencies of $CD4^+Ki67^+$ (31) and CD4 naive $Ki67^+$ T cells (4) is a feature of immunological non-responders to HAART treatment. Chronic immune

activation, as reflected by high CD38 or Ki67, in the absence of detectable viremia has been associated with increased cellular viral load (32) and has been proposed to be driven by altered gut permeability (31, 33). Microbial translocation has been suggested as a feature of immunological non-responders due to their higher levels of LPS (31). Increased levels of IFN-α are also associated with inflammation and chronic immune activation (33), and the inverse correlation we detected between high levels of IFN-α and low Δ RTE could reflect increased apoptosis as a result of activation-induced cell death. The fact that elevated levels of IFN-α impeded recovery of RTEs in HAART-treated subjects despite them having high levels of IL-7 and that correlations between levels of IL-7 and Δ RTE as well as with frequencies of $CD127^+$ cells within RTEs were only detected in subjects that decreased levels of IFN-α post-HAART suggests that IFN-α counteracts IL-7/IL-7R-mediated signaling within RTE cells. This hypothesis is supported by previous studies demonstrating that IFN-α inhibits the IL-7-mediated growth of immature B cells and induces Bcl-2 down-regulation and cell death (34). In addition, we also detected a negative correlation between changes in the levels of IFN-α and changes in the sj/β TREC ratio, suggesting an inhibitory effect for IFN-α on thymic function. IFN-α has previously been shown to have anti-proliferative effects on immature thymocytes and to reduce thymic cellularity following injection into mice (16). IFN-α producing pDCs have been isolated from the thymus (35), and humanized mice were found to secrete high levels of IFN-α in response to HIV infection (36), suggesting that high levels of IFN-α could be detected in the thymus as well as in the periphery and could very well impair T cell development.

We also noticed that subjects that increased the sj/βTREC ratio, a robust measure of thymic function, showed early increases in RTE cell counts that were generally accompanied by long-term RTE recovery. This is in agreement with a previous study that detected increases in thymic volume and TREC-bearing cells per millilitre after 12 weeks of HAART (37). The positive correlation observed between changes in the sj/β TREC ratio and changes in RTE cell counts 52 weeks

post-HAART as well as the positive association between changes in Δ RTE cell counts and Δ total CD4 T cell counts highlights the impact of effective thymic function in T cell regeneration and confirms previous work demonstrating larger thymic size (3) and a higher sj/β TREC ratio (4) distinguished immunological responders (IR) from immunological non responders (INR). Our data also indicate that up-regulation of CD127 within RTEs following treatment with HAART is a mechanism involved during long-term RTE recovery and possibly also participates in the observed early RTE number increases by reducing cell death and resulting in an accumulation of TREC-rich T cells. These findings indicate that optimal T cell reconstitution involves both effective output of RTEs by the thymus as well as the ability of RTEs to receive and translate survival signals within their peripheral niche. Poor reconstitution of naive T cell numbers due to low CD127 and Bcl-2 expression levels have been also observed in other immune reconstitution settings such as following allogeneic hematopoietic stem cell transplantation (38).

Material and Methods

Patients and control individuals

Blood or leukapheresis samples were obtained from 10 healthy adult donors and 10 treated HIV-infected patients. Treated HIV-infected individuals were sampled in the acute/early phase of infection and followed-up for 1 year. The clinical specifications of each subject are listed in table S1. All samples were obtained with the informed consent of the subjects and according to the guidelines of the bioethical committee of Centre hospitalier de l'Université de Montreal (CHUM) and McGill University Health Center (MUHC).

Surface and intracellular staining by flow cytometry

Frozen PBMCs were stained simultaneously with the following mAbs for the detection of cell proliferation: FITC labeled anti-Ki67 (BD Pharmingen), PE labeled anti-CD31 (BD Pharmingen), APC-Cy7 labeled anti-CD45RA (BD Pharmingen), PECy7 labeled anti-CCR7 (BD Pharmingen), APC labeled anti-PD-1 (BD Pharmingen), Alexa-700 labeled anti-CD27 (eBioscience) Pacific Blue labeled anti-CD4 (BD Pharmingen) and Amcyan labeled anti-CD3 (BD Pharmingen). For the detection of cell survival, the following mAbs were used: PECy5 labeled anti-CD127 (eBioscience), PE labeled anti-CD31 (BD Pharmingen), APC-Cy7 labeled anti-CD45RA (BD Pharmingen), PECy7 labeled anti-CCR7 (BD Pharmingen), APC labeled anti-PD-1 (BD Pharmingen), Alexa-700 labeled anti-CD27 (eBioscience) Pacific Blue labeled anti-CD4 (BD Pharmingen) and Amcyan labeled anti-CD3 (BD Pharmingen).

Intracellular staining was carried out following surface staining, though the incubation of the permeabilized cells with mAb directed against Ki-67 (Becton Dickinson, Pharmingen) or its respective isotype control in the dark at room temperature for 30 minutes. The cells were then washed of the excess antibody, fixed in 2% FA. Data was acquired on a Becton Dickinson LSR II^{TM} system through 8- or 9-color flow cytometry and analyzed using the DiVa^{TM} software (Becton Dickinson systems).

TREC quantification

Quantification of sj and DJβ TRECs together with the CD3γ chain (used as a housekeeping gene) was performed for 7 HAART-treated HIV-infected individuals using the LightCycler technology (Roche Diagnostics, Mannheim, Germany), as previously described (4, 39). PBMCs were lysed in Tris (10 mM, pH 8.2) Tween-20 (0.05%), NP-40 (0.05%), and Proteinase K (100 μg/mL) for 30 minutes at 56°C and then 15 minutes at 98°C. Multiplex polymerase chain reaction (PCR) was performed for sjTREC or each of the 10 DβJβ TRECs, together with the CD3γ chain (10 minutes initial denaturation at 95°C, 30 seconds at 95°C, 30 seconds at 60°C, 2 minutes at 72°C for 22 cycles) using outer 3'/5' primer pairs. PCR conditions in the LightCycler experiments, performed on 1/100th of the initial PCR, were as follows: 1 minute initial denaturation at 95°C, 1 second at 95°C, 10 seconds at 60°C, 15 seconds at 72°C for 40 cycles. Fluorescence measurements were performed at the end of the elongation steps. TRECs and CD3γ LightCycler quantifications were performed in independent experiments, but on the same first-round, serially diluted standard curve. The sjTRECs were quantified in triplicate, while individual DβJβ TRECs were quantified in duplicate for all studied samples. The sum of DJβTREC frequencies is calculated as 1.3-fold the sum of the 10 measured DJβTREC frequencies (to extrapolate to the 13 principal DβJβ TRECs). The sj/βTREC ratio is the sjTREC frequency divided by the sum of DJβTREC frequencies (sj/β TREC = sjTREC/sum DJβ TRECs).

Quantification of IL-7 and IFN-α

IL-7 and IFN-α levels were quantified in plasma from 10 healthy controls and 8 untreated HIV-infected individuals using the high sensitivity IL-7 Quantikine HS ELISA kit (R&D Systems) and the IFN-alpha Multi-Subtype ELISA Kit (R&D Systems) according to manufacturer's instructions. Samples were assayed in duplicate.

Statistics

Statistical analysis (two-tailed Student's *t* test, Pearson correlation test, *r*, and *P* values) was performed using MS Excel and the Vassar college website. An *r* value ≥ 0.4 or ≤ -0.4, and a *P* value ≤ 0.05, were considered significant.

Bibliography

1. Aiuti, F. and L. Mezzaroma, Failure to reconstitute CD4+T-cells despite suppression of HIV replication under HAART. Aids Reviews, 2006. 8(2): p. 88-97.

2. Schacker, T.W., et al., Measurement of naive CD4 cells reliably predicts potential for immune reconstitution in HIV. J Acquir Immune Defic Syndr, 2010. 54(1): p. 59-62.

3. Teixeira, L., et al., Poor CD4 T cell restoration after suppression of HIV-1 replication may reflect lower thymic function. AIDS, 2001. 15(14): p. 1749-56.

4. Dion, M.L., et al., Slow disease progression and robust therapy-mediated CD4+ T-cell recovery are associated with efficient thymopoiesis during HIV-1 infection. Blood, 2007. 109(7): p. 2912-20.

5. Di Mascio, M., et al., Naive T-cell dynamics in human immunodeficiency virus type 1 infection: effects of highly active antiretroviral therapy provide insights into the mechanisms of naive T-cell depletion. J Virol, 2006. 80(6): p. 2665-74.

6. Nokta, M.A., et al., Entrapment of recent thymic emigrants in lymphoid tissues from HIV-infected patients: association with HIV cellular viral load. AIDS, 2002. 16(16): p. 2119-27.

7. Bucy, R.P., et al., Initial increase in blood CD4(+) lymphocytes after HIV antiretroviral therapy reflects redistribution from lymphoid tissues. J Clin Invest, 1999. 103(10): p. 1391-8.

8. Tan, J.T., et al., IL-7 is critical for homeostatic proliferation and survival of naive T cells. Proc Natl Acad Sci U S A, 2001. 98(15): p. 8732-7.

9. Fry, T.J., et al., A potential role for interleukin-7 in T-cell homeostasis. Blood, 2001. 97(10): p. 2983-90.

10. Napolitano, L.A., et al., Increased production of IL-7 accompanies HIV-1-mediated T-cell depletion: implications for T-cell homeostasis. Nat Med, 2001. 7(1): p. 73-9.

11. Bai, F., et al., Reduced CD127 expression on peripheral CD4+ T cells impairs immunological recovery in course of suppressive highly active antiretroviral therapy. AIDS, 2010. 24(16): p. 2590-3.

12. Pallard, C., et al., Distinct roles of the phosphatidylinositol 3-kinase and STAT5 pathways in IL-7-mediated development of human thymocyte precursors. Immunity, 1999. 10(5): p. 525-35.

13. Beq, S., et al., IL-7 induces immunological improvement in SIV-infected rhesus macaques under antiviral therapy. J Immunol, 2006. 176(2): p. 914-22.

14. Mackall, C.L., et al., IL-7 increases both thymic-dependent and thymic-independent T-cell regeneration after bone marrow transplantation. Blood, 2001. 97(5): p. 1491-7.

15. Boasso, A. and G.M. Shearer, Chronic innate immune activation as a cause of HIV-1 immunopathogenesis. Clin Immunol, 2008. 126(3): p. 235-42.

16. Lin, Q., C. Dong, and M.D. Cooper, Impairment of T and B cell development by treatment with a type I interferon. J Exp Med, 1998. 187(1): p. 79-87.

17. Lachgar, A. and B. Bizzini, Involvement of alpha-interferon in HIV-1 induced immunosuppression. A potential target for AIDS prophylaxis and treatment. Biomed Pharmacother, 1994. 48(2): p. 73-7.

18. Zagury, D., et al., Interferon alpha and Tat involvement in the immunosuppression of uninfected T cells and C-C chemokine decline in AIDS. Proc Natl Acad Sci U S A, 1998. 95(7): p. 3851-6.

19. Boasso, A., et al., HIV-induced type I interferon and tryptophan catabolism drive T cell dysfunction despite phenotypic activation. PLoS One, 2008. 3(8): p. e2961.

20. Mandl, J.N., et al., Divergent TLR7 and TLR9 signaling and type I interferon production distinguish pathogenic and nonpathogenic AIDS virus infections. Nat Med, 2008. 14(10): p. 1077-87.

21. Herbeuval, J.P., et al., Differential expression of IFN-alpha and TRAIL/DR5 in lymphoid tissue of progressor versus nonprogressor HIV-1-infected patients. Proc Natl Acad Sci U S A, 2006. 103(18): p. 7000-5.

22. Notermans, D.W., et al., Decrease of HIV-1 RNA levels in lymphoid tissue and peripheral blood during treatment with ritonavir, lamivudine and zidovudine. Ritonavir/3TC/ZDV Study Group. AIDS, 1998. 12(2): p. 167-73.

23. Diaz, M., et al., T cells containing T cell receptor excision circles are inversely related to HIV replication and are selectively and rapidly released into circulation with antiretroviral treatment. AIDS, 2003. 17(8): p. 1145-9.

24. Douek, D.C., et al., Changes in thymic function with age and during the treatment of HIV infection. Nature, 1998. 396(6712): p. 690-5.

25. Autran, B., et al., Positive effects of combined antiretroviral therapy on CD4+ T cell homeostasis and function in advanced HIV disease. Science, 1997. 277(5322): p. 112-6.

26. Cavert, W., et al., Kinetics of response in lymphoid tissues to antiretroviral therapy of HIV-1 infection. Science, 1997. 276(5314): p. 960-4.

27. Zhang, Z.Q., et al., Kinetics of CD4+ T cell repopulation of lymphoid tissues after treatment of HIV-1 infection. Proc Natl Acad Sci U S A, 1998. 95(3): p. 1154-9.

28. Schacker, T.W., et al., Lymphatic tissue fibrosis is associated with reduced numbers of naive CD4+ T cells in human immunodeficiency virus type 1 infection. Clin Vaccine Immunol, 2006. 13(5): p. 556-60.

29. Bazdar, D.A. and S.F. Sieg, Interleukin-7 enhances proliferation responses to T-cell receptor stimulation in naive CD4+ T cells from human immunodeficiency virus-infected persons. J Virol, 2007. 81(22): p. 12670-4.

30. Murali-Krishna, K. and R. Ahmed, Cutting edge: naive T cells masquerading as memory cells. J Immunol, 2000. 165(4): p. 1733-7.

31. Piconi, S., et al., Immune activation, apoptosis, and Treg activity are associated with persistently reduced CD4+ T-cell counts during antiretroviral therapy. AIDS, 2010. 24(13): p. 1991-2000.

32. Marchetti, G., et al., Comparative analysis of T-cell turnover and homeostatic parameters in HIV-infected patients with discordant immune-virological responses to HAART. AIDS, 2006. 20(13): p. 1727-36.

33. Brenchley, J.M., et al., Microbial translocation is a cause of systemic immune activation in chronic HIV infection. Nat Med, 2006. 12(12): p. 1365-71.

34. Wang, J., et al., Resident bone marrow macrophages produce type 1 interferons that can selectively inhibit interleukin-7-driven growth of B lineage cells. Immunity, 1995. 3(4): p. 475-84.

35. Bendriss-Vermare, N., et al., Human thymus contains IFN-alpha-producing CD11c(-), myeloid CD11c(+), and mature interdigitating dendritic cells. J Clin Invest, 2001. 107(7): p. 835-44.

36. Gurney, K.B., et al., Endogenous IFN-alpha production by plasmacytoid dendritic cells exerts an antiviral effect on thymic HIV-1 infection. J Immunol, 2004. 173(12): p. 7269-76.

37. Ruiz-Mateos, E., et al., Endogenous IL-7 is associated with increased thymic volume in adult HIV-infected patients under highly active antiretroviral therapy. AIDS, 2003. 17(7): p. 947-54.

38. Poulin, J.F., et al., Evidence for adequate thymic function but impaired naive T-cell survival following allogeneic hematopoietic stem cell transplantation in the absence of chronic graft-versus-host disease. Blood, 2003. 102(13): p. 4600-7.

39. Dion, M.L., et al., HIV infection rapidly induces and maintains a substantial suppression of thymocyte proliferation. Immunity, 2004. 21(6): p. 757-68.

Figure Legends

Figure 1. Impact of RTEs on total CD4 T cell reconstitution following HAART. (A) Representative FACS histograms of CD31 expression within CD4 naive T cells are shown for a subject with baseline CD4 T cell counts > 550 cells/µl and a subject with baseline CD4 T cell counts < 550 cells/µl. Grey lines represent baseline CD31 expression, thin black lines represent CD31 expression 4 weeks post-HAART and thick black lines represent CD31 expression 52 weeks post-HAART (*Upper panel).* Longitudinal assessment of RTE numbers at baseline, 4 weeks and 52 weeks post-HAART for subjects with baseline CD4 T cell counts > 550 cells/µl (N=3) and subjects with baseline CD4 T cell counts < 550 cells/µl (N=7). Bars represent standard deviations (*Lower panel).* (B) The changes RTE cell counts 4 and 52 weeks post-HAART were measured in correlation with CD4 T cell counts (cell/µl) 4 and 52 weeks post-HAART.

Figure 2. Thymic function, immune activation as well as survival of RTEs influence the magnitude of increases in RTE numbers post-HAART. (A) Correlation between Δ RTE numbers and the sj/β TREC ratio measured at 52 weeks post-HAART in 7 subjects. (B) Correlation between Δ RTE numbers and frequencies of $Ki67^+$ cells within RTEs measured at 52 weeks post-HAART in all 10 subjects. (C) Correlation between Δ RTE numbers and frequencies of $CD127^+$ cells within RTEs measured at consecutive time points post-HAART in 5 subjects.

Figure 3. Representative examples of longitudinal analysis of RTEs together with measurement of thymic function and peripheral proliferation. Two examples are shown for subjects with baseline CD4 T cell counts > 550 cells/µl as well as subjects with baseline CD4 T cell counts < 550 cells/µl. RTE numbers (■) were analyzed in parallel with RTE frequencies within naive CD4 T cells (◆). Frequencies of $Ki67^+$ cells within RTEs (●) were analyzed in parallel with the sj/β TREC ratio (▲)

Figure 4. Impact of IFN-α levels post-HAART on changes in RTE and CD4 T cell numbers and in the sj/β TREC ratio. (A) Levels of IFN-α at baseline and 52 weeks post-HAART from the 10 HAART-treated HIV-infected subjects were compared to 20 healthy controls. (B) Correlation between Δ IFN-α levels and Δ RTE numbers measured at 52 weeks post-HAART (N= 10) as well as between Δ IFN-α levels and Δ CD4 numbers measured at 52 weeks post-HAART (N= 10). (C) Correlation between Δ IFN-α levels and Δ sj/β TREC ratio numbers measured at 52 weeks post-HAART (N= 10).

Figure 5. Role for IL-7 in immune reconstitution following HAART. (A) Longitudinal assessment of IL-7 levels for each of the 10 HAART-treated HIV-infected subjects at 4 weeks and 52 weeks post-HAART. (B) Correlation between Δ IL-7 levels and Δ RTE numbers 4 weeks post-HAART as well as Δ IL-7 levels and Δ CD4 numbers 4 weeks post-HAART in subjects that showed a negative Δ IFN-α (N=7). (C) Correlation between frequencies of $Ki67^+$ cells within RTEs and Δ IL-7 in subjects that showed a negative Δ IFN-α (N=7) as well as between frequencies of $CD127^+$ cells within RTEs and Δ IL-7 at 52 weeks post-HAART (N=13 treated time points corresponding to 4 subjects which showed a negative Δ IFN-α and for which CD127 measurements were performed).

Figure S1. Impact of the levels of IL-7 prior to HAART treatment on thymic function post-HAART. Levels of IL-7 prior to HAART treatment were assessed in correlation with the sj/β TREC ratio at 52 weeks post-HAART.

Figure 1

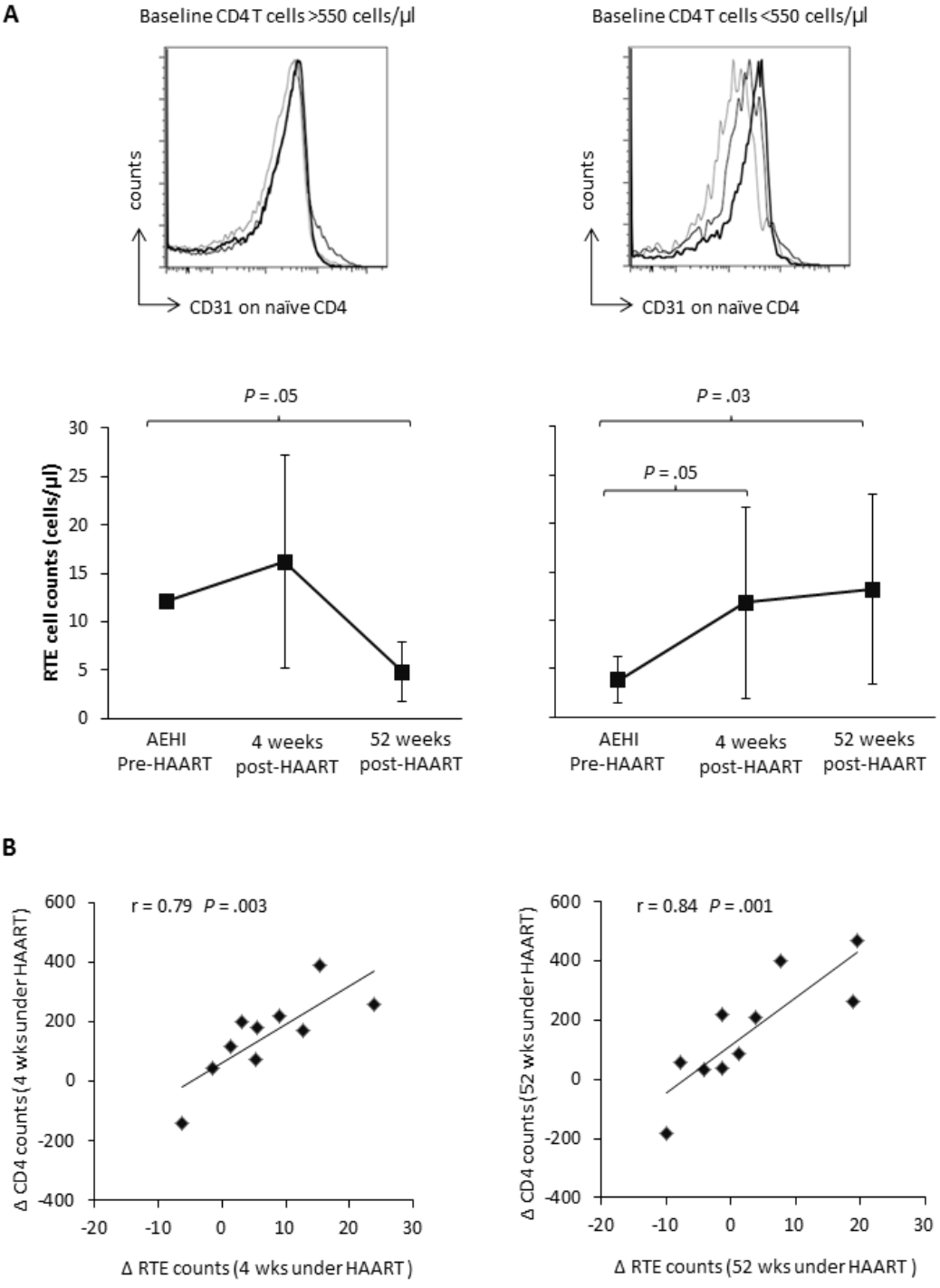
A
Baseline CD4 T cells >550 cells/µl
Baseline CD4 T cells <550 cells/µl
counts
CD31 on naïve CD4
P = .05
P = .03
RTE cell counts (cells/µl)
AEHI Pre-HAART
4 weeks post-HAART
52 weeks post-HAART
B
r = 0.79 P = .003
r = 0.84 P = .001
Δ CD4 counts (4 wks under HAART)
Δ CD4 counts (52 wks under HAART)
Δ RTE counts (4 wks under HAART)
Δ RTE counts (52 wks under HAART)

Table 1. Baseline demographic and immuno-virological characteristics of HAART-treated HIV+ individuals according to baseline CD4 T cell counts

	Subjects with baseline CD4 > 550 cells/µl (N = 3)	Subjects with baseline CD4 < 550 cells/µl (N = 7)	*P*
Age (years)	34 ± 10	41 ± 10	0.427
Baseline RTE levels	12.2 ± 1.8	3.8 ± 2.4	0.001
Baseline VL (log)	2.65 ± 0.75	5.66 ± 0.84	0.004
Baseline IL-7 levels (pg/ml)	7.9 ± 1.9	9.6 ± 3	0.331
Baseline IFN-a levels (pg/ml)	32.5 ± 38.6	14.6 ± 8.5	0.507

Figure 2

A

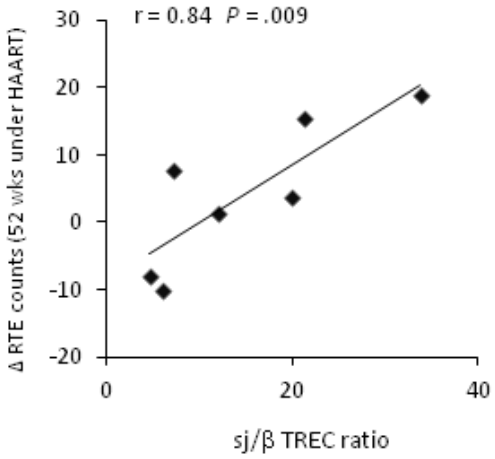
r = 0.84 P = .009
Δ RTE counts (52 wks under HAART)
sj/β TREC ratio

B

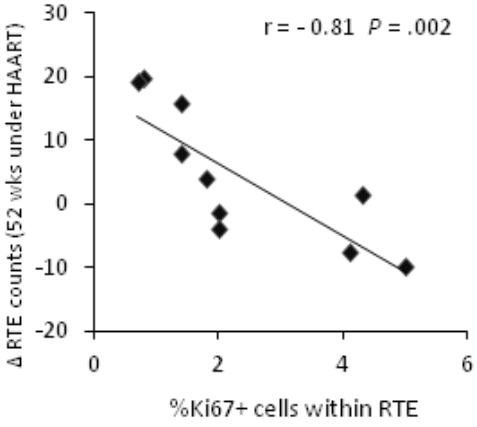
r = - 0.81 P = .002
Δ RTE counts (52 wks under HAART)
%Ki67+ cells within RTE

C

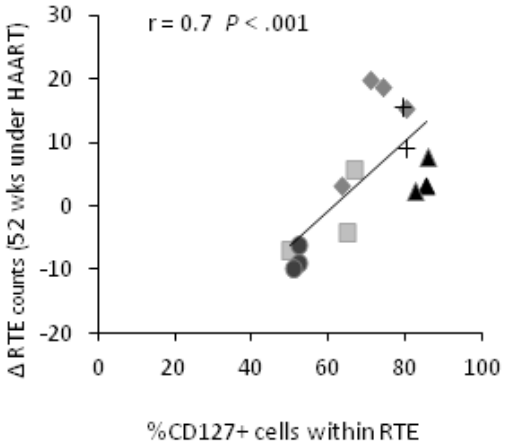
r = 0.7 P < .001
Δ RTE counts (52 wks under HAART)
%CD127+ cells within RTE

Figure 3

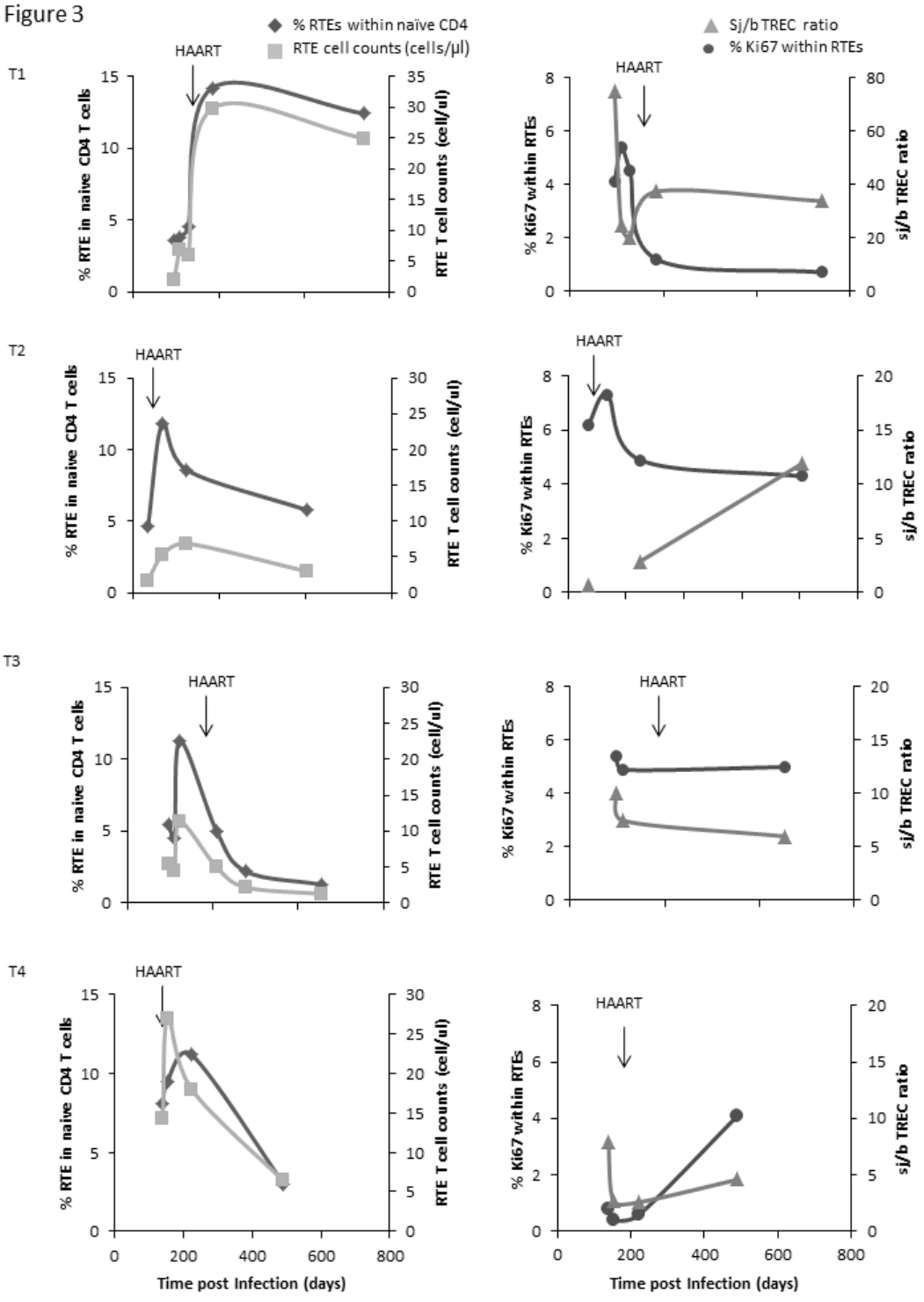
% RTEs within naïve CD4
RTE cell counts (cells/µl)
Sj/b TREC ratio
% Ki67 within RTEs
HAART
T1
T2
T3
T4
% RTE in naive CD4 T cells
RTE T cell counts (cell/ul)
% Ki67 within RTEs
sj/b TREC ratio
Time post Infection (days)

Figure 4

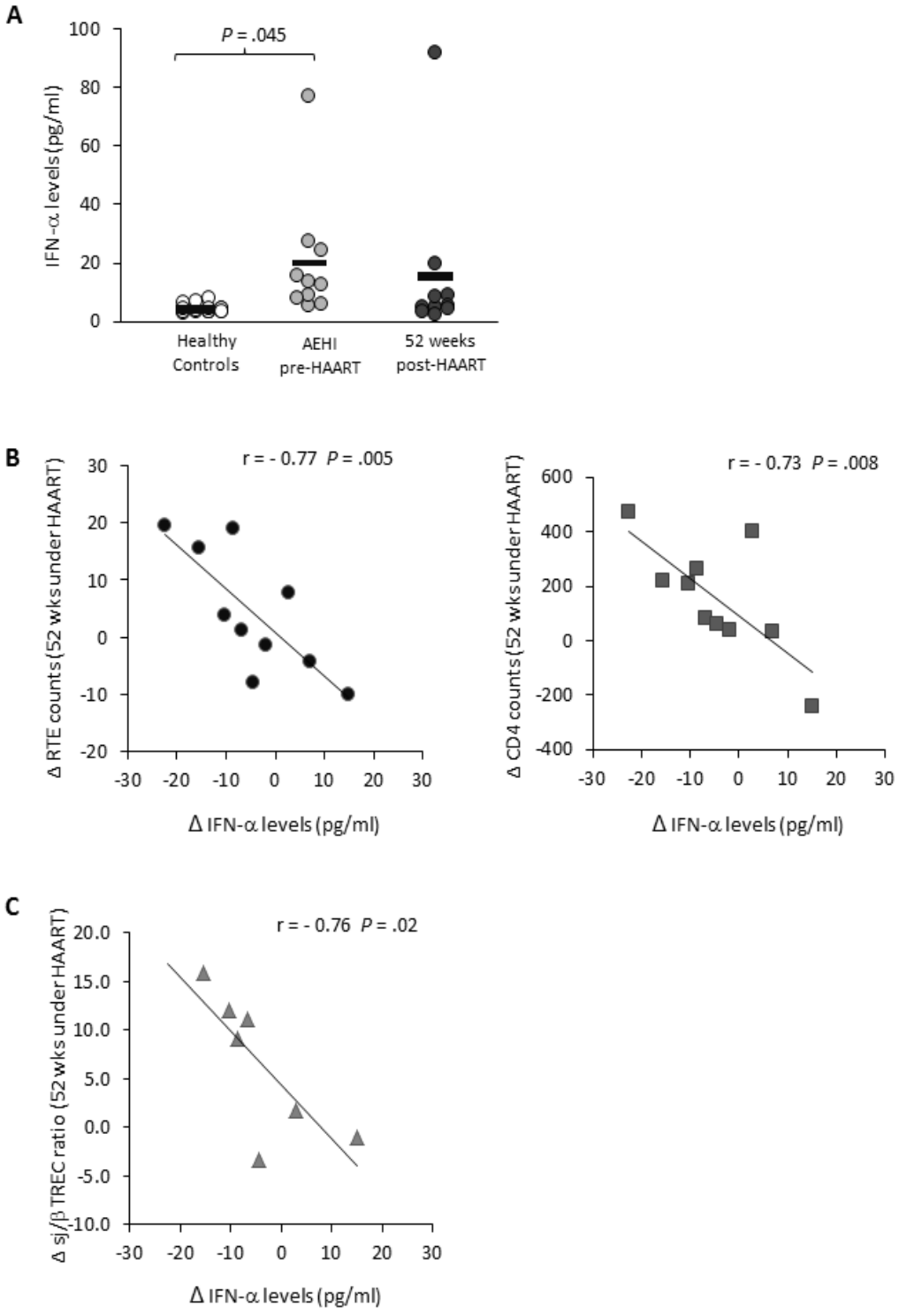
A
P = .045
IFN-α levels (pg/ml)
100
80
60
40
20
0
Healthy Controls
AEHI pre-HAART
52 weeks post-HAART
B
r = - 0.77 P = .005
Δ RTE counts (52 wks under HAART)
Δ IFN-α levels (pg/ml)
r = - 0.73 P = .008
Δ CD4 counts (52 wks under HAART)
Δ IFN-α levels (pg/ml)
C
r = - 0.76 P = .02
Δ sj/β TREC ratio (52 wks under HAART)
Δ IFN-α levels (pg/ml)

Figure 5

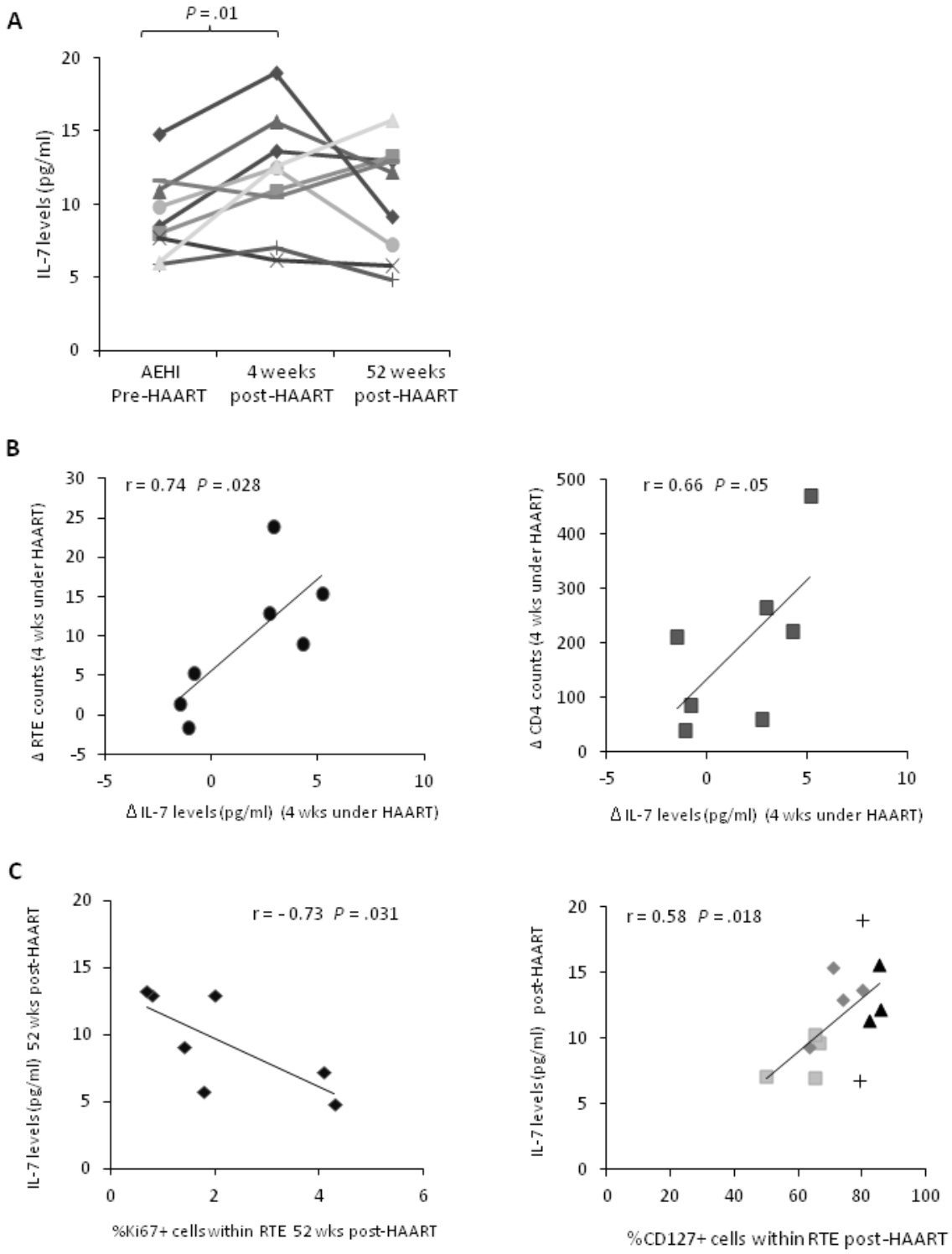
A
P = .01
IL-7 levels (pg/ml)
AEHI Pre-HAART
4 weeks post-HAART
52 weeks post-HAART
B
r = 0.74 P = .028
Δ RTE counts (4 wks under HAART)
Δ IL-7 levels (pg/ml) (4 wks under HAART)
r = 0.66 P = .05
Δ CD4 counts (4 wks under HAART)
Δ IL-7 levels (pg/ml) (4 wks under HAART)
C
r = - 0.73 P = .031
IL-7 levels (pg/ml) 52 wks post-HAART
%Ki67+ cells within RTE 52 wks post-HAART
r = 0.58 P = .018
IL-7 levels (pg/ml) post-HAART
%CD127+ cells within RTE post-HAART

Table S1: Characteristics of HAART-treated subjects infected during AEHI

Patient	Age	Time P.I (days) *	Baseline CD4 count	Δ CD4	Baseline Viral Load (log)	On HAART Viral load (log)	Baseline RTE counts	Δ RTE	Treatment **
T1	24	36	90	470	5.72	1.7	1.3	19.5	I LPV + RTV/ II ATZ + RTV
T2	33	140	460	265	5.59	1.7	6	18.9	III EFV/I DLV
T3	38	140	320	400	5.45	1.7	2.8	7.7	III IDV
T4	41	97	271	209	5.12	1.7	3.6	3.9	III IDV
T5	53	40	540	220	6.65	1.7	8	15	IV RTV/IV IDV
T6	44	159	840	59	3.23	1.7	14.2	-7.8	IV IDV
T7	45	65	357	85	6.76	1.7	1.7	1.3	IV RTV
T8	52	151	281	38	4.35	1.7	3.2	-1.4	IV NVP
T9	36	36	956	34	2.93	1.7	11	-4.2	IV RTV + SQV
T10	24	77	560	-240	1.80	1.7	11.3	-10	IV IDV

•Elapsed time between the sampling date and date of infection. This date was estimated based on the AIEDRP 2002 guidelines

** All patients were treated with a combination of two reverse transcriptase inhibitors (RTI) along with various protease inhibitors (PI). Changes are indicated by a slash (/). Treatment abbreviations:

RTI I. Emtricitabine + Tenofovir (TDF)
II. Lamivudine (3TC) + Tenofovir (TDF)
III. Lamivudine (3TC) + Zidovudine (AZT)
IV. Lamivudine (3TC) + Stavudine (d4T)

PI Lopinavir (LPV); Ritonavir (RTV); Atazanavir (ATZ); Efavirenz (EFV); Delavirdine (DLV); Indivavir (IDV); Saquinavir (SQV)

Figure S1

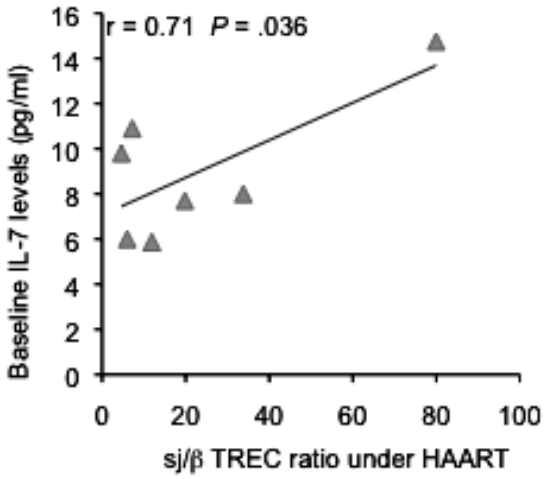
r = 0.71 P = .036
Baseline IL-7 levels (pg/ml)
16
14
12
10
8
6
4
2
0
0
20
40
60
80
100
sj/β TREC ratio under HAART

In Chapter 3, we have identified a role for enhanced intrathymic proliferation versus increased cell cycle entry of RTEs in the long-term recovery of RTEs following treatment with HAART. Restoration of the magnitude of the RTE cell pool post-HAART was correlated with the magnitude of CD4 T cell reconstitution.

We also demonstrated that the levels of IL-7 measured four weeks post-HAART correlated with the magnitude of RTE recovery. However, this effect was only observed in subjects that had decreased their levels of IFN-α following treatment with HAART. This, together with the finding of a negative association between failure to reduce levels of IFN-α post-HAART and levels of intrathymic proliferation, as measured by the sj/β TREC ratio, suggested that IFN-α could interfere with the survival-mediated effects of IL-7 on RTEs as well as with the IL-7- and/or pre-TCR-mediated expansion of thymic progenitors.

The vast majority of intrathymic proliferation occurs in TCR β-selected thymocytes. Therefore, identifying a phenotype that would permit the isolation of thymocytes undergoing β-selection by flow cytometry is crucial to the understanding of the role that IFN-α might exert on thymic function.

Overall, in Chapter 4, we will isolate pre-β-selected and post-β-selected thymocytes from human thymic tissues and use the OP9-DL1 culture system, an *in vitro* system that supports differentiation of human thymocytes, to characterize the point of αβ and γδ lineage divergence and to determine molecular factors that are induced following β-selection in humans.

CHAPTER 4.

CD31 and CD1a identify human β-selected thymocytes and delineate cells committed to the αβ lineage

Joumana Zeidan (1,2,3), Lionel Filion (4), Rebeka Bordi (2,3), Geneve Awong (5), Mohamed El-Far (2), Bader Yassine-Diab (2), Ali Fellali (3), Sylvain Gimmig (2), Elias K. Haddad (2,3,6), Juan Carlos Zúñiga-Pflücker (5) and Rafick-Pierre Sekaly (1,2,3,6)*.

1) *Dept. of Microbiology and Immunology, McGill University, Montreal, Quebec, Canada* 2) *Laboratoire d'Immunologie, CHUM Research Center, Montreal, Quebec, Canada,* 3) *Vaccine and Gene Therapy Institute of Florida Corp, Florida, USA, 4) Dept. of Biochemistry Microbiology and Immunology, University of Ottawa, Ottawa, Ontario, Canada, 5) Department of Immunology, University of Toronto, Toronto, Canada, 6*) *Dept. Microbiologie et Immunologie, Université de Montreal, Montreal, Quebec, Canada.*

*****Corresponding author:
Dr. Rafick-Pierre Sekaly
Vaccine & Gene Therapy Institute Florida
11350 SW Village Pkwy, 3rd Floor
Port St. Lucie, FL 34987
Telephone Number: 772-345-4785
Fax Number: 772-345-3675
Email: sekaly@vgti-fl.org

Abstract

T cell lineage specification is characterized by successive developmental stages that generate mature αβ and γδ T cells. The first TCR-dependent checkpoint determining β-selection is not well described in humans due to a lack of specific cell surface markers. Extensive phenotypic analysis of *ex vivo* $CD3^-$ thymocytes demonstrated that down-regulation of CD31 together with CD1a up-regulation identified immature single positive (ISP) *and* early double positive (EDP) subsets that were enriched for intracellular (ic) T cell receptor β-chain (TCRβ). Flow cytometry analysis revealed that $CD31^-CD1a^{hi}$ $CD3^-$ subsets were activated (as measured by the up-regulation of CD28 and PD-1) and cycling (as measured by Ki67). Gene expression analysis confirmed β-selection of $CD31^-CD1a^{hi}$ ISP and EDP thymocytes versus the unselected $CD31^+CD1a^{low}$ ISP and EDP thymocytes by highlighting changes of expression in genes regulating proliferation (such as Cyclin D3, Cpeb4, GADD45a, and SOCS-1), gene rearrangements (HEB and RAG enzymes), as well as in several candidate genes involved in the Notch signaling pathway (Notch-1, Notch-3, HES-1, pTα and c- myc). Coculture with the Notch-ligand presenting OP9-DL1 stromal cells confirmed that $CD31^+CD1a^{low}$ ISP and EDP thymocytes were the uncommitted precursors to both the αβ- and γδ-lineages, albeit they differentiated primarily into $TCR\gamma\delta^+$ DN cells. Specific isolation of the $CD31^-CD1a^{hi}$ β-selected thymocytes revealed that β-selection ensures αβ-lineage commitment and rapid differentiation into $TCR\alpha\beta^+$ DP and SP cells. Together, these findings pinpoint the stage of TCRαβ and TCRγδ lineage divergence and are compatible with an instructive model of human intrathymic development in which the γδ-lineage is the default pathway of differentiation.

Introduction

T cell development occurs through a series of phenotypically distinct stages. In the human thymus, developmental stages are monitored by expression of cell surface markers (CD34, CD1a, CD4, CD8α, CD8β and CD3). The most immature cells do not express CD4 and CD8 and therefore are called double negative (DN). This stage can be further subdivided using the markers CD34 and CD1a (1). The earliest precursors express CD34, but have not acquired CD1a, and retain the potential to differentiate into cells of the myeloid and erythroid lineage (2). Acquisition of CD1a ($CD34^+CD1a^+$) defines an irreversible commitment to the T cell lineage and acquisition of a T cell specific gene expression program (2). Thymocyte maturation occurs via a CD4 immature single positive (ISP) intermediate (3) before up-regulating CD8β to become early double positive thymocytes (EDP) (4) and CD8β, resulting in $CD3^-$ DP thymocytes. Double positive thymocytes up-regulate CD3 to become the first cells to express a functional αβ T cell receptor (TCR). Positive selection on MHC class I or II and intrathymic cytokines dictate lineage choice and survival of mature CD8 and CD4 single positive (SP) thymocytes respectively (5).

The first checkpoint in T cell development is β-selection, during which a functionally rearranged TCRβ chain pairs with the pre-TCRα protein forming the pre-TCR. Since DP thymocytes are refractory to IL-7 prosurvival cytokine, they are dependent on signals downstream of the TCR for survival and clonal expansion (6, 7). Cells with non-productive TCRβ rearrangements do not form a pre-TCR and do not undergo further maturation (6). In mice, β-selection occurs at the DN3 ($CD44^-CD25^+$) stage of development, resulting in rapid down-regulation of CD25 leading to DN4 ($CD44^-CD25^-$), followed by up-regulation of CD4 and CD8 leading to DP thymocytes (8), the immediate precursors of $CD4^+$ $TCR\alpha\beta^+$ and $CD8^+$ $TCR\alpha\beta^+$ mature SP thymocytes (9). CD27 expression has been shown to identify post-β-selected thymocytes within the DN3 compartment (DN3b) (10) and is useful in distinguishing the earliest emerging αβ and γδ T cells from

unselected DN3 cells thereby allowing the identification of factors regulating the αβ and γδ lineages (10). More recently, the DN3 population was further subdivided by the expression of CD28 and CD25 (11). While the up-regulation of both CD27 and CD28 differentiated DN3b from DN3a, CD28 expression identified a more mature β-selected subset (DN3c) that was intermediate for CD25 and consisted of the first DN3 population that could give rise to DP thymocytes following coculture with OP9-DL1 stromal cells (11).

Beta-selection is not fully characterized in humans due to the fact that specific cell surface markers characterizing this process have not been identified. Consequently, little is known about the development stage from which the αβ and γδ lineages diverge and genetic programs that underlie these different developmental pathways. The detection of intracellular (ic) TCRβ has yielded controversial results; one study proposed that β-selection occurs at the EDP to $CD3^-$DP transition (12) while other studies have suggested that selection begins earlier at the ISP or $CD1a^+$ DN stage (13, 14). More recently, a study has shown that β-selection and γδ-lineage commitment both take place within DN, ISP and EDP populations with the frequencies of β-selected thymocytes increasing, and γδ potential decreasing, as thymocytes progress from the DN to the EDP stage (14).

In order to more precisely identify the β-selection checkpoint in humans we first isolated specific cell populations to characterize surface markers that are modulated during β-selection that differentiate αβ and γδ lineage divergence and then examined molecular programs that are engaged following β-selection. We investigated changes in expression of CD31 and CD1a as potential markers that identify β-selected subpopulations. To the best of our knowledge, this is the first study describing CD31 expression during the different stages of thymocyte development in the human thymus. However, in peripheral blood CD4 T cells the transition from $CD31^+$ to $CD31^-$ CD4 T cells occurs following a strong TCR signal that results in robust cell division (15), making it a good candidate for the identification of proliferating thymocytes in response to β-selection. CD1a, on

the other hand begins to emerge on DN thymocytes that are committed to the T cell lineage (2) and its expression gradually increases with progression to the DP stage of development (5). Therefore, we hypothesized that the combination of these two markers might allow for the identification of ISP and EDP subsets that stained positive for icTCRβ, upregulated activation markers and underwent robust proliferation. In this study we have deciphered surface markers specific for the isolation of β-selected thymocytes and examined phenotypic and transcriptional events associated with this thymic checkpoint. Using the OP9-DL1 expressing stromal cell line, we were able to identify various maturation intermediates and pinpoint the stage of TCRαβ and TCRγδ lineage divergence.

Results

Expression of icTCRβ is associated with the down-regulation of CD31 and the up-regulation of CD1a.

In order to identify markers that would distinguish β-selected subpopulations within ISP and EDP cells, we used multi-parametric flow cytometry to analyze the expression of various markers that are modulated during thymocyte maturation (such as CD1a), or TCR-mediated proliferation (such as CD31). We observed that the expression of CD31 was not uniform in the thymus; the highest levels were measured early during thymopoeisis on DN $CD34^+CD1a^-$ (N=7, mean frequency of 100% $CD31^+$ cells) and $CD34^+CD1a^+$ thymocytes (N=7, mean of 100%). However, $CD3^-$ thymocytes progressively down-regulated CD31 as they gained CD4 (mean of 73% ± 14.5), CD8α (mean of 57% ± 20.5), and CD8β (mean of 2.8% ± 1) (Fig. 1*A*). CD31 was then re-expressed on cells that have rearranged their TCRs and expressed CD3 (data not shown). In both CD4 ISP and EDP, CD31 loss was accompanied with a marked up-regulation of CD1a which resulted in the identification of two subsets; $CD31^+CD1a^{low}$ and $CD31^-CD1a^{high}$. While $CD31^+CD1a^{low}$ thymocytes were first detected at the DN stage, $CD31^-CD1a^{high}$ thymocytes appeared later at the ISP stage and their frequencies increased with further maturation into the EDP and $CD3^-$DPs (Fig. 1*A*). $CD3^-$DP ($CD4^+CD8\alpha^+\beta^+$), a population known to have completed β-selection, undergone extensive proliferation (16) and begun TCRA rearrangements (17, 18), consisted predominately of the $CD31^-CD1a^{high}$ phenotype (Fig. 1*A*), suggesting that the $CD31^-CD1a^{high}$ phenotype could be associated with β-selection.

The fact that the proportion of $CD31^-CD1a^{high}$ thymocytes increased as cells progressed from the ISP to the EDP stage and reached 100% at the EDP stage highly suggests that $CD31^-CD1a^{high}$ thymocytes are cells at a more advanced maturation stage than $CD31^+CD1a^{low}$ thymocytes. To confirm this, we analyzed the expression levels of the hematopoietic stem cell (HSC) marker CD34 in the various $CD3^-$ thymocyte subsets. Although levels of CD34 decreased

considerably as thymocytes matured from the DN to the ISP stage and from the ISP to EDP stage (data not shown), we find that $CD31^{+}CD1a^{low}$ ISP and EDP thymocytes contained significantly higher levels of CD34 than $CD31^{-}CD1a^{high}$ ISP and EDP thymocytes (N=10, average fold change of 3, $P = .001$, and 3.4, $P = .001$; respectively) (Fig. S1). Joachims et al. previously reported that a subset of ISP and EDP thymocytes expressed CD34 (14). Interestingly, they showed that $CD34^{-}$ ISP thymocytes contained considerably higher frequencies of intracellular (ic) $TCR\beta^{+}$ cells as compared to $CD34^{+}$ ISP. The fact that $CD31^{-}CD1a^{high}$ ISP and EDP thymocytes were negative for CD34 further suggests that this phenotype could enrich for β-selected cells.

To determine if the isolation of $CD31^{-}CD1a^{high}$ thymocytes identified cells that have undergone β-selection, we stained thymocytes with icTCRβ. Our results indicate that icTCRβ was significantly upregulated in ISP and EDP thymocytes that harbored the $CD31^{-}CD1a^{high}$ phenotype compared to thymocytes of the $CD31^{+}CD1a^{low}$ phenotype (N=8, 18% ± 8.7 versus 4% ± 3.7, $P = .001$ and 21% ± 11 versus 4% ± 3.7, $P = .001$; respectively) (Figs. 1*B* and S1*C*). In addition, the vast majority of $CD3^{-}$ $icTCR\beta^{+}$ thymocytes, whether ISP or EDP, were negative for CD31 and expressed high levels of CD1a (Fig. 1*C*). Although both $CD31^{+}CD1a^{low}$ and $CD31^{-}CD1a^{high}$ ISP and EDP subsets were gated on $CD3^{-}$ thymocytes, the mean fluorescence intensity (MFI) of CD3 was higher within $CD31^{-}CD1a^{high}$ than $CD31^{+}CD1a^{low}$ thymocytes (N=10, mean fold difference of 1.6 for ISP, Student's *t* test $P = .001$ and mean fold difference of 2.3 for EDP, $P = .001$), suggesting that low levels of the pre-TCR complex could be detected on the surface of these cells (Fig. S2). This low level of CD3 expression is in agreement with the findings that formation of the pre-TCR results in internalization and lysosomal degradation of the pre-TCR (19). Taken together, these findings identify the inverse expression of CD31 and CD1a as markers that enrich for β-selected thymocytes.

The CD31^{-}CD1a^{high} phenotype identifies β-selection-associated phenotypic and transcriptional events

The finding that icTCRβ was detected in CD31^{-}CD1a^{high} thymocytes from both the ISP and EDP stages of maturation suggests that β-selection is not restricted to a specific development stage, i.e. DN, ISP or EDP, in contrast to what is observed in mouse models (10) and explains why previous human studies have proposed that β-selection occurs at distinct stages of development (13, 14). Our results suggest that ISP and EDP thymocytes of the CD31^{-}CD1a^{high} phenotype are at the same differentiation (or maturation) stage compared to the total population of ISP or EDP populations. To test this hypothesis, we analyzed the expression of maturation, activation, proliferation and survival gene expression in CD3^{-} thymocytes using quantitative RT-PCR and performed a two-way cluster analysis of ISP (from three thymi) and EDP (from two thymi) subsets according to their gene expression profile. Fig. 2 represents a heatmap of genes differentially regulated between CD31^{+}CD1a^{low} and CD31^{-}CD1a^{high} ISP thymocytes (*Limma P* < .05). Consistent with our hypothesis, the genes differentiating CD31^{+}CD1a^{low} and CD31^{-}CD1a^{high} ISP thymocytes were also differently expressed between CD31^{+}CD1a^{low} and CD31^{-}CD1a^{high} EDP thymocytes. Consequently, CD31^{+}CD1a^{low} EDP clustered together with CD31^{+}CD1a^{low} ISP thymocytes while CD31^{-}CD1a^{high} EDP clustered together with CD31^{-}CD1a^{high} ISP thymocytes (Fig. 2). The finding that ISP and EDP subsets clustered according to their expression of CD31 and CD1a but not of CD4 and CD8 confirms that all subsets bearing the CD31^{+}CD1a^{low} or the CD31^{-}CD1a^{high} phenotype had similar gene expression and represented cells of similar differentiation stages regardless of whether they were sorted from the ISP or EDP populations. This observation suggests that human T cell maturation as determined by β–selection can occur across developmental stages.

During β-selection, the expression of the pTα-TCRβ complex triggers intracellular signaling that result in clonal expansion, cell survival and allelic exclusion (inhibition of further rearrangements of the TCRβ locus) (7). To

confirm that $CD31^{-}CD1a^{high}$ ISP and EDP subsets had received β-selection-induced signals, we used flow cytometry as well as quantitative RT-PCR to analyze modulation of markers of T cell activation (such as PD-1, CD28, CD62L and CD5) as well as key molecules involved in cell cycling. Our data show that the expression of the activation markers PD-1 and CD28 was markedly up-regulated within ISP and EDP $CD31^{-}CD1a^{high}$ thymocytes compared to their $CD31^{+}CD1a^{low}$ counterparts (PD-1: N=7, mean fold difference of 3.4, $P = .001$, and 3.1, $P < .001$; respectively. CD28: N=6, mean fold difference of 4.6, $P = .006$, and 4.4, $P = .007$; respectively) (Fig. 3*A* and Fig. S3). A similar upregulation was detected for levels of CD5 expression, which correlates with the intensity of pre-TCR and TCR-mediated signals (20) (N=6, mean fold difference of 1.82, $P = .005$, and 1.78, $P = .002$; respectively) (Fig. 3*A* and Fig. S3). CD62L, a marker down-regulated following activation and differentiation of naive to effector T cells (21), was significantly down-regulated within ISP and EDP $CD31^{+}CD1a^{low}$ thymocytes (N=4, mean fold difference of 0.5, $P = .039$, and 0.33, $P = .006$; respectively) (Fig. 3*A* and Fig. S3). In agreement with the observation that ISP and EDP thymocytes bearing the $CD31^{-}CD1a^{high}$ phenotype were activated, we detected that this population was larger in size, as measured by forward scatter (FSC) analysis, than $CD31^{+}CD1a^{low}$ ISP and EDP thymocytes (N=10, $P = .001$ for both ISP and EDP) (representative example in Fig. 3*B*). Moreover, $CD31^{-}CD1a^{high}$ ISP and EDP thymocytes expressed higher levels of the nuclear marker of proliferation Ki67 than $CD31^{+}CD1a^{low}$ ISP and EDP thymocytes (N=7, mean frequencies of 15% ± 10 versus 4.6% ± 2, $P = .026$ and 21% ± 15 versus 3.7% ± 2, $P = .020$; respectively) (Fig. 3*B* and Fig. S3).

Mouse studies have revealed abrupt changes in genes regulating cell-cycle progression during the β-selection transition (16). Similarly, quantitative gene expression analysis confirmed that the expression of two proto-oncogenes, Myeloblastosis oncogene-like 2 (Mybl2) and Cyclin D3, were elevated within thymocytes of the $CD31^{-}CD1a^{high}$ ISP phenotype compared to $CD31^{+}CD1a^{low}$ ISP thymocytes (N = 3, fold change of 2, $P = .042$ and of 1.7, $P = .043$; respectively)

(Fig.3*B*), consistent with the fact that β-selected cells exhibit a rapid burst of proliferation (7). We also observed changes in expression of factors involved in the negative control of proliferation (inhibitors of the cell cycle) during thymocyte development such as Cytoplasmic polyadenylation element binding protein 4 (Cpeb4) (7), Cyclin-dependent kinase inhibitor 1A (Cdkn1a, also known as p21Cip1) (22), Growth arrest and DNA-damage-inducible protein (Gadd45a) (23) and Suppressor of cytokine signaling-1 (Socs-1). These genes, which play a role in the shutdown of proliferation during TCR rearrangements (7) were all selectively down-regulated following differentiation of $CD31^{+}CD1a^{low}$ ISP into $CD31^{-}CD1a^{high}$ ISP thymocytes (N = 3, fold change of 5.1, $P < .001$; fold change of 4.3, $P = .015$, fold change of 2.8, $P = < .001$; and fold change of 1.7, $P = .002$; respectively) (Fig.3*B*).

Following β-selection, pre-TCR signaling must provide survival signals necessary for progression to the DP stage when cells become unresponsive to IL-7. In agreement with mouse studies, we detected a significant down-regulation of the IL-7 pathway, namely in the expression of CD127 (IL-7Rα) and Bcl-2 within $CD31^{-}CD1a^{hi}$ ISP thymocytes (N = 3, fold difference of 2.6, $P < .001$; and 3.3, $P = .002$; respectively). The reduced expression of CD127 and Bcl-2 in $CD31^{-}CD1a^{hi}$ ISP and EDP thymocytes was further demonstrated by flow cytometric analysis (data not shown). In contrast, we detected that Survivin, a member of the inhibitor of apoptosis (IAP) family that has a crucial role in promoting cell survival following pre-TCR triggering (24), was up-regulated during differentiation from the $CD31^{+}CD1a^{low}$ to the $CD31^{-}CD1a^{hi}$ phenotype (N = 3, fold change of 1.7, $P = .027$ for ISP thymocytes and of 2, $P = .029$ for EDP thymocytes) (Fig.3*C*).

Rearrangement of the TCRβ locus is controlled by regulation of the RAG genes, which are down-regulated upon β-selection. As expected, our results demonstrate that expression of the RAG-1 and RAG-2 genes is down-regulated within $CD31^{-}CD1a^{high}$ thymocytes (N = 3, fold change of 2 and 1.7; respectively, $P = .022$), but is re-expressed in $CD3^{-}$DP thymocytes (Fig.3*D*). This pattern of expression was

similar for two additional transcription factors, HEB (P = .015) and c-myb (P = .004) (Fig.3*D*) that positively activate the RAG-1 and RAG-2 promoters (25, 26).

Gene expression analysis also showed that differentiation from the $CD31^{+}CD1a^{low}$ to the $CD31^{-}CD1a^{high}$ phenotype in humans resulted in the down-regulation of members of the Notch signaling pathway such as Notch-1 and Notch-3 (N = 3, fold change of 3.3, P = .011 and 2.5, P = .022; respectively) (Fig. 3*E*). This pattern was similarly observed for downstream targets of Notch signaling such as Hes-1 and pTα (N = 3, fold change of 7.8, P = .005 and 7.8, P = .003; respectively) (Fig. 3*E*). These findings are in agreement with those observed during β-selection in mouse studies in which pTα peaks within DN3a thymocytes (10).

Taken together, these results suggest that the down-regulation of CD31, concomitant with the up-regulation of CD1a, is the result of pre-TCR-triggered activation and proliferation. Therefore, identification of the $CD31^{-}CD1a^{high}$ phenotype permits isolation of thymocytes that have undergone β-selection-mediated events. *In toto*, our results define the dynamic transcriptional profile regulating differentiation and lineage commitment, and identify similarities between human and mouse T cell development. Robust proliferation of immature and early precursors followed by the down-regulation of proliferation, and upregulation of survival pathways direct cells toward the DP stage and establish the epigenetic modifications that prime further differentiation events. DP thymocytes that lack expression of the IL-7R and express high levels of SOCS1 are refractory to prosurvival cytokines. This ensures positive selection of potentially useful TCRs and lineage choice decisions of $CD4^{+}$ and $CD8^{+}$ T cells based solely on TCR signal strength and subsequent cytokine signals.

$CD31^{+}CD1a^{low}$ ISP differentiate into both DP and DN thymocytes while $CD31^{-}$ $CD1a^{high}$ ISP differentiate only into DP thymocytes.

Having established a phenotype that allows the discrimination of β-selected thymocytes from unselected thymocytes, we used the OP9-DL1 system, previously shown to support *ex vivo* human T cell differentiation (27), to monitor development of the pre-β-selected and post-β-selected thymic subsets. This system consists of the bone marrow stromal line OP9 which was retrovirally transduced to express the Notch ligand Delta-like-1. This system has previously been shown to preferentially promote T-cell development of both αβ and γδ lineages from BM derived clonal lymphoid precursors (CLP) but not B cell differentiation (28).

We isolated $CD31^{+}CD1a^{low}$ and $CD31^{-}CD1a^{high}$ ISP thymocytes by FACS sorting from 3 different thymi which were then separately cultured within the OP9-DL1 system. We determined the differentiation potential of each subset by analyzing the frequencies of $CD3^{-}$ DN, ISP, EDP and DP as well as $CD3^{+}$ DN, DP, and single positive CD4 and CD8 (SP4 and SP8) cells from sorted ISP subsets at Day 5, 9 and 14 (a representative example is shown in Fig. 4*A* and 4*B*). At day 5, the majority of $CD31^{+}CD1a^{low}$ ISP thymocytes had down-regulated CD4 and differentiated into $CD3^{-}$DN thymocytes (50% ± 13.2), while a smaller subset had upregulated CD8 and differentiated into $CD3^{-}$DP thymocytes (11% ± 13.2). A smaller fraction of thymocytes had up-regulated CD3 in the cocultures at day 5 (6% ± 1.2) and consisted predominantly of the DN phenotype (Fig. 4*A*). With time, the frequency of developing $CD3^{-}$DP thymocytes increased; this population became predominant at day 14 (35% ± 11). The frequency of $CD3^{+}$ DN cells also increased at day 14 (15% ± 3.6) while $CD3^{+}$DP, SP8 and SP4 were detected at extremely low frequencies throughout the coculture. The developing SP8 were $CD8\alpha^{+}\beta^{-/low}$ (Fig. 4*A*).

In contrast to $CD31^{+}CD1a^{low}$ ISP, $CD31^{-}CD1a^{high}$ ISP thymocytes did not down-regulate CD4 in coculture; instead, they up-regulated CD8 at an accelerated pace.

$CD3^-$ DP represented the majority of developing thymocytes throughout the cocultures (day 5: 53% ± 5.5, day 14: 59% ± 17) (Fig. 4*B*). The emerging $CD3^+$ thymocytes at day 5 (5.3% ± 0.5) consisted of the DP and SP4 phenotype (Fig. 4*B*). SP8 thymocytes were detected at very low frequencies at day 14 (< 1%) but unlike $CD31^+CD1a^{low}$ ISP, SP8 thymocytes developing from $CD31^-CD1a^{high}$ ISP were uniformly $CD8\alpha^+\beta^+$ (Fig. 4*B*).

There were few EDP thymocytes detected throughout the coculture from either $CD31^+CD1a^{low}$ or $CD31^-CD1a^{high}$ ISP thymocytes (day 5: 1.6 ± 0.5 and 2.3 ± 1.2; respectively, day 14: 2.7 ± 2 and 2 ± 1.2; respectively). This might be due to the transient nature of EDPs, as demonstrated by the detection of CD8β in $CD3^-$ $CD8\alpha^+$ thymocytes from day 1 cocultures of $CD31^-CD1a^{high}$ ISP and day 2 cocultures of $CD31^+CD1a^{low}$ ISP thymocytes (data not shown). Of note, $CD31^+CD1a^{low}$ ISP expressed similar frequencies of $CD3^+$ cells as their $CD31^-$ $CD1a^{high}$ counterparts for each time point (data not shown), however; the $CD3^+$ cells arising from $CD31^+CD1a^{low}$ ISP consisted mostly of the $CD4^-CD8^-$ DN phenotype while those developing from $CD31^-CD1a^{high}$ consisted of DP cells and to a lower extent SP CD4 and SP CD8 cells. These results demonstrate that $CD31^-$ $CD1a^{high}$ ISP thymocytes develop directly into the αβ lineage, which further confirms the β-selection transition point. It is important to note that OP9-DL1 stromal cell cocultures lack thymic epithelial cells which express MHC class I and II and therefore differentiation of SP4 and SP8 cells is most likely dependent upon T-T cell interactions. In addition, lineage choice decision between SP4 and SP8 are dependent upon TCR signal strength and cytokines not present in our unsupplemented cultures and therefore these populations are underrepresented in our culture conditions.

CD31^{+}CD1a^{low} EDP differentiate into both DP and CD8 thymocytes while CD31^{-}CD1a^{high} EDP differentiate only into DP thymocytes.

Since EDP thymocytes were not detected in ISP cocultures due to their brief transitional stage, we directly isolated EDP CD31^{+}CD1a^{low} and CD31^{-}CD1a^{high} from 3 different thymi, cocultured them in the OP9-DL1 system and determined their differentiation potential by analyzing the frequencies of CD3^{-} and CD3^{+} thymocyte subsets at Day 5, 9 and 14 (representative example in Fig. 4*C* and 4*D*). As expected, CD31^{+}CD1a^{low} EDP thymocytes underwent rapid phenotype differentiation following coculture; consequently few EDP cells were remaining in cocultures at day 5 (3% ± 1.5). At this time, EDP thymocytes had either up-regulated the CD8β chain and differentiated into CD3^{-}DP (40% ± 8) or down-regulated CD4 to give rise to CD3^{-}CD4^{-}CD8α^{+} thymocytes (48% ± 7) (Fig. 4*D*). Of note, CD3^{-}CD4^{-}CD8α^{+} thymocytes were CD8β$^{low/+}$, a phenotype not normally detected *in-vivo* (Fig.1 *A*). With time, CD3^{-}DP thymocytes increased in frequencies and became the dominant population at day 14 (65% ± 4). A small subset of EDP thymocytes down-regulated both CD4 and CD8α and gave rise to DN thymocytes (7.5% ± 1 at day 14). CD3^{+} thymocytes reached 10% ± 1 at day 14 (data not shown) and consisted of SP8, CD3^{+}DN or CD3^{+}DP (Fig. 4*D*). In contrast to CD3^{-}CD4^{-}CD8α^{+}, CD3^{+} SP8 were CD8α^{+}β$^{-/low}$ (Fig. 4*D*). The transient up-regulation of CD8β on CD3^{-}CD4^{-}CD8α^{+}β^{+} might be a result of the continual presence of Notch activation which has been shown in mice to induce the up-regulation CD8β on CD8^{+} TCRγδ^{+} thymocytes (29).

On the other hand, CD31^{-}CD1a^{high} EDP developed into two main populations: CD3^{-}DP and CD3^{+}DP (75% ± 10 and 15% ± 5 at day 5; respectively) (Fig. 4*D*). CD4 and CD8 SP were detected at very low frequencies at day 14 (< 1%); however, CD8 SP were CD8α^{+}β^{+}, unlike those from CD31^{+}CD1a^{low} that were exclusively CD8α^{+}β$^{-/low}$ (Fig. 4*D*). These results demonstrate that CD31^{-}CD1a^{high} EDP developed into cells of the αβ lineage, which further confirms this β-selected checkpoint.

CD31^{+}CD1a^{low} cells are the precursors of CD31^{-}CD1a^{high} β-selected thymocytes.

The finding that CD31^{+}CD1a^{low} ISP and EDP thymocytes differentiated into both DN and DP cells suggests that CD31^{+}CD1a^{low} thymocytes consist of unselected precursors. To determine whether the transition from the CD31^{+}CD1a^{low} to the CD31^{-}CD1a^{high} phenotype coincided with β-selection-induced proliferation, we sorted CD31^{+}CD1a^{low} ISP thymocytes from three thymi, labeled them with CFSE and cocultured them with OP9-DL1 stromal cells. We then monitored the regulation of CD31 and CD1a expression in proliferating thymocytes at early time points (day 3, 5 and 7). A representative example is shown in Fig. 5. By gating on thymocytes that retained the ISP phenotype in coculture at day 3, we observed that a subset of ISP (13% of total ISP thymocytes) had up-regulated levels of CD1a but had not yet down-regulated levels of CD31, resulting in a transitory population of the CD31^{+}CD1a^{high} phenotype (Fig. 5*A*). This new population, similar to the CD31^{+}CD1a^{low} subset, was CFSE^{high}, demonstrating that CD31^{+}CD1a^{high} thymocytes had not yet undergone proliferation. At day 5, we observed that the majority of the thymocytes in coculture had developed into the CD31^{+}CD1a^{high} phenotype (21% of total ISP thymocytes) or the CD31^{-}CD1a^{high} phenotype (38% of total ISP thymocytes). The proportion of CD31^{-}CD1a^{high} thymocytes further increased at day 9 (48% of total ISP thymocytes). In contrast to CD31^{+}CD1a^{low} and CD31^{+}CD1a^{high} thymocytes, CD31^{-}CD1a^{high} thymocytes were CFSE^{low} (Fig. 5*A*), demonstrating that CD1a upregulation occurred prior to the down-regulation of CD31, and that the transition from CD31^{+}CD1a^{high} to CD31^{-}CD1a^{high} was associated with robust proliferation. The increased frequencies of proliferating CD31^{-}CD1a^{high} ISP thymocytes at day 5 and 7 could explain the observed transient increase in the proportions of ISP between day 5 and day 9 following coculture of CD31^{+}CD1a^{low} ISP thymocytes (Fig. 4*A*). Long-term cocultures of CD31^{+}CD1a^{low} ISP thymocytes indicated that CD3^{-} thymocytes became a homogenous CD31^{-}CD1a^{high} population by day 14 or 19 (data not shown). CD31 was later up-regulated during coculture when thymocytes reached the CD3^{+}CD4^{+}CD8^{+} DP stage of differentiation (data not shown).

To further confirm that the $CD31^{-}CD1a^{high}$ ISP generated in coculture from $CD31^{+}CD1a^{low}$ ISP were similar to those isolated from the thymus *ex-vivo*, we analyzed this emerging population for additional markers that characterized the $CD31^{-}CD1a^{high}$ phenotype such as PD-1 and CD28. Our data confirmed that the transition from $CD31^{+}$ $CD1a^{high}$ to $CD31^{-}$ $CD1a^{high}$ was linked with proliferation as well as activation markers, demonstrated by the up-regulation of PD-1 (Fig. 5*A*) and CD28 (data not shown). PD-1 and CD28 were slightly up-regulated on $CD31^{+}CD1a^{high}$ ISP thymocytes, highlighting this key transitional state (Fig. 5*A* and data not shown).

We then analyzed the emerging 3^{-}DP thymocytes ($CD3^{-}CD4^{-}CD8\alpha^{+}CD8\beta^{low/+}$) for the expression of CD31 and CD1a together with CFSE. At day 3, a subset of 3^{-}DP (18% of total 3^{-}DP thymocytes) had up-regulated CD1a without down-regulating CD31, resulting in the previously described transitory population $CD31^{+}CD1a^{high}$ (Fig. 5*B*). $CD31^{-}CD1a^{high}$ 3^{-}DP were observed at day 5 and consisted of the vast majority of the thymocytes in cocultures (78% of total 3^{-}DP thymocytes). The emerging $CD31^{-}CD1a^{high}$ 3^{-}DP were proliferating, as indicated by the low levels of CFSE (Fig. 5*B*), and recently activated, as demonstrated by their $PD\text{-}1^{+}CD28^{+}$ expression (data not shown), which is in agreement with what was observed for developing $CD31^{-}CD1a^{high}$ ISP thymocytes (Fig. 5*A*). The faster kinetics of CD31 down-regulation in emerging $CD3^{-}$DP thymocytes is not surprising since $CD3^{-}$DP do not express CD31 *ex-vivo* (Fig. 1*A*).

The finding that cells of the $CD31^{+}CD1a^{low}$ phenotype were the precursors of $CD31^{-}CD1a^{high}$ thymocytes was further confirmed by sorting $CD31^{+}CD1a^{low}$ EDP thymocytes from the same three thymi. $CD31^{+}CD1a^{low}$ EDP were labeled with CFSE and cocultured on OP9-DL1 stromal cells. A representative example is shown in fig. 5*C* (same thymus as in fig. 5*A*). We detected that EDP thymocytes differentiate in coculture at a rapid rate: 70% of $CD3^{-}CD4^{+}CD8\alpha^{+}$ DP had up-regulated CD8β by day 3, and 93% by day 5 (data not shown), leaving few EDP thymocytes present in culture and limiting further analysis on this population. Therefore, the emerging $CD3^{-}CD4^{+}CD8\alpha^{+}\beta^{+}$ DP population was analyzed for

CD31, CD1a and CFSE levels. This population consisted mainly of $CD31^{-}$ $CD1a^{high}$ thymocytes (43% at day 3, 58% at day 5 and 80% at day 7) that were $CFSE^{low}$ (Fig. 5*C*) and PD-$1^{+}CD28^{+}$ (data not shown). This is consistent with the fact that EDP thymocytes are more mature than ISP and with *ex-vivo* findings that they contain higher frequencies of $CD31^{-}CD1a^{high}$ cells (Fig. 1*A*). All together, these findings confirm that $CD3^{-}CD31^{+}$ cells are the precursors of the $CD3^{-}CD31^{-}$ β-selected thymocytes and suggest that the down-regulation of CD31 is more specific to β-selection than the up-regulation of CD1a.

CD31 down-regulation is specific to β-selected thymocytes.

In order to determine whether the down-regulation of CD31 alone was sufficient for identifying the β-selection checkpoint, we analyzed thymocytes developing into non-αβ lineages such $CD3^{-}CD4^{-}CD8^{-}$ DN thymocytes, isolated following coculture of $CD31^{+}CD1a^{low}$ ISP, and $CD3^{-}CD4^{-}CD8\alpha^{+}\beta^{low/+}$ thymocytes, isolated following coculture of $CD31^{+}CD1a^{low}$ EDP, for the expression of CD31, CD1a and CFSE. Our data show that although CD1a was moderately up-regulated (16% of DN thymocytes emerging from ISP cocultures *vs.* 12% for $CD3^{-}CD4^{-}$ $CD8\alpha^{+}\beta^{low/+}$ thymocytes emerging from EDP cocultures at day 7) (Figs. 6*A* and 6*B*), CD31 was not down-regulated (1% of DN thymocytes emerging from ISP cocultures *vs.* 5% of $CD3^{-}CD4^{-}CD8\alpha^{+}\beta^{low/+}$ thymocytes emerging from EDP cocultures at day 7). In addition, emerging DN and $CD3^{-}CD4^{-}CD8\alpha^{+}\beta^{low/+}$ thymocytes slightly diluted CFSE levels (Fig. 6*A* and 6*B*) and moderately up-regulated levels of PD-1 and CD28 (data not shown), demonstrating that thymocytes developing into non-αβ lineages can undergo minimal levels of activation and proliferation but do not down-regulate levels of CD31. This suggests that CD31 down-regulation is specific to β-selection while activation markers such as PD-1 and CD28 are not restricted to β-selection-induced activation and should not be used to isolate β-selected thymocytes.

CD31$^+$CD1a^{low} thymocytes favor development into the γδ-lineage while CD31$^-$ CD1a^{high} thymocytes progress to the αβ-lineage.

To investigate lineage commitment, thymocyte development was monitored in the OP9-DL1 system by staining sorted CD31$^+$CD1a^{low} and CD31$^-$CD1a^{high} ISP and EDP thymocytes with both anti-TCRαβ and anti-TCRγδ antibodies at various time points (1 represented out of 4 in Figs. 7*A* and 1 represented out of 3 in Fig. 7*C*). Our results show that CD3$^+$ cells arising from CD31$^+$CD1a^{low} ISP and EDP thymocytes differentiated mostly into the γδ-lineage: the frequency of TCRγδ$^+$ thymocytes peaked at early time points after which it slowly decreased (77% of CD3$^+$ thymocytes at day 9 following coculture of CD31$^+$CD1a^{low} ISP and 55% of CD3$^+$ thymocytes at day 5 following coculture of CD31$^+$CD1a^{low} EDP) (Figs. 7*A* and 7*C*). On the other hand, TCRαβ$^+$ thymocytes were slower to emerge (8.5% of CD3$^+$ thymocytes at day 14 following coculture of CD31$^+$CD1a^{low} ISP and 14% of CD3$^+$ thymocytes at day 5 following coculture of CD31$^+$CD1a^{low} EDP) (Fig. 7*A*). These results strongly suggest that CD31$^+$CD1a^{low} ISP thymocytes are uncommitted precursors. In contrast, the rapid and selective development of TCRγδ$^-$ TCRαβ$^+$ CD3$^+$ cells from coculture of CD31$^-$CD1a^{high} ISP and EDP thymocytes indicated that a significant proportion of CD31$^-$CD1a^{high} ISP thymocytes were previously β-selected and committed to the αβ-lineage. However, CD31$^+$CD1a^{low} EDP generated more TCRαβ$^+$ cells than did ISP (26% of CD3$^+$ thymocytes following coculture of CD31$^-$CD1a^{high} EDP *vs.* 4% of CD3$^+$ thymocytes following coculture of CD31$^-$CD1a^{high} ISP thymocytes at day 9) (Figs. 7*A* and Fig. 7*C*). This is in agreement with the fact that EDP down-regulated CD31 at a faster rate (Fig. 5*C*), suggesting that EDP thymocytes were more differentiated than ISP thymocytes.

Next, we sought to characterize the phenotype of the emerging CD3$^+$ TCRαβ$^+$ and TCRγδ$^+$ thymocytes from ISP and EDP subsets at various time points. TCRγδ$^+$ cells developed only from CD31$^+$CD1a^{low} ISP and EDP cocultures (Figs. 7*A* and 7*C*) and consisted mostly of the DN phenotype (following ISP cocultures)

(Fig. 7*B*) or of both the DN and SP8 phenotypes (following EDP cocultures) (Fig. 7*D*). TCR$\alpha\beta^+$ cells developing from sorted CD31$^+$CD1a^{low} ISP and EDP were DP thymocytes while TCR$\alpha\beta^+$ cells developing from CD31$^-$CD1a^{high} ISP were DP, SP8 and SP4 (Figs. 7*B* and S4) while TCR$\alpha\beta^+$ cells developing from CD31$^-$ CD1a^{high} EDP were DP (Fig. 7*D*) and SP4 (detected at day 14, data not shown).

SP8 thymocytes emerging from CD31$^+$CD1a^{low} ISP thymocytes expressed high levels of TCR$\gamma\delta$ in contrast to the TCR$\alpha\beta^+$ TCR$\gamma\delta^-$ SP8 emerging from CD31$^-$ CD1a^{high} ISP thymocytes (Fig. S3). SP4 developing from CD31$^+$CD1a^{low} ISP thymocytes were detected at very low frequencies at day 14 (< 1%) and a subset of these cells was TCR$\gamma\delta^+$ in contrast to the TCR$\alpha\beta^+$TCR$\gamma\delta^-$ SP4 emerging from CD31$^-$CD1a^{high} ISP thymocytes (Fig. S4). These results, together with the fact that SP8 developing in coculture from CD31$^+$CD1a^{low} ISP thymocytes were CD8$\alpha^+\beta^-$ (Fig. 4*A*), suggest that CD31$^+$CD1a^{low} ISP can give rise to TCR$\gamma\delta^+$ DN and CD8$\alpha^+\alpha^+$ thymocytes, with the former representing the larger population.

In summary, these results show that β-unselected ISP and EDP could generate cells of the γδ-lineage, suggesting that β-selection occurs within a developmental window that is not tightly coupled to either CD4 or CD8 expression. This is in contrast to studies in mice in which it has been demonstrated that β-selection occurs specifically at the DN3 stage of development (10).

Discussion

In mice, up-regulation of CD27 at the DN3 stage of intrathymic differentiation identifies thymocytes that are undergoing β-selection or γδ-selection (10). In contrast to mice, the stage of human T cell development during which β-selection occurs is unclear and several intermediates have been suggested (12, 13). The discrepancies in these reports have been attributed to the lack of surface markers that identify thymocytes undergoing β-selection. Recently, CD28 has been proposed as a marker of β-selection in humans (30). However, CD28 is an activation marker that is often transiently expressed on proliferating cells and therefore may not be specific to signals triggered from either β- or γδ-selection. In this study, we report that the $CD31^{-}CD1a^{high}$ phenotype identifies β-selected thymocytes that are committed to the αβ-lineage while the $CD31^{+}CD1a^{low}$ phenotype consists of immature thymocytes that have not undergone β-selection or lineage commitment. Furthermore, we show that, in contrast to mice, β-selection can occur during the transition from ISP to EDP as well as from EDP to 3^{-}DP.

Due to the fact that the expression of Platelet endothelial cell adhesion molecule (PECAM-1)/CD31, an endothelial cell marker also expressed on HSC, is down-regulated on naive T cells in the periphery following TCR-triggered proliferation (15) and that β-selection is the result of pre-TCR signaling that induces proliferation (7), we hypothesized that modulation of CD31 expression might characterize β-selected thymocytes. In addition, CD31 is a member of the Immunoglobulin superfamily (31) whose intracellular domain contains immunoreceptor tyrosine-based inhibitory motifs (ITIMs) that could influence TCR-driven proliferation (32). This would justify the requirement for CD31 down-regulation in cells undergoing TCR-mediated proliferation. Re-expression of CD31 at later time points is also a marker of recent thymic emigrants and correlates with thymic function and the origin of $CD4^{+}$ T cells in HIV patients receiving ART (33).

In this study we analyzed thymocytes for the expression of CD31 together with CD1a since it was previously reported that expression of CD1a was elevated in icTCRβ$^+$ thymocytes (34). The use of these markers together allowed for the clear identification of distinct subsets in the ISP and EDP populations: CD31$^+$CD1a^{low} and CD31$^-$CD1a^{high}, with the vast majority of icTCRβ$^+$ cells belonging to the CD31$^-$CD1a^{high} phenotype (Fig.1). Genetic analysis confirmed that CD31$^+$CD1a^{low} ISP and EDP thymocytes had similar gene expression and clustered together. They were clearly distinct from CD31$^-$CD1a^{hi} ISP and EDP thymocytes which also clustered together (Fig. 2). This suggests that in human T cell development, the expression of CD31 and CD1a, opposed to CD4 and CD8, delineates the transcription profile of thymocytes and consequently clusters together cells of similar maturation stages. As ISP contained significantly less CD31$^-$CD1a^{high} than EDP (Fig. 1), gating on the total ISP population may lead to the dilution of the genes that are regulated with β-selection. This could explain why previous studies analyzing gene expression within the total ISP and EDP population concluded that β-selection was not initiated at the ISP stage (13).

The CD31$^-$CD1a^{hi} phenotype is associated with β-selection events

To determine whether cells encompassing the CD31$^-$CD1a^{high} phenotype had completed β-selection and received signals associated with this maturation checkpoint, we used both flow cytometry and real time RT-PCR to investigate the expression of various cell markers and/or genes that would be modulated following β-selection. Our data shows that CD31$^-$CD1a^{high} thymocytes expressed higher levels of activation markers such as CD28 and PD-1 than their CD31$^+$CD1a^{low} counterparts (Fig. 3). In addition, these subsets had increased cell size (as determined by FSC) and were cycling (as determined by intracellular staining with Ki67) in agreement with the fact that β-selection induces activation and proliferation (Fig. 3). Analysis of gene expression confirmed that CD31$^-$CD1a^{high} ISP and EDP subsets had increased proliferative history; the transition from CD31$^+$CD1a^{low} to CD31$^-$CD1a^{hi} subsets resulted in the up-regulation of two

proto-oncogenes: Mybl2 and Cyclin D3 (Fig. 3). These genes are important during mouse intrathymic development and are both up-regulated following β-selection (10). Cell-cycle inhibitors such as Cpeb4, Cdkn1a, Gadd45a and Socs-1 were all down-regulated at this transition (Fig. 2). These genes play a role in the shutdown of proliferation during TCR rearrangements: Cdkn1a, Gadd45a and Socs-1 are targets of the helix-loop-helix protein E47 (35) whose activity is blocked as a result of pre-TCR signaling (7). Cpeb4 is induced by RORγt, which in turn is controlled by E47 (7). A recent study showed a pivotal role for the nucelosome remodeling complex and histone deacetylation (NuRD) complex in orchestrating chromatin modifications that regulate β-selection, CD4 coreceptor expression, and thymic maturation (36).

Selective gene down-regulation in $CD31^{-}CD1a^{high}$ subsets was similarly seen for other proteins known to be modulated following β-selection, such as the RAG enzymes as well as Notch-1 and Notch-3. Notch signaling is important for human thymocyte differentiation; it plays a role in early T cell development by inducing T cell commitment and proliferation of progenitors (37, 38) and is also required for the generation of thymocytes of the γδ-lineage (39). In addition, Notch signaling is crucial for VDJβ rearrangements in both humans and mice (38, 40-41) but is not required for differentiation past the β-selection checkpoint, although proliferation is reduced in its absence (30). However, in our in vitro coculture system continued Notch signaling within $CD3^{low}$ DP β-selected thymocytes resulted in the deregulated expansion of TCRαβ thymocytes (37). Therefore, down-regulation of the Notch receptors could be part of a mechanism by which proliferating $CD31^{-}CD1a^{high}$ subsets shut off transcription of genes inducing proliferation in order to allow TCRA gene rearrangement and subsequent maturation into the DP stage. This notion is supported by the findings of Van de Walle et al. that demonstrated that reduction in Notch activation induces TCR-Cα expression (39).

The CD31$^-$CD1a^{high} phenotype is specific to β-selection.

In mice, CD27 distinguishes DN3 cells that have rearranged either the β chain or both the γ and δ chains. Using β gene knockout mice, Taghon et al. (10) showed that γδ-selection, similarly to β-selection, induces proliferation albeit at considerably lower levels. This is in line with the study of Prinz et al. (42) in which γδ-selection triggered 4-5 cell cycle divisions. In addition, qRT-PCR of DN3b thymocytes from wild-type mice and TCRβ knockout mice indicated that many genes were similarly modulated in γδ- and β-selection (such as RAG-1, Notch-1 and -3, HES-1 and pTα) (10). Despite the fact that we detected expression of icTCRβ (Fig. 1) but not icTCRγδ (data not shown) within CD31$^-$ CD1a^{high} thymocytes, it is plausible that the CD31$^-$CD1a^{high} subset might contain γδ-selected thymocytes. To investigate this possibility, sorted subsets were cocultured with OP9-DL1 stromal cells, which have been previously shown to support *ex-vivo* human T cell development (27). Our data show that thymocytes of the CD31$^-$CD1a^{high} phenotype generated CD3$^-$ DP as well as CD3$^+$ DP, SP4 and SP8 cells that solely expressed TCRαβ. These results differ from the mouse study of Taghon et al. (10), in which CD27$^+$ DN3b cells developing on OP9-control cells gave rise to TCRαβ$^+$ as well as TCRγδ$^+$ cells, albeit at lower frequencies.

In addition, our finding that DN cells generated from sorted CD31$^+$CD1a^{low} ISP thymocytes had moderately up-regulated levels of CD1a, CD28 and PD-1 but did not down-regulate levels of CD31 further confirms that the CD31$^-$CD1a^{high} phenotype is specific for thymocytes undergoing β-selection. If CD3$^-$DN thymocytes are indeed the precursors of CD3$^+$DN TCRγδ$^+$ thymocytes, this would suggest that γδ-selection in humans, similarly to what was previously reported in mouse studies (42), is accompanied with low levels of activation and proliferation (that do not lead to CD31 down-regulation). In addition, our results suggest, in contrast to what was recently proposed by others (30), that activation markers such as CD28 may not be specific for the isolation of β-selected thymocytes. In fact, it was recently reported that CD28$^+$ ISP generated both TCRαβ$^+$ and TCRγδ$^+$

thymocytes when cocultured on OP9-DL1 (30). In addition, $CD28^-$ ISP that were transduced with TCR-β did not up-regulate CD28 in the absence of Notch signaling although they did up-regulate other markers associated with β-selection such as CD1. The lack of CD28 up-regulation was attributed to the absence of proliferation (30). Therefore, the activation marker CD28, although capable of enriching for β-selected cells (30), is not specific for β-selection.

Model of human T cell development

In mice, two main lineage models are suggested for αβ- or γδ-lineage commitment: the instructive models which stipulates that the TCR determines the fate of a cell, and the separate lineage models in which it is thought that lineage commitment is pre-determined and that productive rearrangement of the matching TCR rescues the cells from cell death (reviewed by (43)). Mechanisms that have been shown to prevent cells from expressing a TCR of the wrong lineage such as γ-silencing triggered by the pre-TCR (44) and down-regulation of pTα by the γδ-TCR further support this model (45). The data presented here is compatible with the instructive model of lineage commitment, in which αβ and γδ T cells develop from common T-cell progenitors.

Our data has established that $CD31^+CD1a^{low}$ thymocytes as the uncommitted precursors of β-selected $CD31^-CD1a^{high}$ thymocytes. Both $CD31^+CD1a^{low}$ ISP and EDP thymocytes were capable of proliferating (as measured by CFSE dilution) and differentiating into $CD31^-CD1a^{high}$ thymocytes. In addition to generating $CD3^+TCR\alpha\beta^+$ thymocytes, they also gave rise to cells of the γδ-lineage (Figs. 7 and S4), demonstrating that they are the common precursors of cells committed to either the αβ- or γδ-lineage. However, the αβ potential of ISP $CD31^+CD1a^{low}$ was lower than that of EDP $CD31^+CD1a^{low}$, since they generated $CD3^+TCR\gamma\delta^+$ thymocytes in coculture at later time points (day 9 *vs.* day 14, Fig. 7). When $CD34^+CD1a^-$ DN were sorted and cocultured in the OP9-DL1 system, they showed a lower capacity to generate cells of the αβ-lineage and $CD3^+$ DP

TCR$\alpha\beta^+$ did not emerge prior to day 23 (data not shown). These results demonstrate that TCR$\gamma\delta$ T cells are the first to be produced in the thymus and suggest that the $\gamma\delta$-lineage is the default pathway in human thymocyte development. This is in agreement with the study of Blom et al. (13), in which it was shown that completed TCRδ and TCRγ rearrangements occurred prior to TCRβ at the $CD34^+CD1a^+$ DN and ISP stages. This is also compatible with the study of Joachims et al. (14), in which it was shown that $\gamma\delta$ thymocytes contain very few (9%) V-DJβ rearrangements which when present, were predominantly out-of-frame.

Our data also suggest that in humans, β-selection is concomitant with $\alpha\beta$-lineage commitment, as cells that are icTCRβ^+ ($CD31^-CD1a^{high}$ ISP and EDP) do not develop into TCR$\gamma\delta^+$ thymocytes (Fig. 7). These findings are concordant with the instructive model of lineage commitment and suggest that signals issued during β-selection are capable of diverting cells away from the $\gamma\delta$-lineage. The finding that $CD3^+$DN thymocytes are negative for icTCRβ while positive for icTCR$\gamma\delta$ further supports this (data not shown). Our findings contrast with those from studies in mice in which 15% of TCR$\gamma\delta^+$ cells were icTCRβ^+ (46).

Conclusions

The integration of our data with the findings of others is summarized in a model for thymocyte development (Fig. 8). In this model, $\gamma\delta$-lineage is the default pathway in which β-selection is needed to re-direct the cells away from this lineage into the $\alpha\beta$-lineage. Unlike the study of Carrasco et al. (12), which supports the successive rearrangement model, our data suggest that intrathymic development is not linear. Instead, we propose that β-selection is a branched pathway that, unlike that for mice, is not linked to the expression of either CD4 or CD8α. This is in agreement with the study by Joachims et al. (14), in which it was shown that icTCRβ was expressed on ISP, EDP as well as 3^-DP thymocytes

and that thymocytes lost their ability to become a γδ-T cell once they up-regulated CD8β and became $CD3^-$DPs. In this branched model, both γδ- and αβ-lineages arise from a common $CD31^+CD1a^{low}$ precursor. However, a cell's potential to commit to the γδ-lineage decreases as thymocytes up-regulate CD4 and CD8α, while the opposite is true for an αβ-T cell. DN thymocytes first rearrange their TCRδ and TCRγ genes and consequently rapidly develop into $TCR\gamma\delta^+$ DN in coculture. DN thymocytes can up-regulate their CD4 levels to become ISP thymocytes before committing to the γδ-lineage. CD4, once up-regulated on ISP cells, is able to be down-regulated if ISP have successfully rearranged their TCRδ and TCRγ loci, generating $TCR\gamma\delta^+$ DN. During differentiation, ISP thymocytes which have successfully rearranged their TCRβ alleles will up-regulate CD1a and down-regulate CD31 to give rise to $CD31^-CD1a^{high}$ ISP thymocytes. If neither δ, γ or β rearrangements occur, ISPs could still up-regulate CD8α but will not down-regulate CD31. If at the EDP level they are able to produce a productive TCRγδ, they then down-regulate CD4 (and to a lesser extent, CD8) this leads to $TCR\gamma\delta^+$ $CD8\alpha^+\beta^-$ thymocytes (and to a lower extent, $TCR\gamma\delta^+$ DN). In mice, $TCR\gamma\delta^+$ are predominantly DN, sometimes $CD8\alpha^+\alpha^+$, but rarely $CD4^+$ (47). Our data show that in humans, $TCR\gamma\delta^+$ are mostly DN, but CD8 and CD4 $TCR\gamma\delta^+$ are also present (5% and 12%, respectively) (data not shown). These differences are attributed to the fact that mouse $TCR\gamma\delta^+$ cells develop from DN3 and DN4 thymocytes, while human $TCR\gamma\delta^+$ arise from DN, ISP and EDP thymocytes. If EDP thymocytes fail to produce a functional TCRγδ molecule, they can still be rescued by productive rearrangement of TCRβ.

The finding that the γδ-lineage is the default pathway seems contradictory at first glance, since there are 300-fold more DP than γδ-thymocytes, but this observation can be reconciled by the fact that productive rearrangements of 2 TCR chains is more difficult than one, and it is also possible that not all productive δ and γ rearrangements lead to a functional TCRγδ.

Previously, cell surface expression of the TCR was the first time point at which lineage committed cells could be identified. The identification of surface markers that mark β-selected cells has made it possible to identify the precursor stage of β-selection and investigate early sequential events involved in this process and lineage commitment. Our data provides evidence that the $CD31^{+}CD1a^{low}$ population is the common uncommitted precursor for both lineages as well as the point of lineage divergence in human intrathymic development. This has enabled the characterization of a branched instructive model of intrathymic development.

Materials and Methods

Isolation of thymocytes from thymus samples.

Thymic tissues were obtained from children undergoing thoracic surgery at Children's Hospital of Eastern Ontario, with the informed consent of the child's parents and according to the guidelines of the bioethical committee of the Centre hospitalier de l'Université de Montreal (CHUM) and Research Ethics Board of the Children's Hospital of Eastern Ontario. Following mechanical dissociation of thymic tissue using cell strainers (Falcon), isolated thymocytes were harvested and stained.

Flow cytometry

Surface and intracellular staining by flow cytometry

Fresh thymocytes were stained simultaneously with the following mAbs for phenotypic characterization: FITC labeled anti-CD31 (BD Pharmingen), PerCP-Cy5-5 labeled anti-CD8α (BD Pharmingen), ECD labeled anti-CD8β (Coulter), PECy7 labeled anti-CD45RO (BD Pharmingen), APC labeled anti-CD34 (BD Pharmingen), Alexa-700 labeled anti-CD3 (BD Pharmingen) Pacific Blue labeled anti-CD1a (BD Pharmingen) and Amcyan labeled anti-CD4 (BD Pharmingen) with one of the following: PE labeled anti-CD5 (BD Pharmingen), PE labeled anti-CD28 (BD Pharmingen), PE labeled anti-CD62L (BD Pharmingen), PE labeled anti-CD38 (BD Pharmingen), or PE labeled anti-PD-1 (clone EH12.2H7, Biolegend).

For detection of the intracellular TCRβ chain or Ki67, surface staining was performed using the mAbs described above, after which permeabilized cells were incubated with PE-labeled Ki67 (Becton Dickinson, Pharmingen) or PE-labeled TCRβ (Ancell) or an isotype control in the dark for 30 minutes on ice. The cells

were then washed of the excess antibody, fixed in 2% PFA for 30 min and re-washed and resuspended in PBS 2%FCS overnight. Data was acquired on a Becton Dickinson LSR II^{TM} system through 9-color flow cytometry and analyzed using the DiVa^{TM} (Becton Dickinson systems) and FlowJo software (Tree Star, Ashland, OR).

Cell sorting and culture with OP9-DL1

Cell Sorting

Fresh thymocytes were sorted following surface staining with PECy7 labeled anti-CD8α (BD Pharmingen), ECD labeled anti-CD8β (Coulter), APC labeled anti-CD31 (BD Pharmingen), Alexa-700 labeled anti-CD3 (BD Pharmingen) Pacific Blue labeled anti-CD1a (BD Pharmingen) and Amcyan labeled anti-CD4 (BD Pharmingen). Six-color cell sorting was performed using the FACSAria (Becton Dickinson). The populations sorted include: ISP and EDP $CD31^{-}CD1a^{low}$ and $CD31^{+}CD1a^{hi}$. Isolated subsets were sorted at >99% purity.

OP9-DL1 culture

A minimum of 2 X 10^4 sorted ISP and EDP were added in individual wells from a 6-well plate confluent with OP9-DL1 cells in α-minimal essential medium (αMEM) media supplemented with 20% FBS, penicillin (50 U/mL) and streptomycin (50 g/mL). The recombinant human cytokines Flt-3L (1 ng/mL) (Peprotech) and interleukin-7 (IL-7) (1 ng/mL) (Cedarlane) were added at the initiation of coculture and every 4-5 days during harvesting. At the time points indicated, thymocytes were collected and passaged through a 70-μm filter to reduce stromal cell line aggregates. Half of the thymocytes from each well were used for flow analysis and the remaining thymocytes were cocultured in new wells confluent with OP9-DL1 cells.

Characterization of developing thymocytes

To monitor thymocyte proliferation ex vivo, sorted cells were labeled with CFSE prior to coculture with OP9-DL1 cells. Briefly, sorted thymocytes were incubated with 0.2 μM CFSE for 8 minutes at room temperature after which the reaction was stopped with FBS and cells were washed twiced.

At the time points indicated, CFSE-labeled thymocytes were stained with the following mAbs for phenotypic characterization: 7-AAD (BD Pharmingen) to remove dead cells from the analysis, ECD labeled anti-CD8β (Coulter), PECy7 labeled anti-CD8α (BD Pharmingen), APC labeled anti-CD31 (BD Pharmingen), Alexa-700 labeled anti-CD3 (BD Pharmingen) Pacific Blue labeled anti-CD1a (BD Pharmingen) and Amcyan labeled anti-CD4 (BD Pharmingen) with PE labeled anti-PD-1 (clone EH12.2H7, Biolegend) or PE labeled anti-CD28 (BD Pharmingen). CFSE-unlabeled thymocytes were stained with the following mAbs for visualization of lineage commitment: 7-AAD (BD Pharmingen) to remove dead cells from the analysis, FITC labeled anti-CD31 (BD Pharmingen), PerCy7-labeled anti-CD8α (BD Pharmingen), ECD labeled anti-CD8β (Coulter), Alexa-700 labeled anti-CD3 (BD Pharmingen) Pacific Blue labeled anti-CD1a (BD Pharmingen), APC-Cy7 labeled anti-CD27 (eBioscience), Amcyan labeled anti-CD4 (BD Pharmingen), APC labeled anti-TCRγδ (BD Pharmingen), and PE labeled anti-TCRαβ (BD Pharmingen). Data was acquired on a Becton Dickinson LSR II™ system through 9- or 10-color flow cytometry and analyzed over a 4-log scale using DiVa™ software (Becton Dickinson systems) and FlowJo software (Tree Star, Ashland, OR).

Cell sorting and mRNA quantification

Fresh thymocytes were sorted following surface staining with violet-fluorescent dye from LIVE/DEAD Fixable Dead Cell Stain Kits (Invitrogen) to remove dead cells, FITC labeled anti-CD31 (BD Pharmingen), PE labeled anti-CD1a (Coulter), PerCP-Cy5-5 labeled anti-CD8α (BD Pharmingen), ECD labeled anti-CD8β (Coulter), PECy7 labeled anti-CD3 (BD Pharmingen), APC labeled anti-CD34

(BD Pharmingen), Alexa-700 labeled anti-CD4 (BD Pharmingen). Eight-color cell sorting was performed using the FACSAria (Becton Dickinson). Six populations were sorted (DN $CD34^{+}CD1a^{-}$, ISP and EDP $CD31^{-}CD1a^{low}$ and $CD31^{+}CD1a^{hi}$ and $CD3^{-}$DP) into RPMI media after which cells were lysed with RLT buffer supplemented with β-mercaptoethanol. RNA from these subsets was purified using RNA extraction kits (QIAGEN). Quantification and RNA quality was assessed using the Bioanalyzer (Agilent Technologies). qPCR was performed at the genomics platform of the Institute for Research in Immunology and Cancer (Montreal), as previously described (48). qPCR analysis was performed using the normalized ΔCt method, with TBP as housekeeping gene. Gene expression levels in $CD3^{-}$ thymocyte subsets were normalized to levels in the purified $CD31^{+}CD1a^{low}$ ISP population.

Statistics and Analysis

RT-PCR gene expression data was analyzed using Bioconductor (49), an open-source software library for the analyses of genomic data based on R, a language and environment for statistical computing and graphics (www.r-project.org). The normalized ΔCt expression matrix showing gene expression as rows and samples as columns was used as input for linear modeling using the Bioconductor's *Limma* package (50), which estimates the fold-change between predefined groups by fitting a linear model and using an empirical Bayes method to moderate standard errors of the estimated log-fold changes for expression values from each gene. *P* values from the resulting comparison were adjusted for multiple testing according to the method of Benjamini and Hochberg (51). This method controls the false discovery rate, which was set to 0.05 in this analysis.

Pie charts for phenotypic characterization of developing thymocytes in OP9-DL1 cells were obtained using the Spice software (Version 5.1, Mario Roederer, Vaccine Research Center, NIAID, NIH).

Statistical analysis (two-tailed paired Student t-test) was performed using MS Excel. A *P* value $\leq .05$ was considered statistically significant.

Bibliography

1. Spits, H., Development of alphabeta T cells in the human thymus. Nat Rev Immunol, 2002. 2(10): p. 760-72.

2. Weerkamp, F., et al., Human thymus contains multipotent progenitors with T/B lymphoid, myeloid, and erythroid lineage potential. Blood, 2006. 107(8): p. 3131-7.

3. Kraft, D.L., I.L. Weissman, and E.K. Waller, Differentiation of CD3-4-8- human fetal thymocytes in vivo: characterization of a CD3-4+8- intermediate. J Exp Med, 1993. 178(1): p. 265-77.

4. Hori, T., et al., Identification of a novel human thymocyte subset with a phenotype of CD3- CD4+ CD8 alpha + beta-1. Possible progeny of the CD3- CD4- CD8- subset. J Immunol, 1991. 146(12): p. 4078-84.

5. Vanhecke, D., et al., Characterization of distinct stages during the differentiation of human CD69+CD3+ thymocytes and identification of thymic emigrants. J Immunol, 1995. 155(4): p. 1862-72.

6. Fehling, H.J., et al., Crucial role of the pre-T-cell receptor alpha gene in development of alpha beta but not gamma delta T cells. Nature, 1995. 375(6534): p. 795-8.

7. Xi, H., et al., Interplay between RORgammat, Egr3, and E proteins controls proliferation in response to pre-TCR signals. Immunity, 2006. 24(6): p. 813-26.

8. Kruisbeek, A.M., et al., Branching out to gain control: how the pre-TCR is linked to multiple functions. Immunol Today, 2000. 21(12): p. 637-44.

9. Borowski, C., et al., On the brink of becoming a T cell. Curr Opin Immunol, 2002. 14(2): p. 200-6.

10. Taghon, T., et al., Developmental and molecular characterization of emerging beta- and gammadelta-selected pre-T cells in the adult mouse thymus. Immunity, 2006. 24(1): p. 53-64.

11. Teague, T.K., et al., CD28 expression redefines thymocyte development during the pre-T to DP transition. Int Immunol, 2010. 22(5): p. 387-97.

12. Carrasco, Y.R., et al., Beta-selection is associated with the onset of CD8beta chain expression on CD4(+)CD8alphaalpha(+) pre-T cells during human intrathymic development. Blood, 1999. 94(10): p. 3491-8.

13. Blom, B., et al., TCR gene rearrangements and expression of the pre-T cell receptor complex during human T-cell differentiation. Blood, 1999. 93(9): p. 3033-43.

14. Joachims, M.L., et al., Human alpha beta and gamma delta thymocyte development: TCR gene rearrangements, intracellular TCR beta expression, and gamma delta developmental potential--differences between men and mice. J Immunol, 2006. 176(3): p. 1543-52.

15. Kimmig, S., et al., Two subsets of naive T helper cells with distinct T cell receptor excision circle content in human adult peripheral blood. J Exp Med, 2002. 195(6): p. 789-94.

16. Ramiro, A.R., et al., Regulation of pre-T cell receptor (pT alpha-TCR beta) gene expression during human thymic development. J Exp Med, 1996. 184(2): p. 519-30.

17. Verschuren, M.C., et al., PJA-BP expression and TCR delta deletion during human T cell differentiation. Int Immunol, 1998. 10(12): p. 1873-80.

18. Dion, M.L., et al., HIV infection rapidly induces and maintains a substantial suppression of thymocyte proliferation. Immunity, 2004. 21(6): p. 757-68.

19. Panigada, M., et al., Constitutive endocytosis and degradation of the pre-T cell receptor. J Exp Med, 2002. 195(12): p. 1585-97.

20. Azzam, H.S., et al., Fine tuning of TCR signaling by CD5. J Immunol, 2001. 166(9): p. 5464-72.

21. Tanel, A., et al., Cellular and molecular mechanisms of memory T-cell survival. Expert Rev Vaccines, 2009. 8(3): p. 299-312.

22. Harper, J.W., et al., The p21 Cdk-interacting protein Cip1 is a potent inhibitor of G1 cyclin-dependent kinases. Cell, 1993. 75(4): p. 805-16.

23. Smith, M.L., et al., Interaction of the p53-regulated protein Gadd45 with proliferating cell nuclear antigen. Science, 1994. 266(5189): p. 1376-80.

24. Okada, H., et al., Survivin loss in thymocytes triggers p53-mediated growth arrest and p53-independent cell death. J Exp Med, 2004. 199(3): p. 399-410.

25. Bain, G., et al., E2A proteins are required for proper B cell development and initiation of immunoglobulin gene rearrangements. Cell, 1994. 79(5): p. 885-92.

26. Miranda, G.A., et al., Combinatorial regulation of the murine RAG-2 promoter by Sp1 and distinct lymphocyte-specific transcription factors. Mol Immunol, 2002. 38(15): p. 1151-9.

27. La Motte-Mohs, R.N., E. Herer, and J.C. Zuniga-Pflucker, Induction of T-cell development from human cord blood hematopoietic stem cells by Delta-like 1 in vitro. Blood, 2005. 105(4): p. 1431-9.

28. Schmitt, T.M. and J.C. Zuniga-Pflucker, Induction of T cell development from hematopoietic progenitor cells by delta-like-1 in vitro. Immunity, 2002. 17(6): p. 749-56.

29. Washburn, T., et al., Notch activity influences the alphabeta versus gammadelta T cell lineage decision. Cell, 1997. 88(6): p. 833-43.

30. Taghon, T., et al., Notch signaling is required for proliferation but not for differentiation at a well-defined beta-selection checkpoint during human T-cell development. Blood, 2009. 113(14): p. 3254-63.

31. Newman, P.J., et al., PECAM-1 (CD31) cloning and relation to adhesion molecules of the immunoglobulin gene superfamily. Science, 1990. 247(4947): p. 1219-22.

32. Sagawa, K., et al., The protein-tyrosine phosphatase SHP-2 associates with tyrosine-phosphorylated adhesion molecule PECAM-1 (CD31). J Biol Chem, 1997. 272(49): p. 31086-91.

33. Tanaskovic, S., et al., CD31 (PECAM-1) is a marker of recent thymic emigrants among CD4+ T-cells, but not CD8+ T-cells or gammadelta T-cells, in HIV patients responding to ART. Immunol Cell Biol, 2010. 88(3): p. 321-7.

34. Blom, B. and H. Spits, Development of human lymphoid cells. Annu Rev Immunol, 2006. 24: p. 287-320.

35. Schwartz, R., et al., Gene expression patterns define novel roles for E47 in cell cycle progression, cytokine-mediated signaling, and T lineage development. Proc Natl Acad Sci U S A, 2006. 103(26): p. 9976-81.

36. Landry, J.W., et al., Chromatin remodeling complex NURF regulates thymocyte maturation. Genes Dev, 2011. 25(3): p. 275-86.

37. Garcia-Peydro, M., V.G. de Yebenes, and M.L. Toribio, Notch1 and IL-7 receptor interplay maintains proliferation of human thymic progenitors while suppressing non-T cell fates. J Immunol, 2006. 177(6): p. 3711-20.

38. De Smedt, M., et al., Active form of Notch imposes T cell fate in human progenitor cells. J Immunol, 2002. 169(6): p. 3021-9.

39. Van de Walle, I., et al., An early decrease in Notch activation is required for human TCR-alphabeta lineage differentiation at the expense of TCR-gammadelta T cells. Blood, 2009. 113(13): p. 2988-98.

40. Radtke, F., et al., Deficient T cell fate specification in mice with an induced inactivation of Notch1. Immunity, 1999. 10(5): p. 547-58.

41. Radtke, F., et al., The role of Notch signaling during hematopoietic lineage commitment. Immunol Rev, 2002. 187: p. 65-74.

42. Prinz, I., et al., Visualization of the earliest steps of gammadelta T cell development in the adult thymus. Nat Immunol, 2006. 7(9): p. 995-1003.

43. MacDonald, H.R. and A. Wilson, The role of the T-cell receptor (TCR) in alpha beta/gamma delta lineage commitment: clues from intracellular TCR staining. Immunol Rev, 1998. 165: p. 87-94.

44. Ferrero, I., et al., TCRgamma silencing during alphabeta T cell development depends upon pre-TCR-induced proliferation. J Immunol, 2006. 177(9): p. 6038-43.

45. Aifantis, I., et al., On the role of the pre-T cell receptor in alphabeta versus gammadelta T lineage commitment. Immunity, 1998. 9(5): p. 649-55.

46. Wilson, A. and H.R. MacDonald, A limited role for beta-selection during gamma delta T cell development. J Immunol, 1998. 161(11): p. 5851-4.

47. Bluestone, J.A., et al., Ligand specificity and repertoire development of murine TCR gamma delta cells. Curr Top Microbiol Immunol, 1991. 173: p. 133-9.

48. Younes, S.A., et al., HIV-1 viremia prevents the establishment of interleukin 2-producing HIV-specific memory CD4+ T cells endowed with proliferative capacity. J Exp Med, 2003. 198(12): p. 1909-22.

49. Gentleman, R.C., et al., Bioconductor: open software development for computational biology and bioinformatics. Genome Biol, 2004. 5(10): p. R80.

50. Smyth, G.K., J. Michaud, and H.S. Scott, Use of within-array replicate spots for assessing differential expression in microarray experiments. Bioinformatics, 2005. 21(9): p. 2067-75.

51. Klipper-Aurbach, Y., et al., Mathematical formulae for the prediction of the residual beta cell function during the first two years of disease in children and adolescents with insulin-dependent diabetes mellitus. Med Hypotheses, 1995. 45(5): p. 486-90.

Figure Legends

Figure 1. Expression of intracellular (ic) TCRβ in $CD3^-$ thymocytes (A) Representative characterization of thymocyte maturation stages using multiparameter flow cytometry. Thymocyte subpopulations are listed from the most immature to the most mature on the *left panel*. $CD3^-$ thymocytes were divided based on the markers CD4, CD8α, CD8β and CD34, after which the expression of CD31 and CD1a was analyzed and used to further characterize ISP and EDP cells as $CD31^+CD1a^{low}$ or $CD31^-CD1a^{high}$. (B) The expression of icTCRβ was analyzed in DN, ISP $CD31^+CD1a^{low}$ and CD34 $CD31^-CD1a^{high}$, EDP $CD31^+CD1a^{low}$ and $CD31^-CD1a^{high}$, and 3^-DP (** $P < .001$). (C) Expression of CD31 and CD1a within icTCRβ^+ ISP and EDP.

Figure 2. Quantitative real-time RT-PCR gene expression analysis of T cell related genes in $CD3^-$ thymocytes subsets. Two way hierarchical clustering of the gene expression profiles of ISP (N=3) and EDP (N=2) samples using the differentially expressed genes obtained following a two-class *Limma* comparison between $CD31^+CD1a^{low}$ and $CD31^-CD1a^{high}$ ISP samples. The clustering analysis discriminates between $CD31^+CD1a^{low}$ and $CD31^-CD1a^{high}$ samples which cluster in two main clusters whether they originated from ISP or EDP thymocytes. Genes with significant modulations between the $CD31^+CD1a^{low}$ and $CD31^-CD1a^{high}$ ISP subsets are shown (*P* values was set to 0.05).

Figure 3. Phenotypic and transcriptional characterization of $CD3^-$ thymocytes. **A.** The $CD31^-CD1a^{high}$ phenotype is associated with increased levels of activation. Flow cytometric analysis of the activation markers PD-1, CD28, CD5 and CD62L in DN, ISP $CD31^+CD1a^{low}$ and CD34 $CD31^-CD1a^{high}$, EDP $CD31^+CD1a^{low}$ and $CD31^-CD1a^{high}$, and 3^-DP. **B.** The $CD31^-CD1a^{high}$ phenotype is associated with proliferation. Representative example of flow cytometric analysis of cell size (as measured by FSC). Detection of the nuclear antigen Ki67 by flow cytometry in DN, ISP $CD31^+CD1a^{low}$ and CD34 $CD31^-CD1a^{high}$, EDP $CD31^+CD1a^{low}$ and $CD31^-CD1a^{high}$, and 3^-DP. Detection of Mybl2, Cyclin D3, Cdkn1a, and Socs-1 in

DN, ISP $CD31^{+}CD1a^{low}$ and CD34 $CD31^{-}CD1a^{high}$, EDP $CD31^{+}CD1a^{low}$ and $CD31^{-}CD1a^{high}$, and 3^{-}DP by qRT-PCR. Data shown are the average ± STDV from at least two sets of independent samples (three sets of independent samples for ISP subsets), relative to levels in the purified ISP $CD31^{+}CD1a^{low}$ population. **C.** The $CD31^{-}CD1a^{high}$ phenotype is associated with decreased IL-7 signaling. Detection of CD127, Bcl-2 and Survivin in DN, ISP $CD31^{+}CD1a^{low}$ and CD34 $CD31^{-}CD1a^{high}$, EDP $CD31^{+}CD1a^{low}$ and $CD31^{-}CD1a^{high}$, and 3^{-}DP by qRT-PCR. Data shown are the average ± STDV from at least two sets of independent samples (three sets of independent samples for ISP subsets), relative to levels in the purified ISP $CD31^{+}CD1a^{low}$ population. **D.** The $CD31^{-}CD1a^{high}$ phenotype is associated with allelic exclusion. Detection of RAG-1. RAG-2, HEB and c-myb in DN, ISP $CD31^{+}CD1a^{low}$ and CD34 $CD31^{-}CD1a^{high}$, EDP $CD31^{+}CD1a^{low}$ and $CD31^{-}CD1a^{high}$, and 3^{-}DP by qRT-PCR. Data shown are the average ± STDV from at least two sets of independent samples (three sets of independent samples for ISP subsets), relative to levels in the purified ISP $CD31^{+}CD1a^{low}$ population. **E.** The $CD31^{-}CD1a^{high}$ phenotype is associated with decreased Notch signaling. Detection of Notch-1, Notch-3, Hes-1 and pTα in DN, ISP $CD31^{+}CD1a^{low}$ and CD34 $CD31^{-}CD1a^{high}$, EDP $CD31^{+}CD1a^{low}$ and $CD31^{-}CD1a^{high}$, and 3^{-}DP by qRT-PCR. Data shown are the average ± STDV from at least two sets of independent samples (three sets of independent samples for ISP subsets), relative to levels in the purified ISP $CD31^{+}CD1a^{low}$ population. (* $P < .05$, ** $P < .001$).

Figure 4. Development of $CD31^{+}CD1a^{low}$ and $CD31^{-}CD1a^{high}$ thymocytes in the OP9-DL1 culture system. At day 5, 9, and 14, cells were taken out from culture from ISP $CD31^{+}CD1a^{low}$ (A) and $CD31^{-}CD1a^{high}$ subsets (B) as well as EDP $CD31^{+}CD1a^{low}$ (C) and $CD31^{-}CD1a^{high}$ subsets (D) and stained for CD3, CD4, CD8α and CD8β. Maturation was analyzed by comparing the frequencies of $CD3^{-}$ DN, $CD3^{-}$ISP, $CD3^{-}$EDP, $CD3^{-}$DP, $CD3^{+}$DN, $CD3^{+}$DP, SP4 and SP8 developing at each time point using the Spice software. Results shown are representative for 4 independent experiments for ISP subsets and 3 independent experiments for EDP subsets.

Figure 5. $CD31^{+}CD1a^{low}$ subsets are the precursors of $CD31^{-}CD1a^{high}$ thymocytes. $CD4^{+}$ ISP $CD31^{+}CD1a^{low}$ were sorted and cultured in the OP9-DL1 system. CFSE-stained subsets were taken out from coculture at day 3, 5 and 7 and monitored for the down-regulation of CD31 and up-regulation of CD1a for ISP remaining in coculture from ISP $CD31^{+}CD1a^{low}$ (A), $CD3^{-}$DP emerging in coculture from ISP $CD31^{+}CD1a^{low}$ (B), and $CD3^{-}$DP emerging in coculture from EDP $CD31^{+}CD1a^{low}$ (C). Results shown are representative for 3 independent experiments.

Figure 6. Thymocytes not progressing towards the αβ-lineage do not down-regulate CD31. CFSE-stained subsets were monitored for the down-regulation of CD31 and up-regulation of CD1a within $CD3^{-}$DN developing in coculture from sorted ISP $CD31^{+}CD1a^{low}$ (A), and $CD3^{-}CD4^{-}CD8\alpha^{+}$ emerging in coculture from sorted EDP $CD31^{+}CD1a^{low}$ (B) at day 3, 5 and 7. Results shown are representative for 3 independent experiments.

Figure 7. $CD31^{+}CD1a^{low}$ subsets are uncommitted precursors, while $CD31^{-}CD1a^{high}$ are β-selected. $CD31^{+}CD1a^{low}$ and $CD31^{-}CD1a^{high}$ ISP and EDP were sorted and cocultured in the OP9-DL1 system. (A) At day 5, 9, and 14, cells were taken out from culture from each subset and stained for CD3, TCRαβ and TCRδγ to monitor their progress into the αβ- and δγ-lineage. Cells were first gated on $CD3^{+}$ then TCRαβ and TCRδγ expression were analyzed. (B) At day 5, 9 and 14, cells were taken out from culture from each subset and $CD3^{+}$ $TCR\alpha\beta^{+}$ and $TCR\delta\gamma^{+}$ thymocytes were analyzed for CD4, CD8α, and CD8β expression. (C) At day 5 and 9, cells were taken out from culture from $CD31^{+}CD1a^{low}$ and $CD31^{-}CD1a^{hi}$ EDP subsets and stained for CD3, TCRαβ and TCRδγ to monitor their progress into the αβ- and δγ-lineage. Cells were first gated on $CD3^{+}$ then TCRαβ and TCRδγ expression were analyzed. (D) At day 5 and 9, cells were taken out from culture from each subset and $CD3^{+}$ $TCR\alpha\beta^{+}$ and $TCR\delta\gamma^{+}$ thymocytes were analyzed for CD4, CD8α, and CD8β expression. Results shown

are representative for 4 independent experiments for ISP subsets and 3 independent experiments for EDP subsets.

Figure 8. Schematic model of human thymocyte differentiation. β-selection occurs in human over a prolonged window of development as thymocytes progress from ISP to EDP and 3-DP. Thymocytes having received β-selection signals will adopt the $CD31^{-}CD1a^{high}$ phenotype and develop into αβ T-cells. Both lineages arise from the common $CD31^{+}CD1a^{low}$ precursor and the cell's potential to become a γδ-T cell decreases as thymocytes up-regulate CD4 and CD8α, while the opposite is true for an αβ-T cell, as confirmed by the decrease of the percent of CD31 with increasing maturation.

Figure S1. Expression of the stem cell marker CD34 and icTCRβ within $CD3^{-}$ thymocyte subsets. **A.** Representative example of flow cytometric expression of CD34 and **B.** average MFI of expression of CD34 in DN, ISP $CD31^{+}CD1a^{low}$ and CD34 $CD31^{-}CD1a^{high}$, EDP $CD31^{+}CD1a^{low}$ and $CD31^{-}CD1a^{high}$, and 3^{-}DP. **C.** Average frequencies of icTCRβ in DN, ISP $CD31^{+}CD1a^{low}$ and CD34 $CD31^{-}CD1a^{high}$, EDP $CD31^{+}CD1a^{low}$ and $CD31^{-}CD1a^{high}$, and 3^{-}DP. (* $P < .05$, ** $P < .001$).

Figure S2. The $CD31^{-}CD1a^{high}$ phenotype is associated with the formation of the pTα:βTCR complex. Average frequencies of the MFI of CD3 in DN, ISP $CD31^{+}CD1a^{low}$ and CD34 $CD31^{-}CD1a^{high}$, EDP $CD31^{+}CD1a^{low}$ and $CD31^{-}CD1a^{high}$, and 3^{-}DP. (** $P < .001$).

Figure S3. The $CD31^{-}CD1a^{high}$ phenotype is associated with increased levels of activation and proliferation. Average MFI of the expression of PD-1, CD28 and CD5 as well as average frequencies of CD62L and Ki67 in DN, ISP $CD31^{+}CD1a^{low}$ and CD34 $CD31^{-}CD1a^{high}$, EDP $CD31^{+}CD1a^{low}$ and $CD31^{-}CD1a^{high}$, and 3^{-}DP. (* $P < .05$, ** $P < .001$).

Figure S4. TCRαβ and TCRγδ expression of SP cells developing from $CD31^{+}CD1a^{low}$ and $CD31^{-}CD1a^{hi}$ ISP thymocytes. Characterization of SP CD8 and CD4 thymocytes developing from $CD31^{+}CD1a^{low}$ and $CD31^{-}CD1a^{hi}$ ISP at day 14. Both subsets were gated on $CD3^{+}$ and then analyzed for the expression of surface TCRαβ and TCRγδ.

Figure 1

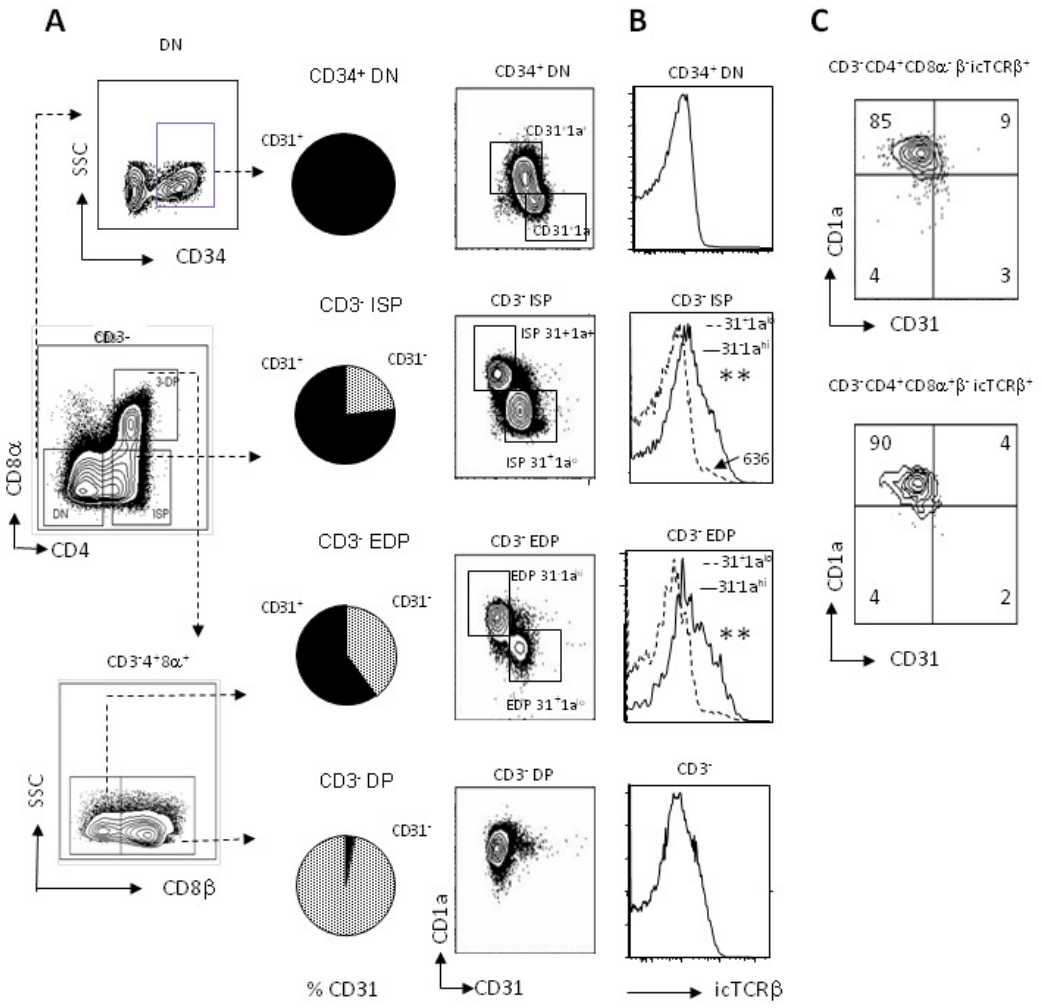
A
B
C
DN
CD34+ DN
SSC
CD34
CD31+
CD34+ DN
CD31-1a-
CD31-1a+
CD34+ DN
CD3- ISP
CD3-
3-DP
DN
ISP
CD8α
CD4
CD31+
CD31-
CD3- ISP
ISP 31+1a+
ISP 31+1a-
CD3- ISP
--31+1ahi
—31-1ahi
**
636
CD3-4+8α+
CD3- EDP
CD31+
CD31-
CD3- EDP
EDP 31-1ahi
EDP 31+1a-
CD3- EDP
--31+1ahi
—31-1ahi
**
SSC
CD8β
CD3- DP
CD31-
CD3- DP
CD3-
CD1a
CD31
% CD31
icTCRβ
CD3-CD4+CD8α-β-icTCRβ+
85
9
4
3
CD1a
CD31
CD3-CD4+CD8α+β- icTCRβ+
90
4
4
2
CD1a
CD31

Figure 2

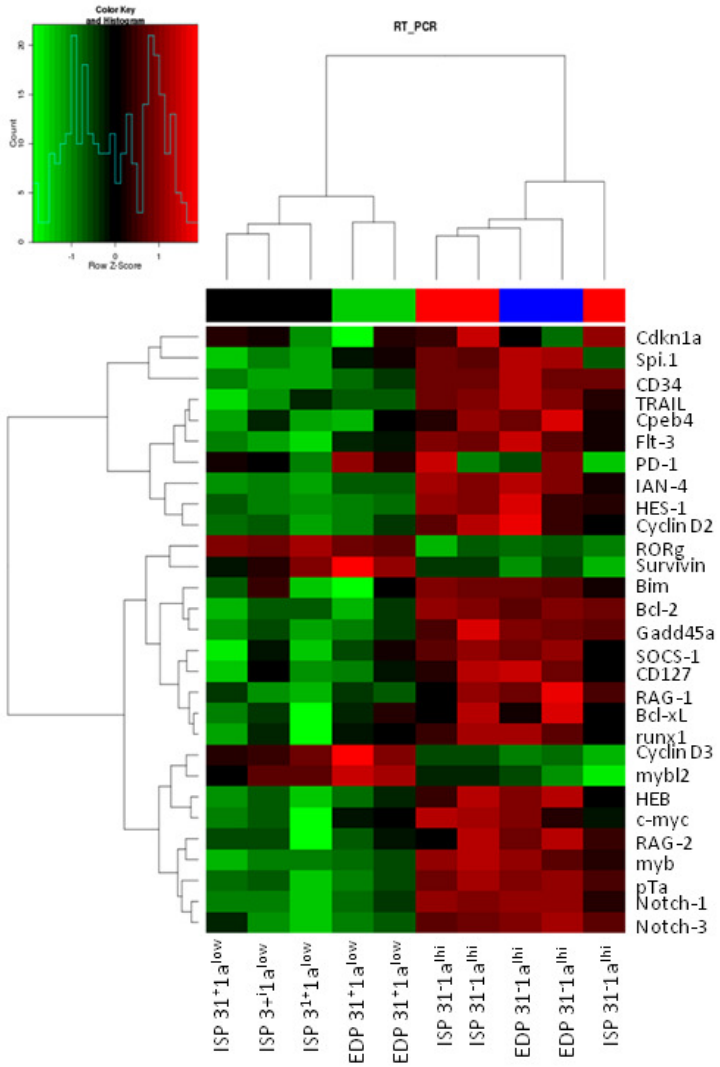
Color Key and Histogram
Count
Row Z-Score
RT_PCR
Cdkn1a
Spi.1
CD34
TRAIL
Cpeb4
Flt-3
PD-1
IAN-4
HES-1
Cyclin D2
RORg
Survivin
Bim
Bcl-2
Gadd45a
SOCS-1
CD127
RAG-1
Bcl-xL
runx1
Cyclin D3
mybl2
HEB
c-myc
RAG-2
myb
pTa
Notch-1
Notch-3
ISP 31+1alow
ISP 3-i1alow
ISP 31+1alow
EDP 31+1alow
EDP 31+1alow
ISP 31-1alhi
ISP 31-1alhi
EDP 31-1alhi
EDP 31-1alhi
ISP 31-1alhi

Figure 3
A

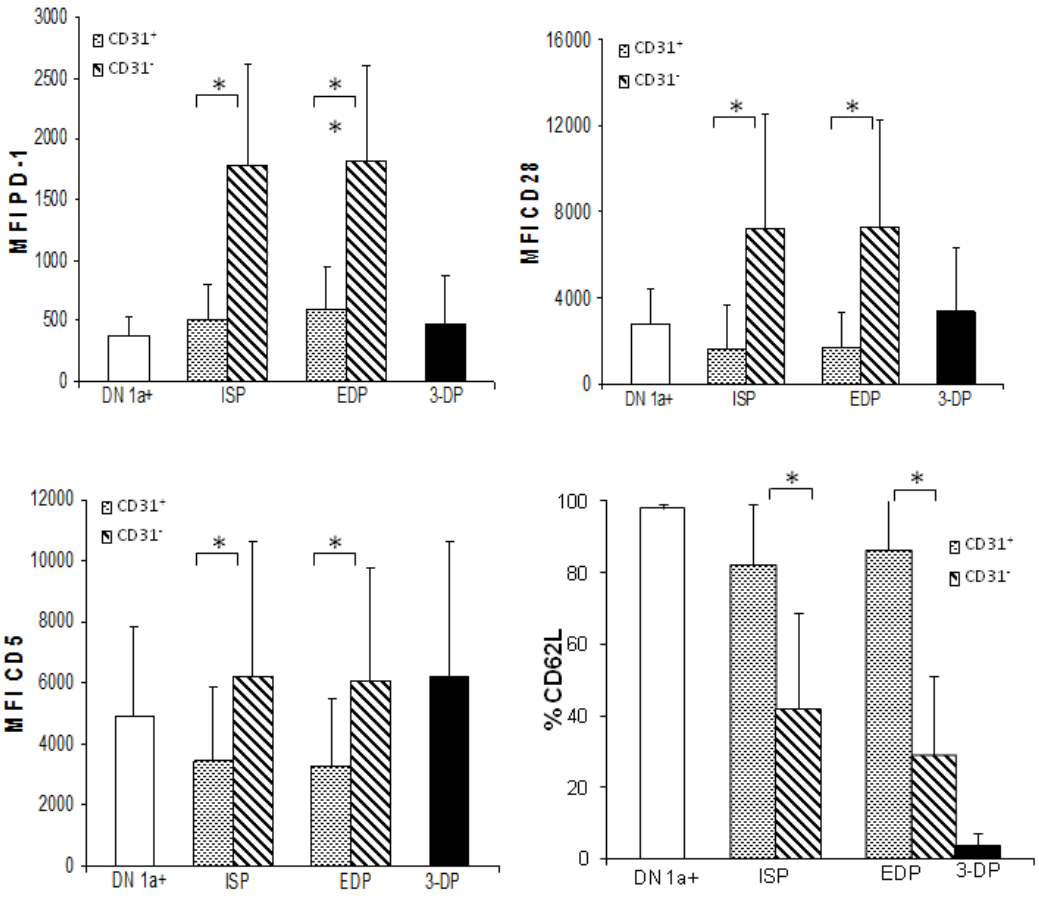

Figure 3

B

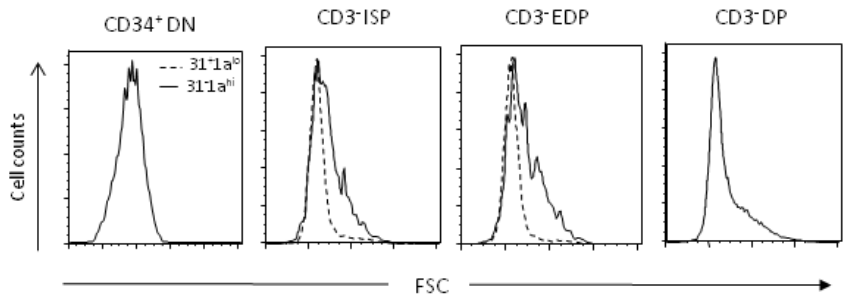
CD34+ DN
CD3-ISP
CD3-EDP
CD3-DP
31-1a-
31-1a+
Cell counts
FSC

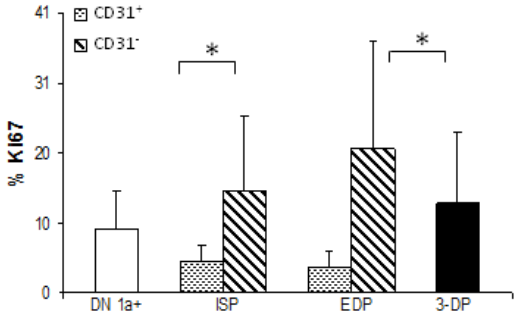
CD31+
CD31-
% KI67
41
31
20
10
0
DN 1a+
ISP
EDP
3-DP

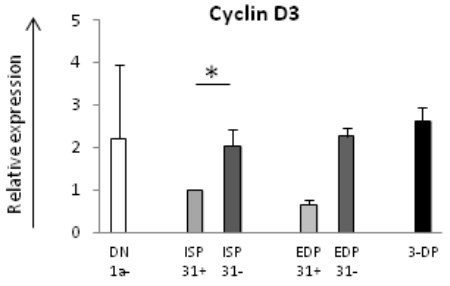
Cyclin D3
Relative expression
DN 1a-
ISP 31+
ISP 31-
EDP 31+
EDP 31-
3-DP

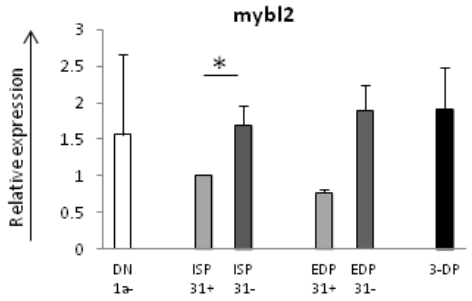
mybl2
Relative expression
DN 1a-
ISP 31+
ISP 31-
EDP 31+
EDP 31-
3-DP

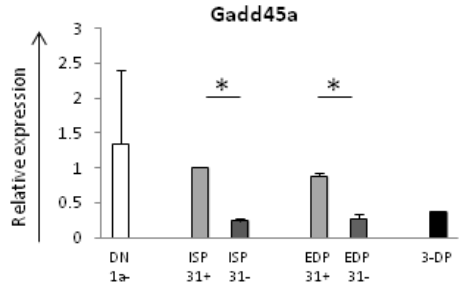
Gadd45a
Relative expression
DN 1a-
ISP 31+
ISP 31-
EDP 31+
EDP 31-
3-DP

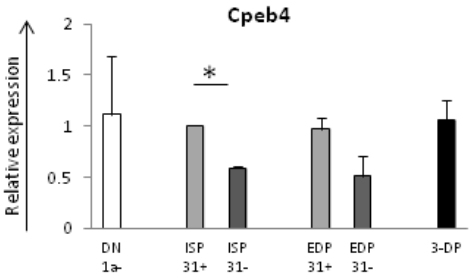
Cpeb4
Relative expression
DN 1a-
ISP 31+
ISP 31-
EDP 31+
EDP 31-
3-DP

C

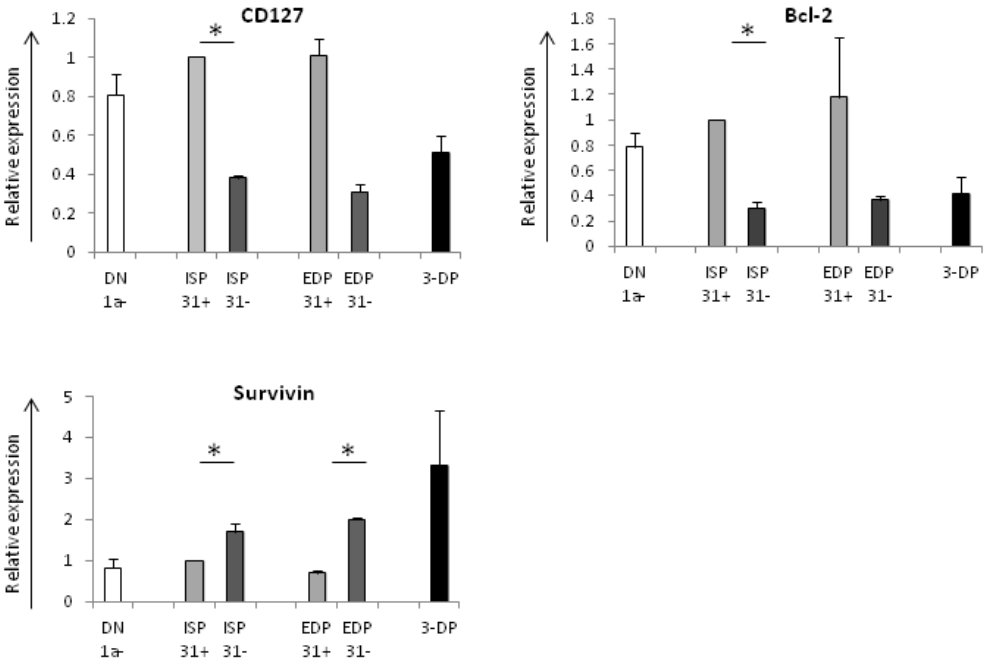
CD127
Relative expression
1.2
1
0.8
0.6
0.4
0.2
0
*
DN 1a-
ISP 31+
ISP 31-
EDP 31+
EDP 31-
3-DP
Bcl-2
Relative expression
1.8
1.6
1.4
1.2
1
0.8
0.6
0.4
0.2
0
*
DN 1a-
ISP 31+
ISP 31-
EDP 31+
EDP 31-
3-DP
Survivin
Relative expression
5
4
3
2
1
0
*
*
DN 1a-
ISP 31+
ISP 31-
EDP 31+
EDP 31-
3-DP

Figure 3

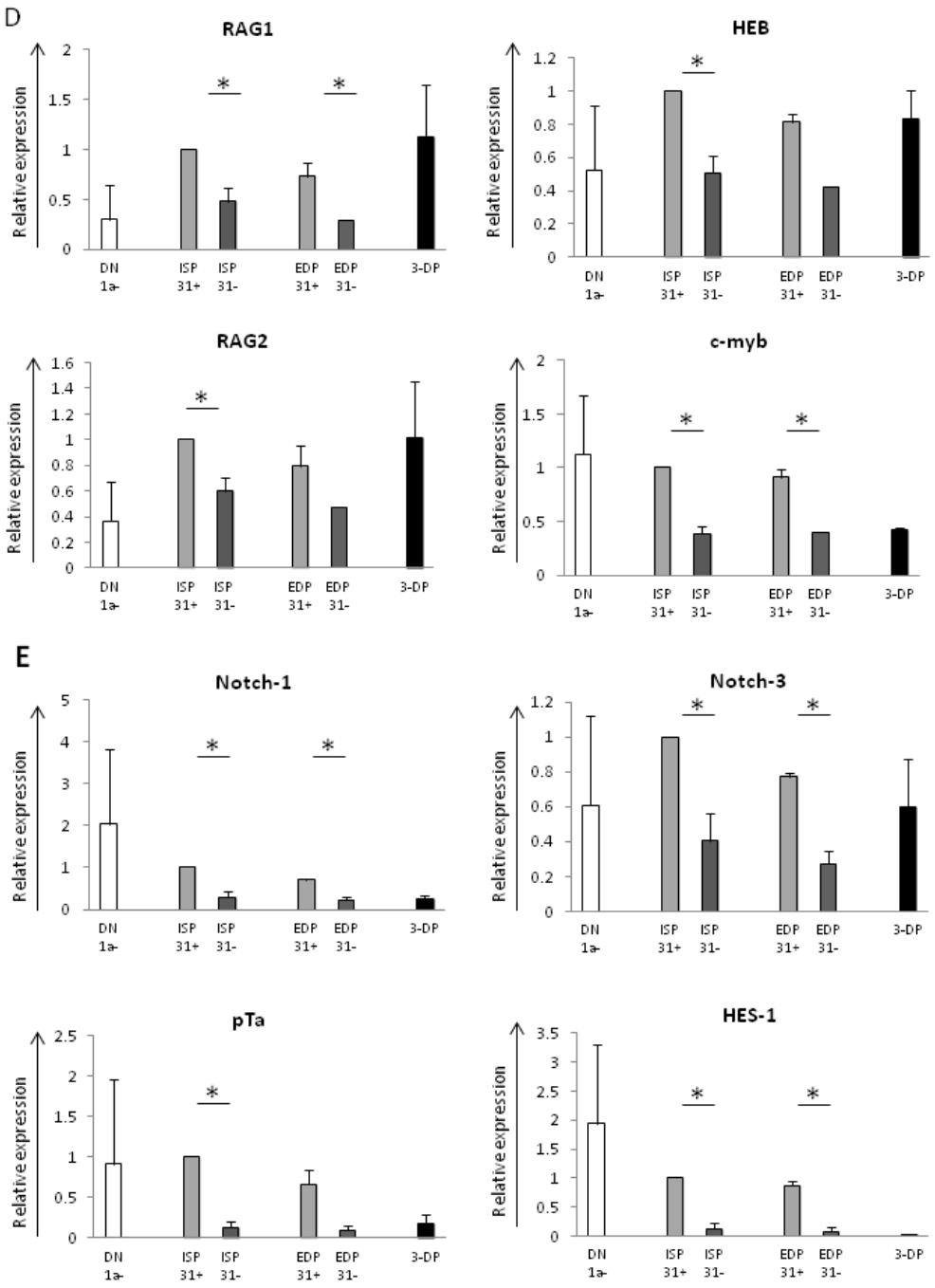
D
RAG1
HEB
RAG2
c-myb
E
Notch-1
Notch-3
pTa
HES-1
Relative expression
DN 1a-
ISP 31+
ISP 31-
EDP 31+
EDP 31-
3-DP

Figure 4

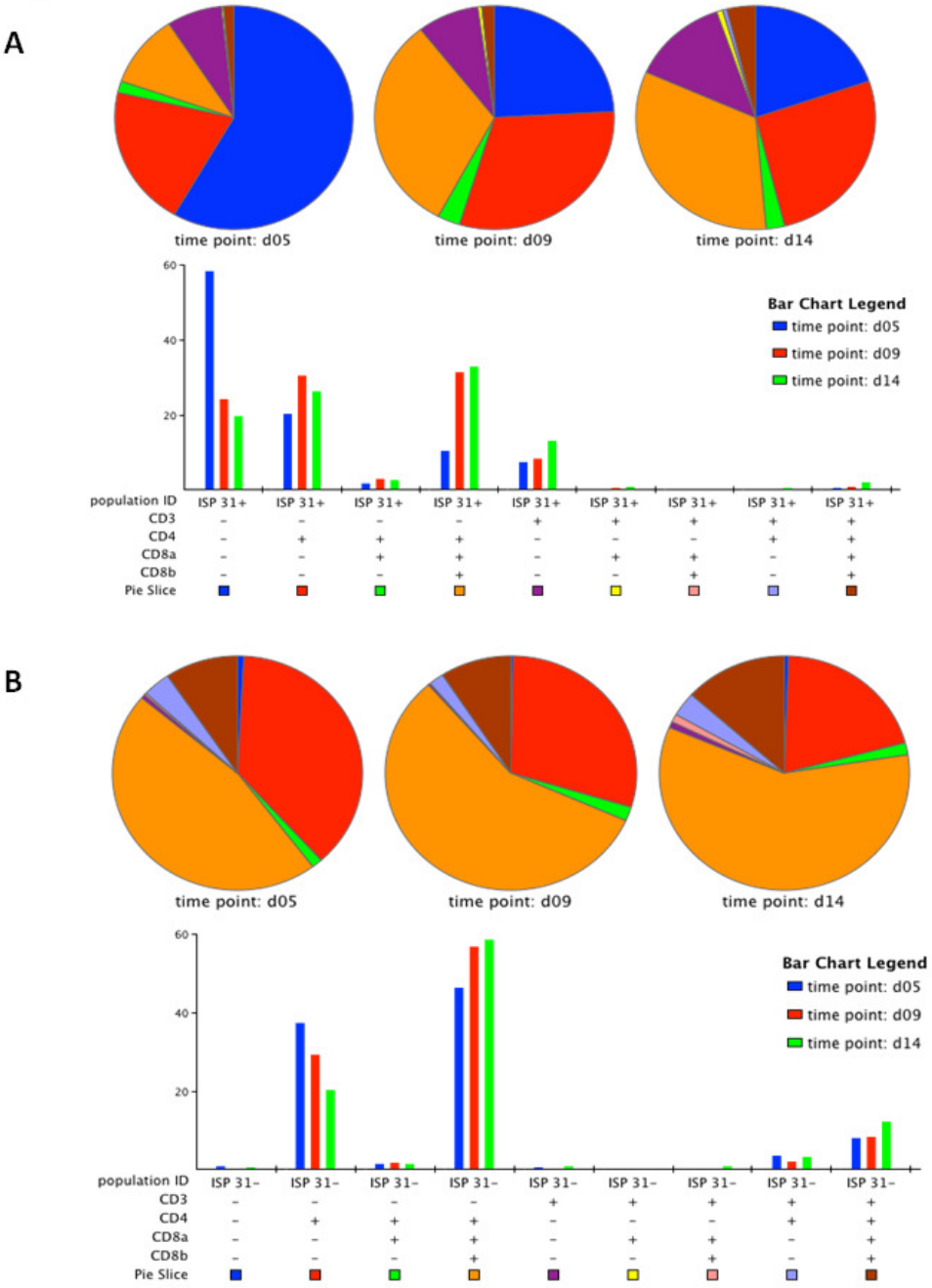
A
time point: d05
time point: d09
time point: d14
Bar Chart Legend
time point: d05
time point: d09
time point: d14
60
40
20
population ID
CD3
CD4
CD8a
CD8b
Pie Slice
ISP 31+
B
time point: d05
time point: d09
time point: d14
Bar Chart Legend
time point: d05
time point: d09
time point: d14
60
40
20
population ID
CD3
CD4
CD8a
CD8b
Pie Slice
ISP 31−

C

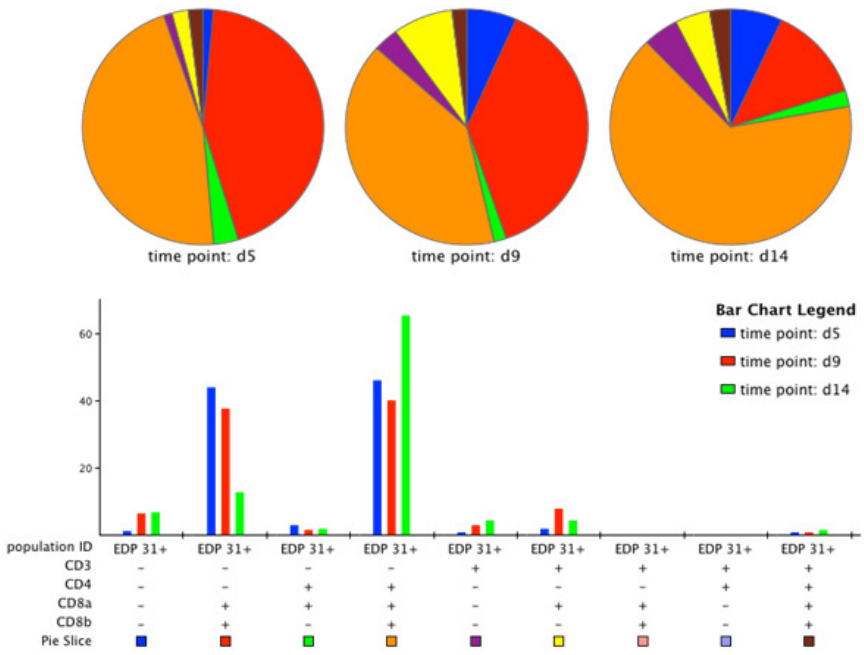
time point: d5
time point: d9
time point: d14
Bar Chart Legend
time point: d5
time point: d9
time point: d14
60
40
20
population ID EDP 31+ EDP 31+ EDP 31+ EDP 31+ EDP 31+ EDP 31+ EDP 31+ EDP 31+ EDP 31+
CD3 – – – – + + + + +
CD4 – – + + – – – + +
CD8a – + + + – + + – +
CD8b – + – + – – + – +
Pie Slice

D

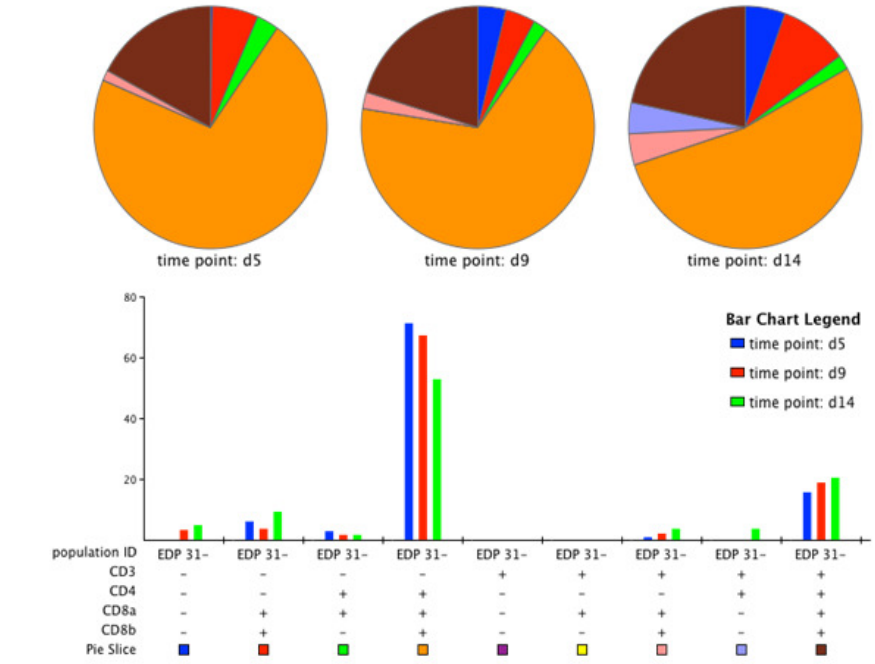
time point: d5
time point: d9
time point: d14
Bar Chart Legend
time point: d5
time point: d9
time point: d14
80
60
40
20
population ID EDP 31- EDP 31- EDP 31- EDP 31- EDP 31- EDP 31- EDP 31- EDP 31- EDP 31-
CD3 – – – – + + + + +
CD4 – – + + – – – + +
CD8a – + + + – + + – +
CD8b – + – + – – + – +
Pie Slice

Figure 5

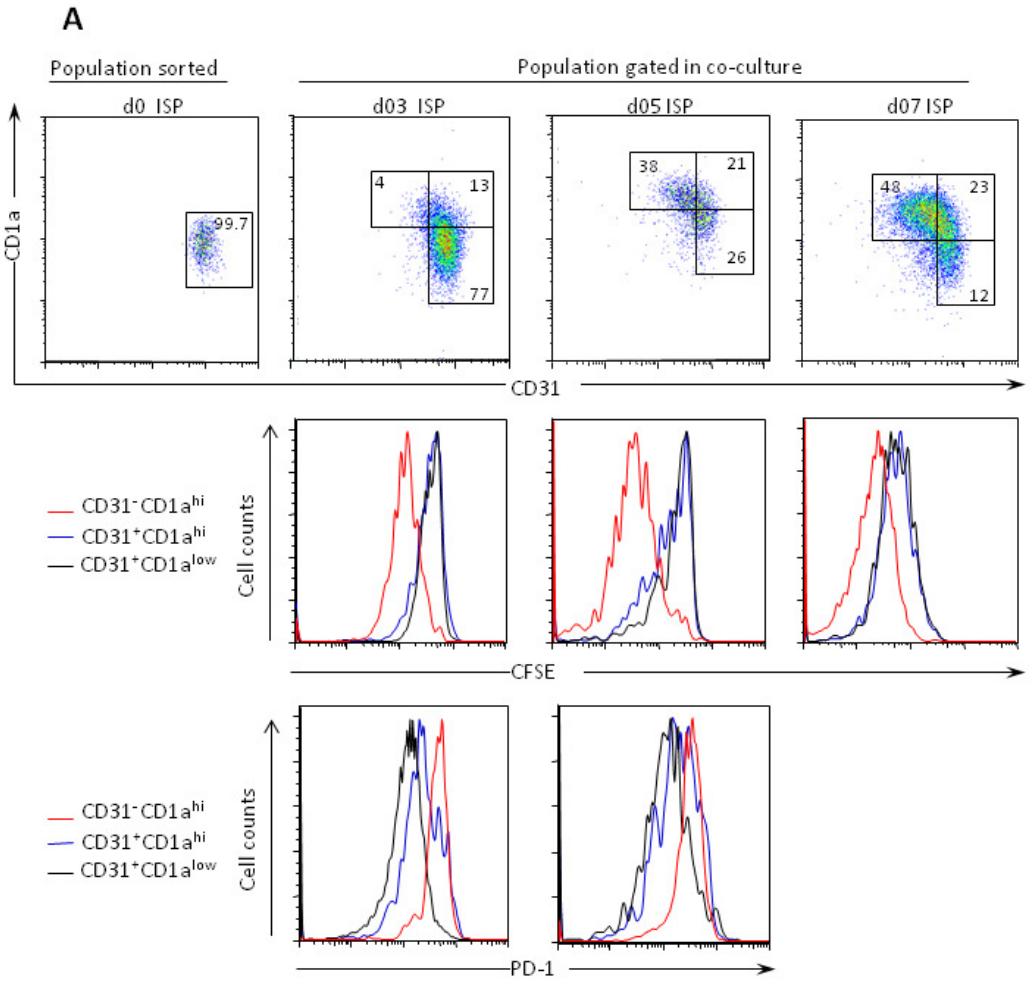
A
Population sorted
Population gated in co-culture
d0 ISP
d03 ISP
d05 ISP
d07 ISP
CD1a
CD31
99.7
4
13
77
38
21
26
48
23
12
CD31⁻CD1a^hi
CD31⁺CD1a^hi
CD31⁺CD1a^low
Cell counts
CFSE
PD-1

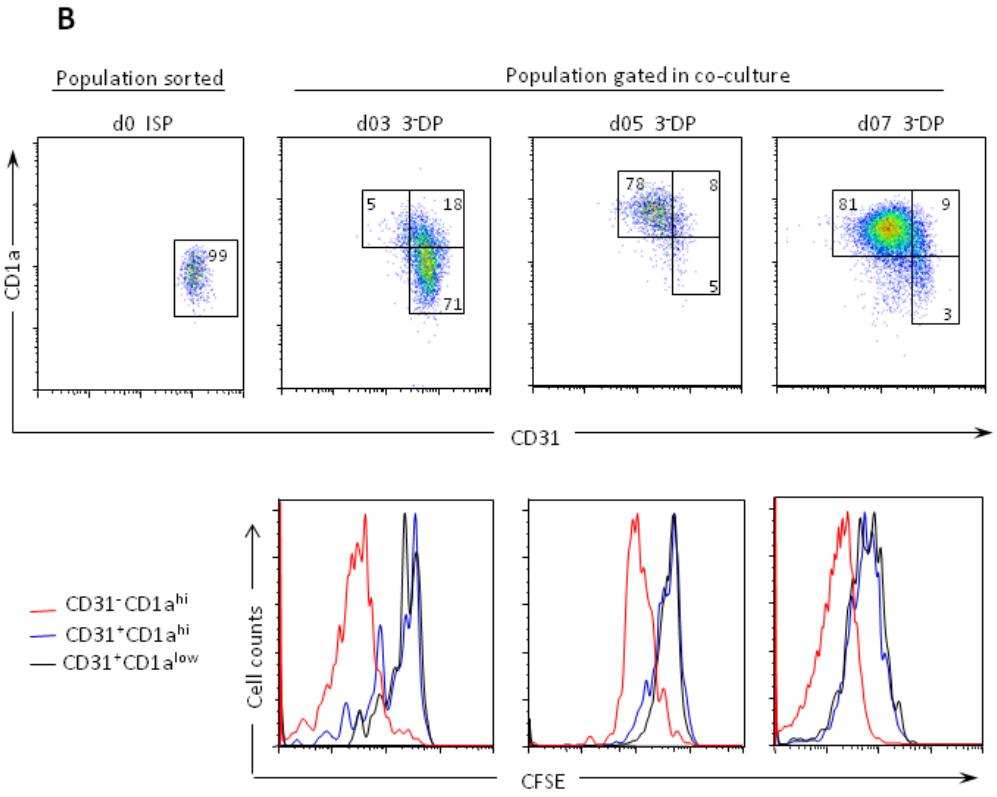
B
Population sorted
Population gated in co-culture
d0 ISP
d03 3-DP
d05 3-DP
d07 3-DP
CD1a
CD31
99
5
18
71
78
8
5
81
9
3
CD31-CD1a^hi
CD31+CD1a^hi
CD31+CD1a^low
Cell counts
CFSE

C

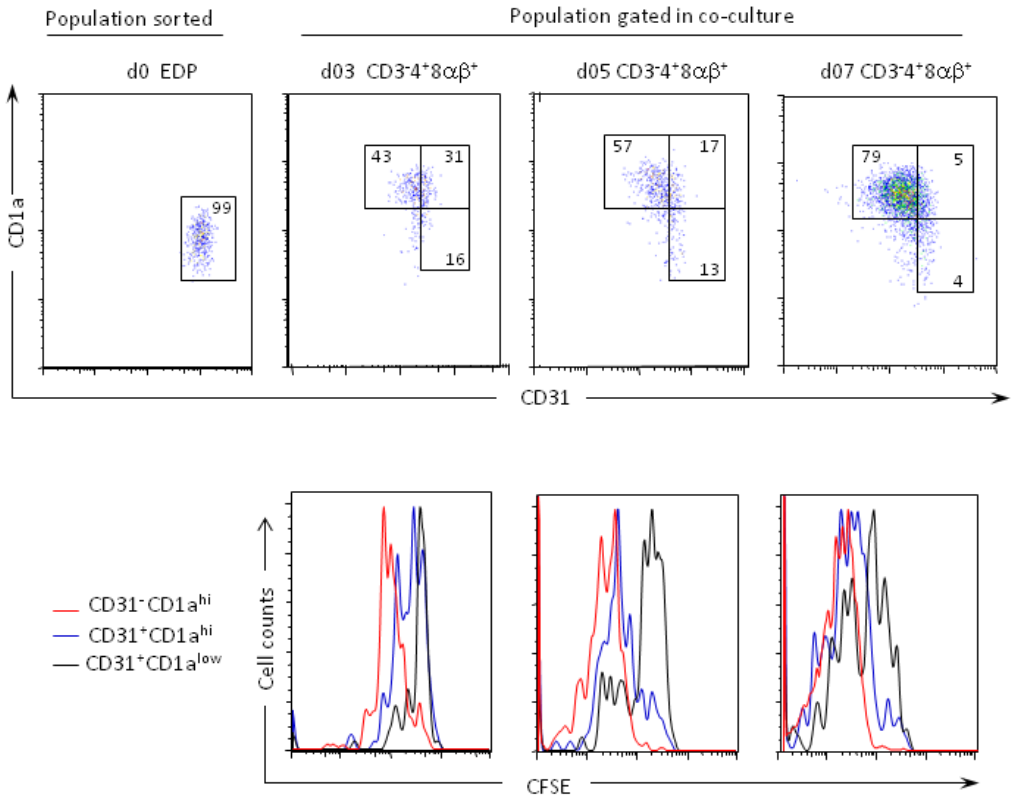
Population sorted
Population gated in co-culture
d0 EDP
d03 CD3-4+8αβ+
d05 CD3-4+8αβ+
d07 CD3-4+8αβ+
CD1a
CD31
99
43
31
16
57
17
13
79
5
4
CD31-CD1ahi
CD31+CD1ahi
CD31+CD1alow
Cell counts
CFSE

Figure 6

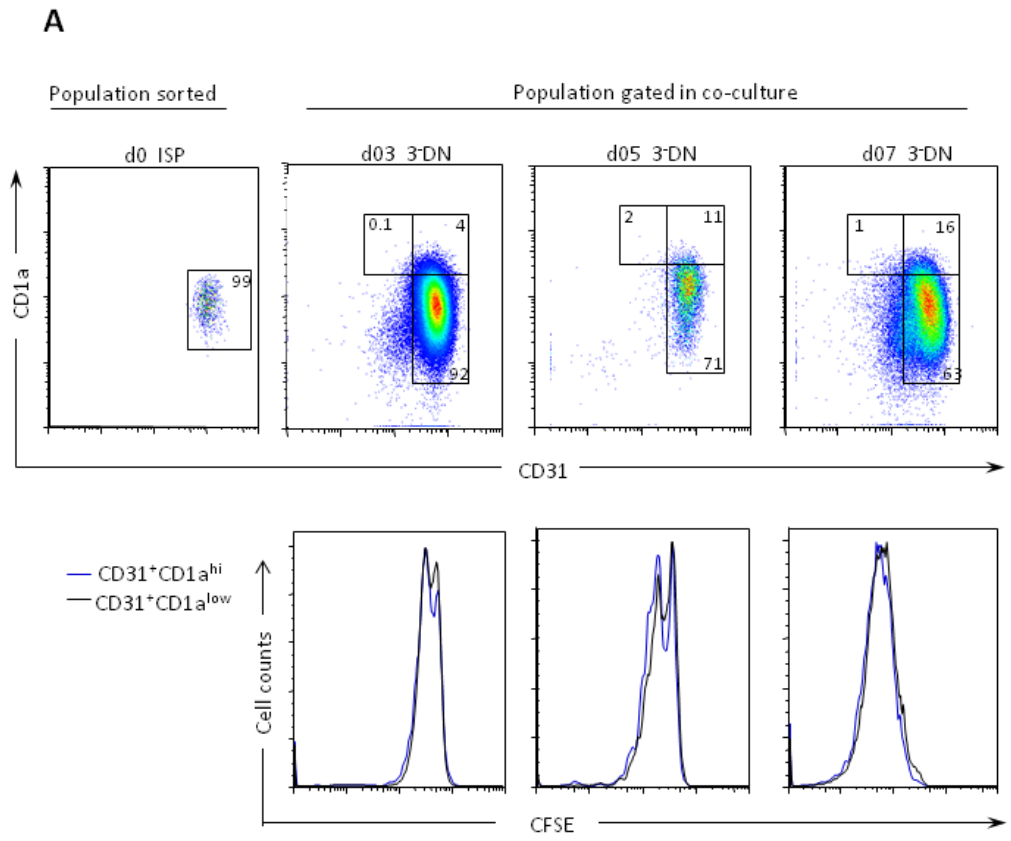
A
Population sorted
Population gated in co-culture
d0 ISP
d03 3-DN
d05 3-DN
d07 3-DN
CD1a
CD31
99
0.1
4
92
2
11
71
1
16
63
CD31+CD1ahi
CD31+CD1alow
Cell counts
CFSE

B

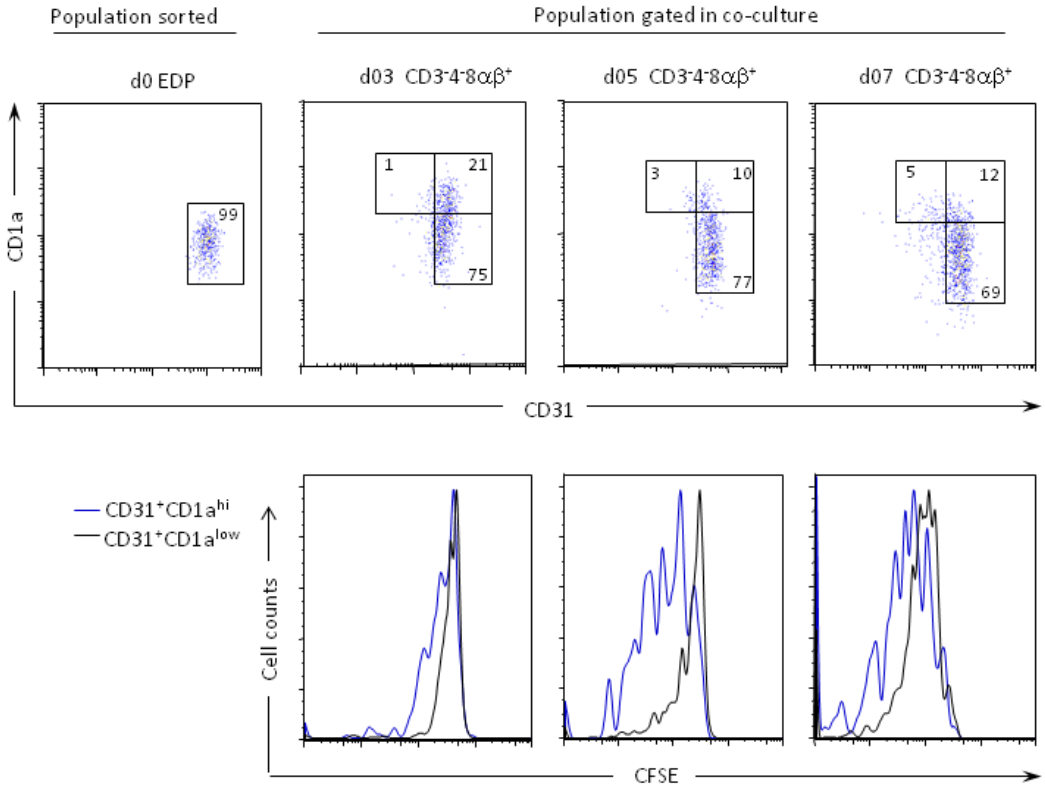
Population sorted
Population gated in co-culture
d0 EDP
d03 CD3-4-8αβ+
d05 CD3-4-8αβ+
d07 CD3-4-8αβ+
99
1
21
75
3
10
77
5
12
69
CD1a
CD31
CD31+CD1ahi
CD31+CD1alow
Cell counts
CFSE

Figure 7

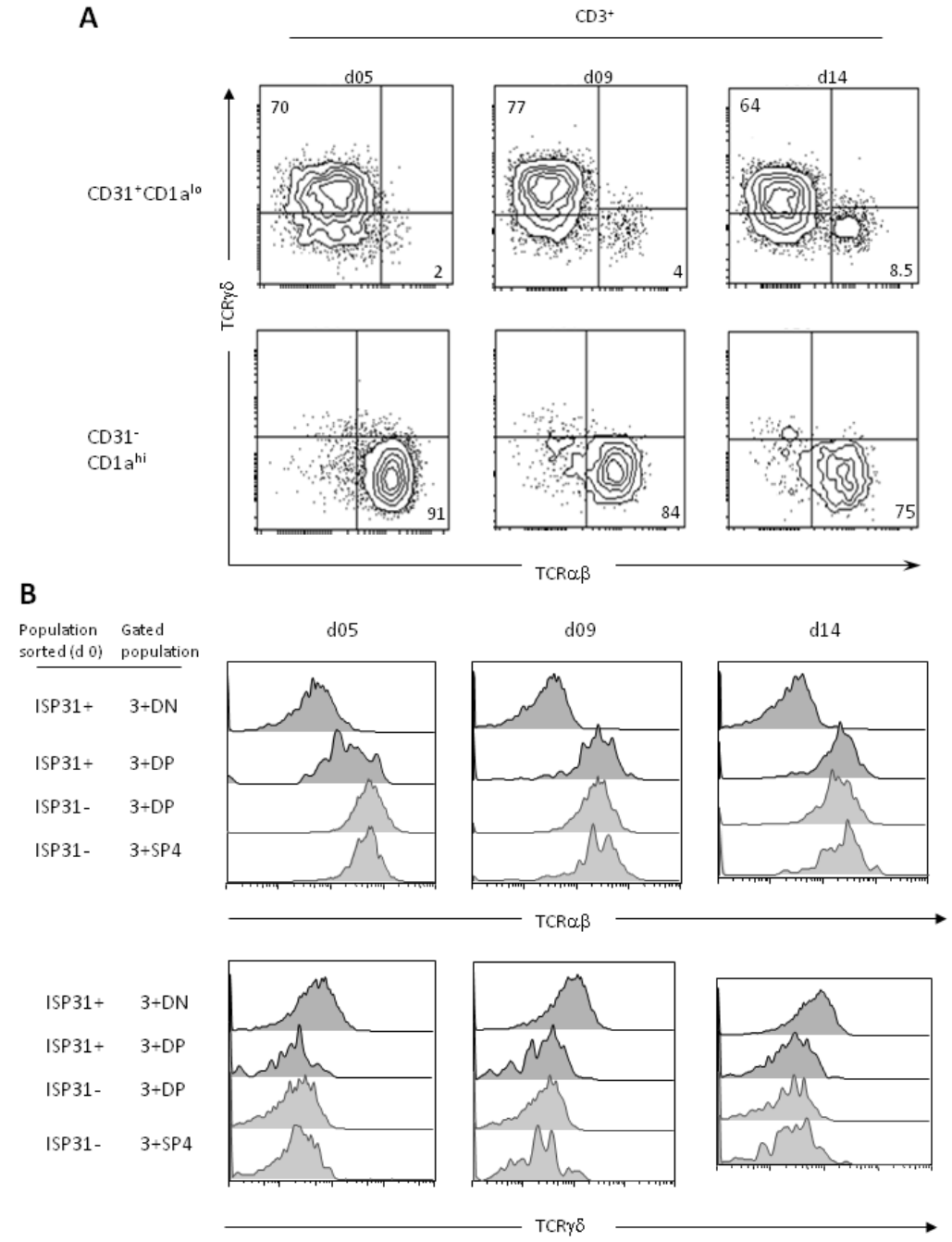
A
CD3+
d05
d09
d14
CD31+CD1alo
CD31-
CD1ahi
70
2
77
4
64
8.5
91
84
75
TCRγδ
TCRαβ
B
Population sorted (d 0)
Gated population
ISP31+ 3+DN
ISP31+ 3+DP
ISP31- 3+DP
ISP31- 3+SP4
d05
d09
d14
TCRαβ
ISP31+ 3+DN
ISP31+ 3+DP
ISP31- 3+DP
ISP31- 3+SP4
TCRγδ

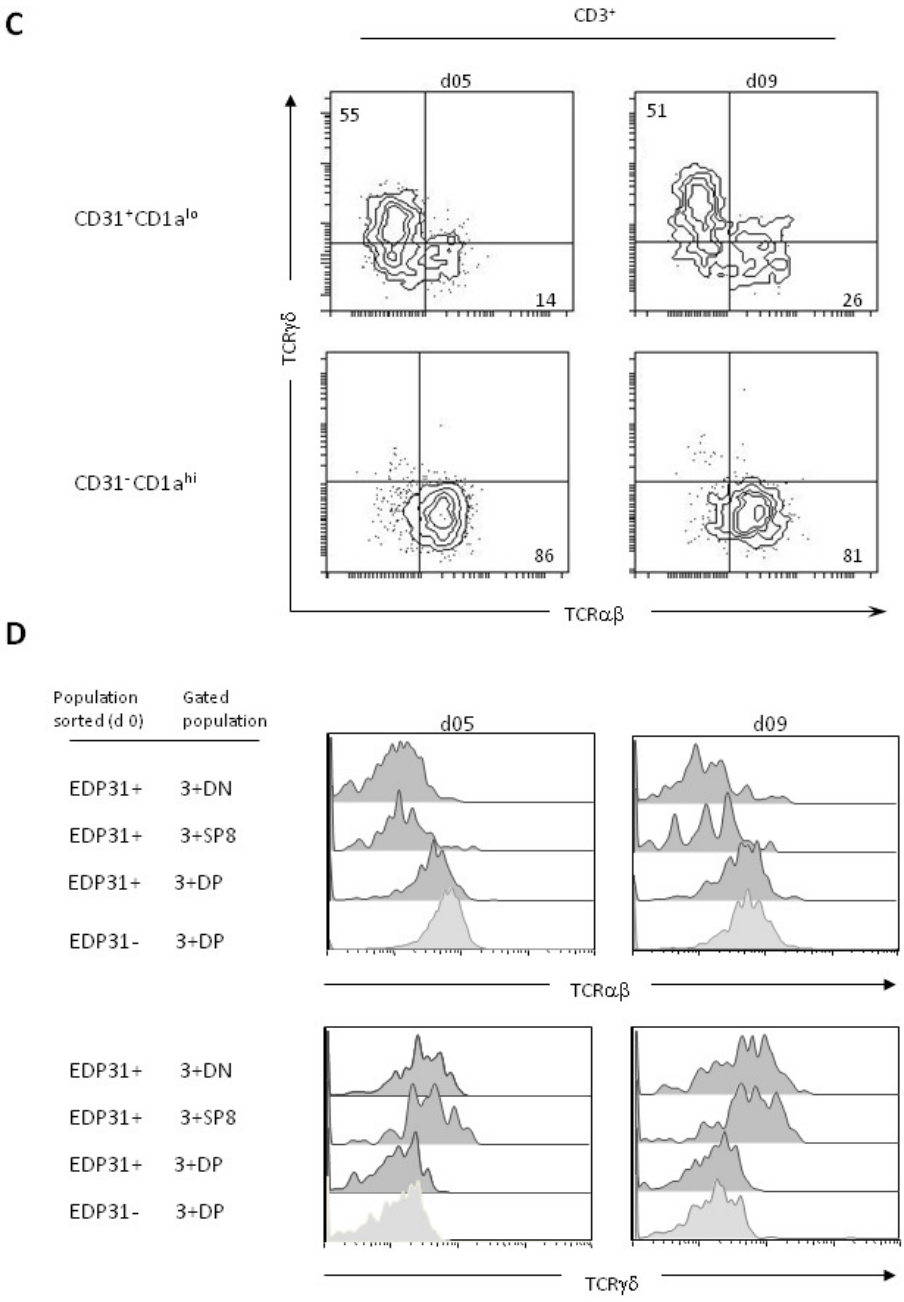
C
CD3+
d05
d09
55
51
14
26
CD31+CD1alo
CD31-CD1ahi
TCRγδ
86
81
TCRαβ
D
Population sorted (d 0)
Gated population
EDP31+ 3+DN
EDP31+ 3+SP8
EDP31+ 3+DP
EDP31- 3+DP
d05
d09
TCRαβ
EDP31+ 3+DN
EDP31+ 3+SP8
EDP31+ 3+DP
EDP31- 3+DP
TCRγδ

Figure 8

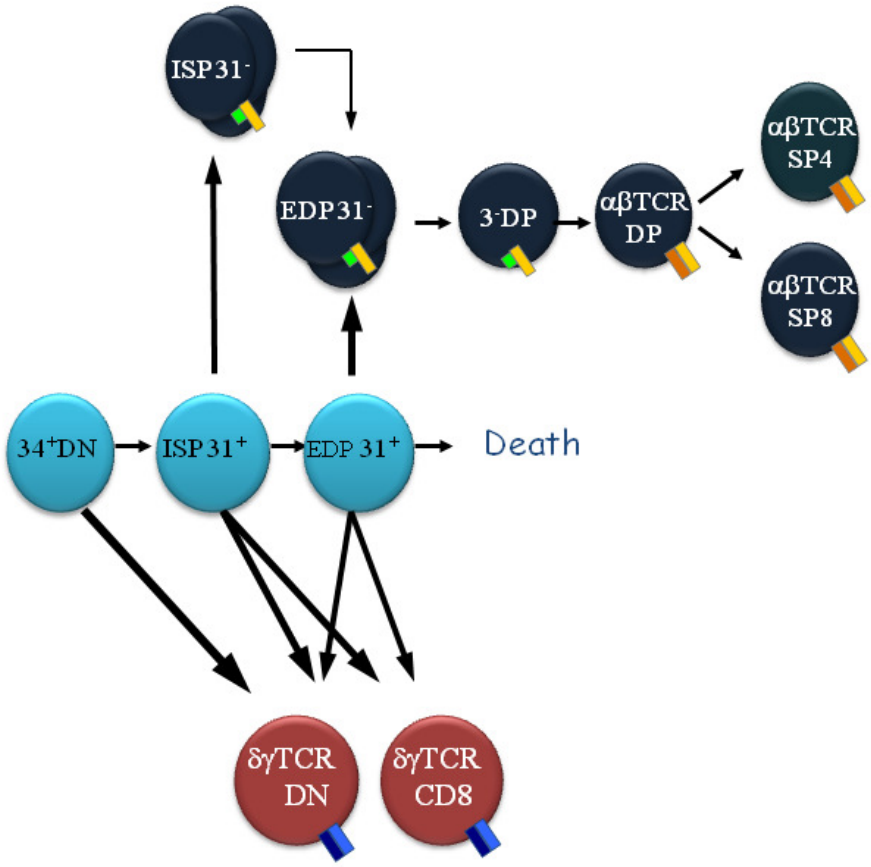
ISP31-
EDP31-
3-DP
αβTCR DP
αβTCR SP4
αβTCR SP8
34+DN
ISP 31+
EDP 31+
Death
δγTCR DN
δγTCR CD8

Figure S1

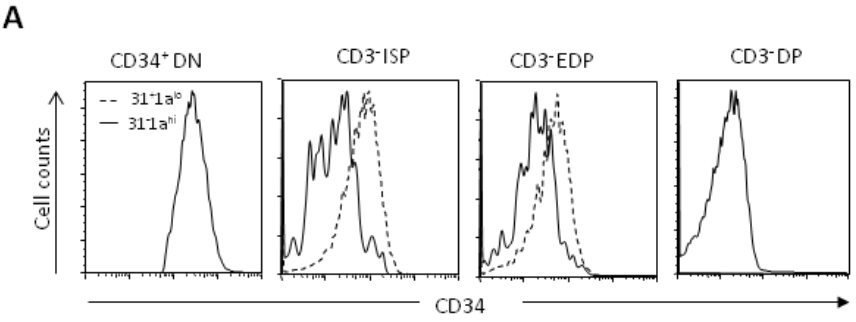
A
CD34+ DN
CD3-ISP
CD3-EDP
CD3-DP
31+1alo
31+1ahi
Cell counts
CD34

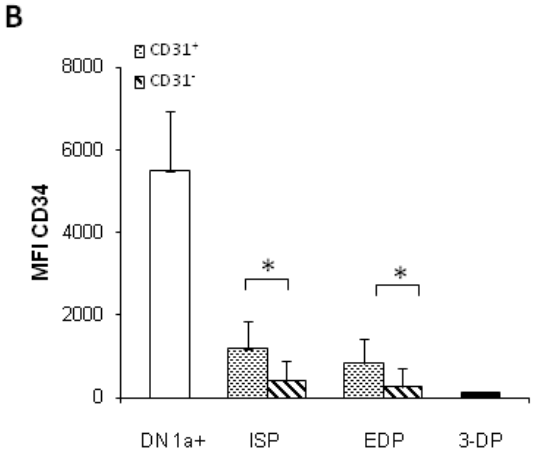
B
CD31+
CD31-
8000
6000
4000
2000
0
MFI CD34
*
*
DN 1a+
ISP
EDP
3-DP

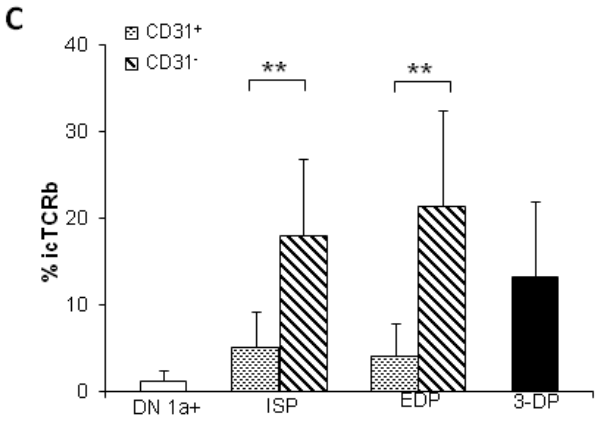
C
CD31+
CD31-
40
30
20
10
0
% icTCRb
**
**
DN 1a+
ISP
EDP
3-DP

Figure S2

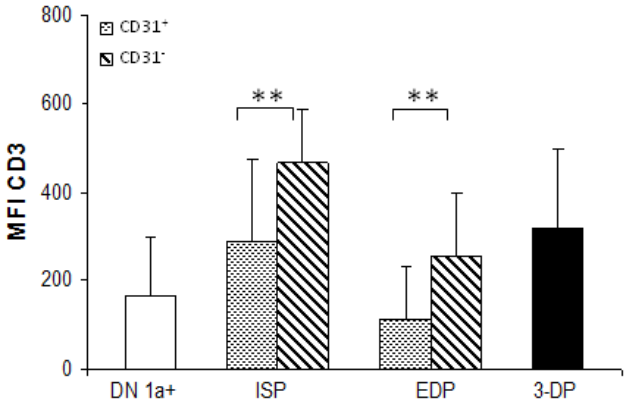

Figure S3

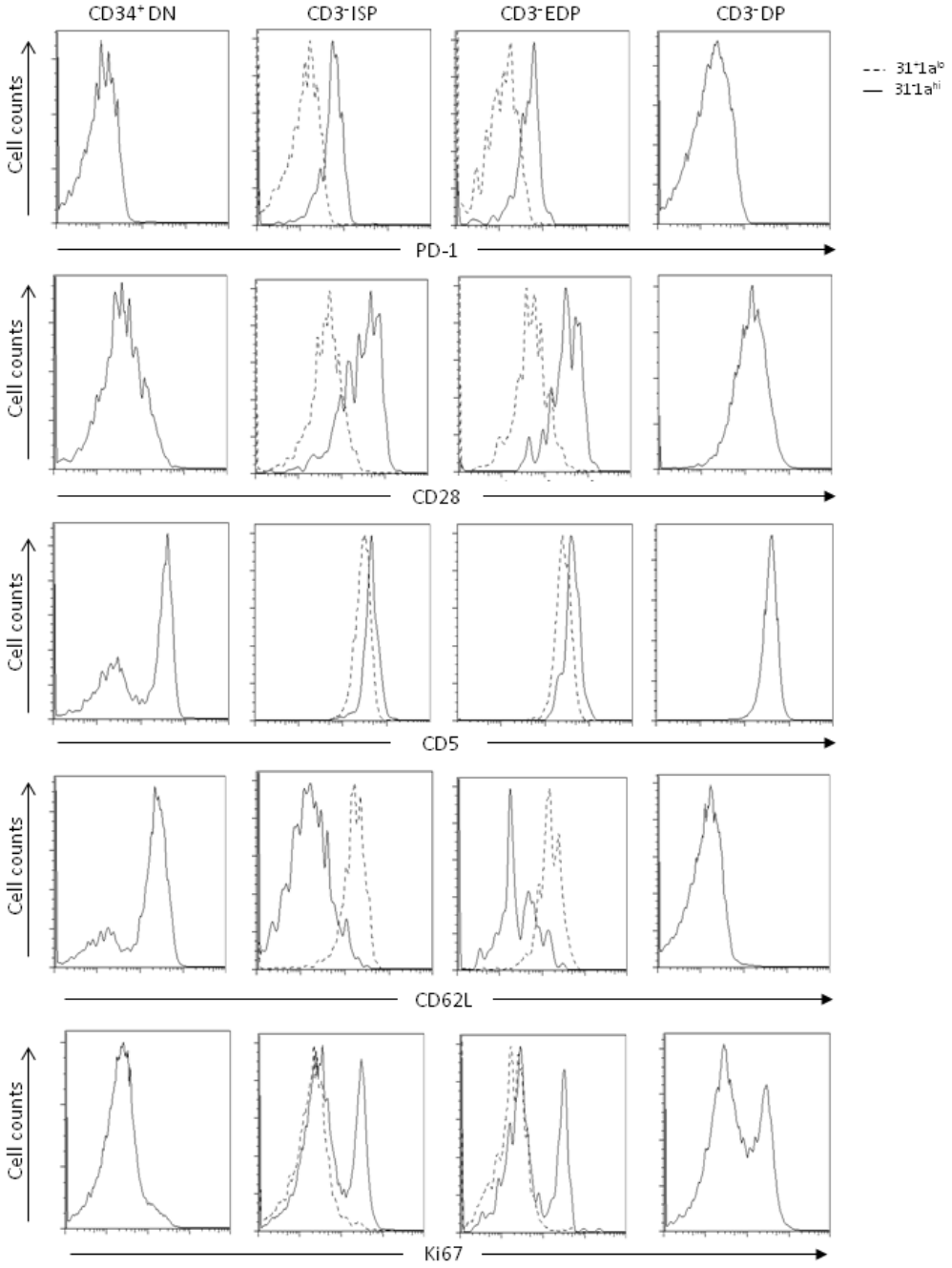
CD34+ DN
CD3-ISP
CD3-EDP
CD3-DP
Cell counts
PD-1
CD28
CD5
CD62L
Ki67
31+1alo
31+1ahi

Figure S4

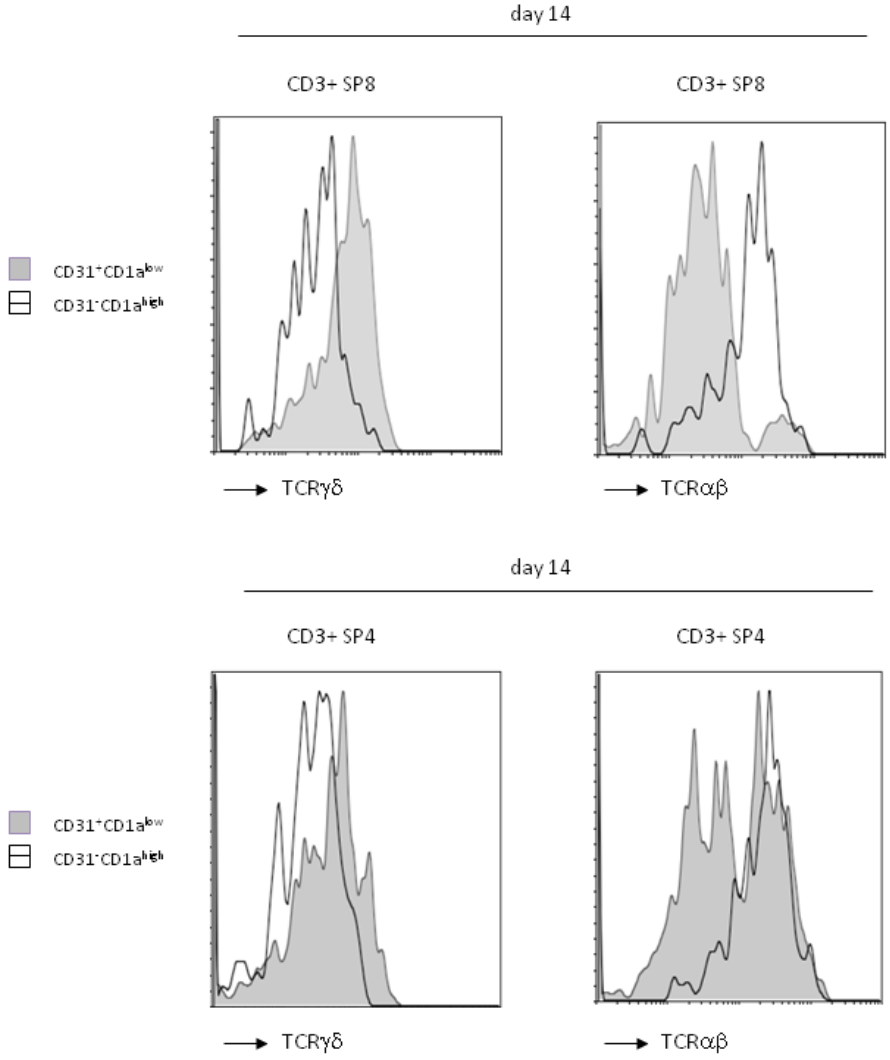
day 14
CD3+ SP8
CD3+ SP8
CD31+CD1alow
CD31-CD1ahigh
TCRγδ
TCRαβ
day 14
CD3+ SP4
CD3+ SP4
CD31+CD1alow
CD31-CD1ahigh
TCRγδ
TCRαβ

CHAPTER 5: DISCUSSION

1. Summary of findings

A hallmark of HIV infection is the gradual decline in CD4 T cells ultimately leading to immunodeficiency. The thymus, the primary source of *de novo* T cells, was previously shown to be impacted during HIV Infection. To further elucidate the perturbations induced by HIV on thymic function and homeostasis of RTEs, a CD4 RTE-specific phenotype ($CD45RA^{+}CD27^{+}CCR7^{+}CD31^{hi}$) was recently identified in our laboratory.

Using the CD31-defined phenotype, we established that both RTE frequencies within naive CD4 T cells *and* absolute numbers were rapidly diminished in the periphery during AEHI when compared to seronegative controls. Longitudinal analysis revealed variability in the evolution of RTE frequencies and numbers with disease progression. In fact, following the initial decline observed in acute/early HIV infection (AEHI), slow progressors (SP) were able to recover the RTE population to amounts similar to those observed in healthy controls, while progressors (P) experienced a greater loss of RTE cells. Our results highlight the impact of the maintenance of the RTE pool in SP subjects on the preservation of central memory T cells (T_{CM}) and total CD4 T cell counts during chronic HIV infection (CHI), suggesting that the loss of RTEs is an upstream event of CD4 T cell depletion.

Our data illustrated that the mechanisms leading to the loss of RTEs from the periphery during AEHI differed from those taking place during CHI. While differentiation of RTEs into T_{CM} could account for the depletion of RTEs during AEHI, increased hyperimmune activation of RTEs, as measured by Ki67 and up-regulation of PD-1 expression, associated with lower survival of RTEs, as measured by Bcl-2, seemed to lead to the depletion of RTE and total CD4 T cells during CHI.

Long-term RTE recovery following treatment with HAART was associated with restoration of the total CD4 T cell pool, providing further evidence for the role of RTEs in stabilizing CD4 T cell absolute numbers. Our data highlights the important role of enhanced thymic output, as measured by the sj/β TREC ratio, and survival of RTEs in the periphery, as measured by the IL-7R α-chain, versus

peripheral proliferation of RTEs, as measured by Ki67, in the recovery of the RTE cell pool following HAART.

Our data also revealed negative correlations between failure to reduce the levels of IFN-α post-HAART and the levels of intrathymic proliferation as well as the magnitude of RTE recovery, suggesting a role for IFN-α in the impaired reconstitution of the RTE and CD4 T cell pools observed in a subset of individuals following treatment with HAART. This has prompted us to dissect early human T cell differentiation and identify a phenotype that permits the isolation of thymocytes undergoing β-selection, namely the $CD31^{-}CD1a^{high}$ phenotype. This provides a novel tool for the assessment of the impact of IFN-α production during HIV infection on intrathymic proliferation.

2. Dynamics of the RTE compartment in HIV-infected individuals

2.1. Direct and indirect virus-mediated factors

HIV infection can lead to the direct destruction of various target CD4 T cells (that express the co-receptors CCR5 or CXCR4). Furthermore, the persistent presence and replication of HIV virions can lead to the exhaustion of the immune system through relentless T cell activation.

2.1.1. Impact of viral replication

AEHI generally starts with the less pathogenic, non-syncytium inducing (NSI) variants that use CCR5 as a co-receptor and consequently only target macrophages and a subset of memory T cells: T_{EM} [175]. In fact, the major population destroyed by the virus during AEHI is the T_{EM} subset due to their high expression of the HIV co-receptor CCR5 [176]. The proportion of $CCR5^{+}$ T_{EM} is much more elevated in the gut than in the blood or lymph nodes. Consequently, mucosal CD4 T cells are targeted for infection and massively depleted early in infection [149, 176]. We have previously shown that RTEs, similar to other naive T cells, express CXCR4 but not CCR5 (unpublished data) and are therefore

spared from viral infection during AEHI [177]. As the infection progresses, the virus can evolve into syncytium-inducing (SI) variants capable of infecting and inducing cell death in CD4 naive T cells in addition to T_{CM} [178, 179] through the use of the CXCR4 co-receptor. In agreement with this, emergence of SI variants was correlated with massive loss of CD4 naive T cells [177], rapid total CD4 T cell depletion [178], and poor naive T cell reconstitution following HAART [180]. This illustrates a potential mechanism by which RTEs could be depleted during CHI. Genotyping of the virus in P versus SP subjects would allow us to assess the impact of virus co-receptor usage on RTE depletion. The destruction of RTEs during AEHI and early stages of CHI is most likely due to indirect effects of HIV infection such as cell death following repeated cell activation, as suggested by the inverse correlation between frequencies of Bcl-2 and Ki67 (as well as between frequencies of Bcl-2 and PD-1) within RTEs (Ch.2 fig.7).

2.1.2. Impact of peripheral activation and proliferation

Heightened immune activation is a hallmark of HIV infection and plays an important role in CD4 T cell depletion and immune dysfunction. Immune activation can be manifested as increased expression of activation markers such as HLA-DR and CD38 [181] or increased T cell proliferation and increased T cell turnover, as demonstrated in studies utilizing deuterated glucose labelling [182], intracellular expression of the nuclear antigen Ki67 [183] and DNA incorporation of BrdU [184-186]. Heightened immune activation has detrimental consequences on pathogenesis and has been linked with disease progression: levels of CD38 within CD4 and CD8 T cells correlated with the rate of progression to AIDS independently of viral load [181], and levels of HLA-DR within CD8 T cells were elevated in rhesus macaques and correlated with CD4 depletion and progression to AIDS [187]. Furthermore, levels of immune activation were found to be a better predictor of survival in advanced stages of disease than viral burden or chemokine receptor usage [188], further emphasizing the impact of hyperimmune activation on disease progression.

It has been proposed that CD4 naive T cells do not undergo proliferation and increased turn-over rates during HIV infection. This is based on the findings that naive T cells from HIV-infected individuals did not exhibit increased Ki67 frequencies when compared to healthy controls during acute infection [162] as well as in later stages of disease [183]. However, the data presented in this thesis demonstrates that CD4 RTEs versus non-RTE naive T cells expressed higher frequencies of $Ki67^+$ and $PD\text{-}1^+$ cells during AEHI when compared to healthy controls (Ch.2 fig.3 and fig.4). In fact, the frequencies of $Ki67^+$ and $PD\text{-}1^+$ cells within RTEs were comparable to those observed within memory subsets, reflecting that RTEs can indeed be activated and undergoing proliferation (Ch.2 fig.3 and fig.4). Since RTEs, especially in the context of HIV infection, represent the minority of naive T cells, the increased Ki67 frequencies within RTEs is under-represented when analysing the entire naive population. High frequencies of $Ki67^+$ cells within RTEs were associated with low RTE cell counts during both AEHI and CHI (Ch.2 fig.6), illustrating that hyperimmune activation of RTEs, as measured by Ki67 and PD-1, is a potential mechanism by which these cells are depleted in the periphery.

There are many ways by which immune activation of CD4 T cells during HIV infection could lead to depletion of the various CD4 T cell pools. For example, antigenic activation of naive T cells could lead to their recruitment into the memory phenotype [189], and chronic activation of T_{CM} cells has been linked with activation-induced cell death (AICD) [190]. However, the mechanisms responsible for activation-mediated depletion of RTEs have not yet been explored. The results presented in Chapter 2 indicate that hyperimmune activation within the RTE subset, as measured by high frequencies of $KI67^+$ and $PD\text{-}1^+$ cells, was positively correlated with viral load throughout the course of infection (Ch.2 fig.3 and fig.4). Analysis of recent TCR activation such as CD69, CD71 or CD25 is needed to confirm that cell cycle entry of RTEs is indeed triggered by viral antigens.

Nonetheless, there is indication of TCR triggering since in AEHI, RTE proliferation was associated with loss of RTE phenotype and gain of a subset of

T_{CM} that express CD31 (Ch.2 fig.6). The ability of RTEs to differentiate into T_{CM} was demonstrated by analyzing sjTRECs within the various CD4 naive ($CD31^{hi}$, $CD31^{low}$, $CD31^{-}$) and T_{CM} ($CD31^{+}$ and $CD31^{-}$) subsets in four HIV-uninfected individuals. A small proportion of T_{CM} was $CD31^{+}$ (but not $CD31^{hi}$) (data not shown), contained on average as many sjTRECs as $CD31^{+}$ naive T cells (Appendix A fig.S1) and is therefore closer in differential status to RTEs than is the $CD31^{-}$ naive subset, suggesting that RTEs can be directly recruited into the memory T cell pool. This is in agreement with a previous study that detected the expression of CD31 on $CD45RA^{low}RO^{low}$ transitory CD4 T cells [89]; however, TREC levels were not quantified in that subset. During AEHI, we observed lower TREC levels within the RTE subset in HIV-infected individuals as compared to uninfected controls; however, TREC levels were similar across the various CD4 naive and T_{CM} subsets, suggesting increased homeostatic proliferation of RTEs (and hence dilution of TRECs within the RTE subset) and/or redistribution of TRECs into normally TREC-poor compartments due to accelerated differentiation of RTEs into $CD31^{-}$ naive and $CD31^{+}$ T_{CM} (Appendix A fig.S1). In agreement with our results, Lewin et al. reported that as much as 50% of the TRECs were contained within the $CD45RA^{-}$ population for both $CD4^{+}$ and $CD4^{-}$ T cells during AEHI and CHI [191]. The fact that we detected an equal distribution of TRECs within all naive and T_{CM} subsets implies that cell death is not the primary mechanism leading to depletion of RTEs during AEHI. Instead, they are most likely recruited into the lymph nodes soon after their release into the periphery where they become activated and differentiate into memory T cells (most likely T_{CM}). This is supported by the detection of a positive correlation between frequencies of $Ki67^{+}$ cells within RTEs and T_{CM} cell counts during AEHI (Ch.2, fig.6).

Recruitment of RTEs into the memory T cell pool could also occur at later stages of infection since a positive correlation between viral load and frequencies of $Ki67^{+}$ cells within RTEs was detected during CHI. However, the correlation between frequencies of $Ki67^{+}$ cells within RTEs and T_{CM} counts (as well as with total CD4 T cell counts) was negative during CHI, suggesting that RTEs are not a

constant supply of memory T cells (Ch.2 fig.6). The finding that P subjects have low RTE frequencies and counts in CHI despite RTEs having high frequencies of $Ki67^+$ cells could be a result of proliferation-induced anergy (or dysfunction) leading to impaired cell cycle progression, diminished T cell differentiation capacity, and eventually cell death [192]. On the other hand, SP subjects had low frequencies of $Ki67^+$ cells within RTEs during CHI and had normalized their RTE and total CD4 T cell counts (Ch.2 fig.6), further demonstrating a role for chronic immune activation in CD4 T cell depletion. The inability of RTEs from P subjects to proliferate and/or differentiate during CHI can be confirmed by *in vitro* assays (such as CFSE-labelling) evaluating the capacity of $Ki67^+$ RTEs to complete cell cycle following TCR triggering.

The notion that chronic immune activation contributes to cell death during CHI is well supported. Since the virus preferentially infects cycling cells, chronic immune activation would provide a consistent and large supply of target cells; however, the low number of cells actively infected following the initial burst of viremia argues for the contribution of apoptosis of bystander cells in the contraction of the CD4 T cell pool [193, 194]. Previous studies have shown that CD4 and CD8 T cells were both activated and experienced similar increases in proliferation rates during HIV infection. If chronic immune activation is responsible for increased cell death, one would observe depletion of both CD4 and CD8 T cell subsets. Instead, HIV infection is characterized by depletion of the CD4 T cell pool and expansion of the CD8 T cell pool. Using mathematical modeling, these discrepancies have been attributed to inherent differences between CD4 and CD8 T cells in the response to stimulation during HIV infection: while the rate of activated CD4 T cells increased, CD4 T cell numbers did not [195]. This is in contrast to the observation that the rate of activation and proportions of CD8 T cells both increased, which led to the conclusion that HIV infection increases the rates of cell death of activated CD4 but not CD8 T cells, consistent with CD8 T cells undergoing more rounds of proliferation than CD4 T cells [195]. This was later confirmed by Sieg et al. in a study whereby T cell proliferation was monitored by both BrdU and CFSE labelling [190]. In contrast

to CD8 S-phase T cells, CD4 S-phase T cells did not dilute CFSE levels (and complete cell cycle) but stained positive for Annexin V (a marker of apoptosis) and disappeared from culture [190]. Our analysis suggested that a similar mechanism might also be behind RTE depletion. In agreement with that observed for S-phase CD4 T_{CM} [190], high frequencies of $Ki67^+$ cells within RTEs were associated with lower frequencies of $Bcl\text{-}2^+$ cells within RTEs (Ch.2 fig.7), suggesting that increased cell cycle entry of RTEs rendered them more susceptible to apoptosis and that cell death could represent a significant mechanism that leads to depletion of RTEs in CHI. Analysis of Annexin V and/or Caspase-3, markers of apoptosis, in conjunction with Fas (CD95), a death receptor involved in apoptosis, within RTEs in P subjects would further confirm this hypothesis. Nonetheless, continuous cell cycle entry during HIV infection had a negative impact on disease progression as it distinguished individuals that showed severe RTE loss from those that recuperated RTE levels during CHI. The negative correlation between low CD4 T cell counts and high Ki67 frequencies within total CD4 T cells has already been established [183]. However, we are the first to show that high Ki67 frequencies within RTEs during CHI negatively impacted the CD4 T cell pool (Ch.2 fig.6).

2.2. Impact of inflammatory cytokines

We (Ch.2 fig.3 and fig.4) and others [183, 196] have shown that hyperimmune activation observed within the various CD4 T cell subsets during HIV infection is correlated with the amount of HIV RNA in the blood, indicating that CD4 T cells might be directly activated by continuous virus production or viral gene products. However, increased viremia is not the sole factor leading to T cell activation since subjects with HIV-2 infection, characterized by low levels (mostly undetectable) of viremia [197], exhibited signs of activation that were directly correlated with CD4 T cell depletion [198]. Furthermore, it was shown that while S-phase T cells expressed activation markers such as CD38, this was not accompanied by markers of recent TCR engagement such as CD69 and CD25 [184]. In fact, it was shown that only a small amount of activated T cells were HIV-specific T cells [199,

200]. This is highly suggestive of cell cycling induced by bystander activation and/or homeostatic mechanisms versus specific TCR stimulation by viral antigens.

HIV viremia creates an inflammatory environment due to APC [7] and T cell activation for prolonged periods, and increased levels of pro-inflammatory cytokines such as IFN-α, TNF-α, and IL-6 have been detected in HIV-infected individuals [7, 8]. Amongst those cytokines, IFN-α is up-regulated transiently during AEHI and reaches high levels in late-stage disease which correlate with poor prognosis [8]. IFN-α induces up-regulation of the activation marker CD38 in HIV-infected T cells [201] and is associated with increased interferon-stimulated transcripts in activated CD4 T cells from untreated HIV individuals [202]. The role of persistent IFN-α responses in disease pathogenesis was shown in SIV models of infection in which failure to down-regulate IFN-α 30-days post-infection distinguished pathogenic (infection of rhesus macaques) from non-pathogenic (infection of natural hosts) SIV infection [203]. IFN-α may contribute to bystander apoptosis of uninfected T cells through the up-regulation of TRAIL ligands on T cells within lymphoid tissues [204]. Brenchely et al. identified a positive correlation between IFN-α levels and LPS, a common component of the bacterial cell wall during CHI, and markers of immune activation [205], illustrating the role of the inflammatory environment in damaging mucosal immunity and exacerbating disease. Our finding of a positive correlation between levels of IFN-α and frequencies of $Ki67^+$ cells within RTEs during CHI (Ch. 2) suggest that the pro-inflammatory environment created by HIV infection could also negatively impact the RTE cell pool.

2.3. Regenerative factors

As mentioned above, our data show that relentless activation and recruitment of RTEs into the memory T cell pool during AEHI creates a void in the RTE cell pool. Generation of new RTEs can be mediated through *de novo* T cell production by the thymus or peripheral proliferation of pre-existing T cells. The data we

presented in Chapter 2 demonstrates that defective regeneration of RTEs ultimately leads to total CD4 T cell depletion.

2.3.1. Impact of T cell homeostasis

HIV infection, similarly to other lymphopenic conditions, is characterized by high levels of IL-7 in both AEHI and CHI (Ch.2 fig.S1), which were shown to be associated with the magnitude of CD4 T cell depletion [206]. This was not found for other homeostatic cytokines such as IL-2 and IL-15 [196] and raises the question of whether IL-7 has a role in T cell regeneration. The results presented in Chapter 2 demonstrate that levels of IL-7 were positively associated with frequencies of $Ki67^+$ cells within RTEs during AEHI as well as CHI and therefore could be driving proliferation of RTEs in response to the initial decline of RTE numbers (Ch.2 fig.3). This is in agreement with a recent study demonstrating that proliferation of CD4 T cells, as determined by BrdU incorporation, correlated more strongly with low CD4 T cell counts than with high viral load [196]. In contrast, levels of CD8 T cell proliferation only correlated with viral load [196], illustrating different forces driving CD4 and CD8 T cell cycling in HIV infection. However, our data shows that subjects with increased frequencies of $Ki67^+$ cells within RTEs did not increase RTE numbers throughout the period of study (Ch.2 fig.5), demonstrating the limited capacity of IL-7-driven proliferation in the restoration of the RTE cell pool during untreated HIV infection.

It is not clear whether the negative correlation observed between levels of IL-7 and RTE cell counts (Ch.2 fig.5) reflects a response to low RTE numbers or is rather the cause of low RTE numbers. In lymphopenic settings, IL-7 can promote slow rates of naive T cell proliferation in the absence of foreign antigen (mediated by low affinity self-peptides) [130, 207]. However, this is associated with irreversible acquisition of the memory phenotype, which could help explain why IL-7-mediated proliferation failed to increase RTE cell counts during CHI in subjects with low CD4 counts. On the other hand, IL-7 facilitates naive T cell proliferation in response to antigenic stimulation [208], and it is therefore conceivable that high levels of IL-7 together with persistent TCR triggering could lead to over-activation of RTEs resulting in accelerated cell death or "propriocidal

regulation", as shown for IL-2 and IL-4 in the apoptosis of CD4 T cells [209]. This suggests a role for IL-7 in the pathogenesis of RTE depletion, which will be further discussed in section 3.

2.3.2. Impact of thymic output

In Chapter 2, we demonstrated that the depletion of RTEs in untreated HIV-infected individuals during AEHI was associated with differentiation into T_{CM} while the depletion of RTEs during CHI was associated with lower survival. However, a subset of individuals was shown capable of restoring RTE numbers and the total CD4 T cell pool during CHI (Ch.2 fig.1). Although we did not quantify the sj/β TREC ratio in those subjects, it is likely that these individuals maintained adequate thymic function throughout CHI. However, 3 out of those 4 subjects showed low viral load (Ch.2 Table S1) and we could not discriminate between adequate thymic output and low hyperimmune activation-mediated cell death as the cause of RTE maintenance. To provide convincing evidence for the role of the thymus in the generation of new RTE cells and the maintenance of the total CD4 T cell pool, we would need to assess the sj/β TREC ratio in SP subjects that show high viral load.

The notion that the thymus is capable of generating and exporting large amounts of new T cells despite the presence of high viral load is supported by studies detecting abundant thymic tissue (using CT scans) in a subset of HIV-infected adults when compared to age-matched healthy controls, which was associated with increased levels of circulating CD4 naive T cells [72].

3. Role of IL-7 in HIV Infection

In addition to its central role in early thymocyte development, IL-7 is crucial for naive and T_{CM} cell survival by inhibiting programmed cell death-induced signaling through the up-regulation of anti-apoptotic molecules such as Bcl-2 and Kruppel–like factor 2 [210]. In addition, IL-7 induces the proliferation of peripheral T cells in lymphopenic settings and therefore plays a role as a regulator of homeostasis [211]. In healthy subjects, surface expression levels of the IL-7

receptor α-chain (CD127) but not the common γ-chain (CD132) were predictive of the magnitude of the response to IL-7 [212, 213]. Our data and that of others demonstrated that levels of IL-7 were increased in HIV-infected individuals (Ch.2 fig.S1, [214]). This is similar to what was initially described in other lymphopenic conditions such as bone marrow transplantation [215] and chemotherapy [206]. Many studies have found that high levels of IL-7 correlated with lower CD4 T cell counts in both HIV^+ adults [197, 214, 216, 217] and children [218], especially when subjects with severe lymphopenia (CD4 count < 100 cells/mL) were included in the study [206]. Similar relationships were not observed between CD4 T cell counts and levels of other cytokines such as IL-2, IL-4, IL-6, IL-12 or IL-15 [206]. As a result, IL-7 is thought to be involved in HIV-induced CD4 T cell depletion.

3.1. IL-7 levels in HIV: increased production or decreased consumption?

Whether increased levels of plasma IL-7 observed in HIV infection are part of a regulatory pathway triggered following lymphopenia to drive immune restoration or simply occur as a consequence of lymphopenia and depletion of T cells expressing the IL-7 receptor is not fully clear and support in the literature exits for both models. Support for the hypothesis that IL-7 production is regulated as part of a homeostatic response to the T cell depletion observed in HIV infection stems from the detection of relatively low levels of IL-7 in a subset of individuals with idiopathic CD4 lymphopenia despite their severe CD4 T cell depletion [206]. Similarly, HIV-infected individuals with reduced IL-7 levels despite low CD4 T cell counts were indentified and this seemed to be associated with poor reconstitution following therapy [219]. If increased levels of IL-7 were strictly a result of diminished target cell consumption, this would then take place in all clinical settings associated with CD4 depletion, which is clearly not always the case. Further evidence for this model stems from reports of delayed increases of IL-7 levels following CD4 T cell depletion during HIV infection [220] and delayed normalization of IL-7 levels following restoration of CD4 T cell counts after completion of chemotherapy [206], since increased consumption of IL-7

would be expected to normalize levels of IL-7 at faster rates. This hypothesis is further backed by the finding of increased IL-7 production by dendritic-like cells within lymphocyte-depleted lymph nodes [214]. This model invokes the ability of IL-7-producing cells to 'sense' T cell depletion either through cell to cell interactions [221] or via soluble factors secreted by T cells such as TGF-β which has been shown to regulate IL-7 production by bone marrow stromal cells [222].

The other explanation for the negative association between CD4 T cell counts and levels of IL-7 is that as a consequence of CD4 T cell depletion, there are fewer cells expressing the IL-7 receptor resulting in decreased IL-7 consumption and consequently, increased levels of plasma IL-7. This model states that IL-7 is produced at a constant rate by stromal cells within lymphoid tissues and that lymphocyte depletion increases availability of IL-7. During HIV infection, CD4 T cells are depleted whereas CD8 T cells are doubled in numbers when compared to uninfected controls. For that reason, it was initially thought that cell target reduction was an unlikely cause of the observed increased levels of IL-7 [214]. However, recent studies analyzing the expression of CD127 on CD4 and CD8 T cell subsets from HIV-infected individuals during CHI reinforced this hypothesis. Although CD127 expression was only slightly down-regulated on CD4 T cells [213, 216, 217], specifically within T_{CM} and T_{EM} subsets [216, 217, 223], there was a drastic reduction in CD127 levels on all CD8 T cell subsets especially within naive T cells [216]. Therefore, it is plausible that decreased consumption generated by decreased CD127 availability on CD8 T cells was enough to markedly increase circulating levels of IL-7. This is further supported by the finding of an inverse correlation between CD127 expression on T cells and serum levels of IL-7 in HIV-infected patients at different clinical stages of HIV infection [217, 224]. Certainly, one can argue that high levels of IL-7 can be the cause rather than a consequence of CD127 down-regulation. However, long-term non-progressors (LTNPs) were shown to also contain low expression levels of CD127 despite having normal concentrations of circulating IL-7 [224], suggesting that CD127 down-regulation is, at least in some part, mediated by factors other than IL-7 itself.

The two models discussed are most likely not mutually exclusive and may both contribute to the observed increased levels of IL-7. For instance, CD127 expression on CD8 T cells have also been shown to be greatly decreased during AEHI [224], which could explain the increased levels of IL-7 observed in AEHI that do not correlate with peripheral CD4 T cell counts [224]. On the other hand, mucosal CD4 T cells are massively depleted in the gut during AEHI [225] and although it has not been shown, it is likely that IL-7 increases in the periphery reflect a 'spill-over' from increased production in the gut.

3.2. Defects in the IL-7/IL-7R system in HIV infection

Many mechanisms can lead to the down-regulation of CD127 from the surface of T cells. *In vitro* as well *in vivo* IL-7 administration studies have shown that IL-7 leads to the rapid but transient down-regulation of its own receptor [224, 226]. This is reversed following withdrawal of IL-7 and involves new receptor synthesis [224]. CD127 down-regulation in response to IL-7 has been proposed to be part of an altruistic mechanism during which T cells that engage IL-7 halt future consumption of IL-7 [227]. During HIV infection, the correlation between high levels of IL-7 and low CD127 expression on T cells is unlikely to be a result of increased signaling and receptor internalization since T cells expressing low levels of CD127 contained significantly lower levels of Bcl-2 when compared to T cells expressing high levels of CD127 [217], suggesting that IL-7 down-regulation is induced by factors other than IL-7. Indeed, it was demonstrated that loss of CD127 on CD8 and CD4 memory T cells was tightly associated with increased cell activation, as assessed by expression levels of CD38, within these subsets [216, 217]. In addition, the HIV protein Tat has been shown to lead to CD127 down-regulation by binding to the cytoplasmic tail of CD127, inducing its internalization and degradation thereby impairing CD8 T cell proliferation and function [228].

Longitudinal analysis of HIV-infected individuals revealed that despite increases in the levels of IL-7, CD4 T cells continued to be progressively depleted, suggesting alteration in the IL-7 signaling pathway [229] and raising the question

of why elevated levels of IL-7 during CHI are incapable of restoring T cell counts. Indeed, normal expression levels of the IL-7R does not guarantee normal function and we observed significantly lower frequencies of Bcl-2^+ cells within RTEs in P subjects during AEHI and CHI when compared to uninfected controls, despite unchanged frequencies of $CD127^+$ cells within RTEs (Ch.2 fig.7). This is in line with a previous study demonstrating that CHI is characterized by a loss of correlation between levels of CD127 on CD4 T cells and up-regulation of Bcl-2 following IL-7 stimulation when compared to healthy individuals [230]. This defective up-regulation of Bcl-2 was found in both CD4 naive and memory T cell subsets, despite preserved levels of CD127 and preserved IL-7 binding to its receptor [212]. The observed decrease in IL-7 responsiveness has been recently shown to involve the JAK/STAT transduction pathway: the ability of IL-7 to induce the phosphorylation of signal transducer and activator of transcription 5 (STAT-5) was greatly reduced in CD4 naive and memory T cell populations from HIV-infected individuals and this was not correlated with levels of CD127 within CD4 T cells [223].

The results presented in this thesis demonstrate that unresponsiveness of RTEs to IL-7 is a phenomenon of CHI that is dependent on viral load. In SP subjects which showed consistent low viral load throughout the study period (<500 HIV RNA copies/ml), we detected a significant positive correlation between levels of IL-7 and *ex vivo* frequencies of Bcl-2^+ cells within RTEs in both AEHI and CHI, implying that the IL-7 signaling pathway was intact in those subjects (Ch.2 fig.S1). However, this correlation was no longer significant in P subjects which showed high viral load (>10,000 HIV RNA copies/ml) (Ch.2 fig.S1). We hypothesized that these differences might be due to an inability of RTEs from P subjects to respond to IL-7 in CHI. In fact, both *ex vivo* and IL-7-induced phosphorylation of STAT-5 were positively associated with levels of plasma IL-7 during AEHI in P subjects, a correlation lost during CHI (Ch.2 fig.8). This indicates preserved signaling in response to IL-7 early in infection and suggests desensitization of the IL-7R in CHI due to chronic immune activation. This is supported by the fact that we detected an inverse correlation between levels of

STAT-5 phosphorylation within RTEs and viral load during CHI (Ch.2 fig.8). Since STAT-5 is a potentially oncogenic protein [231], chronic stimulation of the JAK/STAT signaling pathway [212, 232] may result in the up-regulation of elements (such as SLIM proteins (E3 ubiquitin ligases) or the transcription factor PIAS) that would negatively regulate its expression or activity [233, 234].

In addition to defects in IL-7 responsiveness, it is also possible that T cells have limited access to the IL-7 stores. For example, higher levels of circulating soluble IL-7R (sCD127) were detected in HIV-infected individuals as compared to uninfected controls which may potentially bind to plasma IL-7 and diminish its bioavailability [235]. *In vitro* co-culture of IL-7 with sCD127 led to marked inhibitions in the phosphorylation of STAT-5 and Akt, as well as diminished T cell proliferation and Bcl-2 expression [235]. Furthermore, increased fibrosis in lymph nodes during CHI possibly exerts physical constraints that alter trafficking of T cells and consequently limit the access of RTEs to cytokines such as IL-7 that are required to maintain their survival and homeostasis [2].

Consequently, the inability of HIV-infected individuals to reconstitute CD4 T cell counts in the presence of high levels of IL-7 may be merely a result of the inability of the IL-7 receptor to bind circulating IL-7 and/or to respond to its signals. This, in turn, can represent an additional mechanism responsible for increased levels of IL-7 and can explain why we observed decreased RTE cell survival and CD4 T cell depletion despite abundance of IL-7.

3.3. Are increased IL-7 levels during HIV infection beneficial or harmful?

Although IL-7 is known to play a positive role on the survival of thymocytes and mature T cells, the benefits of increased levels of IL-7 in the context of HIV infection remain unclear especially in subjects with high viral replication. We show in Chapter 2 that levels of IL-7 during AEHI were higher in P subjects (that showed low RTE frequencies) than in SP subjects (that showed higher RTE frequencies) despite both groups having similar CD4 T cell counts. Therefore, it is possible that IL-7 is increased as a feedback compensatory mechanism in response to low RTE numbers and/or reduced thymic activity to stimulate *de novo*

T cell production in the thymus [52]. However, this notion is challenged by the findings of Ruiz-Mateos et al, which demonstrated that levels of IL-7 in HIV-infected adults were inversely correlated with thymic measures (thymus volume, frequencies of TRECs and naive T cells) [236]. Similar findings were reported in HIV-infected untreated children [218]. On the other hand, levels of IL-7 prior to HAART therapy were positively correlated with changes in thymus volume [236], as well as with CD4 T cell recovery post-HAART [224, 237]. In addition, increased levels of IL-7 during HIV-2 infection (an "attenuated" form of HIV disease characterized by low viral load throughout all stages of disease), seemed to be associated with increased frequencies of $CD31^+$ naive CD4 T cells [197]. Whether the positive correlation between levels of IL-7 and frequencies of $CD31^+$ naive T cells in HIV-2 infected individuals was due to enhanced thymic production or peripheral expansion remains to be clarified through measurement of TRECs and Ki67 expression levels.

Taken together, these findings suggest that the absence of a correlation between high levels of IL-7 and increased thymic activity in untreated HIV infection might be due to a limited capacity of the thymus and RTEs to respond to IL-7 in the presence of uncontrolled viral suppression. Furthermore, high levels of plasma IL-7 during AEHI have been suggested as a biomarker of disease progression to AIDS [238] and are mostly associated with a poor prognosis in HIV-infected individuals [238] and in SIV-infected macaques [220]. Therefore, it is conceivable that IL-7 plays a role in the pathogenesis of HIV infection.

3.3.1. Role for IL-7 in HIV pathogenesis

As mentioned above, T cells are unresponsive to IL-7 and its pro-survival signals in settings with high viral load. However, several studies have proposed that high levels of IL-7 may actually exacerbate HIV-induced CD4 T cell depletion. In fact, IL-7 has been suggested to directly induce apoptosis of bystander T cells in HIV infection. Treatment of T cells with IL-7 as well as *in vivo* injections of IL-7 to rhesus macaques induced the up-regulation of Fas [239], a death receptor involved in apoptosis [240]. In addition, it was found that high levels of serum IL-

7 were correlated with increased Fas expression within both naive and memory T cell populations in HIV-infected individuals [239]. Furthermore, HIV proteins such as gp120, Tat and Nef have been shown to induce Fas ligand expression [241], which explains why treatment of HIV-infected T cells with IL-7 rendered them sensitive to Fas-mediated apoptosis [242]. It would be of interest to determine whether RTEs from P subjects also up-regulate Fas during CHI and if that correlates with levels of IL-7.

Furthermore, we show that levels of IL-7 were positively correlated with viral load during both AEHI and CHI (Appendix A fig.S3). This supports the findings of Napolitano et al [214] and suggests a role for IL-7 in enhancing viral replication *in vivo*. *In vitro* studies have previously demonstrated that exogenous IL-7 could enhance HIV replication in CD4 T cells from chronically infected subjects [243] as well as in $CD4^+$ thymocytes within FTOCs [244]. In addition, pre-treatment of CD4 naive T cells with IL-7 rendered them permissive to HIV infection by inducing the up-regulation of the transcriptional factor NFAT [245]. Therefore, IL-7 may be involved in a positive feedback loop that promotes viral spread whereby high levels of IL-7 produced following onset of infection lead to increased viral replication and higher viral loads. This in turn accelerates CD4 T cell depletion and results in even greater levels of IL-7.

In addition, by enhancing viral replication, high levels of IL-7 might indirectly favour virus evolution. In fact, IL-7 was shown to be higher in the plasma of children harbouring the syncytium-inducing (or X4) phenotype versus those with non-syncytium-inducing (or R5) variants [218]. Furthermore, decreases in levels of IL-7 and viral load following HAART therapy resulted in the switch from the X4/S1 to the R5/NSI phenotype [218]. In addition, it was shown that IL-7 up-regulated the expression of CXCR4 on thymocytes [246], naive T cells [247] and T_{CM} [248], thereby increasing target cell availability. These results imply that high levels of IL-7 may eventually lead to the destruction of $CXCR4^+CD4^+$ progenitor cells in the thymus and mature naive T cells in the periphery consequently impairing production of new T cells and aggravating disease.

Further evidence for a role of IL-7 in pathogenesis stems from analyzing IL-7 levels in HIV-infected LTNPs, characterized by CD4 T cell counts of above 500 cells/μl and controlled viral replication for 7-10 years [249], as well as in non-pathogenic SIV infection. Levels of IL-7 within LTNP subjects were within the normal range [224, 229]; however, subjects that lost viral control (and LTNP status) during the follow-up period had significantly increased their levels of IL-7 prior to loss of viral control [224]. In addition, it was reported that SIV-infected sooty mangabeys, monkeys that maintain stable CD4 T cell numbers and do not progress to simian AIDS, have significantly lower levels of IL-7 compared to rhesus macaques, despite the presence of high viral load in both animals [220].

We have previously demonstrated that HIV-infected subjects that maintained high CD4 T cell counts for many years despite high viremia had unaltered intrathymic proliferation whereas subjects with low CD4 T cell counts were characterized by reduced intrathymic proliferation [5]. Determining whether differences existed in the levels of IL-7 between these distinct groups would help further elucidate the role of IL-7 in RTE and CD4 T cell depletion. The contribution of IL-7 in enhanced viral replication can help explain why regardless of its origin (increased production, low CD4 T cells, low $CD127^+$ T cells, or unresponsive receptor) high levels of IL-7 are associated with accelerated disease progression.

4. HIV-mediated constraints on thymocyte development

In the early stages of HIV infection, CCR5-using strains predominate. Emergence of X4 virus takes place in approximately 50% of infected individuals and precedes the symptomatic phase of HIV infection [250]. Having identified specific phenotypes associated with the different development stages in $CD3^-$ immature human thymocytes (Ch. 4), we were able to determine which subsets expressed which co-receptors. Using RT-PCR on sorted thymocytes, we confirmed that CXCR4 was abundantly expressed on all immature $CD3^-$ thymocytes (Appendix A fig.S4), which explains why CXCR4-using strains have detrimental consequences on the regeneration of naive T cells during late-stage HIV infection [218] and following treatment with HAART [180]. However, we

did not detect CCR5 gene expression in any of the $CD3^-CD4^+$ thymocytes (Appendix A fig.S4). This is compatible with previous studies reporting very low CCR5 frequencies within thymocytes (1-3%) [4] that seemed restricted to DP and SP thymocytes [251]. While these results imply that thymocytes are less susceptible to HIV infection and viral-mediated lysis during AEHI (characterized by R5-using strains [250]), it was shown that levels of CCR5 on mature CD4 thymocytes were significantly higher in thymi from HIV-infected individuals when compared to thymi from uninfected controls [167]. This was correlated with enhanced bystander activation in $CD3^-CD4^-CD8^-$ immature thymocytes [167], demonstrating a role for immune activation in facilitating infection and/or viral-meditated destruction of thymocytes. The consequences of enhanced infection of mature SP thymocytes include diminished thymic output as well as export of latently infected naive T cells into the periphery.

The impaired intrathymic proliferation observed in a subset of HIV-infected individuals during AEHI [6] is likely derived from indirect effects associated with infection of thymic dendritic cells (DC) and thymic epithelial cells (TEC), which are both susceptible to R5 virus [252]. Infection of these cells can lead to their degeneration, creating disorganization of the thymic microenvironment [253] that thymocytes depend on for their survival. Furthermore, thymic DCs can be stimulated by HIV antigens to secrete inflammatory cytokines such as IL-4, IFN-γ, IL-6 and IL-10 which could alter thymocyte differentiation [166]. In addition, plasmacytoid DCs (pDCs) have been shown to produce IFN-α upon HIV infection in SCID-Hu Thy-Liv mice [254]. Our laboratory has previously demonstrated the inhibitory impact of TLR-triggered IFN-α production on thymopoiesis in mice [255, 256]. Administration of IFN-α has been shown to directly inhibit IL-7-driven proliferation of $CD3^-$ immature thymocytes *in vitro* [257] as well as to down-regulate the expression of the IL-7R α-chain and increase the expression of suppressor of cytokine signaling-1 (SOCS-1) [255]. Interestingly, the IFN-α receptor seemed to be expressed at higher levels in ISP and EDP thymocytes that were $CD31^+$ (pre-β-selection) (Appendix A fig.S4) and it is therefore probable that IFN-α is involved in impaired proliferation following

the β-selection stage leading to reduced sj/β TREC ratio. The impact of IFN-α and other anti-proliferative cytokines on intrathymic proliferation can now be tested by co-culturing $CD3^-$ thymocytes sorted at various differentiation stages together with the cytokine(s) of interest on OP9-DL1 stromal cells, as described in Chapter 4. Having established phenotypes associated with pre- and post-β-selection, we can now identify the various players involved in halting thymocyte proliferation and differentiation. This could provide added therapeutic value to patients with discordant responses to HAART treatment. Preliminary work using this system suggested that IFN-α inhibited proliferation of cells undergoing β-selection (as measured by CFSE) in a dose-dependent manner (data not shown).

5. Dynamics of RTEs following HAART

Highly Active Antiretroviral Therapy (HAART) results in viral suppression and increases of total CD4 T cell counts in the majority of patients. However, up to 30% of HIV-infected individuals do not increase CD4 T cells more than 100 cells/μl in response to HAART and are termed immunological non-responders (INR) [258]. It was previously described that increases in CD4 T cells following treatment with HAART occur in two phases: a first phase, as early as two weeks after the start of therapy, consisting primarily of increases in memory T cells and a second late phase, consisting of increases in naive T cells [170]. It remains unclear whether these naive T cells originated from the thymus or from peripheral expansion. Difficulties in assessing thymic function by measuring naive T cells arise from the fact that a conversion from a memory $CD45RO^+$ to a naive $CD45RA^+$ phenotype has been reported following treatment with HAART [259]. Using the RTE-specific phenotype, the data presented in this thesis demonstrate that RTEs are increased in the early phase of reconstitution (Ch.3 fig.1). While recirculation may be involved in this early rise, especially in subjects that began treatment before their CD4 T cell counts dropped below 550 cells/μl, our results confirm that enhanced thymic function, as measured by the sj/β TREC ratio, contributed to the observed increases in RTE cell counts during the early phase of T cell reconstitution (Ch.3 fig.3) and, unlike recirculation or peripheral

proliferation, was involved in long-term RTE maintenance (Ch.3 fig.2). Our findings of a positive correlation between the magnitude of RTE gain and total CD4 T cell recovery highlights the importance of thymic output in T cell reconstitution and supports previous studies conducted by us and others that reported higher sj/β TREC ratio [5] and abundant thymic tissue [260] in immunological responders (IR) versus immunological non responders (INR).

Our data also suggested that enhanced thymic function is not the sole determinant of the magnitude of the RTE and CD4 T cell recovery following treatment with HAART. In fact, high frequencies of $Ki67^+$ cells as well as low frequencies of $CD127^+$ cells within RTEs 52 weeks post-HAART correlated with poor RTE recovery despite increased intrathymic proliferation (Ch.3 fig.2 and fig.3). These findings promote a role for enhanced RTE survival in immune reconstitution following treatment with HAART and support the notion that HIV infection induces severe disruptions in the 'thymus-naive T cell' axis. Scarring of lymph nodes due to collagen deposition during HIV infection has been demonstrated [2], and this could impact the ability of newly exported RTEs to survive in the periphery following therapy with HAART. Increased immune activation can represent another mechanism that leads to defective survival of RTE and naive T cells despite continuous thymic output. This notion is supported by a recently published report demonstrating that INR, when compared to IR, showed depletion of naive T cells despite similar sj/β TREC ratio that was associated with increased activation levels due to the presence of predominant X4 virus strains [180].

A role for the IL-7/IL-7R system in the normalization of CD4 T cell numbers during HAART has also been suggested by previous studies demonstrating that reduced levels of CD127 within CD4 T cells correlated with low CD4 naive T cell counts in INR [261] and that high levels of CD127 within CD4 and CD8 T cells were associated with successful immune reconstitution in chronically infected HIV patients treated with HAART [262, 263]. Longitudinal studies have revealed that normalization of CD127 on CD8 T cells occurs after 24 months of HAART treatment [216] but not after 12 months [216, 224]. It is therefore possible that restoration in the levels of CD127 and normalization of CD4 T cell counts

following HAART lead to decreased levels of IL-7. Conflicting data in the literature exist on whether levels of IL-7 are reduced following treatment with HAART. Some studies have shown that levels of IL-7 are decreased as early as 10 months post-HAART [224, 236, 264] while another reported that levels of IL-7 decreased, although not significantly, 24 months following HAART [216]. In addition, there is evidence that levels of IL-7 do not normalize after initiation of HAART even after 33 months [265] and that high levels of IL-7 are a prominent feature of INR [264, 266]. We also detected great variations in the levels of IL-7 following HAART. While the majority of HAART-treated individuals experienced a transient increase in the levels of IL-7 shortly following onset of HAART (Ch.3 fig.5*A*), a subset of individuals maintained high levels of IL-7 52 weeks post-HAART while others reduced IL-7 levels.

However, none of these studies detected any correlations between levels of IL-7 following treatment with HAART and CD4 T cell recovery, which questions the role of endogenous IL-7 during HAART therapy. The differences observed in IL-7 normalization can be reconciled by a recent study demonstrating that a positive correlation between levels of IL-7 following HAART and CD4 T cell recovery existed only in subjects that responded to IL-7 (as measured by their high STAT-5 phosphorylation levels following IL-7 stimulation). This highlights the need to assess levels of IL-7 in conjunction with levels of its receptor and receptor functionality in order to have a clearer picture on the role of IL-7 in T cell reconstitution. For instance, our data demonstrated that increased levels of IL-7 post-HAART correlated with higher frequencies of $CD127^{+}$ cells within RTEs (Ch.3 fig.5C). Both of these measurements, in turn, correlated with a higher RTE gain post-HAART (Ch.3 fig.2 and fig.5B). This is supported by previous reports indicating that higher CD127 expression was correlated with increased CD4 T cell recovery in 'CD4-exploders' [262] and that high levels of IL-7 in conjunction with low expression of CD127 and low CD4 T cell counts were characteristic of INR [263], a pattern reminiscent of untreated HIV infection. Evaluation of IL-7 responses such as phosphorylation of STAT-5 and up-regulation of Bcl-2 are necessary in order to allow us to confirm restoration of the IL-7/IL-7R pathway in

HAART-treated patients. Nonetheless, it has recently been shown that the loss of a correlation between CD127 expression and responsiveness to IL-7 during untreated HIV infection is reversed following HAART and that frequencies of $CD127^+$ within CD4 T cells correlated with the magnitude of STAT-5 phosphorylation in response to IL-7 stimulation [267].

Although certain groups have identified a positive correlation between levels of IL-7 prior to HAART treatment and CD4 T cell recovery following HAART [216, 224, 237], we found no such correlation for RTE or total CD4 T cell gain. Instead, we detected a positive correlation between levels of IL-7 prior to HAART treatment and the sj/β TREC ratio following treatment with HAART (Ch.3 fig.S1). This is in agreement with previous reports showing positive correlations between levels of IL-7 prior to HAART and increased thymic volume [236] as well as TREC content in HIV-infected adults and children [262, 268] following initiation of HAART. The absence of these correlations prior to HAART most likely reflects the inhibitory effects of HIV on thymic activity [269] and the ability of IL-7 to augment thymocyte infection [244].

In summary, the results presented in Chapter 3 suggest that IL-7 promotes CD4 T cell recovery following viral suppression mediated by HAART through two complementary mechanisms. First, levels of IL-7 detected prior to initiation of HAART treatment might act to increase thymic function and accelerate the release of newly produced T cells into the periphery that would be more functional than resident (pre-HAART) T cells provided viral replication is suppressed. Second, increased levels of IL-7 following HAART play a possible role in transferring survival signals to newly exported RTEs, thereby facilitating CD4 T cell regeneration. Our findings suggest that the IL-7-IL-7R axis might be an important therapeutic target adjunct to HAART treatment. Recombinant IL-7 therapy in SIV-infected rhesus macaques under antiviral treatment and in phase I human clinical trials in cancer patients and HAART-treated HIV-infected subjects have shown that subcutaneous injections of IL-7 were well tolerated with minimal toxicity [226, 270-272]. IL-7 administration led to significant dose-dependent increases in T cell numbers which persisted even after cessation of therapy and

were accompanied by rapid polyclonal expansion of most T cell subsets [226, 270-272]. Repeated dose injections demonstrated a preferential expansion of naive T cells and T_{CM} concomitant with up-regulation of Bcl-2 levels [271, 272]. This demonstrates that IL-7 therapy resulted in quantitative and qualitative enhancement of the immune system. In fact, Sportes et al. [272] have shown that IL-7 therapy resulted in increased repertoire diversity in the majority of cancer patients. Increases in naive (and RTE) T cell counts were shown to correlate with enhanced thymopoiesis, as measured by the sj/β TREC ratio in SIV-infected macaques [270] but this remains to be confirmed for the human clinical trials. The identification and validation of the $CD31^{hi}$ phenotype as a tool to measure T cell reconstitution by the thymus would now permit such an assessment, and would allow the isolation of RTEs and the discrimination of the various effects (i.e survival and/or proliferation) that are exerted by administration of this cytokine. Further support of the use of IL-7 in conjunction to HAART therapy stems from a recent study that demonstrated that administration of recombinant IL-7 to SIV-infected rhesus macaques following treatment with IFN-α abrogated the lymphopenic effect induced by IFN-α [273]. Our data showed that failure to decrease levels of IFN-α following treatment with HAART correlated with decreased sj/β TREC ratio and RTE cell counts, despite high levels of IL-7 (Ch.3 fig.4). It is conceivable that treatment with exogenous IL-7 could stimulate intrathymic proliferation despite high levels of IFN-α in these subjects, similarly to what was reported in the non human primate model.

A limitation of the use of IL-7 therapy in HIV stems from the previously discussed mechanisms by which IL-7 can accelerate HIV disease progression and increase thymocyte and naive T cell susceptibility to HIV infection. In these trials, IL-7 administration did not increase serum viral loads, although dose-dependent transient peaks in viral replication were detected [226, 271]. Nonetheless, it is also possible that IL-7 increases HIV DNA content within T cells [266]. Results from these clinical trials suggested that IL-7 is a safe and promising candidate for the treatment of conditions associated with lymphopenia but viral load and HIV reservoir need to be carefully monitored and thymic function needs to be assessed

using reliable tools such as the sj/β TREC ratio and the $CD31^{hi}$ phenotype in order to determine whether IL-7 reshapes the immune system without impacting viral replication.

CONCLUSIONS AND PERSPECTIVES

The work presented in this thesis is aimed at investigating the role of thymic output, homeostatic proliferation and survival in the maintenance of RTEs during untreated AEHI and CHI as well as in reconstitution of RTEs following treatment with HAART. The impact of homeostatic cytokines, including IL-7 and IFN-α, on intrathymic proliferation and RTE homeostasis was also evaluated.

We have gained insight into RTE dynamics during natural HIV infection, as well as following treatment with HAART, and the factors associated with their depletion. We detected a significant loss of circulating RTEs at early stages of infection, and determined that the magnitude of loss directly predicted slow disease progression versus accelerated progression. Lower RTE numbers in association with high levels of IL-7, elevated immune activation (as measure by frequencies of Ki67 and PD-1) and defective survival (as demonstrated by low Bcl-2 frequencies) distinguished slow progressors (SP) from progressors (P). On the other hand, long-term RTE reconstitution following treatment with HAART, when present, involved increases in intrathymic proliferation concomitant with increases in the frequencies of RTE cells expressing CD127 and decreases in the frequencies of RTE cells expressing Ki67. Taken together, these results highlight the role of thymic output versus homeostatic expansion in the replenishment of the RTE cell pool.

In fact, our data suggest that thymic function dictates the rate of disease progression since untreated subjects with normal RTE frequencies within naive T cells and RTE absolute numbers maintained higher numbers of circulating T_{CM} and total CD4 T cells when compared to subjects with low RTE frequencies and absolute numbers. Based on these results, one could question whether continuous production of RTEs by the thymus keeps T_{CM} and total CD4 T cell numbers constant throughout infection in the face of increased priming, differentiation and cell death observed during HIV infection. On the other hand, one could wonder if

hyperimmune activation, mediated by high viral loads and/or increased inflammation, is the major culprit behind RTE depletion despite effective thymic function. To answer these questions, we would need to evaluate levels of activation within RTEs in conjunction with the sj/β TREC ratio in a subset of HIV-infected individuals that maintain high CD4 T cell counts despite high levels of viremia.

Further evidence for the importance of intact thymic output during HIV infection stems from the finding that RTEs, unlike $CD31^{low}$ or $CD31^{-}$ CD4 naive subsets, are the only population to show increased frequencies of proliferating cells during AEHI, which in turn correlated with T_{CM} absolute numbers. These results suggest that RTEs are the key naive T cell population capable of differentiating and generating T_{CM} in response to antigen encounter. These findings raise two key questions: Do $CD31^{low}$ and $CD31^{-}$ CD4 naive subsets represent cells at 'dead end' stages of maturation that have extensively proliferated and are no longer capable of responding to either TCR or IL-7 triggering? Does the severe impact of RTE depletion on disease progression result not only from quantitative defects but also from impaired T_{CM} generation? If this is indeed the case, adequate thymic output during HIV infection would not only increase repertoire diversity, but also provide cells that are more adept in the immune response (See figure 4). To confirm this hypothesis, the proliferative capacity and differentiation potential of RTEs and other naive T cells would have to be tested following IL-7 or TCR triggering from both healthy and HIV-infected individuals.

Our data also show distinct roles for IL-7 in untreated versus treated HIV infection; while levels of IL-7 early in infection predict faster disease progression and are involved in increased proliferation during untreated HIV infection, increases in levels of IL-7 following treatment with HAART are positively associated with RTE reconstitution.

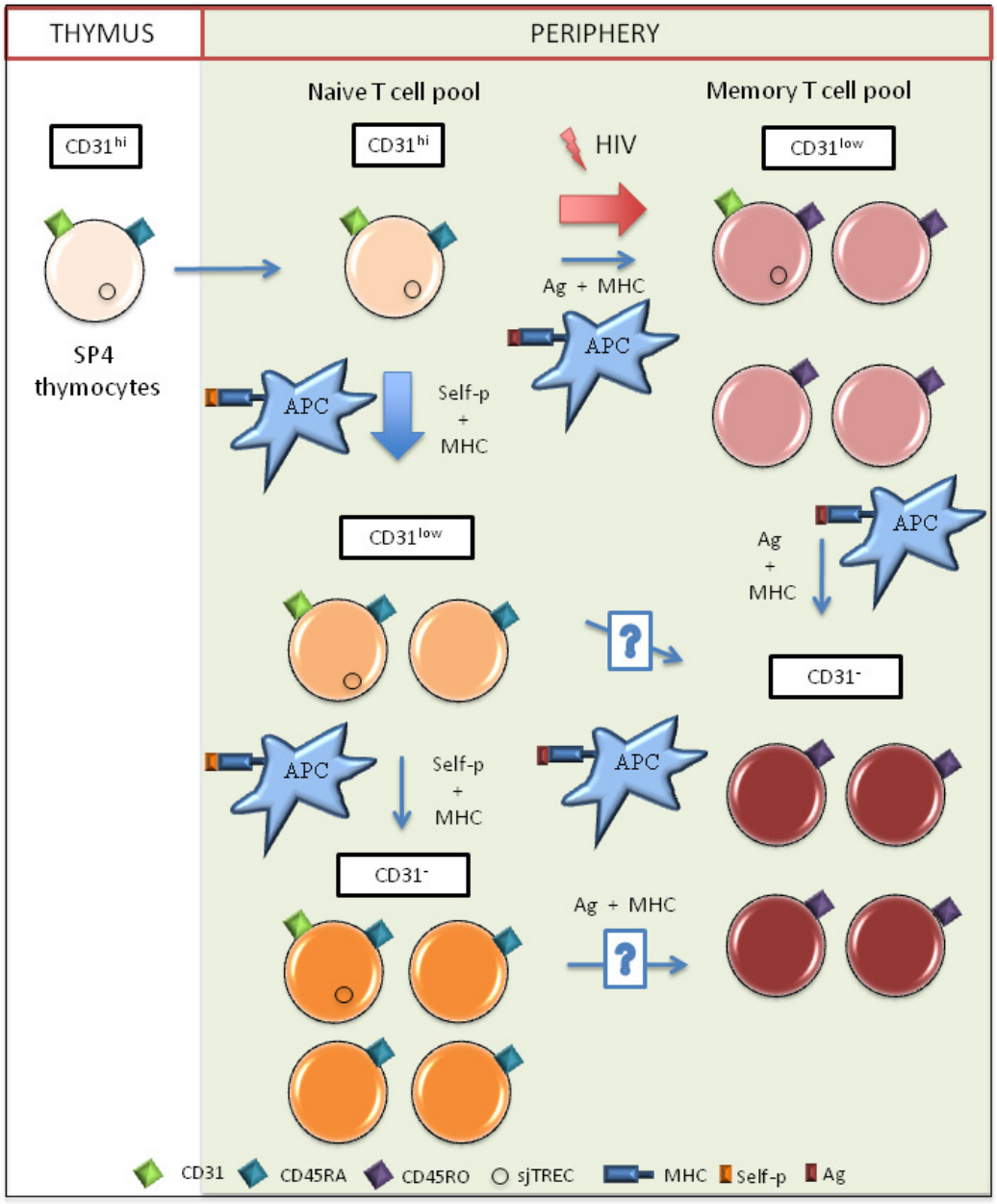

Figure 4: RTE homeostasis in health and HIV Infection.

Following their exit from the thymus, RTEs join the naive T cell compartment. Interactions with self-peptide:MHC complex within secondary lymphoid tissues lead to homeostatic proliferation as well as down-regulation of $CD31^{hi}$ and dilutions of TRECs. Upon recognition of foreign antigens, RTEs can differentiate directly into T_{CM}, a process amplified during HIV infection. Due to the very low frequencies of cycling cells within the $CD31^{low}$ and $CD31^{-}$ T cell subsets and to the lack of a correlation between cell cycle entry within these subsets and HIV RNA, we hypothesize that $CD31^{low}$ and $CD31^{-}$ naive T cells might be cells that have undergone extensive differentiation and can no longer respond to antigen-triggered differentiation (original figure).

This is most likely a result of enhanced survival signals, as suggested by the presence of a positive correlation between levels IL-7 and CD127 frequencies within RTEs, and the absence of an association between levels of IL-7 and Ki67 frequencies within RTEs. These viremia-dependent differences in the role of IL-7 support the use of IL-7 administration as an adjuvant to HAART treatment. Robust and non-invasive tools to study thymic function, such as the ones used in the work outlined in this thesis, permit quantification of the contribution of the thymus versus peripheral expansion in on-going human clinical trials. Our data also suggest a crucial role for the ability of RTEs to survive in the periphery following their release from the thymus. To discriminate between poor RTE reconstitution due to their inability to receive survival signals as a result of a scarred lymphatic environment or as a result of a loss of responsiveness to IL-7 due to persistent T cell activation, we would need to measure the levels of pSTAT-5 and Bcl-2 induced following IL-7 stimulation in RTEs from these treated subjects.

Lastly, our data suggest that high levels of IFN-α following treatment with HAART could inhibit the positive effects of IL-7 on RTE and CD4 T cell reconstitution as well as impair thymic activity. If high levels of IFN-α generated during HIV infection can indeed impair intrathymic proliferation, this would result not only in numerical depletion of RTEs, but in the output of population with a skewed repertoire. Having extensively characterized the human β-selection stage of development, we can now test this hypothesis by co-culturing isolated $CD31^{-}CD1a^{hi}$ thymocytes in the OP9-DL1 system and directly assess any blockages IFN-α might exert on intrathymic proliferation by monitoring phenotype progression as well as proliferative and survival capacities. This will allow the elucidation of the specific mechanism of HIV-altered thymopoeisis which will be crucial in the development of therapeutic approaches aiming at restoring the capacity of the thymus to reconstitute the immune system depleted by HIV.

BIBLIOGRAPHY

1. McCune, J.M., *The dynamics of CD4+ T-cell depletion in HIV disease.* Nature, 2001. **410**(6831): p. 974-9.
2. Schacker, T.W., et al., *Lymphatic tissue fibrosis is associated with reduced numbers of naive CD4+ T cells in human immunodeficiency virus type 1 infection.* Clin Vaccine Immunol, 2006. **13**(5): p. 556-60.
3. Schuurman, H.J., et al., *The thymus in acquired immune deficiency syndrome. Comparison with other types of immunodeficiency diseases, and presence of components of human immunodeficiency virus type 1.* Am J Pathol, 1989. **134**(6): p. 1329-38.
4. Taylor, J.R., Jr., et al., *Expression and function of chemokine receptors on human thymocytes: implications for infection by human immunodeficiency virus type 1.* J Virol, 2001. **75**(18): p. 8752-60.
5. Dion, M.L., et al., *Slow disease progression and robust therapy-mediated CD4+ T-cell recovery are associated with efficient thymopoiesis during HIV-1 infection.* Blood, 2007. **109**(7): p. 2912-20.
6. Dion, M.L., et al., *HIV infection rapidly induces and maintains a substantial suppression of thymocyte proliferation.* Immunity, 2004. **21**(6): p. 757-68.
7. Boasso, A. and G.M. Shearer, *Chronic innate immune activation as a cause of HIV-1 immunopathogenesis.* Clin Immunol, 2008. **126**(3): p. 235-42.
8. Nixon, D.E. and A.L. Landay, *Biomarkers of immune dysfunction in HIV.* Curr Opin HIV AIDS, 2010. **5**(6): p. 498-503.

9. Zagury, D., et al., *Interferon alpha and Tat involvement in the immunosuppression of uninfected T cells and C-C chemokine decline in AIDS.* Proc Natl Acad Sci U S A, 1998. **95**(7): p. 3851-6.
10. Gurney, K.B., et al., *Endogenous IFN-alpha production by plasmacytoid dendritic cells exerts an antiviral effect on thymic HIV-1 infection.* J Immunol, 2004. **173**(12): p. 7269-76.
11. Lin, Q., C. Dong, and M.D. Cooper, *Impairment of T and B cell development by treatment with a type I interferon.* J Exp Med, 1998. **187**(1): p. 79-87.
12. Markert, M.L., et al., *Transplantation of thymus tissue in complete DiGeorge syndrome.* N Engl J Med, 1999. **341**(16): p. 1180-9.
13. van Ewijk, W., E.W. Shores, and A. Singer, *Crosstalk in the mouse thymus.* Immunol Today, 1994. **15**(5): p. 214-7.
14. Spits, H., *Development of alphabeta T cells in the human thymus.* Nat Rev Immunol, 2002. **2**(10): p. 760-72.
15. Lind, E.F., et al., *Mapping precursor movement through the postnatal thymus reveals specific microenvironments supporting defined stages of early lymphoid development.* J Exp Med, 2001. **194**(2): p. 127-34.
16. Prockop, S.E. and H.T. Petrie, *Regulation of thymus size by competition for stromal niches among early T cell progenitors.* J Immunol, 2004. **173**(3): p. 1604-11.
17. Rossi, F.M., et al., *Recruitment of adult thymic progenitors is regulated by P-selectin and its ligand PSGL-1.* Nat Immunol, 2005. **6**(6): p. 626-34.
18. Weijer, K., et al., *Intrathymic and extrathymic development of human plasmacytoid dendritic cell precursors in vivo.* Blood, 2002. **99**(8): p. 2752-9.

19. Ikawa, T., et al., *Commitment of common T/Natural killer (NK) progenitors to unipotent T and NK progenitors in the murine fetal thymus revealed by a single progenitor assay.* J Exp Med, 1999. **190**(11): p. 1617-26.
20. Michie, A.M., et al., *Clonal characterization of a bipotent T cell and NK cell progenitor in the mouse fetal thymus.* J Immunol, 2000. **164**(4): p. 1730-3.
21. Weerkamp, F., et al., *Human thymus contains multipotent progenitors with T/B lymphoid, myeloid, and erythroid lineage potential.* Blood, 2006. **107**(8): p. 3131-7.
22. Schatz, D.G., *V(D)J recombination.* Immunol Rev, 2004. **200**: p. 5-11.
23. Godfrey, D.I., et al., *A developmental pathway involving four phenotypically and functionally distinct subsets of CD3-CD4-CD8-triple-negative adult mouse thymocytes defined by CD44 and CD25 expression.* J Immunol, 1993. **150**(10): p. 4244-52.
24. Taghon, T., et al., *Developmental and molecular characterization of emerging beta- and gammadelta-selected pre-T cells in the adult mouse thymus.* Immunity, 2006. **24**(1): p. 53-64.
25. Fehling, H.J., et al., *Crucial role of the pre-T-cell receptor alpha gene in development of alpha beta but not gamma delta T cells.* Nature, 1995. **375**(6534): p. 795-8.
26. von Boehmer, H., *Unique features of the pre-T-cell receptor alpha-chain: not just a surrogate.* Nat Rev Immunol, 2005. **5**(7): p. 571-7.
27. Yamasaki, S., et al., *Mechanistic basis of pre-T cell receptor-mediated autonomous signaling critical for thymocyte development.* Nat Immunol, 2006. **7**(1): p. 67-75.
28. Aifantis, I., et al., *Constitutive pre-TCR signaling promotes differentiation through Ca2+ mobilization and activation of NF-kappaB and NFAT.* Nat Immunol, 2001. **2**(5): p. 403-9.

29. Xi, H., et al., *Interplay between RORgammat, Egr3, and E proteins controls proliferation in response to pre-TCR signals.* Immunity, 2006. **24**(6): p. 813-26.
30. Panigada, M., et al., *Constitutive endocytosis and degradation of the pre-T cell receptor.* J Exp Med, 2002. **195**(12): p. 1585-97.
31. Blom, B., et al., *TCR gene rearrangements and expression of the pre-T cell receptor complex during human T-cell differentiation.* Blood, 1999. **93**(9): p. 3033-43.
32. Haas, W., P. Pereira, and S. Tonegawa, *Gamma/delta cells.* Annu Rev Immunol, 1993. **11**: p. 637-85.
33. Yashiro-Ohtani, Y., T. Ohtani, and W.S. Pear, *Notch regulation of early thymocyte development.* Semin Immunol, 2010. **22**(5): p. 261-9.
34. Kraft, D.L., I.L. Weissman, and E.K. Waller, *Differentiation of CD3-4-8- human fetal thymocytes in vivo: characterization of a CD3-4+8- intermediate.* J Exp Med, 1993. **178**(1): p. 265-77.
35. Verschuren, M.C., et al., *T-cell receptor V delta-J alpha rearrangements in human thymocytes: the role of V delta-J alpha rearrangements in T-cell receptor-delta gene deletion.* Immunology, 1998. **93**(2): p. 208-12.
36. Palmer, E., *Negative selection--clearing out the bad apples from the T-cell repertoire.* Nat Rev Immunol, 2003. **3**(5): p. 383-91.
37. Ueno, T., et al., *CCR7 signals are essential for cortex-medulla migration of developing thymocytes.* J Exp Med, 2004. **200**(4): p. 493-505.
38. Anderson, M.S., et al., *The cellular mechanism of Aire control of T cell tolerance.* Immunity, 2005. **23**(2): p. 227-39.
39. van Meerwijk, J.P., et al., *Quantitative impact of thymic clonal deletion on the T cell repertoire.* J Exp Med, 1997. **185**(3): p. 377-83.

40. Cyster, J.G., *Chemokines, sphingosine-1-phosphate, and cell migration in secondary lymphoid organs.* Annu Rev Immunol, 2005. **23**: p. 127-59.
41. Carlson, C.M., et al., *Kruppel-like factor 2 regulates thymocyte and T-cell migration.* Nature, 2006. **442**(7100): p. 299-302.
42. Feng, C., et al., *A potential role for CD69 in thymocyte emigration.* Int Immunol, 2002. **14**(6): p. 535-44.
43. Raulet, D.H., *The structure, function, and molecular genetics of the gamma/delta T cell receptor.* Annu Rev Immunol, 1989. **7**: p. 175-207.
44. Jiang, Q., et al., *Cell biology of IL-7, a key lymphotrophin.* Cytokine Growth Factor Rev, 2005. **16**(4-5): p. 513-33.
45. DiSanto, J.P., et al., *Defective human interleukin 2 receptor gamma chain in an atypical X chromosome-linked severe combined immunodeficiency with peripheral T cells.* Proc Natl Acad Sci U S A, 1994. **91**(20): p. 9466-70.
46. Roberts, J.L., et al., *Janus kinase 3 (JAK3) deficiency: clinical, immunologic, and molecular analyses of 10 patients and outcomes of stem cell transplantation.* Blood, 2004. **103**(6): p. 2009-18.
47. Nosaka, T., et al., *Defective lymphoid development in mice lacking Jak3.* Science, 1995. **270**(5237): p. 800-2.
48. Peschon, J.J., et al., *Early lymphocyte expansion is severely impaired in interleukin 7 receptor-deficient mice.* J Exp Med, 1994. **180**(5): p. 1955-60.
49. Garcia-Peydro, M., V.G. de Yebenes, and M.L. Toribio, *Notch1 and IL-7 receptor interplay maintains proliferation of human thymic progenitors while suppressing non-T cell fates.* J Immunol, 2006. **177**(6): p. 3711-20.

50. Pallard, C., et al., *Distinct roles of the phosphatidylinositol 3-kinase and STAT5 pathways in IL-7-mediated development of human thymocyte precursors.* Immunity, 1999. **10**(5): p. 525-35.
51. Akashi, K., et al., *Bcl-2 rescues T lymphopoiesis in interleukin-7 receptor-deficient mice.* Cell, 1997. **89**(7): p. 1033-41.
52. Okamoto, Y., et al., *Effects of exogenous interleukin-7 on human thymus function.* Blood, 2002. **99**(8): p. 2851-8.
53. Durum, S.K., et al., *Interleukin 7 receptor control of T cell receptor gamma gene rearrangement: role of receptor-associated chains and locus accessibility.* J Exp Med, 1998. **188**(12): p. 2233-41.
54. van Tetering, G., et al., *Metalloprotease ADAM10 is required for Notch1 site 2 cleavage.* J Biol Chem, 2009. **284**(45): p. 31018-27.
55. Kopan, R. and M.X. Ilagan, *The canonical Notch signaling pathway: unfolding the activation mechanism.* Cell, 2009. **137**(2): p. 216-33.
56. De Smedt, M., et al., *Active form of Notch imposes T cell fate in human progenitor cells.* J Immunol, 2002. **169**(6): p. 3021-9.
57. Pui, J.C., et al., *Notch1 expression in early lymphopoiesis influences B versus T lineage determination.* Immunity, 1999. **11**(3): p. 299-308.
58. Radtke, F., et al., *Deficient T cell fate specification in mice with an induced inactivation of Notch1.* Immunity, 1999. **10**(5): p. 547-58.
59. Wilson, A., H.R. MacDonald, and F. Radtke, *Notch 1-deficient common lymphoid precursors adopt a B cell fate in the thymus.* J Exp Med, 2001. **194**(7): p. 1003-12.
60. Wolfer, A., et al., *Inactivation of Notch1 impairs VDJbeta rearrangement and allows pre-TCR-independent survival of early alpha beta Lineage Thymocytes.* Immunity, 2002. **16**(6): p. 869-79.
61. Washburn, T., et al., *Notch activity influences the alphabeta versus gammadelta T cell lineage decision.* Cell, 1997. **88**(6): p. 833-43.

62. Van de Walle, I., et al., *An early decrease in Notch activation is required for human TCR-alphabeta lineage differentiation at the expense of TCR-gammadelta T cells.* Blood, 2009. **113**(13): p. 2988-98.
63. McCune, J.M., et al., *The SCID-hu mouse: murine model for the analysis of human hematolymphoid differentiation and function.* Science, 1988. **241**(4873): p. 1632-9.
64. de Villartay, J.P., *V(D)J recombination deficiencies.* Adv Exp Med Biol, 2009. **650**: p. 46-58.
65. Galy, A., et al., *Precursors of CD3+CD4+CD8+ cells in the human thymus are defined by expression of CD34. Delineation of early events in human thymic development.* J Exp Med, 1993. **178**(2): p. 391-401.
66. Fisher, A.G., et al., *Human thymocyte development in mouse organ cultures.* Int Immunol, 1990. **2**(6): p. 571-8.
67. Schmitt, T.M. and J.C. Zuniga-Pflucker, *Induction of T cell development from hematopoietic progenitor cells by delta-like-1 in vitro.* Immunity, 2002. **17**(6): p. 749-56.
68. La Motte-Mohs, R.N., E. Herer, and J.C. Zuniga-Pflucker, *Induction of T-cell development from human cord blood hematopoietic stem cells by Delta-like 1 in vitro.* Blood, 2005. **105**(4): p. 1431-9.
69. Jaleco, A.C., et al., *Differential effects of Notch ligands Delta-1 and Jagged-1 in human lymphoid differentiation.* J Exp Med, 2001. **194**(7): p. 991-1002.
70. Mohtashami, M. and J.C. Zuniga-Pflucker, *Three-dimensional architecture of the thymus is required to maintain delta-like expression necessary for inducing T cell development.* J Immunol, 2006. **176**(2): p. 730-4.
71. Baron, R.L., et al., *Computed tomography of the normal thymus.* Radiology, 1982. **142**(1): p. 121-5.

72. McCune, J.M., et al., *High prevalence of thymic tissue in adults with human immunodeficiency virus-1 infection.* J Clin Invest, 1998. **101**(11): p. 2301-8.
73. Flores, K.G., et al., *Analysis of the human thymic perivascular space during aging.* J Clin Invest, 1999. **104**(8): p. 1031-9.
74. Douek, D.C., et al., *Changes in thymic function with age and during the treatment of HIV infection.* Nature, 1998. **396**(6712): p. 690-5.
75. Verschuren, M.C., et al., *PJA-BP expression and TCR delta deletion during human T cell differentiation.* Int Immunol, 1998. **10**(12): p. 1873-80.
76. Livak, F. and D.G. Schatz, *T-cell receptor alpha locus V(D)J recombination by-products are abundant in thymocytes and mature T cells.* Mol Cell Biol, 1996. **16**(2): p. 609-18.
77. Takeshita, S., M. Toda, and H. Yamagishi, *Excision products of the T cell receptor gene support a progressive rearrangement model of the alpha/delta locus.* EMBO J, 1989. **8**(11): p. 3261-70.
78. Arellano, M.V., et al., *Thymic function-related markers within the thymus and peripheral blood: Are they comparable?* J Clin Immunol, 2006. **26**(1): p. 96-100.
79. De Rosa, S.C., L.A. Herzenberg, and M. Roederer, *11-color, 13-parameter flow cytometry: identification of human naive T cells by phenotype, function, and T-cell receptor diversity.* Nat Med, 2001. **7**(2): p. 245-8.
80. Tough, D.F. and J. Sprent, *Turnover of naive- and memory-phenotype T cells.* J Exp Med, 1994. **179**(4): p. 1127-35.
81. Sempowski, G., et al., *Effect of thymectomy on human peripheral blood T cell pools in myasthenia gravis.* J Immunol, 2001. **166**(4): p. 2808-17.

82. Newman, P.J., et al., *PECAM-1 (CD31) cloning and relation to adhesion molecules of the immunoglobulin gene superfamily.* Science, 1990. **247**(4947): p. 1219-22.
83. Kimmig, S., et al., *Two subsets of naive T helper cells with distinct T cell receptor excision circle content in human adult peripheral blood.* J Exp Med, 2002. **195**(6): p. 789-94.
84. Albelda, S.M., et al., *EndoCAM: a novel endothelial cell-cell adhesion molecule.* J Cell Biol, 1990. **110**(4): p. 1227-37.
85. Tenca, C., et al., *Death of T cell precursors in the human thymus: a role for CD38.* Int Immunol, 2003. **15**(9): p. 1105-16.
86. Tanaka, Y., et al., *CD31 expressed on distinctive T cell subsets is a preferential amplifier of beta 1 integrin-mediated adhesion.* J Exp Med, 1992. **176**(1): p. 245-53.
87. Muller, W.A., et al., *PECAM-1 is required for transendothelial migration of leukocytes.* J Exp Med, 1993. **178**(2): p. 449-60.
88. Demeure, C.E., et al., *CD31 (PECAM-1) is a differentiation antigen lost during human CD4 T-cell maturation into Th1 or Th2 effector cells.* Immunology, 1996. **88**(1): p. 110-5.
89. Junge, S., et al., *Correlation between recent thymic emigrants and CD31+ (PECAM-1) CD4+ T cells in normal individuals during aging and in lymphopenic children.* Eur J Immunol, 2007. **37**(11): p. 3270-80.
90. Kilpatrick, R.D., et al., *Homeostasis of the naive CD4+ T cell compartment during aging.* J Immunol, 2008. **180**(3): p. 1499-507.
91. Hellerstein, M.K., et al., *Subpopulations of long-lived and short-lived T cells in advanced HIV-1 infection.* J Clin Invest, 2003. **112**(6): p. 956-66.
92. Tanchot, C., et al., *Differential requirements for survival and proliferation of CD8 naive or memory T cells.* Science, 1997. **276**(5321): p. 2057-62.

93. Nesic, D. and S. Vukmanovic, *MHC class I is required for peripheral accumulation of CD8+ thymic emigrants.* J Immunol, 1998. **160**(8): p. 3705-12.
94. Kirberg, J., A. Berns, and H. von Boehmer, *Peripheral T cell survival requires continual ligation of the T cell receptor to major histocompatibility complex-encoded molecules.* J Exp Med, 1997. **186**(8): p. 1269-75.
95. Labrecque, N., et al., *How much TCR does a T cell need?* Immunity, 2001. **15**(1): p. 71-82.
96. Martin, B., et al., *Self-recognition is crucial for maintaining the peripheral CD4+ T-cell pool in a nonlymphopenic environment.* Blood, 2006. **108**(1): p. 270-7.
97. Takada, K. and S.C. Jameson, *Self-class I MHC molecules support survival of naive CD8 T cells, but depress their functional sensitivity through regulation of CD8 expression levels.* J Exp Med, 2009. **206**(10): p. 2253-69.
98. von Boehmer, H. and K. Hafen, *The life span of naive alpha/beta T cells in secondary lymphoid organs.* J Exp Med, 1993. **177**(4): p. 891-6.
99. Moses, C.T., et al., *Competition for self ligands restrains homeostatic proliferation of naive CD4 T cells.* Proc Natl Acad Sci U S A, 2003. **100**(3): p. 1185-90.
100. Hao, Y., N. Legrand, and A.A. Freitas, *The clone size of peripheral CD8 T cells is regulated by TCR promiscuity.* J Exp Med, 2006. **203**(7): p. 1643-9.
101. Hataye, J., et al., *Naive and memory CD4+ T cell survival controlled by clonal abundance.* Science, 2006. **312**(5770): p. 114-6.
102. Hassan, J. and D.J. Reen, *IL-7 promotes the survival and maturation but not differentiation of human post-thymic CD4+ T cells.* Eur J Immunol, 1998. **28**(10): p. 3057-65.

103. Kondrack, R.M., et al., *Interleukin 7 regulates the survival and generation of memory CD4 cells.* J Exp Med, 2003. **198**(12): p. 1797-806.
104. Vivien, L., C. Benoist, and D. Mathis, *T lymphocytes need IL-7 but not IL-4 or IL-6 to survive in vivo.* Int Immunol, 2001. **13**(6): p. 763-8.
105. Tan, J.T., et al., *IL-7 is critical for homeostatic proliferation and survival of naive T cells.* Proc Natl Acad Sci U S A, 2001. **98**(15): p. 8732-7.
106. Yao, Z., et al., *Stat5a/b are essential for normal lymphoid development and differentiation.* Proc Natl Acad Sci U S A, 2006. **103**(4): p. 1000-5.
107. Pellegrini, M., et al., *Loss of Bim increases T cell production and function in interleukin 7 receptor-deficient mice.* J Exp Med, 2004. **200**(9): p. 1189-95.
108. Park, J.H., et al., *Suppression of IL7Ralpha transcription by IL-7 and other prosurvival cytokines: a novel mechanism for maximizing IL-7-dependent T cell survival.* Immunity, 2004. **21**(2): p. 289-302.
109. Kittipatarin, C. and A.R. Khaled, *Interlinking interleukin-7.* Cytokine, 2007. **39**(1): p. 75-83.
110. Burgering, B.M., *A brief introduction to FOXOlogy.* Oncogene, 2008. **27**(16): p. 2258-62.
111. Kerdiles, Y.M., et al., *Foxo1 links homing and survival of naive T cells by regulating L-selectin, CCR7 and interleukin 7 receptor.* Nat Immunol, 2009. **10**(2): p. 176-84.
112. Link, A., et al., *Fibroblastic reticular cells in lymph nodes regulate the homeostasis of naive T cells.* Nat Immunol, 2007. **8**(11): p. 1255-65.
113. Tanel, A., et al., *Cellular and molecular mechanisms of memory T-cell survival.* Expert Rev Vaccines, 2009. **8**(3): p. 299-312.

114. Sallusto, F., J. Geginat, and A. Lanzavecchia, *Central memory and effector memory T cell subsets: function, generation, and maintenance.* Annu Rev Immunol, 2004. **22**: p. 745-63.
115. Swain, S.L., H. Hu, and G. Huston, *Class II-independent generation of CD4 memory T cells from effectors.* Science, 1999. **286**(5443): p. 1381-3.
116. Murali-Krishna, K., et al., *Persistence of memory CD8 T cells in MHC class I-deficient mice.* Science, 1999. **286**(5443): p. 1377-81.
117. Judge, A.D., et al., *Interleukin 15 controls both proliferation and survival of a subset of memory-phenotype CD8(+) T cells.* J Exp Med, 2002. **196**(7): p. 935-46.
118. Kieper, W.C., et al., *Overexpression of interleukin (IL)-7 leads to IL-15-independent generation of memory phenotype CD8+ T cells.* J Exp Med, 2002. **195**(12): p. 1533-9.
119. Lenz, D.C., et al., *IL-7 regulates basal homeostatic proliferation of antiviral CD4+T cell memory.* Proc Natl Acad Sci U S A, 2004. **101**(25): p. 9357-62.
120. Purton, J.F., et al., *Antiviral CD4+ memory T cells are IL-15 dependent.* J Exp Med, 2007. **204**(4): p. 951-61.
121. Hou, S., et al., *Virus-specific CD8+ T-cell memory determined by clonal burst size.* Nature, 1994. **369**(6482): p. 652-4.
122. Tanchot, C., et al., *Conversion of naive T cells to a memory-like phenotype in lymphopenic hosts is not related to a homeostatic mechanism that fills the peripheral naive T cell pool.* J Immunol, 2002. **168**(10): p. 5042-6.
123. Min, B., et al., *Neonates support lymphopenia-induced proliferation.* Immunity, 2003. **18**(1): p. 131-40.

124. Ge, Q., et al., *Different contributions of thymopoiesis and homeostasis-driven proliferation to the reconstitution of naive and memory T cell compartments.* Proc Natl Acad Sci U S A, 2002. **99**(5): p. 2989-94.
125. Ernst, B., et al., *The peptide ligands mediating positive selection in the thymus control T cell survival and homeostatic proliferation in the periphery.* Immunity, 1999. **11**(2): p. 173-81.
126. Kieper, W.C., J.T. Burghardt, and C.D. Surh, *A role for TCR affinity in regulating naive T cell homeostasis.* J Immunol, 2004. **172**(1): p. 40-4.
127. Workman, C.J. and D.A. Vignali, *Negative regulation of T cell homeostasis by lymphocyte activation gene-3 (CD223).* J Immunol, 2005. **174**(2): p. 688-95.
128. Krieg, C., et al., *B and T lymphocyte attenuator regulates CD8+ T cell-intrinsic homeostasis and memory cell generation.* Nat Immunol, 2007. **8**(2): p. 162-71.
129. Posevitz, V., et al., *Regulation of T cell homeostasis by the transmembrane adaptor protein SIT.* J Immunol, 2008. **180**(3): p. 1634-42.
130. Cho, B.K., et al., *Homeostasis-stimulated proliferation drives naive T cells to differentiate directly into memory T cells.* J Exp Med, 2000. **192**(4): p. 549-56.
131. Kittipatarin, C., et al., *Cell cycling through Cdc25A: transducer of cytokine proliferative signals.* Cell Cycle, 2006. **5**(9): p. 907-12.
132. Fry, T.J., et al., *IL-7 therapy dramatically alters peripheral T-cell homeostasis in normal and SIV-infected nonhuman primates.* Blood, 2003. **101**(6): p. 2294-9.
133. Swainson, L., et al., *IL-7-induced proliferation of recent thymic emigrants requires activation of the PI3K pathway.* Blood, 2007. **109**(3): p. 1034-42.

134. Li, W.Q., et al., *IL-7 promotes T cell proliferation through destabilization of p27Kip1.* J Exp Med, 2006. **203**(3): p. 573-82.
135. Sherr, C.J. and J.M. Roberts, *CDK inhibitors: positive and negative regulators of G1-phase progression.* Genes Dev, 1999. **13**(12): p. 1501-12.
136. Le Campion, A., et al., *Naive T cells proliferate strongly in neonatal mice in response to self-peptide/self-MHC complexes.* Proc Natl Acad Sci U S A, 2002. **99**(7): p. 4538-43.
137. Tanchot, C. and B. Rocha, *The peripheral T cell repertoire: independent homeostatic regulation of virgin and activated CD8+ T cell pools.* Eur J Immunol, 1995. **25**(8): p. 2127-36.
138. Berzins, S.P., et al., *A central role for thymic emigrants in peripheral T cell homeostasis.* Proc Natl Acad Sci U S A, 1999. **96**(17): p. 9787-91.
139. Olkinuora, H., et al., *T cell regeneration in pediatric allogeneic stem cell transplantation.* Bone Marrow Transplant, 2007. **39**(3): p. 149-56.
140. Hakim, F.T., et al., *Age-dependent incidence, time course, and consequences of thymic renewal in adults.* J Clin Invest, 2005. **115**(4): p. 930-9.
141. Mackall, C.L., et al., *Age, thymopoiesis, and CD4+ T-lymphocyte regeneration after intensive chemotherapy.* N Engl J Med, 1995. **332**(3): p. 143-9.
142. Gabor, M.J., R. Scollay, and D.I. Godfrey, *Thymic T cell export is not influenced by the peripheral T cell pool.* Eur J Immunol, 1997. **27**(11): p. 2986-93.
143. Doitsh, G., et al., *Abortive HIV infection mediates CD4 T cell depletion and inflammation in human lymphoid tissue.* Cell, 2010. **143**(5): p. 789-801.

144. Zack, J.A., et al., *HIV-1 entry into quiescent primary lymphocytes: molecular analysis reveals a labile, latent viral structure.* Cell, 1990. **61**(2): p. 213-22.
145. Miller, C.J., et al., *Propagation and dissemination of infection after vaginal transmission of simian immunodeficiency virus.* J Virol, 2005. **79**(14): p. 9217-27.
146. McMichael, A.J., et al., *The immune response during acute HIV-1 infection: clues for vaccine development.* Nat Rev Immunol, 2010. **10**(1): p. 11-23.
147. Rosok, B.I., et al., *Reduced CD4 cell counts in blood do not reflect CD4 cell depletion in tonsillar tissue in asymptomatic HIV-1 infection.* AIDS, 1996. **10**(10): p. F35-8.
148. Brenchley, J.M., et al., *CD4+ T cell depletion during all stages of HIV disease occurs predominantly in the gastrointestinal tract.* J Exp Med, 2004. **200**(6): p. 749-59.
149. Mattapallil, J.J., et al., *Massive infection and loss of memory CD4+ T cells in multiple tissues during acute SIV infection.* Nature, 2005. **434**(7037): p. 1093-7.
150. Mellors, J.W., et al., *Prognostic value of HIV-1 RNA, CD4 cell count, and CD4 Cell count slope for progression to AIDS and death in untreated HIV-1 infection.* JAMA, 2007. **297**(21): p. 2349-50.
151. Goonetilleke, N., et al., *The first T cell response to transmitted/founder virus contributes to the control of acute viremia in HIV-1 infection.* J Exp Med, 2009. **206**(6): p. 1253-72.
152. Streeck, H., et al., *Human immunodeficiency virus type 1-specific CD8+ T-cell responses during primary infection are major determinants of the viral set point and loss of CD4+ T cells.* J Virol, 2009. **83**(15): p. 7641-8.

153. Tomaras, G.D., et al., *Initial B-cell responses to transmitted human immunodeficiency virus type 1: virion-binding immunoglobulin M (IgM) and IgG antibodies followed by plasma anti-gp41 antibodies with ineffective control of initial viremia.* J Virol, 2008. **82**(24): p. 12449-63.
154. Streeck, H. and D.F. Nixon, *T cell immunity in acute HIV-1 infection.* J Infect Dis, 2010. **202 Suppl 2**: p. S302-8.
155. Kemball, C.C., et al., *The antiviral CD8+ T cell response is differentially dependent on CD4+ T cell help over the course of persistent infection.* J Immunol, 2007. **179**(2): p. 1113-21.
156. Sun, J.C., M.A. Williams, and M.J. Bevan, *CD4+ T cells are required for the maintenance, not programming, of memory CD8+ T cells after acute infection.* Nat Immunol, 2004. **5**(9): p. 927-33.
157. Gorochov, G., et al., *Perturbation of CD4+ and CD8+ T-cell repertoires during progression to AIDS and regulation of the CD4+ repertoire during antiviral therapy.* Nat Med, 1998. **4**(2): p. 215-21.
158. Joshi, V.V., J.M. Oleske, and E.M. Connor, *Morphologic findings in children with acquired immune deficiency syndrome: pathogenesis and clinical implications.* Pediatr Pathol, 1990. **10**(1-2): p. 155-65.
159. Grody, W.W., S. Fligiel, and F. Naeim, *Thymus involution in the acquired immunodeficiency syndrome.* Am J Clin Pathol, 1985. **84**(1): p. 85-95.
160. Savino, W., et al., *Thymic epithelium in AIDS. An immunohistologic study.* Am J Pathol, 1986. **122**(2): p. 302-7.
161. Bonyhadi, M.L., et al., *HIV induces thymus depletion in vivo.* Nature, 1993. **363**(6431): p. 728-32.
162. Douek, D.C., et al., *Evidence for increased T cell turnover and decreased thymic output in HIV infection.* J Immunol, 2001. **167**(11): p. 6663-8.

163. Ye, P. and D.E. Kirschner, *Reevaluation of T cell receptor excision circles as a measure of human recent thymic emigrants.* J Immunol, 2002. **168**(10): p. 4968-79.
164. Hays, E.F., et al., *In vitro studies of HIV-1 expression in thymocytes from infants and children.* AIDS, 1992. **6**(3): p. 265-72.
165. Tremblay, M., et al., *Infection of human thymic lymphocytes by HIV-1.* J Acquir Immune Defic Syndr, 1990. **3**(4): p. 356-60.
166. Koka, P.S., et al., *HIV type 1 infection alters cytokine mRNA expression in thymus.* AIDS Res Hum Retroviruses, 2003. **19**(1): p. 1-12.
167. Bandera, A., et al., *CD4+ T cell depletion, immune activation and increased production of regulatory T cells in the thymus of HIV-infected individuals.* PLoS One, 2010. **5**(5): p. e10788.
168. Shiow, L.R., et al., *CD69 acts downstream of interferon-alpha/beta to inhibit S1P1 and lymphocyte egress from lymphoid organs.* Nature, 2006. **440**(7083): p. 540-4.
169. Perelson, A.S., et al., *Decay characteristics of HIV-1-infected compartments during combination therapy.* Nature, 1997. **387**(6629): p. 188-91.
170. Autran, B., et al., *Positive effects of combined antiretroviral therapy on CD4+ T cell homeostasis and function in advanced HIV disease.* Science, 1997. **277**(5322): p. 112-6.
171. Haase, A.T., *Population biology of HIV-1 infection: viral and CD4+ T cell demographics and dynamics in lymphatic tissues.* Annu Rev Immunol, 1999. **17**: p. 625-56.
172. Mocroft, A., et al., *Normalisation of CD4 counts in patients with HIV-1 infection and maximum virological suppression who are taking combination antiretroviral therapy: an observational cohort study.* Lancet, 2007. **370**(9585): p. 407-13.

173. Kaufmann, G.R., et al., *CD4 T-lymphocyte recovery in individuals with advanced HIV-1 infection receiving potent antiretroviral therapy for 4 years: the Swiss HIV Cohort Study.* Arch Intern Med, 2003. **163**(18): p. 2187-95.
174. Smith, K.Y., et al., *Thymic size and lymphocyte restoration in patients with human immunodeficiency virus infection after 48 weeks of zidovudine, lamivudine, and ritonavir therapy.* J Infect Dis, 2000. **181**(1): p. 141-7.
175. Schuitemaker, H., et al., *Biological phenotype of human immunodeficiency virus type 1 clones at different stages of infection: progression of disease is associated with a shift from monocytotropic to T-cell-tropic virus population.* J Virol, 1992. **66**(3): p. 1354-60.
176. Kunkel, E.J., et al., *Expression of the chemokine receptors CCR4, CCR5, and CXCR3 by human tissue-infiltrating lymphocytes.* Am J Pathol, 2002. **160**(1): p. 347-55.
177. Picker, L.J., et al., *Insufficient production and tissue delivery of CD4+ memory T cells in rapidly progressive simian immunodeficiency virus infection.* J Exp Med, 2004. **200**(10): p. 1299-314.
178. Blaak, H., et al., *In vivo HIV-1 infection of CD45RA(+)CD4(+) T cells is established primarily by syncytium-inducing variants and correlates with the rate of CD4(+) T cell decline.* Proc Natl Acad Sci U S A, 2000. **97**(3): p. 1269-74.
179. Hazenberg, M.D., et al., *Depletion of naive CD4 T cells by CXCR4-using HIV-1 variants occurs mainly through increased T-cell death and activation.* AIDS, 2003. **17**(10): p. 1419-24.

180. Delobel, P., et al., *Naive T-cell depletion related to infection by X4 human immunodeficiency virus type 1 in poor immunological responders to highly active antiretroviral therapy.* J Virol, 2006. **80**(20): p. 10229-36.
181. Hazenberg, M.D., et al., *Persistent immune activation in HIV-1 infection is associated with progression to AIDS.* AIDS, 2003. **17**(13): p. 1881-8.
182. Mohri, H., et al., *Increased turnover of T lymphocytes in HIV-1 infection and its reduction by antiretroviral therapy.* J Exp Med, 2001. **194**(9): p. 1277-87.
183. Sachsenberg, N., et al., *Turnover of CD4+ and CD8+ T lymphocytes in HIV-1 infection as measured by Ki-67 antigen.* J Exp Med, 1998. **187**(8): p. 1295-303.
184. Sieg, S.F., et al., *Peripheral S-phase T cells in HIV disease have a central memory phenotype and rarely have evidence of recent T cell receptor engagement.* J Infect Dis, 2005. **192**(1): p. 62-70.
185. Lempicki, R.A., et al., *Impact of HIV-1 infection and highly active antiretroviral therapy on the kinetics of CD4+ and CD8+ T cell turnover in HIV-infected patients.* Proc Natl Acad Sci U S A, 2000. **97**(25): p. 13778-83.
186. Kovacs, J.A., et al., *Identification of dynamically distinct subpopulations of T lymphocytes that are differentially affected by HIV.* J Exp Med, 2001. **194**(12): p. 1731-41.
187. Silvestri, G., et al., *Nonpathogenic SIV infection of sooty mangabeys is characterized by limited bystander immunopathology despite chronic high-level viremia.* Immunity, 2003. **18**(3): p. 441-52.

188. Giorgi, J.V., et al., *Shorter survival in advanced human immunodeficiency virus type 1 infection is more closely associated with T lymphocyte activation than with plasma virus burden or virus chemokine coreceptor usage.* J Infect Dis, 1999. **179**(4): p. 859-70.
189. Hazenberg, M.D., et al., *T cell depletion in HIV-1 infection: how CD4+ T cells go out of stock.* Nat Immunol, 2000. **1**(4): p. 285-9.
190. Sieg, S.F., D.A. Bazdar, and M.M. Lederman, *S-phase entry leads to cell death in circulating T cells from HIV-infected persons.* J Leukoc Biol, 2008. **83**(6): p. 1382-7.
191. Lewin, S.R., et al., *Dynamics of T cells and TCR excision circles differ after treatment of acute and chronic HIV infection.* J Immunol, 2002. **169**(8): p. 4657-66.
192. Petrovas, C., et al., *Differential association of programmed death-1 and CD57 with ex vivo survival of CD8+ T cells in HIV infection.* J Immunol, 2009. **183**(2): p. 1120-32.
193. Chun, T.W., et al., *Quantification of latent tissue reservoirs and total body viral load in HIV-1 infection.* Nature, 1997. **387**(6629): p. 183-8.
194. Finkel, T.H., et al., *Apoptosis occurs predominantly in bystander cells and not in productively infected cells of HIV- and SIV-infected lymph nodes.* Nat Med, 1995. **1**(2): p. 129-34.
195. Ribeiro, R.M., et al., *In vivo dynamics of T cell activation, proliferation, and death in HIV-1 infection: why are CD4+ but not CD8+ T cells depleted?* Proc Natl Acad Sci U S A, 2002. **99**(24): p. 15572-7.
196. Catalfamo, M., et al., *HIV infection-associated immune activation occurs by two distinct pathways that differentially affect CD4 and CD8 T cells.* Proc Natl Acad Sci U S A, 2008. **105**(50): p. 19851-6.

197. Albuquerque, A.S., et al., *Rate of increase in circulating IL-7 and loss of IL-7Ralpha expression differ in HIV-1 and HIV-2 infections: two lymphopenic diseases with similar hyperimmune activation but distinct outcomes.* J Immunol, 2007. **178**(5): p. 3252-9.
198. Sousa, A.E., et al., *CD4 T cell depletion is linked directly to immune activation in the pathogenesis of HIV-1 and HIV-2 but only indirectly to the viral load.* J Immunol, 2002. **169**(6): p. 3400-6.
199. Doisne, J.M., et al., *CD8+ T cells specific for EBV, cytomegalovirus, and influenza virus are activated during primary HIV infection.* J Immunol, 2004. **173**(4): p. 2410-8.
200. Tough, D.F., P. Borrow, and J. Sprent, *Induction of bystander T cell proliferation by viruses and type I interferon in vivo.* Science, 1996. **272**(5270): p. 1947-50.
201. Rodriguez, B., et al., *Interferon-alpha differentially rescues CD4 and CD8 T cells from apoptosis in HIV infection.* AIDS, 2006. **20**(10): p. 1379-89.
202. Sedaghat, A.R., et al., *Chronic CD4+ T-cell activation and depletion in human immunodeficiency virus type 1 infection: type I interferon-mediated disruption of T-cell dynamics.* J Virol, 2008. **82**(4): p. 1870-83.
203. Harris, L.D., et al., *Downregulation of robust acute type I interferon responses distinguishes nonpathogenic simian immunodeficiency virus (SIV) infection of natural hosts from pathogenic SIV infection of rhesus macaques.* J Virol, 2010. **84**(15): p. 7886-91.
204. Herbeuval, J.P., et al., *Differential expression of IFN-alpha and TRAIL/DR5 in lymphoid tissue of progressor versus nonprogressor HIV-1-infected patients.* Proc Natl Acad Sci U S A, 2006. **103**(18): p. 7000-5.

205. Brenchley, J.M., et al., *Microbial translocation is a cause of systemic immune activation in chronic HIV infection.* Nat Med, 2006. **12**(12): p. 1365-71.
206. Fry, T.J., et al., *A potential role for interleukin-7 in T-cell homeostasis.* Blood, 2001. **97**(10): p. 2983-90.
207. Murali-Krishna, K. and R. Ahmed, *Cutting edge: naive T cells masquerading as memory cells.* J Immunol, 2000. **165**(4): p. 1733-7.
208. Bazdar, D.A. and S.F. Sieg, *Interleukin-7 enhances proliferation responses to T-cell receptor stimulation in naive CD4+ T cells from human immunodeficiency virus-infected persons.* J Virol, 2007. **81**(22): p. 12670-4.
209. Boehme, S.A. and M.J. Lenardo, *Propriocidal apoptosis of mature T lymphocytes occurs at S phase of the cell cycle.* Eur J Immunol, 1993. **23**(7): p. 1552-60.
210. Endrizzi, B.T. and S.C. Jameson, *Differential role for IL-7 in inducing lung Kruppel-like factor (Kruppel-like factor 2) expression by naive versus activated T cells.* Int Immunol, 2003. **15**(11): p. 1341-8.
211. Webb, L.M., B.M. Foxwell, and M. Feldmann, *Putative role for interleukin-7 in the maintenance of the recirculating naive CD4+ T-cell pool.* Immunology, 1999. **98**(3): p. 400-5.
212. Juffroy, O., et al., *Dual mechanism of impairment of interleukin-7 (IL-7) responses in human immunodeficiency virus infection: decreased IL-7 binding and abnormal activation of the JAK/STAT5 pathway.* J Virol, 2010. **84**(1): p. 96-108.
213. Colle, J.H., et al., *The correlation between levels of IL-7Ralpha expression and responsiveness to IL-7 is lost in CD4 lymphocytes from HIV-infected patients.* AIDS, 2007. **21**(1): p. 101-3.

214. Napolitano, L.A., et al., *Increased production of IL-7 accompanies HIV-1-mediated T-cell depletion: implications for T-cell homeostasis.* Nat Med, 2001. **7**(1): p. 73-9.
215. Bolotin, E., et al., *Serum levels of IL-7 in bone marrow transplant recipients: relationship to clinical characteristics and lymphocyte count.* Bone Marrow Transplant, 1999. **23**(8): p. 783-8.
216. Benito, J.M., et al., *Down-regulation of interleukin-7 receptor (CD127) in HIV infection is associated with T cell activation and is a main factor influencing restoration of CD4(+) cells after antiretroviral therapy.* J Infect Dis, 2008. **198**(10): p. 1466-73.
217. Rethi, B., et al., *Loss of IL-7Ralpha is associated with CD4 T-cell depletion, high interleukin-7 levels and CD28 down-regulation in HIV infected patients.* AIDS, 2005. **19**(18): p. 2077-86.
218. Resino, S., et al., *Homeostatic role of IL-7 in HIV-1 infected children on HAART: association with immunological and virological parameters.* Acta Paediatr, 2005. **94**(2): p. 170-7.
219. Albuquerque, A.S., et al., *Low CD4 T-cell counts despite low levels of circulating HIV: insights from the comparison of HIV-1 infected patients with a discordant response to antiretroviral therapy to patients with untreated advanced HIV-2 disease.* Clin Immunol, 2007. **125**(1): p. 67-75.
220. Muthukumar, A., et al., *Elevated interleukin-7 levels not sufficient to maintain T-cell homeostasis during simian immunodeficiency virus-induced disease progression.* Blood, 2004. **103**(3): p. 973-9.
221. Ryan, D.H. and J. Tang, *Regulation of human B cell lymphopoiesis by adhesion molecules and cytokines.* Leuk Lymphoma, 1995. **17**(5-6): p. 375-89.
222. Tang, J., et al., *TGF-beta down-regulates stromal IL-7 secretion and inhibits proliferation of human B cell precursors.* J Immunol, 1997. **159**(1): p. 117-25.

223. Bazdar, D.A., M. Kalinowska, and S.F. Sieg, *Interleukin-7 receptor signaling is deficient in CD4+ T cells from HIV-infected persons and is inversely associated with aging.* J Infect Dis, 2009. **199**(7): p. 1019-28.
224. Sasson, S.C., et al., *Increased plasma interleukin-7 level correlates with decreased CD127 and Increased CD132 extracellular expression on T cell subsets in patients with HIV-1 infection.* J Infect Dis, 2006. **193**(4): p. 505-14.
225. Mehandru, S., et al., *Primary HIV-1 infection is associated with preferential depletion of CD4+ T lymphocytes from effector sites in the gastrointestinal tract.* J Exp Med, 2004. **200**(6): p. 761-70.
226. Sereti, I., et al., *IL-7 administration drives T cell-cycle entry and expansion in HIV-1 infection.* Blood, 2009. **113**(25): p. 6304-14.
227. Mazzucchelli, R. and S.K. Durum, *Interleukin-7 receptor expression: intelligent design.* Nat Rev Immunol, 2007. **7**(2): p. 144-54.
228. Faller, E.M., et al., *Soluble HIV Tat protein removes the IL-7 receptor alpha-chain from the surface of resting CD8 T cells and targets it for degradation.* J Immunol, 2010. **185**(5): p. 2854-66.
229. Fluur, C., et al., *Relationship between serum IL-7 concentrations and lymphopenia upon different levels of HIV immune control.* AIDS, 2007. **21**(8): p. 1048-50.
230. Colle, J.H., et al., *Regulatory dysfunction of the interleukin-7 receptor in CD4 and CD8 lymphocytes from HIV-infected patients--effects of antiretroviral therapy.* J Acquir Immune Defic Syndr, 2006. **42**(3): p. 277-85.
231. Hennighausen, L. and G.W. Robinson, *Interpretation of cytokine signaling through the transcription factors STAT5A and STAT5B.* Genes Dev, 2008. **22**(6): p. 711-21.

232. Schweneker, M., et al., *HIV-induced changes in T cell signaling pathways.* J Immunol, 2008. **180**(10): p. 6490-500.
233. Shuai, K. and B. Liu, *Regulation of gene-activation pathways by PIAS proteins in the immune system.* Nat Rev Immunol, 2005. **5**(8): p. 593-605.
234. Ungureanu, D. and O. Silvennoinen, *SLIM trims STATs: ubiquitin E3 ligases provide insights for specificity in the regulation of cytokine signaling.* Sci STKE, 2005. **2005**(304): p. pe49.
235. Crawley, A.M., S. Faucher, and J.B. Angel, *Soluble IL-7R alpha (sCD127) inhibits IL-7 activity and is increased in HIV infection.* J Immunol, 2010. **184**(9): p. 4679-87.
236. Ruiz-Mateos, E., et al., *Endogenous IL-7 is associated with increased thymic volume in adult HIV-infected patients under highly active antiretroviral therapy.* AIDS, 2003. **17**(7): p. 947-54.
237. Beq, S., et al., *HIV infection: pre-highly active antiretroviral therapy IL-7 plasma levels correlate with long-term CD4 cell count increase after treatment.* AIDS, 2004. **18**(3): p. 563-5.
238. Roberts, L., et al., *Plasma cytokine levels during acute HIV-1 infection predict HIV disease progression.* AIDS, 2010. **24**(6): p. 819-31.
239. Fluur, C., et al., *Potential role for IL-7 in Fas-mediated T cell apoptosis during HIV infection.* J Immunol, 2007. **178**(8): p. 5340-50.
240. Wajant, H., *The Fas signaling pathway: more than a paradigm.* Science, 2002. **296**(5573): p. 1635-6.
241. Dockrell, D.H., *The multiple roles of Fas ligand in the pathogenesis of infectious diseases.* Clin Microbiol Infect, 2003. **9**(8): p. 766-79.
242. Lelievre, J.D., et al., *Interleukin 7 increases human immunodeficiency virus type 1 LAI-mediated Fas-induced T-cell death.* J Virol, 2005. **79**(5): p. 3195-9.

243. Smithgall, M.D., et al., *IL-7 up-regulates HIV-1 replication in naturally infected peripheral blood mononuclear cells.* J Immunol, 1996. **156**(6): p. 2324-30.

244. Chene, L., et al., *Thymocyte-thymic epithelial cell interaction leads to high-level replication of human immunodeficiency virus exclusively in mature CD4(+) CD8(-) CD3(+) thymocytes: a critical role for tumor necrosis factor and interleukin-7.* J Virol, 1999. **73**(9): p. 7533-42.

245. Managlia, E.Z., A. Landay, and L. Al-Harthi, *Interleukin-7 induces HIV replication in primary naive T cells through a nuclear factor of activated T cell (NFAT)-dependent pathway.* Virology, 2006. **350**(2): p. 443-52.

246. Schmitt, N., et al., *Positive regulation of CXCR4 expression and signaling by interleukin-7 in CD4+ mature thymocytes correlates with their capacity to favor human immunodeficiency X4 virus replication.* J Virol, 2003. **77**(10): p. 5784-93.

247. Steffens, C.M., et al., *Interleukin-7-treated naive T cells can be productively infected by T-cell-adapted and primary isolates of human immunodeficiency virus 1.* Blood, 2002. **99**(9): p. 3310-8.

248. Jourdan, P., et al., *Cytokines and cell surface molecules independently induce CXCR4 expression on CD4+ CCR7+ human memory T cells.* J Immunol, 2000. **165**(2): p. 716-24.

249. Walker, B.D., *Elite control of HIV Infection: implications for vaccines and treatment.* Top HIV Med, 2007. **15**(4): p. 134-6.

250. van Rij, R.P., et al., *Early viral load and CD4+ T cell count, but not percentage of CCR5+ or CXCR4+ CD4+ T cells, are associated with R5-to-X4 HIV type 1 virus evolution.* AIDS Res Hum Retroviruses, 2003. **19**(5): p. 389-98.

251. Zamarchi, R., et al., *Expression and functional activity of CXCR-4 and CCR-5 chemokine receptors in human thymocytes.* Clin Exp Immunol, 2002. **127**(2): p. 321-30.
252. Schmitt, N., et al., *Differential susceptibility of human thymic dendritic cell subsets to X4 and R5 HIV-1 infection.* AIDS, 2006. **20**(4): p. 533-42.
253. Stanley, S.K., et al., *Human immunodeficiency virus infection of the human thymus and disruption of the thymic microenvironment in the SCID-hu mouse.* J Exp Med, 1993. **178**(4): p. 1151-63.
254. Keir, M.E., et al., *IFN-alpha secretion by type 2 predendritic cells up-regulates MHC class I in the HIV-1-infected thymus.* J Immunol, 2002. **168**(1): p. 325-31.
255. Baron, M.L., et al., *TLR Ligand-Induced Type I IFNs Affect Thymopoiesis.* J Immunol, 2008. **180**(11): p. 7134-46.
256. Demoulins, T., et al., *Reversible blockade of thymic output: an inherent part of TLR ligand-mediated immune response.* J Immunol, 2008. **181**(10): p. 6757-69.
257. Su, D.M., et al., *Interferons alpha/beta inhibit IL-7-induced proliferation of CD4- CD8- CD3- CD44+ CD25+ thymocytes, but do not inhibit that of CD4- CD8- CD3- CD44- CD25- thymocytes.* Immunology, 1997. **90**(4): p. 543-9.
258. Aiuti, F. and L. Mezzaroma, *Failure to reconstitute CD4+T-cells despite suppression of HIV replication under HAART.* Aids Reviews, 2006. **8**(2): p. 88-97.
259. Lecuroux, C., et al., *Identification of a particular HIV-specific CD8+ T-cell subset with a CD27+ CD45RO-/RA+ phenotype and memory characteristics after initiation of HAART during acute primary HIV infection.* Blood, 2009. **113**(14): p. 3209-17.

260. Teixeira, L., et al., *Poor CD4 T cell restoration after suppression of HIV-1 replication may reflect lower thymic function.* AIDS, 2001. **15**(14): p. 1749-56.
261. Marziali, M., et al., *T-cell homeostasis alteration in HIV-1 infected subjects with low CD4 T-cell count despite undetectable virus load during HAART.* AIDS, 2006. **20**(16): p. 2033-41.
262. Mussini, C., et al., *Features of 'CD4-exploders', HIV-positive patients with an optimal immune reconstitution after potent antiretroviral therapy.* AIDS, 2002. **16**(12): p. 1609-16.
263. Bai, F., et al., *Reduced CD127 expression on peripheral CD4+ T cells impairs immunological recovery in course of suppressive highly active antiretroviral therapy.* AIDS, 2010. **24**(16): p. 2590-3.
264. Chiappini, E., et al., *Interleukin-7 and immunologic failure despite treatment with highly active antiretroviral therapy in children perinatally infected with HIV-1.* J Acquir Immune Defic Syndr, 2003. **33**(5): p. 601-4.
265. Darcissac, E.C., et al., *Variations in serum IL-7 and 90K/Mac-2 binding protein (Mac-2 BP) levels analysed in cohorts of HIV-1 patients and correlated with clinical changes following antiretroviral therapy.* Clin Exp Immunol, 2001. **126**(2): p. 287-94.
266. Marchetti, G., et al., *Comparative analysis of T-cell turnover and homeostatic parameters in HIV-infected patients with discordant immune-virological responses to HAART.* AIDS, 2006. **20**(13): p. 1727-36.
267. Camargo, J.F., et al., *Responsiveness of T cells to interleukin-7 is associated with higher CD4+ T cell counts in HIV-1-positive individuals with highly active antiretroviral therapy-induced viral load suppression.* J Infect Dis, 2009. **199**(12): p. 1872-82.

268. Correa, R., S. Resino, and M.A. Munoz-Fernandez, *Increased interleukin-7 plasma levels are associated with recovery of CD4+ T cells in HIV-infected children.* J Clin Immunol, 2003. **23**(5): p. 401-6.
269. McCune, J.M., *Thymic function in HIV-1 disease.* Semin Immunol, 1997. **9**(6): p. 397-404.
270. Beq, S., et al., *IL-7 induces immunological improvement in SIV-infected rhesus macaques under antiviral therapy.* J Immunol, 2006. **176**(2): p. 914-22.
271. Levy, Y., et al., *Enhanced T cell recovery in HIV-1-infected adults through IL-7 treatment.* J Clin Invest, 2009. **119**(4): p. 997-1007.
272. Sportes, C., et al., *Administration of rhIL-7 in humans increases in vivo TCR repertoire diversity by preferential expansion of naive T cell subsets.* J Exp Med, 2008. **205**(7): p. 1701-14.
273. Parker, R., et al., *Interleukin-7 treatment counteracts IFN{alpha} therapy-induced lymphopenia and stimulates SIV-specific CTL responses in SIV-infected rhesus macaques.* Blood, 2010.

APPENDIX A: SUPPLEMENTARY FIGURES

Figure S1

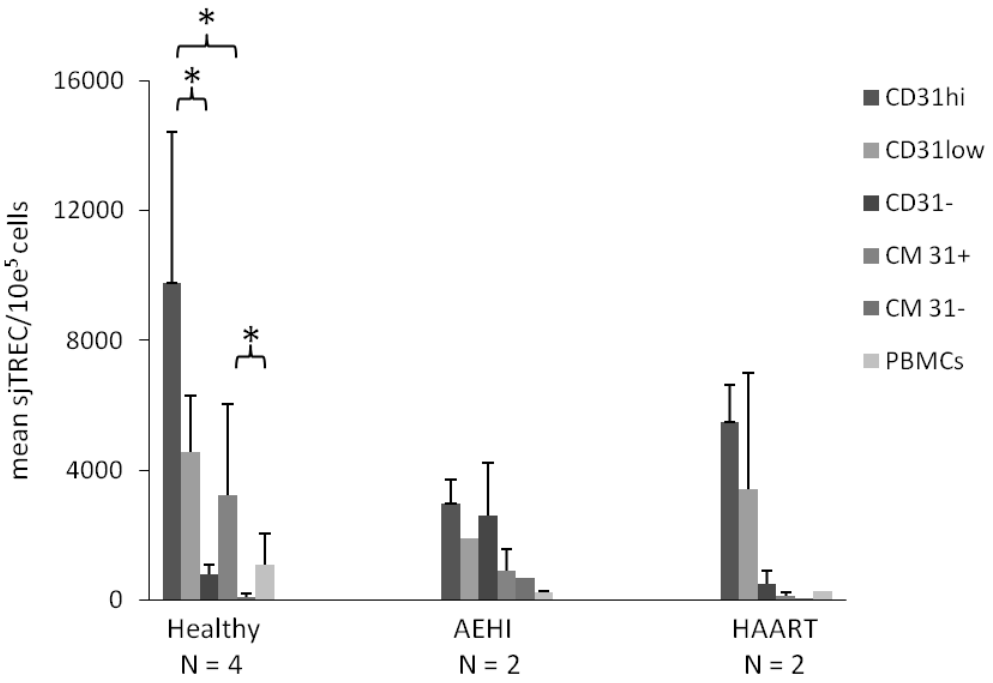

Figure S1. Detection of sjTRECs within CD31$^+$ T_{CM} CD4 T cells. sjTRECs were quantified in sorted naive (RTE, CD31^{low}, and CD31$^-$) and T_{CM} (CD31$^+$ and CD31$^-$) subsets as well as in total PBMCs from healthy controls, HIV-infected individuals as well as HAART-treated individuals. * $P < .05$.

Figure S2

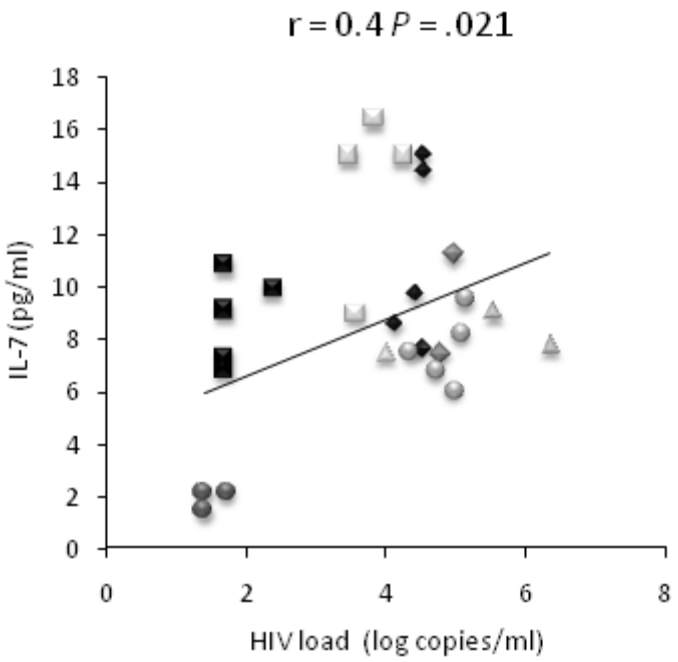

Figure S2. High levels of IL-7 during untreated HIV infection are positively associated with viral load. Correlation between levels of IL-7 and viral load in seven HIV-infected individuals during AEHI and CHI. IL-7 levels were measured by ELISA in the plasma of untreated HIV-infected subjects during follow-up while viral load represents HIV RNA copies per ml of blood.

Figure S3

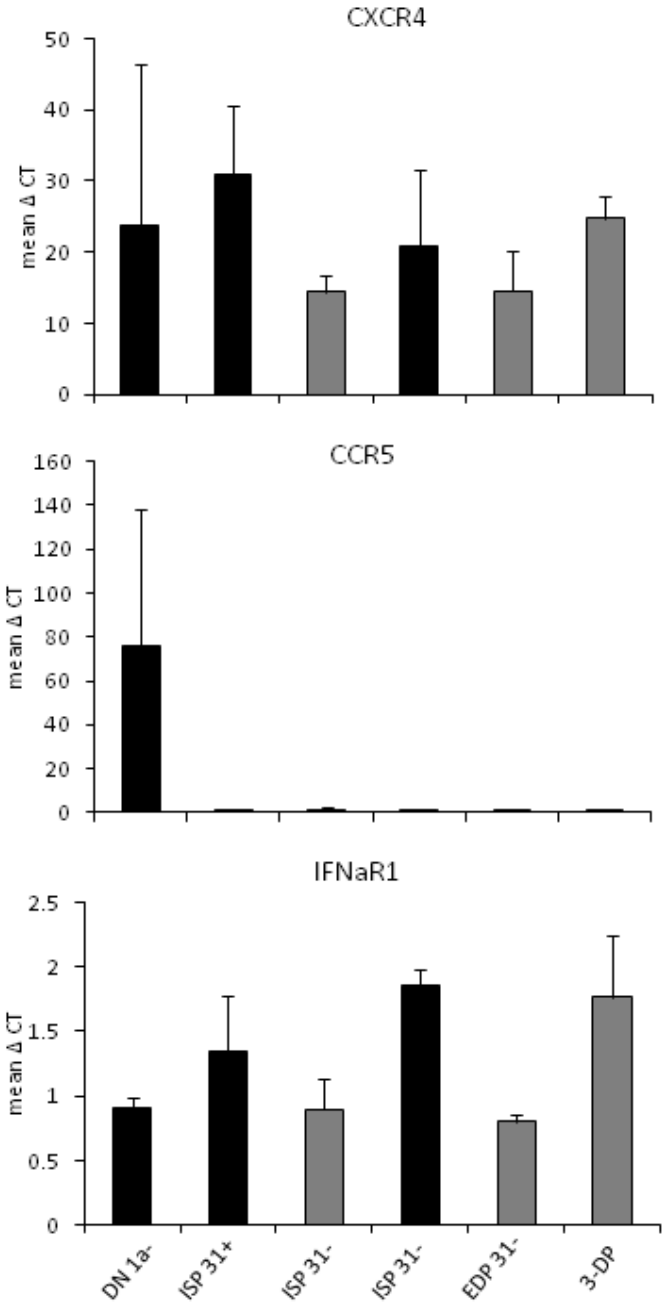

Figure S3. Expression of the HIV co-receptors CXCR4 and CCR5 as well as IFN-αR in sorted CD3$^-$ immature thymocytes by quantitative RT-PCR. Sorted DN CD34$^+$CD1a$^-$, ISP and EDP CD31$^+$CD1a^{low} and CD31$^-$CD1a^{hi} as well as CD3$^-$DP subsets were analyzed by for mRNA expression of CXCR4, CCR5 and IFN-αR by qPCR.